VIRULENCE REGULATORS OF THE SIGNIFICANT HUMAN PATHOGEN *ACINETOBACTER BAUMANNII*

by

SARAH K. GILES

Bachelor of Education

Bachelor of Science (Honours)

Thesis

Submitted to Flinders University

for the degree of

Doctor of Philosophy

College of Science and Engineering

December 2019

TABLE OF CONTENTS

TABLE OF FIGURES

DATA TABLES

ABBREVIATIONS

AC	Adenylyl cyclase
AMK	Amikacin
AMP	Adenosine monophosphate
AMP	Ampicillin
ATCC	American type culture collection
ATP	Adenosine triphosphate
Asp	Aspartate
bp	Base pair
Bap	Biofilm-associated protein
BD	Below detection level
°C	Degree Celsius
Ca^{+}	Calcium
g	Centrifugal force
cAMP	Cyclic adenosine monophosphate
CRP complex	cAMP receptor protein
CFU	Colony forming units
CFU/mL	Colony forming units per millilitre
CFU/well	Colony forming units per well
COG	Clusters of orthologous groups
CHX	Chlorhexidine
CIP	Ciprofloxacin
CHL	Chloramphenicol
CST	Colistin
DNA	Deoxyribonucleic acid
ERY	Erythromycin
FUR	Ferric up-take regulator
GalN	Galactosamine
GEN	Gentamicin
gfp	Green fluorescent protein
H_2O_2	Hydrogen peroxide
HI	Hydrophobicity index

His	Histidine
HiSeq	High throughput sequencing
HK	Histidine kinase
ICU	Intensive care unit
IMVS	Institute of Medical and Veterinary Science
KAN	Kanamycin
KAN^R	Kanamycin resistance
Kan	Kanamycin resistance gene
kb	Kilobase
kDa	Kilo Dalton
KEGG	Kyoto encyclopaedia of genes and genomes
L	Litre
LB	Luria-Bertani
LOS	Lipoologosaccharide
LPS	Lipopolysaccharides
Mg^{2+}	Magnesium
MDR	Multidrug-resistant
mg	Milligram
MH	Mueller-Hinton
µg	Microgram
µL	Microlitre
µM	Micromolar
MIC	Minimal inhibitory concentration
mL	Millilitre
mM	Millimolar
mm	Millimetre
MQ	MilliQ
mRNA	Messenger ribonucleic acid
M9	Minimal media
NA	Not applicable
NCBI	National centre for biotechnology information
ND	Not done

ng	Nanogram
nm	Nanometre
NOV	Novobiocin
NAL	Nalidixic acid
OD	Optical density
OD_{600}	Optical density at 600nm
OmpA	Outer membrane protein A
ORF	Open reading frame
PNAG	poly-β-(1-6)-*N*-acetylglucosamine
%	Percentage
P	Phosphate
P-value	Probability value
P <	Probability value less than
P >	Probability value greater than
PBS	Phosphate buffered saline
PCR	Polymerase chain reaction
PDE	Phosphodiesterase
PEN	Pentamidine
pEtN	Phosphoethanolamine
PMB	Polymyxin
psi	Pounds per square inch
PUM	Potassium urea magnesium
qRT-PCR	Quantitative reverse transcription PCR
^{R}	Resistance
rDNA	Ribosomal deoxyribonucleic acid
RIF	Rifampicin
RNA	Ribonucleic acid
RR	Response regulator
SDS-PAGE	Sodium dodecyl sulphate polyacrylamide gel electrophoresis
sp.	Species
sRNA	small non-coding RNA
STR	Streptomycin

TCSTS	Two-component signal transduction system
TEL	Tellurite
TEM	Transmission electron microscope
TET	Tetracycline
TM	Trans-membrane
TRI	Triclosan
Tn*10*	pLOF mini::Tn*10*:*gfp*:*kan*
TX	Triton X100
V	Volt
v/v	Volume/volume
Vfr	Virulence factor regulator
w/v	Weight/volume
WT	Wild-type
WHO	World health organisation

ABSTRACT

Acinetobacter baumannii is a prolific pathogen and a leading cause in nosocomial infections worldwide. This particular bacterium causes a number of infections including pneumonia which is commonly ventilator-associated, urinary tract and meningitis. Described as multidrug-resistant (MDR) and presenting a high threshold for a number of antibiotics as well as antiseptics, it is now commonplace to hear reports of pandrug-resistant strains. These strains are resistant to all clinically used classes of antibiotics. Epidemiological studies show a rapid global emergence and dissemination of this pathogen, demonstrating the remarkable successfulness and adaptation ability of *A. baumannii* in the hospital environment. This thesis provides insight into the regulation of a variety of genes and their impact on a number of virulence factors. These factors include pellicle formation, antibiotic resistance, adherence to eukaryotic cells and the ability of *A. baumannii* to cause disease in a murine infection model.

The ability to form a biofilm at the air-liquid interface, known as a pellicle, is a factor that is involved in the persistence of *A. baumannii* in various environments and is described in detail in chapter two (Giles *et al.* 2015). To investigate the pellicle forming ability of this bacterium a transposon bank was generated in a pre-existing hypermotile derivative of *A. baumannii* ATCC 17978 called 17978hm. Evaluation of the transposon mutant strains identified 11 mutants that were unable to form a pellicle. Sequencing of the pLOFmini::Tn*10*:*gfp*:*kan* (Tn*10*) insertion site identified three genes essential in pellicle formation. Of significant interest, was the identification of *cpdA*. The *cpdA* gene degrades cyclic adenosine monophosphate (cAMP), a secondary signalling molecule, maintaining the amount of cAMP within a cell. Measurement of cAMP levels within the *A. baumannii* 17978hm*cpdA*::Tn (*cpdA*::Tn) mutant strain confirmed the abundance of cAMP and its role in the ability to form a pellicle.

Two-component signal transduction systems (TCSTS) are known to regulate virulence factors in numerous bacteria, and as these systems are not found within humans they are of interest as potential drug targets therefore warranting investigation. The highly virulent clinical *A. baumannii* 04117201 strain was selected from in a collection of 54 clinical isolates as an appropriate candidate to assess

virulence and antibiotic resistance as described in chapters three and four. Examination of *A. baumannii* 04117201 identified a novel TCSTS designated herein as StkRS. The StkRS system is not present in the avirulent strain SDF and is therefore postulated to regulate virulence factors. Deletion of the *stkR* response regulator (RR) gene in the *A. baumannii* 04117201 parent strain was achieved generating the mutant strain 04117201Δ*stkR* (Δ*stkR*). Assessment of the resulting Δ*stkR* mutant strain identified a number of alterations in the virulence potential of this strain compared to the 04117201 parent strain as described in chapters three and four. Importantly, an increase in resistance to colistin (CST) of the Δ*stkR* mutant strain compared to the 04117201 WT was identified. CST being a polymyxin E antibiotic which has re-emerged as a viable treatment due to the severity of infections caused by *A. baumannii*. Additional differences were identified including an increase in; adherence capabilities to A549 pneumocytes, macrophage survival and resistance to human serum. A murine infection model of the 04117201 WT and Δ*stkR* mutant strains identified an increased bacterial load in the blood, lungs and spleen of mice infected with the Δ*stkR* mutant compared to the 04117201 WT strain. The above alterations plus further discussion in chapters three and four, reveal that the *stkR* RR gene is significant in regulating virulence factors in *A. baumannii* 04117201. Further investigation into this system is necessary to deepen the understanding of this invasive and problematic pathogen.

DECLARATION

I certify that this thesis does not incorporate without acknowledgment any material previously submitted for a degree or diploma in any university; and that to the best of my knowledge and belief it does not contain any material previously published or written by another person except where due reference is made in the text.

Sarah K. Giles

Decmber 2019

ACKNOWLEDGEMENTS

An immense thankyou to my parents Jane and Nigel, for their support both emotionally and physically. Continuing to be there for me throughout my University study, including the years leading up to and including my PhD, starting back in 2006 with my undergraduate in Education and Science. You have been a great help and support I could not have done it without you. To my brothers Brendan and Dylan for their support and encouragement through my many university degrees; you both always gave a shoulder to vent and whinge to when needed (which was a lot).

I would like to take this opportunity to give a gigantic thank you to my loving and always supportive husband Nitin. His encouragement and un-wavering patience was the backbone of my PhD candidature. Through the final stages were we welcomed our first child Collins, Nitin continued to support me in completing my thesis as well as being a loving and beautiful father.

Thank you to my supervisor Melissa Brown, who always gave great laboratory advice to overcome blockages in my research. Thank you for being level headed when I wanted to conduct mammoth experiments and bringing me back to my hypothesis, always asking ‘what are you trying to find out?’. To my co-supervisors Sophie Leterme and Uwe Stroeher, thank you for being there for me. Uwe, for the long and intense scientific discussion over coffee and cake through the years, nutting-out the smallest details of my experiments. Sophie, for being a great friend, giving great statistical advice and always giving a different perspective on a subject. A special thank you to Sylvia for continuing to be a great friend in and outside of the laboratory. To Felise and Jenny, for the laughs and many memories of dancing and chatting in the lab I will never forget. To Mohsen, Betty, and the rest of the laboratory members for their support, encouragement and great friendship; I wish you all the best and thankyou once more.

CONTRIBUTIONS

To Joel Geoghegan and Mark Van Der Hoek from SA health and Adelaide Institute of Medical and Veterinary Science (IMVS), for their help in running the RNA sequencing for the *A. baumannii* 04117201 and Δ*stkR* mutant strains. Mark treated the RNA samples for Ribosomal RNA reduction using the Epicentre Ribo-Zero kit, RNA library bar-coding was undertaken on the treated RNA for Illumina high throughput sequencing (HiSeq). To Lynette Waterhouse from Adelaide Microscopy, the University of Adelaide for her help with instructions and use of the transmission electron microscope (TEM) FEI Tecnai G2 Spirit machine and cutting of the samples in preparation. The Flinders Animal House Adelaide, including Roxanne Collingwood, Sharen Pilkington and colleges for all their help and support while running the mouse models. Ruth Hall from University of Sydney for providing the sequence of 04117201 *A. baumannii* strain. Shashikanth Marri from Flinders University, Adelaide bioinformatics, aligned the *A. baumannii* 04117201 RNA segments from the Illumina sequencing to the 04117201 constructed genome; Shashikanth also aligned the 04117201 strain contiqets to partly construct the *A. baumannii* 04117201 strains genome. To Sophie Leterme at Flinders University, College of Science and Engineering for her contribution in the statistical analysis undertook. David Ogunniyi from the University of South Australia, Future Industries Institute for providing the A549 human pneumocytes cell line and finally, Gillian Diet for professionally edited this thesis. This project was financially supported by the National Health and Medical Research Council Australia Project Grant 535053 and a Flinders Medical Research Foundation Grant both held by Melissa Brown.

PUBLICATIONS

Giles. S K, Stroeher U H, Eijkelkamp B A and Brown M H (2015) Identification of genes essential for pellicle formation in *Acinetobacter baumannii*. *BMC Microbiology* **15**:116.

Giles, S. K., Stroeher, U. H. and Brown, M. H. (2016). Measurement of Intracellular cAMP Levels Using the Cyclic Nucleotide XP Enzymatic Immunoassay Kit in Bacteria. *Bio-protocol* **6**(8): e1792. http://www.bio-protocol.org/e1792

PRESENTATIONS

Sarah Giles, Uwe Stroeher, Shashikanth Marri, Melissa Brown, An *Acinetobacter baumannii* two-component system modulates multiple virulence traits, *Acinetobacter conference*, Seville, Spain Sep 20th - 22nd Sep 2017.

Sarah Giles, Uwe Stroeher, Melissa Brown, The StkRS two-component system influences colistin resistance in *Acinetobacter baumannii*, *Australian Society of Microbiology Conference into Microbial Stress Response Molecular Systems and Community Response*, QT, Canberra, ACT, Australia July 3rd - 6th July 2015.

Sarah Giles, Uwe Stroeher, Melissa Brown, The role of the GerE response regulator in virulence and colistin resistance of *Acinetobacter baumannii*, *Gordon Research Conference into Microbial Stress Response Molecular Systems and Community Response*, Mount Holyoke College, South Hadley, MA, USA July 27th – 1st August 2014.

Sarah Giles, Uwe Stroeher, Melissa Brown, The role of the GerE response regulator in virulence and colistin resistance of *Acinetobacter baumannii*, *Gordon Research Seminar into Microbial Stress Response/ Cross-Disciplinary Studies of Microbes in Changing Environments*, Mount Holyoke College, South Hadley, MA, USA 26th – 27th July 2014.

Sarah Giles, Bart Eijkelkamp, Uwe Stroeher, Melissa Brown, Identification of genes involved in pellicle formation in *Acinetobacter baumannii* ATCC 17978, *Acinetobacter conference 9th International Symposium on the Biology of Acinetobacter*, Maternushaus, Cologne, Germany 19th - 21nd June 2013.

The presenting author has been underlined.

OUTLINE

This thesis is compromised of three result chapters, an introductory chapter, and a final discussion and conclusion chapter. The three results chapters are linked through subject matter as they each focus on the virulence and persistence capacity of the *A. baumannii* bacterium. This thesis contains approximately 38,000 words excluding appendices. The results chapters only contain information that is relevant to the publication. Extensive optimisations and investigations of non publishable research were not included in this thesis. The result chapters are written as individual papers with a preface, abstract, introduction, materials and methods, results and discussion. For ease of interpretation and reference within the thesis, the chapters have been modified to reference previous chapters. Additionally, to reduce repetition within the thesis, the introduction to chapter four is written in context of the thesis referring to the previous chapter rather than repeating information already stated. The preface at the beginning of each chapter describes the contributions of the authors for the articles, excluding paid contributions which are stated in the contributions section (see page XVII).

The chapter two focuses on the formation of pellicle, which is a type of biofilm formed at the air-liquid interface; this virulence trait is postulated to cause numerous issues within the hospital environment, as well as the host, as discussed. Chapter two is titled 'Identification of genes essential for pellicle formation in *A. baumannii*'; and is published as **Giles, S. K., Stroeher, U. H., Eijkelkamp, B. A. and Brown, M. H.** (2015) Identification of genes essential for pellicle formation in *Acinetobacter baumannii*. *BMC Microbiology* **15**:116. This article is presented in paper format in Appendix F. The investigation undertaken in chapter two also led to the development of a new method for measuring cAMP molecules in bacteria using an enzymatic kit as described. As this investigation did not follow the format chosen for this thesis the optimisation and development of this method was not described herein however, it is published as **Giles, S. K., Stroeher, U H. and Brown, M. H.** (2016). Measurement of intracellular cAMP levels using the Cyclic Nucleotide XP Enzymatic Immunoassay kit in Bacteria. *Bio-protocol* **6**: e1792. http://www.bio-protocol.org/e1792. This article is presented in paper format in Appendix G.

Chapters three and four focused on virulence traits related to the StkRS two component signal transduction system which was investigated using a variety of *in vitro* and *in vivo* experiments. Both chapters are written in paper format, to be submitted for publication upon completion of this thesis as the following. Chapter three to be submitted as **Giles. S. K., Stroeher. U. H. and Brown. M. H.** (2018) The StkRS two-component system influences colistin resistance in *Acinetobacter baumannii*, to *Antimicrobial Agents and Chemotherapy*; and chapter four to be submitted as **Giles, S. K, Stroeher, U. H, Marri, S., and Brown, M. H** (2018) *Acinetobacter baumannii* virulence factors and the host immune response influences bacterial morbidity and mortality in a murine pneumonia infection model to *mBio*.

CHAPTER 1 Introduction

1.1 *Acinetobacter baumannii*: new and improved

Acinetobacter baumannii is a Gram-negative coccobacilli bacterium that belongs to the gamma-proteobacterial family (Bergogne-Berezin *et al.* 1996). *A. baumannii* is one of the ESKAPE pathogens, a group of organisms that also includes *Enterococcus faecium*, *Staphylococcus aureus*, *Klebsiella pneumoniae*, *Pseudomonas aeruginosa* and *Enterobacter sp.* (Elhosseiny *et al.* 2018). Two-thirds of the antibiotic-resistant hospital-acquired infections seen today originate from the ESKAPE group. The *A. baumannii* hospital-acquired pathogen is commonly multidrug resistant (MDR), indicating simultaneous resistance to two or more classes of antibiotics, such as aminoglycoside and fluoroquinolones. Significantly, some clinical *A. baumannii* strains are classified as pandrug-resistant, which means they are resistant to all clinically or medically used classes of antibiotics (Hsueh *et al.* 2002, Fernandez-Cuenca *et al.* 2011).

The past 30 years have seen MDR and pandrug-resistant *A. baumannii* infections escalate in frequency and voraciousness. Infections caused by this bacterium include; pneumonia (commonly ventilator-associated), bacteraemia, urinary tract infections, septicaemia, device-associated infections caused by medical implants, open wounds and meningitis (Karageorgopoulos *et al.* 2008, Garnacho-Montero *et al.* 2010). There are several difficulties in treating patients who present with these bacterial infections. Due to the MDR and pandrug-resistant nature of *A. baumannii*, mortality rates have increased in infected patients (Sunenshine *et al.* 2007). Hospitals in the United States are estimated to spend approximately $8,246 to $29,019 per case of infection with *A. baumannii* (Lee *et al.* 2010). These costs are largely due to extended ventilation, extended patient hospital stays (which can be months), endemic contamination and infection, epidemic outbreaks, decontamination of wards, ongoing (sometimes lifelong) treatment for chronic conditions and repetition of surgery to remove infected prosthetics (Fournier *et al.* 2006). As this bacterium evolves, there is a great need to continually investigate and monitor its virulence and genetic capabilities to develop means to better combat this destructive pathogen.

1.2 A historical overview of *A. baumannii* infection

Historically, *A. baumannii* was considered a contaminant that was found in diagnostic laboratories, but as stated previously, through the past 30 years it has presented itself as a significant bacterium. The *A. baumannii* species are part of the *Acinetobacter* family. Originally, more than 15 taxonomic groups were named for what is now known as the *Acinetobacter* genus (Bergogne-Berezin *et al.* 1996). In 1911, Beijerinck first described *Acinetobacter* as *Micrococcus calco-aceticus*, and since then the species had been issued several names until 1968 when the name *Acinetobacter sp.* was allocated. The genus *Acinetobacter* has expanded to contain 32 taxonomically distinct species (Dijkshoorn *et al.* 2007, Gordon *et al.* 2010, Nemec *et al.* 2011), with several being environmental organisms not associated with human disease.

A. baumannii is the most medically relevant of the species. It is pleomorphic, moving between coccoidal and rod shapes when grown under different conditions (Adams *et al.* 2008, Peleg *et al.* 2008). This bacterium does not have fastidious growth requirements; it can grow in a wide range of temperatures, pH levels and can use a variety of carbon sources (Abbo *et al.* 2005). Recorded as naturally transformable, *A. baumannii* can take up foreign DNA from the environment and incorporate this DNA into its own genome. The genetic material, including plasmids, transposons and genomic islands, frequently harbour functional resistance genes contributing to MDR and pandrug-resistance. Technological advances have highlighted the degree to which *A. baumannii* strains can rearrange externally acquired DNA to extend their virulence portfolios.

1.3 Hospital-acquired *A. baumannii* infections

A. baumannii is predominately a hospital-acquired pathogen infecting immune-compromised patients in intensive care units (ICU). One of the more severe *A. baumannii* infections is ventilator-associated pneumonia (Aydemir *et al.* 2012, Celik *et al.* 2012). Surveillance at several hospitals has shown that ventilator-associated pneumonia mortality rates are as high as 73 % for *A. baumannii* infections (Seifert *et al.* 1995, Fagon *et al.* 1996, Makris *et al.* 2018). As such, much is being done to understand the infection pathways of *A. baumannii* as well as develop antibiotic treatment initiatives (e.g. combination therapy and using polypeptides to help reduce

the development of infections) (Parchem *et al.* 2016). Importantly, the implementation of polymyxins like polymyxin B (PMB) and/or colistin (CST) in decontamination regimens has been reported to reduce ventilator-associated pneumonia by up to 50 % (Hurley 2018). However due to the widespread use of PMB and/or CST antibiotic topical applications, hospitals have seen the emergence of Gram-negative bacteria and in particular *A. baumannii* strains, resistant to these antibiotics (Hurley 2018).

A. baumannii is also commonly found on surfaces within hospitals, such as bed railings, walls, medical equipment, computers and bed sheets (Higgins *et al.* 2010, Pakharukova *et al.* 2018). The persistent nature of this pathogen contributes to its endemic spread within hospitals and accounts for some of the increased risks of contracting MDR *A. baumannii* strains. Other risk factors include, but are not limited to, exposure in ICU (especially prolonged stays), receiving mechanical ventilation, exposure to antimicrobial agents, recent surgery and underlying medical issues that contribute to a reduced immunity (Fournier *et al.* 2006, Maragakis *et al.* 2008, Chuang *et al.* 2009). To control hospital outbreaks, strict decontamination and ward closures have been used (Higgins *et al.* 2010).

Compared with the other pathogenic bacteria in the ESKAPE group, *A. baumannii* has been reported to be the most prevalent infective organism associated with invasive operations contributing up to 20 % of infections in ICU (Lee *et al.* 2017, Yue *et al.* 2017). A study conducted in Delhi from 2010 to 2014 assessed 818 samples from patients with open wound infections in isolated burn units. This study found that *A. baumannii* accounted for 12 % of the infections with an increase in resistance to aminoglycosides and ceftazidime (Singh *et al.* 2017). Carbapenem-resistant *A. baumannii* has been identified as contributing to the increased persistence of *A. baumannii* infections (Zarrilli *et al.* 2013). Recently, the World Health Organisation (WHO) released a statement describing the top priority pathogens to investigate on their 'Global priority list of antibiotic-resistant bacteria to guide researcher, discovery, and development of new antibiotics' (WHO 2017). The most critical are *A. baumannii* carbapenem-resistant strains, then *P. aeruginosa* carbapenem-resistant, *Entrobacteriaceae* carbapenem-resistant and 3rd generation cephalosporin-resistant strains. The release of this priority list confirmed the importance of investigating *A. baumannii.*

1.4 *A. baumannii* carriage capacity, persistence and spread to a community-acquired pathogen

While the particulars of the reservoir harbouring *Acinetobacter* are unknown, although hospitals have been suggested as a source, interactions between animals, the environment and humans could be contributing to the emergence and re-emergence of this infectious pathogen exacerbating the situation (Zeana *et al.* 2003, Eveillard *et al.* 2013). *Acinetobacter sp.* are found extensively in the environment; a study of 66 soil samples taken in Hong Kong discovered that more than a third contained *Acinetobacter sp.* with 23 % being *A. baumannii* (Houang *et al.* 2001). Additionally, *A. baumannii* is commonly found in supermarkets and greengrocers as well as other public places (Berlau *et al.* 1999, Choi *et al.* 2012). Other areas identified where *A. baumannii* species persist include manured agricultural soil, pig slurry and fish farms (Huys *et al.* 2007, Byrne-Bailey *et al.* 2009).

As stated above, the hospital has been suggested as a possible reservoir for *A. baumannii*; the surfaces of medical equipment, such as ventilators or catheters are the common places identified with this bacterium (Raad *et al.* 2008, Jang *et al.* 2009, Ju *et al.* 2018, Qin *et al.* 2018). Colonisation of these items, the added exposure to antimicrobial agents in patient treatment and inadequate decontamination practices is suggested to contribute to the MDR, persistence and therefore spread of this pathogen (Hurley 2018). In addition to the cross-contamination between infected and non-infected patients discussed above, inadequate hand hygiene practices by medical staff also plays a role (Dijkshoorn *et al.* 2007, Markogiannakis *et al.* 2008, Garlantezec *et al.* 2011). Therefore, as well as adequate ward decontamination, implementation of stringent hygiene regimes is required for successful control and eradication of *A. baumannii* outbreaks (Chan *et al.* 2007, Hurley 2018).

Recently, community-acquired *A. baumannii* infections have been identified in several countries including North America (Falagas *et al.* 2007, Eveillard *et al.* 2013, Serota *et al.* 2018). Additionally, community-acquired infections in Australasia have been contained to sub-tropical regions of Australia as well as Thailand, the Philippines and the Indonesian island of Bali (Seifert 1999, Anstey *et al.* 2002, Ong *et al.* 2009, Telang *et al.* 2011, Chanchaithong *et al.* 2018, Kim *et al.* 2018). Within Australia, community-acquired infections appear to be related to the physiological

conditions of the patient. Patients who have contracted this bacterium frequently have alcoholism or asthma (Anstey *et al.* 1992, Ong *et al.* 2009). These infections range from pneumonia to open wound and bacteraemia. Climate has been proposed as a possible cofactor in the ability of *A. baumannii* to cause disease within a patient. The likelihood of a patient contracting community-acquired *A. baumannii* pneumonia is highest directly after a change from a temperate to a humid climate (Anstey *et al.* 2002, Eveillard *et al.* 2013). As such, after large natural disasters there is a dramatic increase of *A. baumannii* wound infections in the population within the affected area (Y. Wang *et al.* 2010, Eveillard *et al.* 2013, Suleyman *et al.* 2018).

Disturbingly, several military personnel have contracted this bacterium at army bases in Iraq and Afghanistan (Davis *et al.* 2005, Hujer *et al.* 2006, Arivett *et al.* 2016), with *A. baumannii* causing soft tissue infections in open skin wounds (Griffith *et al.* 2007, Denys *et al.* 2011). The army personnel who contract this bacterium overseas, upon returning to their countries of origin have the potential to transmit the infection to other patients as well as into the wider community, thereby exacerbating the spread of the pathogen (Peleg *et al.* 2008).

Overall, the emergence of community-acquired *A. baumannii* infections could be associated with its general persistence in the environment as suggested above, and therefore the environment could be considered to be involved in the emergence and re-emergence of this infectious disease. As this pathogen becomes more frequently reported in the community, greater measures need to be taken to help prevent its spread; this can be done by reducing patient-to-patient contamination as stated previously, as well as ensuring that hygiene practices are followed by hospital staff and that outbreaks are dealt with quickly.

1.5 Mechanisms of pathogenesis

Pathogenesis is the virulence potential of an organism, and is categorised as the degree to which it can cause disease. *A. baumannii* has multiple virulence factors that contribute to its survival and ability to cause disease. Some of these factors are structures protruding from, or embedded in, the membrane (Harding *et al.* 2018). These include a variety of: adhesion pili; outer membrane proteins such as membrane receptor proteins (Catel-Ferreira *et al.* 2016, Elhosseiny *et al.* 2018); capsular polysaccharide and other surface polysaccharides and oligosaccharides (Russo *et al.*

2010); biofilm-associated protein (Bap) (Brossard *et al.* 2012); type I and type IV pili (Harding *et al.* 2013); and type IV and type VI secretion systems (Cerqueira *et al.* 2011, Fitzsimons *et al.* 2018) (Figure 1.1). Virulence factors that can sequester or expel elements, metals or molecules like iron (Fe^{2+}) include the cation up-take systems (Eijkelkamp *et al.* 2011a) (Section 1.9) and efflux pumps from diverse families including the major facilitator superfamily (MFS), the resistance nodulation division (RND) and the ATP-binding cassette transporter (ABC) families (Yoon *et al.* 2013, Machado *et al.* 2018). Nevertheless, however significant these factors are, the ability to control their expression is ever more important, and as such, these systems are commonly tightly regulated by signal transduction systems (Robinson *et al.* 2000, Adams *et al.* 2009, Dorr *et al.* 2016, Richmond *et al.* 2016, Russo *et al.* 2016, Chen *et al.* 2017, De Silva *et al.* 2018, Liu *et al.* 2018). This regulation enables bacterial cells to respond to environmental pressures by activating these systems (Chen *et al.* 2017, De Silva *et al.* 2018). Finally, several resistance genes and transferable genetic material (such as plasmids) can carry the above mentioned virulence factors to other bacterial cells and strains, allowing them to spread globally (Figure 1.1).

1.5.1 Transfers of plasmid and other mobile genetic elements

Bacteria can adapt and evolve in hostile conditions. One way that they can achieve this is to alter their ability to withstand pressures is acquiring new DNA. Numerous species have been shown to take up DNA from the environment and integrate it into their genome, thereby acquiring new phenotypes (Cameranesi *et al.* 2018). It is thought that *A. baumannii* can not only incorporate foreign DNA but can use mechanisms such as horizontal gene transfer to transfer DNA from one bacterial cell to another (Fournier *et al.* 2006, Vila *et al.* 2007, Rumbo *et al.* 2011). This new genetic material can code for different virulence factors including antibiotic resistance. For example the AmpC β-lactamase genetic element (bla_{ADC}) provides resistance to β-lactams, while the ($bla_{OXA-143}$) and the ($bla_{OXA-235}$) genetic elements have been shown to contribute to carbapenem resistance in various areas in Brazil (Pagano *et al.* 2016). This insertion of new genetic material can also cause mutations affecting the expression of proteins and

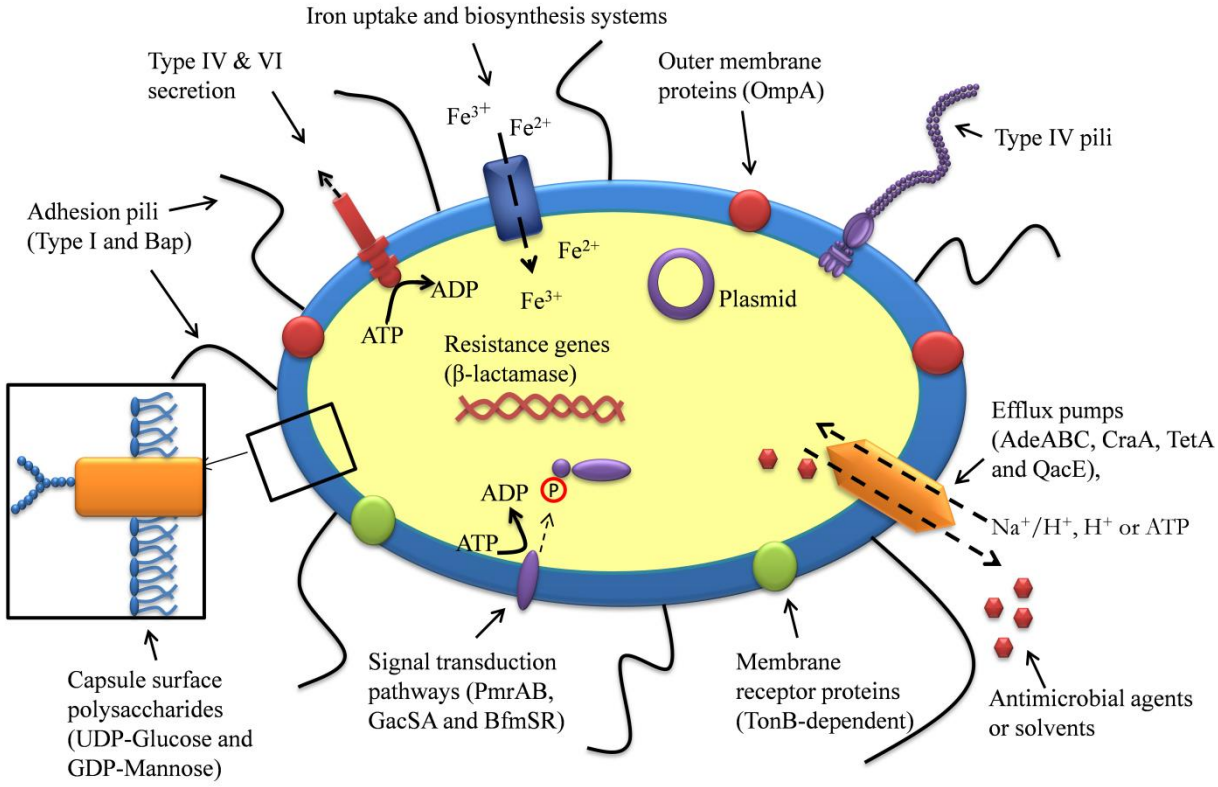

Figure 1.1: A schematic diagram of the virulence factors used by *A. baumannii* strains

Represented are several important virulence factors of *A. baumannii*; type IV pili, iron uptake and biosynthesis systems, surface polysaccharides, efflux pumps, outer membrane proteins, signal transduction pathways, membrane receptor proteins, resistance genes, plasmids, adhesion pili and type IV secretion systems. Figure adapted from (Moatamed 2012).

could alter the expression of outer membrane proteins, efflux pumps and signal transduction pathways effecting virulence (Vila *et al.* 2007).

1.5.2 Adherence to biotic surfaces and biofilm formation

A. baumannii has an intrinsic ability to arrive at a biotic surface and attach to form a biofilm (Draughn *et al.* 2018). A biofilm is described as a collection of bacterial cells surrounded by a polymeric matrix of exopolysaccharides, DNA and other proteins that develops into a multicellular heterogeneous community (Tiwari *et al.* 2018). The developmental changes from planktonic bacteria to a mature biofilm proceeds in the stages shown in Figure 1.2. In stage one, free floating planktonic bacteria arrive at a surface and divide. The bacteria use pili or fimbriae to adhere and this produces a bacterial monolayer. The initial adherence by planktonic bacteria is reversible until the bacteria begin to produce exopolymers. Stage two proceeds with bacterial cell division and exopolysaccharides and proteins being produced (Donlan *et al.* 2002, Hammond *et al.* 2011). Stage three advances with cell division and the production of further exopolysaccharides; this stage shows the beginning of quorum-sensing, which is believed to be involved in advancing the development of a biofilm (Piletska *et al.* 2011). Stage four is development of a mature biofilm exhibiting multicellular characteristics, waste channels and quorum-sensing. Stage five is the spread to the surrounding environment of a mature biofilm by a process called seeding dispersal (Purevdorj-Gage *et al.* 2005).

1.5.2.1 Multiple mechanisms contribute to adherence and biofilm formation

Strain variation has compounded investigation of the molecular mechanisms responsible for formation of *A. baumannii* biofilms because it is unknown whether the molecular mechanisms described are conserved. Adherence is the initial step in colonisation as stated previously and is most commonly mediated by pili and other protein structures embedded on the bacterial cell surface like outer membrane protein A (OmpA) (Pakharukova *et al.* 2018). For example, the CsuA/BABCDE chaperone-usher pili assembly commonly regulated by the TCSTS BfmSR, is composed of six genes important for the assembly of pili; mutations in the *csu* genes have been shown to reduce adherence to abiotic surfaces (Cerqueira *et al.* 2011, Draughn *et al.* 2018). There are many genes associated with adherence and/or biofilm formation, which are not necessarily independent, for example an insertion disruption of either a type I pili

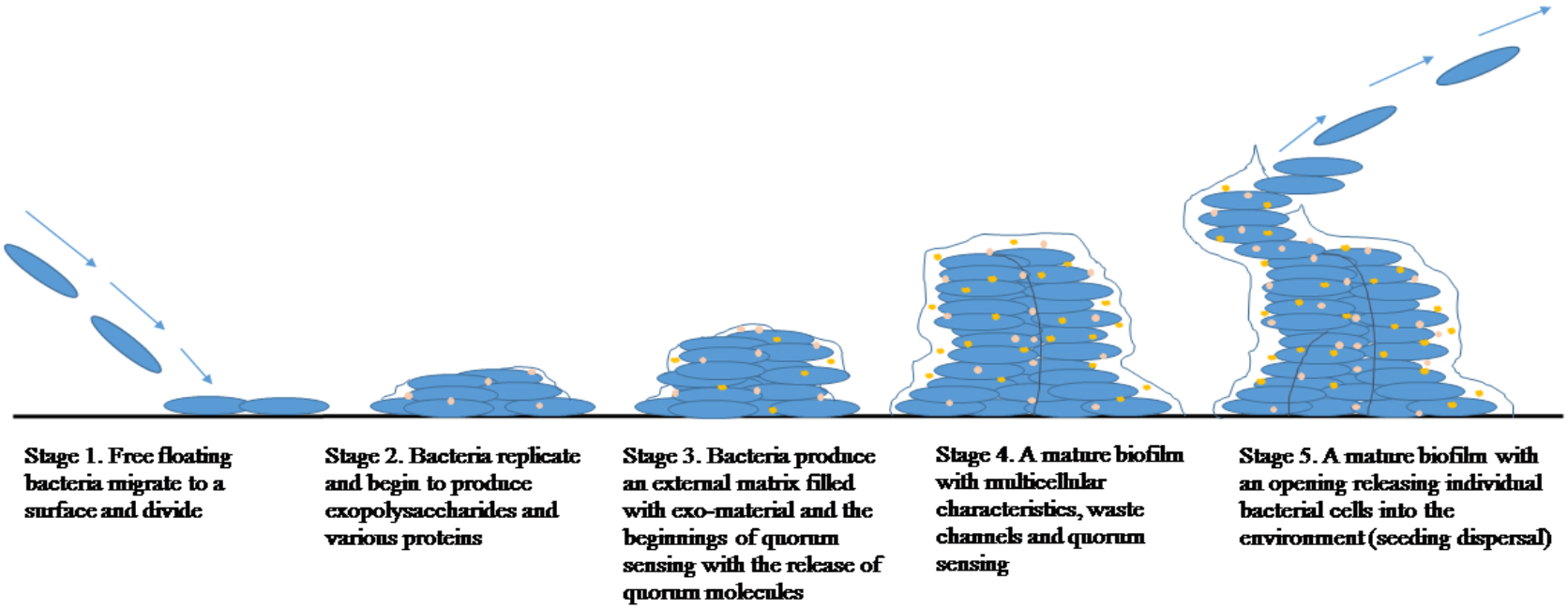

Figure 1.2: Biofilm formation stages one to five

Biofilm formation is established in five stages: stage one free floating bacteria arrive at a surface and divide; stage two, bacteria produce exopolysaccharides and other proteins; stage three, bacteria continue to produce exopolysaccharides and proteins as well as divide and begin excreting quorum-sensing molecules; stage four, a mature biofilm is formed with quorum-sensing and waste channels; and stage five, the biofilm releases individual bacterial cells to infect other areas. Adapted from (Vogeleer *et al.* 2014)

cluster or OmpA can result in altered biofilm levels (Tomaras *et al.* 2003, Gohl *et al.* 2006, Gaddy *et al.* 2009b). Several proteins play a role in the maturation of the *A. baumannii* biofilm; these include Bap (Loehfelm *et al.* 2008, Rahbar *et al.* 2010, Tiwari *et al.* 2018), production of the poly-β-(1-6)-*N*-acetylglucosamine (PNAG) polysaccharide and expression of the *pgaABCD* gene cluster have all been described as critical for *A. baumannii* biofilm formation (Loehfelm *et al.* 2008, Choi *et al.* 2009, Rahbar *et al.* 2010, Deveson Lucas *et al.* 2018, Tiwari *et al.* 2018). In clinical *Acinetobacter* strains, major differences between strains have been identified in their ability to form biofilms (Cevahir *et al.* 2008, Lee *et al.* 2008, de Breij *et al.* 2010, Eijkelkamp *et al.* 2011b). In addition to the above, the control of biofilm formation has been shown to be due to cell-to-cell signalling, which occurs by quorum-sensing (Castillo-Juarez *et al.* 2017). Interestingly, the biofilm structure is of particular interest within the hospital environment as it binds to hydrophobic materials like plastics, as such suggestions to move the medical industry to hydrophilic materials could result in reducing the ability of biofilm forming pathogens to spread (Pakharukova *et al.* 2018).

1.5.2.2 Biofilm and increased antibiotic resistance

Bacteria within a biofilm are largely protected against attacks from antibiotics, disinfectants, germicides and phagocytosis (Bartoszewicz *et al.* 2007). MDR *A. baumannii* isolates commonly show higher levels of biofilm formation than their susceptible counterparts, which confirms a correlation between biofilm formation and increased drug resistance (King *et al.* 2009, Sato *et al.* 2018). The biofilm matrix provides protection via the outer matrix structure against antimicrobial agents and environmental stressors, leaving the bacteria within largely untouched (Stewart *et al.* 2001, Skindersoe *et al.* 2008, Hoiby *et al.* 2011, Draughn *et al.* 2018, Pakharukova *et al.* 2018). Proteins associated with drug resistance, including β-lactamases and aminoglycoside acetyltransferases, are found to be over-expressed in biofilms and contribute to resistance by deactivating the agents entering the biofilm (Mah *et al.* 2001, Darouiche 2004, Shin *et al.* 2009). Interestingly, the production of biofilms can be a result of exposure to sub-inhibitory concentrations of antimicrobial compounds, suggesting that the formation of biofilms can be classified as a virulence mechanism (Nucleo *et al.* 2009).

The structure of a biofilm produce cause gradients of nutrients, oxygen, waste and pH (Stewart *et al.* 2001). These variations can also create anaerobic conditions that can be beneficial in resisting antibiotic attack (Xu *et al.* 2000). Some antibiotics work well in aerobic conditions but lose their effectiveness in anaerobic conditions. For example, aminoglycosides work well in inhibiting bacteria in aerobic environments but they are not effectively taken up by bacteria cells in anaerobic conditions (Bryant *et al.* 1992, Stewart *et al.* 2001).

Within a biofilm, there are many physical and chemical stresses (including osmotic, endogenous oxidative stress and nutrient) (Sutherland 2001, Hoiby *et al.* 2011, Falghoush *et al.* 2017) that could lead to the bacteria entering a slowed growth phase. This phase has been thought to limit division capacity and inhibit antibiotics from reaching the interior of the bacteria cells (Prigent-Combaret *et al.* 1999, Hoiby *et al.* 2010). This is seen as beneficial because bacteria in the middle of a biofilm are largely protected against antibiotic therapy; dormant bacteria have been found to be 15 times more resistant compared with planktonic cells (Desai *et al.* 1998, Stewart *et al.* 2001, Darouiche 2004, Behlau *et al.* 2008). Subsequently, the treatment of biofilms requires not only an antibiotic but also an agent to break down the biofilm itself (Alipour *et al.* 2009).

1.5.2.3 Pellicle formation is the biofilm at the air-liquid interface

There are two distinct forms of biofilms described in the literature. The best known biofilm is formed at the solid–liquid interface, as described above, while the other is the pellicle formed at the air–liquid interface (Kentache *et al.* 2017). Interestingly, a study in *A. baumannii* assessing formed pellicle material, identified 52 differentially-expressed proteins with 32 up-regulated and 20 down-regulated when compared to planktonic growth (Martí *et al.* 2011a). These findings are similar to another investigation of the whole proteome of the pellicle which found that sessile bacteria more are resistant to external pressures than the planktonic bacteria (Kentache *et al.* 2017).

The formation of a pellicle in ventilator tubing has the potential to form a plug where bacteria have access to oxygen as well as nutrients from a liquid media (Jos *et al.* 2009). Interestingly, *A. baumannii* has been found to have an increased ability to form a pellicle compared with other *Acinetobacter sp.* (Martí *et al.* 2011b).

Additionally, the pellicle has been associated with various virulence factors including phospholipases, adhesion factors, the GacSA TCSTS and Type VI secretion system (Kentache *et al.* 2017). The siderophore iron up-take systems described in section 1.10 have also been correlated with pellicle formations (Martí *et al.* 2011a). It has been suggested that the pellicle may not be important in a host niche, but instead its core purpose could be associated with environmental pressures (Martí *et al.* 2011b). Because pellicle formation is more pronounced at room temperature (approximately 25°C compared with incubation temperature of 37°C), it is important to note that biofilm and pellicle formation are not directly correlated when investigating different strains (McQueary *et al.* 2011).

1.6 Regulation of pathogenic factors

As the virulence mechanisms used by bacteria are being investigated so are the regulating factors that control these mechanisms. *A. baumannii* uses an array of virulence mechanisms that facilitate its persistence and resistance within the hospital and host environments. As described above, these include surviving desiccation, forming biofilms and pellicles, using a range of efflux pumps and modification of antibiotic targets to withstand antibiotic therapy (Draughn *et al.* 2018). A number of regulating factors have been identified including small non-coding RNA (sRNA), plasmids and signal transduction pathways shown to regulate virulence factors contributing to increased morbidity and mortality rates with *A. baumannii* infections. A number of, sRNAs have been found to affect the AdeABC efflux pump altering antibiotic resistance as well as influence biofilm formation in ATCC 17978, different sRNA are found in sessile bacteria compared to planktonic (Gholamalipour *et al.* 2018, Hu *et al.* 2018). Other mechanisms are affected by plasmid mediated regulation for example the TeR-like regulator harboured on plasmids pAB3 and pAB04-1 in the ATCC 17978 and Ab04 strains play key roles in the ability of *A. baumannii* to resist antibiotic pressures (Wood *et al.* 2018). As well as the above regulatory mechanisms TCSTS enable bacteria to alter their state when under selective environmental pressures through regulation of the histidine kinase (HK) and RR proteins, discussed below. These systems can regulate a variety of virulence mechanisms including antibiotic resistance by regulating efflux pumps and biofilm formation (Adams *et al.* 2018).

1.6.1 TCSTS

Bacteria can sense, adapt and respond to signals both inside and outside a host. This ability has permitted them to survive adverse conditions as well as invade a wide range of niches (Sheng *et al.* 2012, Adams *et al.* 2018). The TCSTS is one mechanism in which a protein perceives an external stimulus and then activates a regulator to modify gene expression (Calva *et al.* 2006), thereby aiding the bacteria to actively respond to its environment. TCSTS are relatively simple signalling pathways that are found predominantly in prokaryotes. First identified as a distinct class of signalling pathway 25 years ago (Nixon *et al.* 1986), TCSTS are present in bacteria, archaea and eukaryotic organisms (e.g. yeast and plants) but they are not found in higher animals (Hoch 2000). Because of this, TCSTS have been identified as potential drug targets (Gotoh *et al.* 2010, Milton *et al.* 2018). These systems contribute to the pathogenicity of bacterial infections by regulating processes including the surface adhesion, phosphate and iron uptake, antibiotic resistance, and the formation of biofilms and pellicles (Casino *et al.* 2010, Russo *et al.* 2016). A standard TCSTS consists of two proteins, a sensor HK and a cognate RR (Figure 1.3) (Calva *et al.* 2006, Laub *et al.* 2007).

As shown in Figure 1.3, the HK is located in the cell membrane and acts as a sensor protein. When the HK protein receives a stimulus, it undergoes dimerisation and autophosphorylation at a conserved histidine (His) residue. The phosphoryl group is transferred to a conserved aspartate (Asp) residue on the cognate RR in the cytosol. This leads to conformational changes in the RR effector domain that enables the protein to actively increase or decrease gene transcription (Robinson *et al.* 2000, Stock *et al.* 2000). The average bacterial genome encodes 50–60 TCSTS (Ashby *et al.* 2006, Whitworth *et al.* 2008, Wuichet *et al.* 2010). TCSTS regulate a wide range of physiological processes in response to changing environmental parameters (Comeau *et al.* 1985) including environmental pressures experienced during the infection cycle (Ewann *et al.* 2002).

1.6.1.1 HK proteins

HK proteins phosphorylate a number of targets (Robinson *et al.* 2000), but in a typical two-component system, there is a one-to-one relationship between the HK and the RR with very little cross-talk between non-cognate RR proteins. The sensor

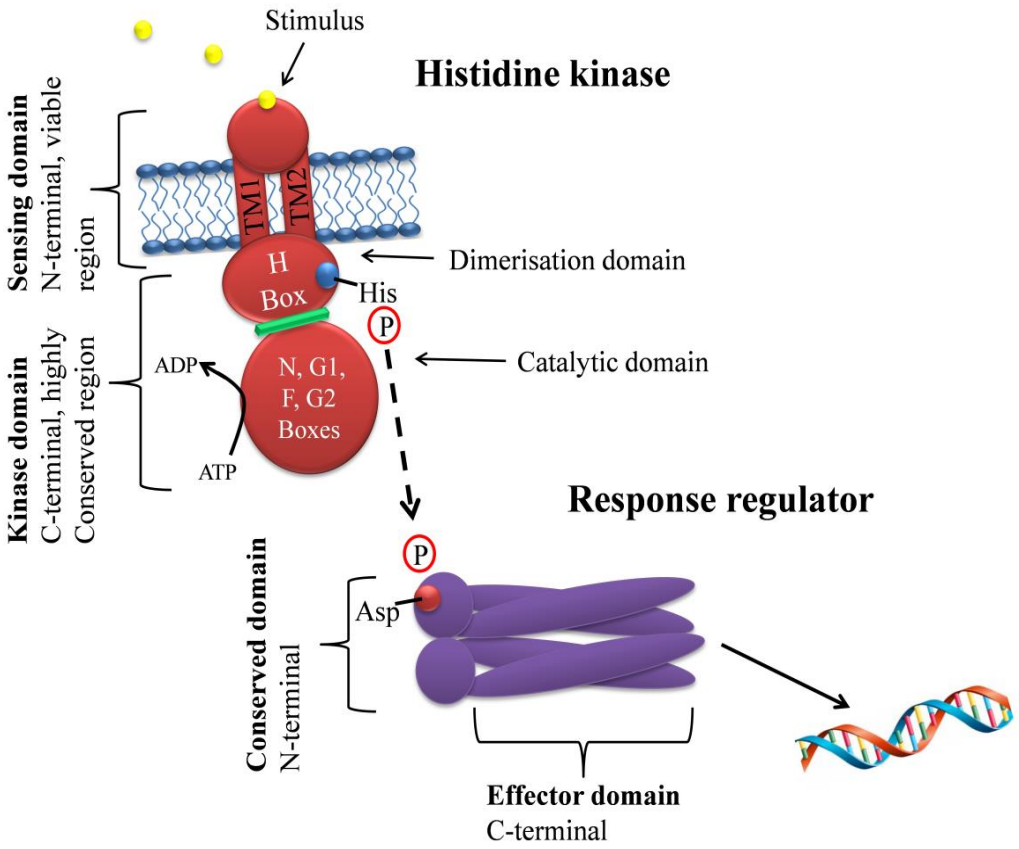

Figure 1.3: Representation of a TCSTS

After receiving an external stimulus (yellow circle), the histidine kinase is autophosphorylated at a conserved His residue (blue circle) in the H box. The subsequent phosphoryl group is transferred to an Asp residue (red circle) in the N-terminal of the response regulator protein. A conformational change in the C-terminal or effector domain of the response regulator leads to an alteration in gene expression in response to the stimulus.

HK protein generally consists of two domains: a variable N-terminal sensing domain and a highly conserved C-terminal kinase domain. The N-terminal sensing domain consists of two trans-membrane (TM) regions, TM1 and TM2 (Figure 1.3), which embeds the protein in the cytoplasmic membrane (Forst *et al.* 1987). The C-terminal kinase domain consists of a dimerisation and a catalytic region. The dimerisation region contains the H box and a conserved histidine (His) residue where autophosphorylation takes place. The catalytic region is comprised of four or five amino acid motifs known as the H, N, G1, F and G2 boxes (Parkinson *et al.* 1992, Stock *et al.* 2000) (Figure 1.3) and is responsible for the adenosine triphosphate (ATP) binding required for autophosphorylation.

The response process starts with a stimulus being detected from the environment leading to a conformational change of the sensing domain. The autophosphorylation of the kinase is a trans-autophosphorylation bimolecular reaction between homodimers where one HK monomer catalyses the phosphorylation of the conserved His residue in the other (Perraud *et al.* 1999, Stock *et al.* 2000, Cardona *et al.* 2018). The phosphoryl group on the Asp residue is transferred to water in a hydrolysis reaction where all autophosphorylation steps require divalent metal ions, with Mg^{2+} assumed to be the relevant cation *in vivo* (Stock *et al.* 2000). Several HK proteins can actively dephosphorylate the cognate RR due to the activity of the phosphate, which limits the RR proteins time in the activated state (Robinson *et al.* 2000).

The HK proteins can be divided into two classes, orthodox and hybrid, which range in size from less than 40 kDa to more than 200 kDa. An example of an orthodox HK is the *Escherichia coli* EnvZ protein, which has two TM regions. However, not all orthodox HKs have this structure. For example, the FixL protein from *Rhizobium meliloti*, which is involved with nitrogen fixation (Stock *et al.* 2000) has four TM regions and UhpB, a part of the sugar transport system in *E. coli*, has eight TM regions (Island *et al.* 1993). Furthermore, not all HK proteins are membrane bound. CheA, which is implicated in chemotaxis, and the nitrogen regulatory kinase NtrB are both soluble cytoplasmic HK proteins. They can be regulated by interaction with intracellular stimuli or by interaction with the cytoplasmic domains of other proteins (Stock *et al.* 2000).

1.6.1.2 RR proteins

The RR protein of a TCSTS generally consist of two domains: the regulatory conserved N-terminal region containing an Asp residue and the variable effector C-terminal domain (See Figure 1.3) (Gross *et al.* 2012). The RR proteins commonly found in the cytosol of a cell are responsible for altering gene transcription. The RR protein has two conformational states; inactive and active. The inactive state is the unphosphorylated RR protein and the active state is the result of phosphorylation of the conserved Asp (Buckler *et al.* 2000). As stated previously, in a TCSTS the phosphoryl group is catalysed from the phosphor-His of the cognate HK protein and transferred to the conserved Asp residue in the RR N-terminal regulatory domain, where a conformational change occurs facilitating transcriptional effects (Stephenson *et al.* 2002). The response is a set of inter- or intra-molecular interactions that alter the surface area of the effector domain to produce a response. This response can be protein-to-protein or act directly on the RNA polymerase (Capra *et al.* 2012).

A RR protein can also activate without the assistance of a cognate HK through interactions with several small molecules. For example, acetyl phosphate, carbamoyl phosphate, imidazole phosphate and phosphoramidate can act as phosphodonors and cause transcriptional effects independently of an external signal (Feng *et al.* 1992, Lukat *et al.* 1992). This provides evidence that the system can be activated without sensing an external stimulus, possibly as a reaction to internal metabolic states. To return to an inactive state, most RR proteins can autodephosphorylate, which limits the lifetime of the activated RR (Perraud *et al.* 1999).

1.6.1.3 Orphan HK and RR proteins

Although a vast majority of HK and RR proteins are identified in pairs with their cognate partner, some are also present as orphan proteins (Capra *et al.* 2012). Different species of bacteria have different orphan proteins. For example, approximately 6.4 % of HK and RR proteins in *E. coli* are orphaned, whereas in *Caulobacter crescentus* this percentage is increased to 57 % (Skerker *et al.* 2005). The orphan proteins are suggested to work in the same manner as the cognate paired TCSTS, but they are able to act on more than one protein, giving rise to an abundance of cross-talk (Section 1.6.1.6) (Laub *et al.* 2007).

1.6.1.4 Prevalence of TCSTS

The occurrence of TCSTS in prokaryotes can vary dramatically across species. For example, in *E. coli* there are 30 HK (five of which have been identified as hybrid kinases) and 32 RR proteins. The number of TCSTS proteins can be as high as 80 in *Synechocystis sp* and 82 in *Burkholderia pseudomallei* (Cardona *et al.* 2018). In contrast there are none in *Mycoplasma genitalium*. There is a large variability in the number of TCSTS presence in different species including 70 in *Bacillus subtilis*, 9 in *Haemophilus influenzae*, 11 in *Helicobacter pylori*, and 19 in *Thermotoga maritime* (Stock *et al.* 2000, Galperin 2006). As more and more species of bacteria have their complete genomes sequenced, TCSTS proteins will be identified and the prevalence of these systems will be known.

1.6.1.5 Typical TCSTS

A typical TCSTS is the EnvZ-OmpR system from *E. coli*. This system responds to changes in the osmolarity of the external environment and ethanol (Tipton *et al.* 2016, Zhang *et al.* 2018). The HK EnvZ and the RR OmpR protein act together to regulate the expression of the outer membrane porin proteins OmpF and OmpC. When activated, the OmpR RR binds to regions upstream of genes encoding these proteins (Cai *et al.* 2002, Yoshida *et al.* 2002). This system has also been thought to contribute to biofilm formation through the phosphorylated OmpR protein binding to the *csgD* promoter that positively regulates the transcription of *csgAB* and *adrA*, which are types of pili known to be involved in biofilm formation (Stanley *et al.* 2004).

1.6.1.5.1 GacSA TCSTS within *A. baumannii*

For the regulation of virulence factors across Gram-negative bacteria, the TCSTS GacSA has been identified as important (Parkins *et al.* 2001, Stanley *et al.* 2004, Gauthier *et al.* 2010, Tahrioui *et al.* 2013, Yan *et al.* 2018). Interestingly, the GacS protein in *A. baumannii* bacteria is an orphan hybrid HK that shares 43 % homology to a protein in *P. aeruginosa* PA01 (Peleg *et al.* 2008). The *gacS* gene contributes to the virulence capacity of *A. baumannii* to kill unicellular eukaryotes, commonly *Candida albicans*, and when this gene is disrupted, this ability is attenuated (Peleg *et al.* 2008). In addition to the above, 674 genes are transcriptionally altered when *gacS* is disrupted in *A. baumannii* ATCC 17978. The affected genes include those involved in biofilm formation, motility and pili

synthesis (Cerqueira *et al.* 2014). TEM studies have visualised significantly shortened pili and a reduction in biofilm mass in the ATCC 17978 WT strain compared with the Δ*gacS* mutant. Expression of two genes essential for pili synthesis and biofilm formation as part of the *csu* operon were found to be significantly reduced in expression in the Δ*gacS* mutant (a 4-fold reduction for *csuB* and a 4.5-fold reduction for *csuC*) (Tomaras *et al.* 2008, Gaddy *et al.* 2009a). Of note, the *csu* operon has been found to be regulated by two TCSTS, the GacSA and the BfmSR systems, and is potentially a cross-talk system within *A. baumannii*.

1.6.1.5.2 BfmSR TCSTS within *A. baumannii*

The BfmSR, also known as the RstAB, TCSTS is involved in various mechanisms correlated to *in vivo* survival, biofilm formation and antibiotic resistance (Tomaras *et al.* 2008, Russo *et al.* 2016, Draughn *et al.* 2018). Regulating these mechanisms involves the expression of several regulatory processes that alter the physiology of the bacterial cell. This system has been associated with the expression of the *csuA/BABCDE* chaperone operon pili system in ATCC 19606; when *bfmR* is disrupted, the cell surface pili were reduced (Tomaras *et al.* 2008) leading to a reduction in biofilm formation. Interestingly, in *A. baumannii* 19606, disruption of *bfmS* was shown to also reduce the total amount of biofilm produced (Tomaras *et al.* 2008, Thompson *et al.* 2012). This finding has contributed to the belief that *bfmR* can be activated by another HK to induce biofilm formation in this strain. Additionally, when the BfmSR TCSTS is disrupted, the shape of the bacterial cell is affected (Olson *et al.* 2012). The BfmSR system also confers resistance to carbapenems and chloramphenicol (CHL) (Geisinger *et al.* 2015). In addition to the above, BfmSR is responsible for increased resistance to complement-mediated bactericidal activity, as well as scaffolding of the outer membrane protein OmpA, thereby increasing the bacterium's survival *in vivo* (Russo *et al.* 2016).

1.6.1.6 Cross-talk within signal transduction networks

Recent investigations into non-specific cross-talk between cognate and non-cognate HK and RR proteins producing some interesting results as the interconnectedness of these systems comes to light. For example, reports have shown that *in vitro* non-cognate pairs interact via cross-talk as suggested above by the BfmSR system (Gaddy *et al.* 2009a, Russo *et al.* 2016). However, the cross-talk identified is at a low affinity compared with cognate pairs and possibly due to the

high concentration of cells *in vitro*. Another example of this phenomenon is found within *B. subtilis* where the PhoPR two-component system interacts with the YycFG two-component system in response to phosphate limitations within the bacterial cell, this reaction also occurs at a reduced level similar to what was identified of the BfmSR system (Howell *et al.* 2006). Moreover a study assessing non-cognate pares *in vitro* of *E. coli* identified 692 non-cognate parings of 27 truncated HK and 34 RR (Yamamoto *et al.* 2005). Bacteria have multiple TCSTS the above described research has demonstrated that these systems can be used in combination to form complex regulatory networks, increasing cellular responses to different conditions (Howell *et al.* 2006).

1.6.1.7 TCSTS are potential drug targets

The need to find an alternative to antibiotic treatment is paramount in the clinical environment. Pathogenic bacteria continue to increase their resistance to antibiotics and have become a considerable burden in hospitals. Because TCSTS are not found in higher eukaryotic organisms, they are good candidates for therapeutic targets without the risk of harming patients. As described, a number of TCSTS have been associated with virulence traits; these systems are the new targets for anti-microbial research (Gross *et al.* 2012). Thus, inhibitors of TCSTS that control virulence factors could reduce virulence mechanisms without killing the bacteria, allowing the host's immune response to eradicate the infection.

Sites of TCSTS that share homology between systems are possible drug targets. Developing an inhibitory compound to disable multiple strains is an important step towards controlling MDR pathogenic bacteria (Gotoh *et al.* 2010). The sites of potential inhibition include the autophosphorylation signal and the autophosphorylation of the HK, which would inhibit interactions between the HK and the cognate RR protein, disrupt the dephosphorylation of the HK and prevent binding of the RR protein to the gene promoter or other downstream protein-to-protein actions (Krueger *et al.* 2012, Draughn *et al.* 2018).

While traditional antibiotics commonly inhibit proteins that perform specific functions (e.g. inhibiting cell wall synthesis, DNA gyrase, protein synthesis and possibly RNA synthesis), TCSTS inhibitors would target the upstream regulatory controls and not the downstream products (Gotoh *et al.* 2010). The BfmSR TCSTS is

being investigated by *in silico* ligand binding analysis assessing potential drug targets (Russo *et al.* 2016). This could enable the development of drugs that will work against MDR pathogens such as *S. aureus*, *P. aeruginosa* and *A. baumannii* (Krueger *et al.* 2012).

Several reports have identified the potential of these new drug targets, including Roychoudhury *et al* (1993), who found an inhibitor that has the capacity to reduce the production of the exopolysaccharide alginate from *P. aeruginosa* (Roychoudhury *et al.* 1993). This finding could potentially benefit cystic fibrosis patients through disruption of the phosphorylation or dephosphorylation of AlgR2 and the DNA-binding activity of AlgR1. Gotoh *et al* (2010) identified several inhibitors for use against TCSTS, three of which are described here. The first inhibitor is walkmycin B (also known as walrycin), which acts on a separate function of the well-characterised TCSTS WalKR that is found in a number of Gram-positive opportunistic pathogens (Gotoh *et al.* 2010). Walkmycin B blocks the autophosphorylation of the HK and interacts with the RR to inhibit the phosphor transfer from the HK. Specifically, the cell wall metabolism of methicillin-resistant *S. aureus* is affected and reduces the virulence of this pathogenic bacterium (Gotoh *et al.* 2010). The second inhibitor is LED209 which can inhibit QseC, the HK of a system in enterohemorrhagic *E. coli*. This inhibitor stops the HK from receiving external activation signals and therefore inhibits autophosphorylation of the system and suppresses the pathogenicity of the strain (Gotoh *et al.* 2010). The third inhibitor is apolipoprotein B, a large protein found in serum of the host that is used by the innate immune defence system. Apolipoprotein B works against the virulent TCSTS AgrCA by sequestering autoinducing cyclic thiolactone peptides that activate the virulence traits via AgrCA within methicillin-resistant *S. aureus* (Gotoh *et al.* 2010). These newly identified compounds could be used in the clinical setting to reduce the effects of these pathogenic bacteria without harming the host or increasing antibiotic resistance.

1.7 cAMP regulation

Signal transduction pathways are used to sense the external environment and react to it; this reaction can be varied and may include the responses discussed above but may also be in the form of chemotaxis, cell differentiation and apoptosis. TCSTS are not the sole mechanisms whereby bacteria can respond; many environmental

signalling pathways use secondary molecules to relay information from receptors to effectors within the cell (Figure 1.4). Many molecules are used in these systems, including cyclic nucleotides, guanosine pentaphosphate and Ca^{2+} (McDonough *et al.* 2012). One of the major signalling molecules, and the best studied, is cAMP. cAMP is synthesised by the enzyme adenylyl cyclase (AC) through biosynthesis of ATP to cAMP (Figure 1.4). To maintain homeostasis within the cell, cAMP levels are controlled by degradation and this occurs via phosphodiesterase (PDE). CpdA, which hydrolyses cAMP leaving AMP (McDonough *et al.* 2012). Thus, regulation of the concentration of cAMP is largely a result of controlling the CpdA enzyme.

The best-described cAMP signalling system is within *E. coli* and controls metabolic responses (Fuchs *et al.* 2010b). The CRP complex regulates more than 100 genes and operons (Fuchs *et al.* 2010b, McDonough *et al.* 2012). Within *Pseudomonas*, cAMP and the virulence factor regulator (Vfr) complex, which shares homology to the CRP complex, have been described as being able to coordinate intracellular processes, control virulence gene expression, relay extracellular signals from the environment and manipulate the host's immunity by increasing cAMP levels during infection (McDonough *et al.* 2012). The regulatory cascade involved is very complex and has not been fully elucidated. Gene expression altered via cAMP can be varied and may include virulence genes such as those that affect biofilm formation, Type III secretion and carbon metabolism (McDonough *et al.* 2012).

1.8 Survival in various media

To cause a disease state, pathogenic bacteria have to persist in a variety of different media, this can include blood, lung fluid and sputum; causing disease like sepsis and pneumonia. A key factor to survival in these niches is the ability to acquire iron from the surrounding environment. Iron is vital in many cellular processes including metabolism, cell-to-cell signalling and biofilm formation (Hazan *et al.* 2010). However, soluble iron (Fe^{2+} and Fe^{3+}) has a limited presence in many environments. Therefore, the ability to acquire Fe^{2+} and Fe^{3+} is a critical mechanism for *A. baumannii* to persist within the host and on abiotic surfaces. Interestingly *A. baumannii* has the ability to grow under iron-limiting conditions

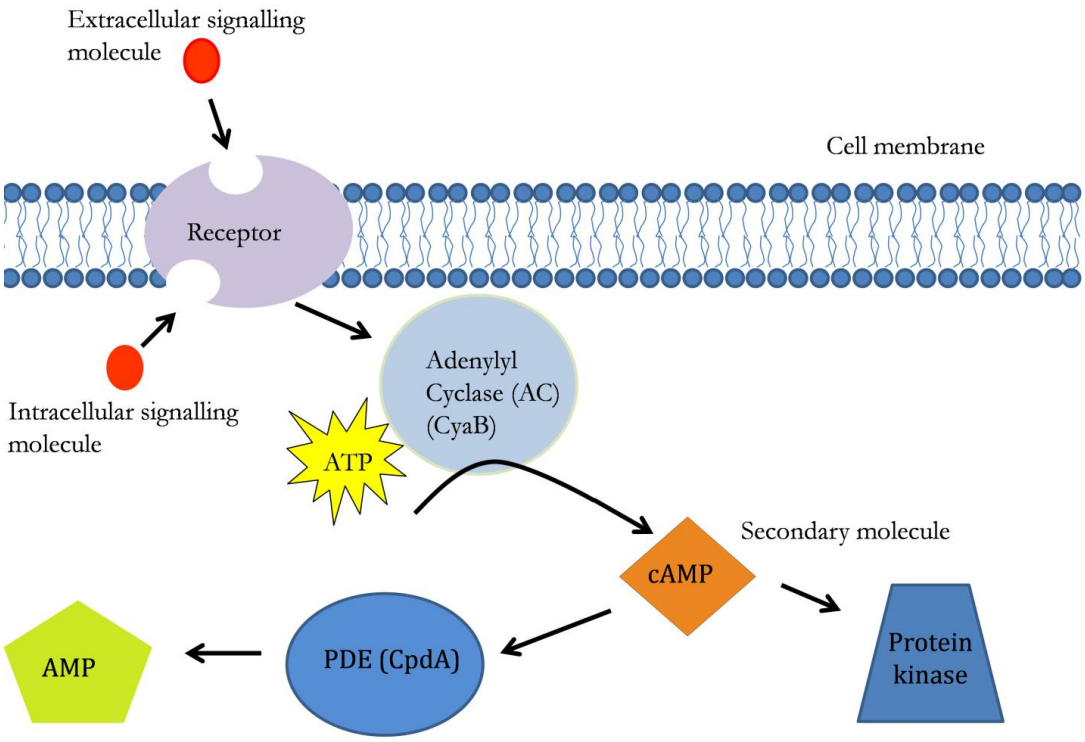

Figure 1.4: cAMP second signalling molecule pathway

An extracellular or intracellular signalling molecule (red circle) is received by the cAMP receptor protein (CRP complex) (purple circle). This activates synthesis of cAMP (orange diamond) from ATP (yellow star) by AC (*cyaB*) (light blue circle). The produced cAMP acts on protein kinases and other effector proteins altering transcriptional expression. The cAMP is degraded by PDE *cpdA* (blue oval), maintaining homeostasis of this molecule within the cell.

(Dorsey *et al.* 2003a). Siderophore-mediated iron acquisition is utilised by the bacterial cell, where siderophore molecules are synthesised and secreted into the extracellular space acquiring iron. Once siderophores bind to iron they are taken up by surface receptors. The TonB-ExbB-ExbD system mediates the up-take of iron-bound siderophores (Braun 2003).

Three types of iron acquisition have been previously described in *A. baumannii*; ferrous iron or heme receptor proteins, siderophore-mediated up-take via synthesis of acinetobactin, and hemophore utilisation mechanisms (Antunes *et al.* 2011). A previous study identified a variety of gene clusters in *A. baumannii* including two siderophore clusters, the acinetobactin cluster, Fe-receptors, fumarase C and ExbB/D to be significantly up-regulated in iron starvation conditions (Eijkelkamp *et al.* 2011a). Another important iron regulatory mechanism is the ferric up-take regulator (FUR), which controls iron homeostasis. In the presence of iron the FUR protein dimerises and binds to the FUR box. This leads to repression of iron acquisition genes, however in the absence of iron FUR dissociates from the binding site which allows gene expression (Stojiljkovic *et al.* 1994). In addition to the above, the BLUF-type photoreceptor BlsA protein has recently been identified as antagonising FUR under temperature, no light and blue light conditions (Tuttobene *et al.* 2018). This enabled growth under iron deficiency conditions in the dark.

1.9 Evading the immune system

Evading the immune system is an essential process for bacteria to cause an infection. One such immune defence system is complement killing, by which complement proteins, found in the serum part of the blood, through an intricate step-by-step process create a pore in invading bacterial cell membrane, releasing the cellular contents and causing the cell to lyse (Kim *et al.* 2009, Li *et al.* 2015, Alves *et al.* 2017). The ability to resist this active process is associated with a number of factors including extracellular polysaccharides (Sarkar *et al.* 2014) and bacterial lipopolysaccharides, namely the lipid A core and the repeat O antigen subunits with alterations in the sugar subunits including the capsule proteins and outer membrane proteins like OmpA (Kim *et al.* 2009, Shashkov *et al.* 2015, Wessels 2016, Harding *et al.* 2018). The proteins help to circumvent complement activity by inhibiting correct attachment to the bacterial cell.

Another important immune defense system is phagocytosis, this is the destruction of bacteria and other foreign particles that invade host systems (Baquir *et al.* 2012, John *et al.* 2012, Weiss *et al.* 2015). Phagocytosis is accomplished by neutrophil and macrophage cells that engulf the foreign bacteria and produce an oxidative burst to kill bacteria within itself (Garcia-Patino *et al.* 2017). Neutrophils and macrophages are recruited to the site of infection by chemoattractant proteins including chemokines and cytokines, commonly triggered by the Toll-like receptor (van Faassen *et al.* 2007, Garcia-Patino *et al.* 2017). The ability to withstand the oxidative stresses produced within the phagocytotic cells enables bacteria to not only survive with the immune cells but replicate as well, causing severe diseases. Additionally, the ability of the bacteria to alter its cell surface protein structures, e.g. capsule and/or lipid A, can reduce the activation of the Toll-like receptor and therefore reduce the recruitment of phagocytosis cells leading to an increased bacterial load (Dikshit *et al.* 2018).

1.10 Focus of the study

A. baumannii is an established human pathogen that colonises hospitals and spreads endemically. *A. baumannii* can cause a range of infections with high morbidity and mortality rates of up to 75 % in some cases. Due to the severity of this pathogen, the focus of this study was to identify and investigate some of the virulence-related mechanisms used by the *A. baumannii* bacterium in causing these lethal disease states.

Biofilm formation is a known virulence trait. Biofilms can be formed in a range of niches including medical device implants and other equipment. However, little is known about pellicle formation which is a type of biofilm, or the specific molecules used to signal its development in *A. baumannii* strains. The biofilm and pellicle states are defined at different physiological phases: the biofilm is a collection of cells grown at the surface-liquid interface, whereas the pellicle grows at the air-liquid interface. As the pellicle enhances the persistence of *A. baumannii* in different settings, investigation of the specific genes involved in its formation is essential in furthering our understanding and to develop strategies to combat this pathogen. The aim of chapter two was to identify the genes involved in the formation of the pellicle. As such the pellicle forming *A. baumannii* strain 17978hm was mutated using a

transposon insertion element, to identify derivatives that could no longer form a pellicle at the air-liquid interface. Comparative HiSeq techniques were used to identify the genes contributing to the regulation, and therefore production, of the pellicle in the identified pellicle deficient *cpdA*::Tn mutant strain.

TCSTS are known to regulate a variety of virulence factors contributing to the ability of *A baumannii* to cause a disease state. These factors contribute to increased antibiotic resistance and the ability to withstand the host immune response. TCSTS in *A. baumannii* represent a relatively new field of research with limited complete pictures of TCSTS and the multiple regulation abilities correlated specifically to virulence potential. Chapters three and four aimed to examine a novel TCSTS and assess its relationship with virulence traits identified in the *A. baumannii* 04117201 strain. This investigation identified the novel TCSTS named here as StkRS in the clinical *A. baumannii* strain 04117201. After deletion of the RR in the StkRS system, the Δ*stkR* mutant strain was analysed together with its progenitor in several virulence assays, including a mouse model assessing bacterial load in the lungs, blood and spleen. Comprehensive genomic transcriptomic analysis of the 04117201 Δ*stkR* mutant and WT strains aided in identifying a plethora of genes that play a role in *A. baumannii* virulence. Investigation of the mouse immune response to the *A. baumannii* infection using an RT^2 profiler array, highlighted the importance of the StkRS system in virulence.

Overall, the wide range of molecular techniques and experimental approaches used in this study generated a wealth of knowledge about *A. baumannii* in relation to virulence capabilities. This project fills the gap of knowledge related to pellicle formation ability in the *A. baumannii* population, substantially connecting three phenotypes; the pellicle, cell surface hydrophobicity and motility through *in vitro* and genetic investigation. Additionally, an assessment of *A. baumannii* 04117201 and the Δ*stkR* mutant strain grown in a wide selection of media generated data indicating the influence of different growth conditions. These data also identified many possible regulatory pathways that were affected by the previously undescribed TCSTS StkRS. A significant increase in virulence potential of the Δ*stkR* mutant compared to its *A. baumannii* 04117201 progenitor, highlighted the importance of the StkRS system. Moreover the ability of *A. baumannii* 04117201 and the Δ*stkR*

mutant to alter the innate immune response by decreasing the expression of a Toll-like receptor, cytokine and chemokine production is a significant finding.

CHAPTER 2 Identification of genes essential for pellicle formation in *A. baumannii*

Declaration for thesis chapter two

Declaration by candidate

In chapter two the nature and extent of my contribution to the work was the following:

Nature of contribution	**Extent of contribution**
Experimental design, performance of experiments, writing, editing and revision of manuscript	75 %

The following co-authors contributed to the work.

Name	**Nature of contribution**	**Extent of contribution**
Bart Eijkelkamp	Experimental design, editing and revision of manuscript	5 %
Uwe Stroeher	Experimental design, editing and revision of manuscript	10 %
Melissa Brown	Experimental design, editing and revision of manuscript	10 %

The undersigned hereby certify the above declaration correctly reflects the nature and extent of the candidates and co-authors contribution to this work

Candidate's Date

Signature 2019

Supervisor's Date

Signature 2019

2.1 Preface

This chapter is heavily based on the article published in BMC Microbiology as **Giles, S. K., Stroeher, U. H., Eijkelkamp, B. A. and Brown, M. H.** (2015) Identification of genes essential for pellicle formation in *Acinetobacter baumannii*. *BMC Microbiology* **15**:116. The printed version of this article appears in Appendix F. In addition to the above article this work also contributed to a protocol paper, whereby a new method for analysing cAMP within bacterial cells was developed using the Cyclic Nucleotide XP Enzymatic Immunoassay Kit. The specific optimisation and development of this method is not described in this thesis; however the article is published in Bio-protocol as **Giles, S. K., Stroeher, U H. and Brown, M. H**. (2016) Measurement of intracellular cAMP levels using the cyclic nucleotide XP enzymatic immunoassay kit in bacteria. *Bio-protocol* **6**: e1792. http://www.bio-protocol.org/e1792. The printed version of this article appears in Appendix G.

2.2 Abstract

A. baumannii is an opportunistic pathogen which has the ability to persist in the clinical environment, causing acute and chronic infections. A possible mechanism contributing to survival of *A. baumannii* is its ability to form a biofilm-like structure at the air-liquid interface, known as a pellicle. This study aimed to identify and characterise the molecular mechanisms required for pellicle formation in *A. baumannii* and to assess a broad range of clinical *A. baumannii* strains for their ability to form these multicellular structures.

Random transposon mutagenesis was undertaken on a previously identified hyper-motile variant of *A. baumannii*, 17978hm. In total three genes critical for pellicle formation were identified; *cpdA*, a PDE required for degradation of cAMP, and A1S_0112 and A1S_0115 which are involved in the production of a secondary metabolite. While motility of the 17978hmA1S_0112::Tn (A1S_0112::Tn) and 17978hmA1S_0115::Tn (A1S_0115::Tn) mutant strains was abolished, the *cpdA*::Tn mutant strain displayed a minor alteration in its motility pattern. Determination of cAMP levels in the *cpdA*::Tn strain revealed an approximate 24-fold increase in cellular cAMP, confirming the role CpdA plays in catabolising this secondary messenger molecule. Interestingly, transcriptional analysis of the *cpdA*::Tn strain showed significant down-regulation of the operon harbouring the A1S_0112 and

A1S_0115 genes, revealing a link between these three genes and pellicle formation. Examination of our collection of 54 clinical *A. baumannii* strains revealed that eight formed a measurable pellicle; all of these strains were motile.

This study shows that pellicle formation is a rare trait in *A. baumannii* and that a limited number of genes are essential for expression of this phenotype. Additionally, an association between pellicle formation and motility was identified. The level of the signalling molecule cAMP was found to be controlled, in part, by the *cpdA* gene product, in addition to playing a critical role in pellicle formation, cellular hydrophobicity and motility. Furthermore, cAMP was identified as a novel regulator of the operon A1S_0112-0118.

2.3 Introduction

A. baumannii is an opportunistic Gram-negative human pathogen that causes severe nosocomial infections primarily in immune-compromised patients; disease states include pneumonia, meningitis and bacteraemia (Bergogne-Bérézin 1997, Dijkshoorn *et al.* 2007, McQueary *et al.* 2011, Roca *et al.* 2012, Shin *et al.* 2012). The bacterium can be found in ICU and is frequently isolated from medical devices (Neely *et al.* 1999, Donlan *et al.* 2002, Peleg *et al.* 2008, Ramirez *et al.* 2010). The capacity to survive in these environments is possibly due to the ability of this organism to survive desiccation and resist a broad spectrum of antibiotics and disinfectants. As a result, *A. baumannii* has entrenched itself in the clinical environment (Karageorgopoulos *et al.* 2008, Strassle *et al.* 2012, Karaiskos *et al.* 2013).

Given the occurrence of *A. baumannii* in ICU and its high level of intrinsic and adapted resistance, there is increased pressure to identify novel drug targets. Therefore, understanding the molecular mechanisms contributing to virulence in *A. baumannii* is essential. Similar to numerous other organisms, *A. baumannii* has the ability to grow a multicellular structure known as a biofilm (Longo *et al.* 2014) of which the pellicle is a specialised form. The pellicle is localised to the interface between air and liquid, and is a structure of connected cells surrounded by a matrix of extracellular polymeric substance (Moonmangmee *et al.* 2002, Yamamoto *et al.* 2012). The formation of a pellicle allows aerobic bacteria to have access in a stagnant environment to high levels of oxygen and nutrients (Yuan *et al.* 2013). The

pellicle can increase bacterial survival under antibiotic pressure as well as contribute to longer than usual persistence in a hostile environment, such as under drying conditions (Kanchanarach *et al.* 2010, Espinal *et al.* 2012, Sambandan *et al.* 2013).

There are numerous molecular mechanisms potentially involved in pellicle formation by *A. baumannii*. One such mechanism is the *csuA/BABCDE* pilus chaperone-usher assembly system which is responsible for the production of pili and is essential in the formation of a biofilm on solid surfaces (Donlan *et al.* 2002, Tomaras *et al.* 2003, McQueary *et al.* 2011). In a study on *B. subtilis*, 288 regulatory and potential regulatory genes were associated with pellicle formation (Kobayashi 2007). Recent analyses of *A. baumannii* in the pellicle state have revealed alterations in the expression of at least 52 membrane proteins (32 up-regulated and 20 down-regulated) (Martí *et al.* 2011a, Nait Chabane *et al.* 2014). These 52 proteins were found to be involved in; iron up-take systems, lipid and carbohydrate transport, cellular metabolism, starvation, porins and pili.

As bacteria encounter a wide range of environmental conditions, there is a requirement to respond to these changes, such as changing from a planktonic state to living within a biofilm and/or pellicle; this can involve deployment of a number of signalling molecules (de Kievit 2009, Lazar 2011). cAMP is a ubiquitous signalling molecule used in conjunction with a variety of regulators for modulating gene expression in both prokaryotes and eukaryotes (Shemarova 2009, Kalivoda *et al.* 2013). In bacteria, it has been found to alter multiple virulence characteristics. For example, in *Vibrio cholerae* cAMP has been implicated in the regulation of the cholera toxin, toxin co-regulated pilus and other pathogenic factors (Skorupski *et al.* 1997). In *Serratia marcescens* the importance of the CRP complex in the formation of biofilm has been established (Kalivoda *et al.* 2013). In this case the type I fimbriae-dependant biofilm is tightly regulated and a deletion in the PDE gene was found to increase cAMP within the bacteria cell and consequently decrease biofilm formation. Conversely, when increased copies of the PDE gene are introduced into the bacterial cell, the bacteria enter into what is described as “hyper biofilm” characteristic (Kalivoda *et al.* 2013). Similarly in *P. aeruginosa*, cAMP has been identified as a key component in biofilm formation, where increased levels of cAMP can inhibit adherence capabilities (Ono *et al.* 2014).

Furthermore, in this organism cAMP functions as a co-factor of the Vfr, where the cAMP-Vfr complex regulates type III secretion systems involved in exporting toxins and other compounds (Yahr *et al.* 1998, Wolfgang *et al.* 2003, Jimenez *et al.* 2012). This complex also regulates virulence factors such as type IV pili, the *las* quorum-sensing system and exotoxin A (Fuchs *et al.* 2010a, Jimenez *et al.* 2012). Although a *vfr*-like gene is present in the *A. baumannii* genome, its role in regulation of virulence factors and interaction with cAMP has not been reported.

The proteomic analyses by Marti *et al*. (2011) and Nait Chabane *et al*. (2014) suggested that pellicle formation in *A. baumannii* is not the result of a single gene or gene products (Martí *et al.* 2011a, Nait Chabane *et al.* 2014). Instead, it is likely that pellicle formation is multifactorial, requiring surface-exposed molecular structures and an adequate level of transcriptional regulation. The aim of this study is to provide insight into the genetic elements that contribute to the ability of *A. baumannii* to migrate to a surface and form a pellicle as well as to assess the prevalence of pellicle formation in a number of clinically-relevant *A. baumannii* strains.

2.4 Materials and Methods

2.4.1 Bacterial strains

The 54 clinical *A. baumannii* bacterial strains used in this study and the hyper-motile derivative of *A. baumannii* 17978hm have been described previously (Eijkelkamp *et al.* 2011a, Eijkelkamp *et al.* 2011b). All *A. baumannii* strains were cultured on Luria-Bertani (LB) media containing 1 % agar overnight at 37°C, and single colonies transferred to LB broth for subsequent use in assays, unless otherwise stated. For maintenance, conjugation, cloning and replicating plasmids, *E. coli* DH5α, SM10 or JM109 cells were used (Hanahan 1983, Simon *et al.* 1983, Yanisch-Perron *et al.* 1985).

A. baumannii ATCC 17978 was one of the first bacteria to be sequenced in 2007 (Smith *et al.* 2007); however, due to limitations in the sequencing technique and annotation, the initial sequence contained several errors (Weber *et al.* 2015b). The old accession number is CP000521 (Smith *et al.* 2007), the new accession number is CP012004 and the plasmid number is CP012005 (Weber *et al.* 2015b).

2.4.2 Assessment of pellicle formation

The pellicle formation assay was adapted from a previously described protocol (Martí *et al.* 2011b). In brief, overnight bacterial cultures were diluted 1:100 in 5 mL of LB broth and grown in polypropylene or glass tubes for 72 hours at 25°C without shaking in the dark (Mussi *et al.* 2010, Golic *et al.* 2013). Quantitative measurement of the pellicle material was assessed by the addition of 1 mL of ethanol into the tube underneath the pellicle material. The floating pellicle was then removed and resuspended in phosphate buffered saline (PBS) and the OD_{600} measured using a spectrophotometer (Beckman DU 640). Quantitative data were collected from at least three experiments on three different days.

2.4.3 Motility assays

Motility was assessed by migration on semi-solid surfaces using media containing 0.25 % agar as described previously (Eijkelkamp *et al.* 2011b). Briefly, an overnight colony was collected using a sterile loop and used to inoculate the centre of LB media containing 0.25 % agar. The plate was then incubated overnight at 37°C. Strains were considered motile if any movement of growth from the original inoculation site was observed.

2.4.4 Eukaryotic cell adherence assays

A. baumannii cell adherence to A549 (human type 2 pneumocytes) was investigated as previously described (Eijkelkamp *et al.* 2011b). In brief, cell lines were grown in Dulbecco's Modified Eagle media (Invitrogen, Australia) supplemented with 10 % foetal bovine serum (Bovogen, Australia). Washed A549 monolayers in 24-well tissue culture plates were infected with bacterial inoculums containing ~$1x10^7$ colony forming units (CFU). After incubation at 37°C for 4 hours the culture media was removed and the monolayers washed with PBS. The cell monolayers were detached from the plate using a treatment of 100 µL of 0.25 % trypsin in PBS. Eukaryotic cells were subsequently lysed by the addition of 400 µL 0.025 % Triton X-100 and serial 10-fold dilutions were spread plated on LB agar to determine the number of CFU of adherent bacteria per well. The collated data for the adherence assay were obtained from at least three independent experiments and represent the data points from each experiment in quadruplicate wells.

2.4.5 Cell surface hydrophobicity tests

Cell surface hydrophobicity was examined as described previously (Rosenberg *et al.* 1983). In brief, overnight cultures were diluted in LB broth and incubated at 37°C for 2 hours. Potassium urea magnesium (PUM) buffer was used to wash the cells twice, before incubation at 30°C for 20 minutes. The cell suspension was adjusted to OD_{600} = 0.25 in the same buffer in glass vials before the addition of xylene (3 mL). The sample was vortexed for 20 seconds and the aqueous phase transferred to a 1.5 mL tube. The OD_{600} of the cell suspension was determined before ($OD_{initial}$) and after (OD_{final}) the addition of xylene. The hydrophobicity index (HI), expressed as a percentage, is calculated as (OD_{inital} − OD_{final}/ $OD_{initial}$)*100. Quantitative data were collected from at least three experiments from three different days.

2.4.6 Transposon mutagenesis

Transposon mutagenesis was undertaken using a modified mini Tn*10* transposon (mini::Tn*10*:*gfp*:*kan*) carried on the plasmid pLOF (Matthysse *et al.* 1996). The pLOFmini::Tn*10*:*gfp*:*kan* plasmid was transformed into the donor *E. coli* SM10 strain and mated with the *A. baumannii* 17978hm recipient at a 1:10 ratio for 4 hours at 37°C on LB agar media. Exconjugates were resuspended in 5 mL of LB broth and plated onto selective media containing 50 μg/mL kanamycin (KAN) and 25 μg/mL CHL to select for transposition events and counter-select against the *E. coli* SM10 donor strain. Approximately, 4000 exconjugates were individually picked using sterile toothpicks to inoculate 200 μL of LB broth in 96 well microtitre plates. The cells were grown at 25°C in the dark for 72 hours and assessed visually for pellicle loss.

2.4.7 Identification of pLOFmini::Tn*10*:*gfp*:*kan* insertion in the chromosome

Chromosomal DNA isolated from *A. baumannii* 17978hm containing the pLOFmini::Tn*10*:*gfp*:*kan* was digested with restriction endonucleases *Xba*I and *Sac*II for 4 hours at 37°C. Digested products were cloned into pBluescript SK II (Agilent technologies, CA, USA) and clones were confirmed by sequencing (Australian Genome Research Facility (AGRF), Adelaide, South Australia). The insertion site of the transposons in the chromosome was determined by Sanger sequencing using an oligonucleotide designed to read out of the end of the transposon (Table 2.1).

2.4.8 Complementation of transposon insertions

For genetic complementation of the non-pellicle forming *A. baumannii* mutants, the genes corresponding to A1S_0112, A1S_0115 and *cpdA* were amplified using polymerase chain reaction (PCR) and cloned into the shuttle vector pWH1266, transformed into *E. coli* DH5α cells, DNA extracted and sequenced. Purified plasmids were transformed via electroporation using a MicroPulser (Bio-Rad, CA, USA) at 2.5 kilovolts, 200 ohms and 25 microfarads into their respective *A. baumannii* transposon insertion strains (Hunger *et al.* 1990). PCR was achieved with VELOCITY^{TM} DNA polymerase (Bioline, Vic, Australia) and the oligonucleotides (Table 2.1) using the following PCR protocols. For amplification of *cpdA*, cycling conditions were 2 minutes at 94°C, 30 cycles of 45 seconds at 94°C, 45 seconds at 55°C, and 90 seconds at 72°C, followed by a final extension of 4 minutes at 72°C. Amplification of A1S_0112 used the same conditions with the exception of the annealing temperature which was increased to 60°C. For amplification of A1S_0115, the cycling conditions were 2 minutes at 94°C, 30 cycles of 90 seconds at 94°C, 90 seconds at 60°C, 4 minutes at 72°C and a final extension of 6 minutes at 72°C.

2.4.9 Measurement of intracellular cAMP levels

Assessment of cAMP levels within *A. baumannii* strains *cpdA*::Tn, *cpdA*::Tn(0249), *cpdA*::Tn(1266) and 17978hm was performed with cells grown to an OD_{600} of 0.7. Cells were pelleted by centrifugation at 4500 *g* for 15 minutes, resuspended in PBS and disrupted at 30,000 psi using the One Shot Head from the TS series bench top disruptor (Constant Systems, United Kingdom). The resulting cellular material in the cell lysis solution was clarified by centrifugation at 4500 *g* for 30 minutes and the supernatant removed and stored at −80°C until required. The concentration of cAMP was measured using the Cyclic Nucleotide XP Enzymatic Immunoassay kit (Cell Signalling Technology, MA, USA) according to the manufacturer's instructions.

Table 2.1: Oligonucleotides used in chapter two

Name /Target	Forward 5'–3'	Reverse 5'–3'
A1S_0112comp	GAGAGAATTCGCAACTTTGGAATCCCGCGCA	GAGAGGATCCTTGCTCCAGACGAGCAGCAG
A1S_0115comp	GAGAGAATTCTTCTGAGTTGCAGCAGGGAG	GAGAGGATCCAACCTGCATCATTGGCTGGG
A1S_0249	GAGAGGATCCCTGTTCGATGAAAATCACCC	GAGAGGATCCCTTTAGGGCTAATAACCTG
Tn*10*- F2	CGGCCGCACGCGTATTCAGG	
A1S_r01 (16SrRNA)	CAGCTCGTGTCGTGAGATGT	CGTAAGGGCCATGATGACTT
A1S_2501 (GapDH)	CAACACTGGTAAATGGCGTG	ACAACGTTTTTCATTTCGCC
A1S_0109	TCTGGTGAGCAGGGATAGG	TGTCGTGGCTCAAGACAGAG
A1S_0112	ACGCCAGTCTGGTGGTATTC	AGGTTCGAACAGCAATACGG
A1S_0115	GCGGTCAAAATCATTATGTG	GCTCTGCTGCTTATCGGCAT
A1S_0118	GGACTCTCTATTATCGGACG	CAGATAAATCGCTCAAGCTGC

In brief, 50 µL of horseradish peroxidase-linked cAMP solution and 50 µL of sample were added to the supplied 96-well tray, which was then covered and incubated at room temperature for 3 hours on a horizontal orbital plate shaker. The contents of the plate were discarded and the plate was washed 4 times with 200 µL/well of wash buffer. Next, 100 µL of 3,3',5,5'-tetramethylbenzidinesubstrate solution was added and incubated for 30 minutes at room temperature, after which 100 µL of stop solution was added and the absorbance measured at 450 nm. Using the inverse for the standards derived from a standard curve and adjusted for the amount of total protein added, the amount of cAMP was calculated. Total protein concentrations were quantified using the Lowry protein assay (Bio-Rad, CA, USA) following the manufacturer's instructions.

2.4.10 Isolation of total cellular RNA

To measure transcriptional levels for either RT-PCR or HiSeq RNA transcriptome analysis conducted by SA Pathology (Central Adelaide local Health Network via an Illumina platform), cells were isolated and RNA extracted as below. Bacterial cells were harvested from either semi-solid media (0.25 % LB agar) for RT-PCR using pre-chilled PBS or harvested from Mueller-Hinton (MH) broth at OD_{600} of 0.6 for HiSeq. Bacterial cells were pelleted by centrifugation at 4500 *g* for 15 minutes and lysed in 1 mL TRIzol reagent (Life Technologies, Australia) and 200 µL of chloroform. Following phase separation, the aqueous layer was collected and RNA isolated using the Isolate RNA Mini Kit (Bioline, NSW, Australia) following the manufacturer's recommendations. Samples for RT-PCR were subsequently treated with DNaseI (Promega, WI, USA) for 30 minutes at 37°C and 1 µL of stop solution was added before a final incubation for 10 minutes at 65°C. Triplicate samples were pooled and sent to SA Pathology for Ribosomal RNA reduction using Epicentre Ribo-Zero kit and RNA library bar-coding was undertaken on RNA for HiSeq. Samples were run on the Illumina HiSeq platform (1X50 base pair (bp) single reads). These data are accessible through GEO Series accession number: GSE64935 (http://www.ncbi.nlm.nih.gov/geo/query/acc.cgi?acc=GSE64935).

2.4.11 Bioinformatic analysis

The quality of the cDNA reads obtained from the HiSeq procedure was checked using 'Fastqc' (http://www.bioinformatics.babraham.ac.uk/projects/fastqc/). Reads

were subsequently mapped to the reference genome using 'bowtie' aligner (http://bowtie-bio.sourceforge.net/index.shtml). For the reads obtained, approximately 95 % were mapped to the ATCC 17978 genome of which 78 % mapped to the coding regions. In order to determine changes in gene expression the number of reads obtained for each ORF was normalised using reads per kilobase (kb) of transcript per million reads mapped.

2.4.12 Quantitative reverse transcription PCR

M-MLV reverse-transcriptase (Promega) and random hexamers (GeneWorks, SA, Australia) were used to synthesise complementary deoxyribonucleic acid (cDNA) following the manufacturer's recommendations. Quantitative reverse transcription-PCR (qRT-PCR) was performed on three biological replicates using DyNAmo SYBR green qRT-PCR kits (ThermoScientific, Vic, Australia) in conjunction with a Rotor-Gene RG-3000 (Corbett Life Science, Australia). A typical qRT-PCR run was as follows: 1 minute at 95°C, 40 cycles of 10 seconds at 95°C, 15 seconds at 55°C and 20 seconds at 72°C (Brazma *et al.* 2001). Transcriptional differences were calculated using the $\Delta\Delta C_T$ method (Livak *et al.* 2001). The 16S rRNA (A1S_r01) and *gapDH* (A1S_2501) transcription levels were used as references.

2.4.13 Measurement of intracellular cAMP levels using the Cyclic Nucleotide XP Enzymatic Immunoassay Kit

Assessment of cAMP levels within a bacterial cell had not previously been reported upon using this intracellular kit. As such, development and optimisation using the cyclic nucleotide XP enzymatic immunoassay kit allowed for the adequate and quantitative analysis of cAMP levels with bacteria cells. This method was then published in Bio-protocols see (Appendix G) "**Giles, S. K., Stroeher, U. H. and Brown, M. H.** (2016) Measurement of intracellular cAMP levels using the cyclic nucleotide XP enzymatic immunoassay kit in bacteria. *Bio-protocol* **6**: e1792". http://www.bio-protocol.org/e1792.

2.5 Results and Discussion

2.5.1 Pellicle formation is a rare trait in clinical *A. baumannii* strains

In this study, the pellicle is defined as a robust layer of connected cells covering the surface of a liquid. To assess the prevalence of pellicle formation, our collection of clinical *A. baumannii* strains (Eijkelkamp *et al.* 2011b) was screened for this phenotype. Pellicle formation was assessed using glass and polypropylene tubes, as these materials are used for a number of implements within the hospital environment and have different surface properties, which may influence the initial attachment and formation of a pellicle. Preliminary assessment of pellicle biomass was conducted at growth temperatures of 25°C and 37°C (data not shown), which revealed that pellicle growth predominantly occurred at 25°C; these results coincided with Marti *et al*. (2011), (Martí *et al.* 2011b)as such all subsequent analyses were performed at 25°C (Martí *et al.* 2011b). Of the 54 clinical strains tested (see Appendix A) only eight formed a robust pellicle, suggesting that this is not a ubiquitous phenotype (Table 2.2). These eight strains produced varying amounts of total pellicle biomass when comparing glass and polypropylene strata (Table 2.2). Pellicle formation was categorised into three groups dependent on the amount of pellicle material measured at OD_{600} where; “small pellicle” was considered >0.19, “moderate pellicle” was considered >0.20 and <0.50 and a “well-developed pellicle” was >0.51. In glass tubes, strains ATCC 17978, 17978hm, WM98c, 04145027 and AYE produced a well-developed pellicle, while, AB0057, 11986752 and 2320495 produced a moderate to small pellicle. Analysis in polypropylene tubes showed that only two strains, 17978hm and 04145027, produced a strong pellicle, while four strains, ATCC 17978, 11986752, 2320495 and WM98c, produced a moderate to small pellicle. Both AYE and AB0057 formed a pellicle in glass tubes, but failed to form a measurable pellicle in polypropylene tubes. Hence, the ability to form a pellicle was not conserved across glass and polypropylene surfaces.

These observed differences could be due to a number of factors related to the specific adherence strategies of each strain, such as the production of pili and other surface-exposed macromolecules. A number of strains, 6772166, 6856775, PW01c, 6877889 and 6870155, produced a weak surface film that could not be extracted

Table 2.2: Pellicle formation in glass and polypropylene, cell hydrophobicity, motility status and isolation site

***A. baumannii* isolate**	**Glass (OD_{600})[a]**	**Polypropylene (OD_{600})[a]**	**Hydrophobicity (%)**	**Motility**	**Isolation site**
Pellicle forming *A. baumannii* strains					
ATCC 17978	0.65±0.16	0.44±0.08	32±0.25	+	Meningitis
17978hm	1.03±0.01	0.94±0.02	42±0.19	+	Meningitis
11986752	0.13±0.01	0.17±0.04	98±0.01	+	Pus
2320495	0.35±0.08	0.28±0.06	98±0.03	+	Pus
WM98c	1.01±0.02	0.37±0.08	94±0.10	+	Unknown
04145027	0.62±0.00	0.79±0.04	100±0.00	+	Vaginal
AYE	0.65±0.11	Not detected	92±0.07	+	Urinary

Table 2.2: Continued

A. baumannii isolate	Glass (OD_{600})[a]	Polypropylene (OD_{600})[a]	Hydrophobicity (%)	Motility	Isolation site
AB0057	0.47±0.06	Not detected	0	+	Blood
Surface forming *A. baumannii* strains					
6772166	BD	BD	0	+	Pus
685775	BD	BD	0	+	Sputum
PW01c	BD	BD	0	+	Unknown
6877889	BD	BD	9±0.09	+	Sputum
6870155	BD	BD	5±0.07	+	Sputum

[a] BD, below detection

using our protocol, attempts to do so by other means such as draining the planktonic growth resulted in destruction of this weak surface film. Structures such as pilin-like proteins and exopolysaccharides have been shown to be present in pellicles (Nait Chabane *et al.* 2014) and it is possible that these structures are expressed at a reduced level in these strains resulting in only a weak surface film. Interestingly, all pellicle forming strains and those that formed a weak surface film have been shown to be motile (Eijkelkamp *et al.* 2011b). This finding highlights the possibility that the molecular mechanisms involved in motility and pellicle formation are linked.

2.5.2 Hydrophobicity across the clinical *A. baumannii* strains is not directly linked to pellicle formation ability

In a number of bacterial species, including *A. baumannii*, a positive association between cell surface hydrophobicity, biofilm formation and adherence capabilities has been reported (Costa *et al.* 2006, Furuhata *et al.* 2009, Pour *et al.* 2011). Evaluation of our collection of 54 clinical *A. baumannii* strains for cell surface hydrophobicity identified major differences (Figure 2.1). Using the divisions of the HI as established by Pour *et al*. (2011) (Pour *et al.* 2011), 42 of the strains displayed a hydrophilic character, nine were found to have a strong hydrophobic character and three showed an intermediate level of cell surface hydrophobicity. Of the eight strains that formed a pellicle (Table 2.2), five (11986752, 2320495, WM98c, 04145027 and AYE) were found to have a strong HI of >70 %, two (ATCC 17978 and 17978hm) showed an intermediate hydrophobic character and AB0057 was found to be hydrophilic.

There are a number of proteins embedded within the outer membrane of Gram-negative bacteria that have a variety of functions including pili for adherence and possibly pellicle formation as well as other physical mechanisms. Surface proteins can alter the surface chemistry of a cell and affect the surface hydrophobicity (Kouidhi *et al.* 2010, Chiku *et al.* 2013). The aforementioned results suggest a high level of correlation between the ability to form an extractable pellicle and an increase in cell surface hydrophobicity. The level of hydrophobicity may have an influence on what surface and how strongly bacteria interact due to a variety of proteins on the cell surface (Delcour 2009, Raut *et al.* 2010). Interestingly, the strains identified as producing a weak surface film all show a hydrophilic nature.

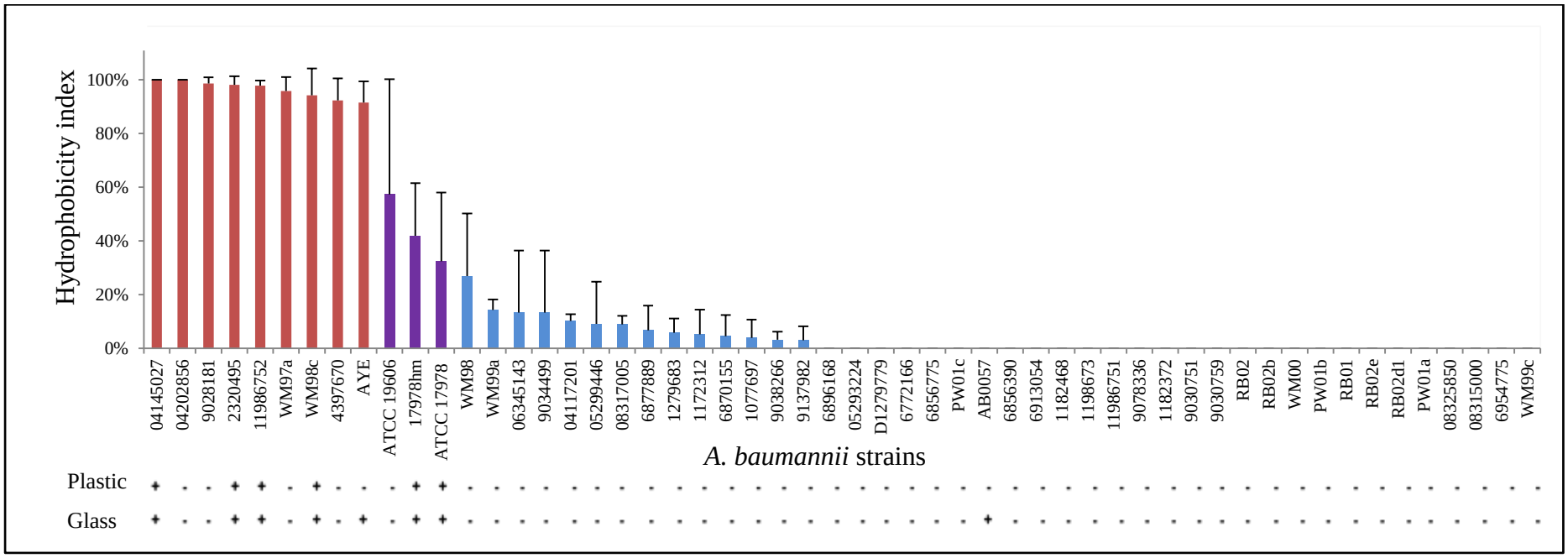

Figure 2.1: Hydrophobicity and pellicle-forming ability of *A. baumannii* clinical strains

Cell surface hydrophobicity was assessed by the affiliation of the bacterial cell to xylene. Strains with a hydrophobic index above 70 % are shown in red, those above 30 % are in purple and those below 30 % are in blue. Those strains where no bar is visible are completely hydrophilic. The ability of each strain to form a pellicle in glass or polypropylene is shown as (+ or -) below the hydrophobic index. Bars indicate the standard deviation of three replicates.

2.5.3 A1S_0112, A1S_0115 and *cpdA* are essential genes for pellicle formation in *A. baumannii* 17978hm

To further investigate the pellicle phenotype, the previously characterised *A. baumannii* 17978hm strain was used (harbouring an insertion in *hns*) (Eijkelkamp *et al.* 2013), which has the ability to produce increased amounts of pellicle material compared to the ATCC 17978 parent strain. This strain was chosen as it allows good discrimination between the pellicle and non-pellicle phenotype allowing ready identification in large scale screen procedures. To identify genes associated with this potential virulence factor a transposon bank of random mutants was constructed in the 17978hm strain using the plasmid pLOFmini::Tn*10*:*gfp*:*kan* (Stretton *et al.* 1998). Approximately 4000 individual transposon insertion mutants were examined in microtitre trays for their ability to form a pellicle. Initial screening identified nine transposon insertion mutants that were incapable of pellicle formation. Subsequent evaluation of these strains in polypropylene and glass tubes confirmed the complete loss of the pellicle phenotype (data not shown). The exact insertion sites of the transposon insertions were identified by cloning the kanamycin resistance gene (*kan*) associated with the transposon (pLOFmini::Tn*10*:*gfp*:*kan*) and subsequent sequencing. Insertions were found to be within three genes: A1S_0249 (*cpdA*), a cAMP PDE; A1S_0112, acyl-CoA synthetase/adenosine monophosphate (AMP) acid ligase II; and A1S_0115, which is annotated to be involved in amino acid adenylation. The precise insertion site of the transposon is given as the nucleotide position relative to the *A. baumannii* ATCC 17978 genome sequence (GenBank CP000521) (Table 2.3). Seven transposon insertions were identified to be within the A1S_0115 gene. A single representative of each of the three mutants, transposon individual mutants one, two and five, was taken for further investigation (Table 2.3).

Transposon mutant one was identified as containing an insertion within *cpdA*, *cpdA*::Tn. Bacteria finely modulate intracellular cAMP levels through adenylate cyclases (synthesis) and cAMP PDE, such as CpdA, which converts cAMP to AMP (degradation) (Fuchs *et al.* 2010b). Therefore, as the insertional inactivation of *cpdA* led to a loss of pellicle, this insertion identified the requirement for cAMP regulation in this process. To confirm that the observed phenotype can be attributed to disruption of *cpdA*, the *cpdA*::Tn mutant strain was complemented by cloning a

Table 2.3: Position of the pLOFmini::Tn*10*:*gfp*:*kan* insertion within the *A. baumannii* 17978hm non-pellicle forming mutants

Mutant	Position within the chromosome[a]	ORF	Description given by KEGG[b]
1	275449	A1S_0249	Cyclic 3'5'-AMP PDE
2	137827	A1S_0115	Amino acid adenylation
3	137821	A1S_0115	Amino acid adenylation
4	137827	A1S_0115	Amino acid adenylation
5	134323	A1S_0112	Acyl-CoA synthetise/AMP-acid ligase II
6	137819	A1S_0115	Amino acid adenylation
7	137827	A1S_0115	Amino acid adenylation
8	137827	A1S_0115	Amino acid adenylation
9	139814	A1S_0115	Amino acid adenylation

[a] Positions are relative to *A. baumannii* ATCC 17978 GenBank (CP000521)
[b] KEGG, Kyoto Encyclopaedia of genes and genomes; www.genome.jp/kegg

WT copy of *cpdA* into the empty shuttle vector pWH1266 (Hunger *et al.* 1990), producing pWH0249. The pWH0249 plasmid was subsequently electroporated into the *cpdA*::Tn mutant strain generating the strain *cpdA*::Tn(0249) (Table 2.4). This strain was found to successfully produce a pellicle in contrast to both the *cpdA*::Tn mutant strain or the *cpdA*::Tn control strain harbouring the empty pWH1266 vector, *cpdA*::Tn(1266) (Table 2.4; Figure 2.2).

Transposon mutant two (A1S_0112::Tn) and transposon mutant five (A1S_0115::Tn) have insertions within the open reading frames (ORFs) A1S_0112 and A1S_0115, respectively, which are located in a large operon comprised of seven genes, A1S_0112-0118 (Figure 2.3). This operon has previously been associated with cell motility, potentially by production and secretion of a biosurfactant via a Type-I secretion system or another mechanism (Stewart *et al.* 2009, Clemmer *et al.* 2011). A recent report has shown that the genes within this operon are significantly up-regulated in biofilm cells in *A. baumannii* ATCC 17978 and a site-specific knockout of A1S_0114 abolished biofilm formation (Rumbo-Feal *et al.* 2013). Efforts to complement the A1S_0112::Tn and A1S_0115::Tn transposon mutant strains with copies of the WT genes cloned into pWH1266 (Table 2.4) were unsuccessful, possibly due to polar effects of the transposon insertions. In order to ensure that the lack of complementation was not due to a lack of transcription of these complementing genes, qRT-PCR was undertaken. This procedure revealed adequate transcription occurred for the WT A1S_0112 and A1S_0115 genes cloned into the pWH1266 vector (Table 2.1 and Table 2.5). As mentioned, pellicle formation was not restored in these mutants, possibly because these ORFs are part of an operon which must be transcribed as a polycistronic message making complementation of these mutants not possible. This is supported by the work of Clemmer *et al.* (2011) who previously isolated transposon mutants in this region which abolished motility and due to the nature of this operon were also unable to complement the mutants (Clemmer *et al.* 2011).

2.5.4 Characterisation of pellicle-deficient mutant strains *cpdA*::Tn, A1S_0112::Tn and A1S_0115::Tn

The three transposon insertion mutant strains described above were examined for potential growth perturbations in LB liquid cultures. All three *A. baumannii*

Table 2.4: *A. baumannii* 17978hm mutant derivatives constructed in chapter two

Abbreviated name	Description[a]
cpdA::Tn	pLOFmini::Tn*10*:*gfp*:*kan* insertion in *cpdA,* KAN^R
cpdA::Tn(0249)	pLOFmini::Tn*10*:*gfp*:*kan* insertion in *cpdA* containing pWH0249, KAN^R, AMP^R
cpdA::Tn(1266)	pLOFmini::Tn*10*:*gfp*:*kan* insertion in *cpdA* containing shuttle vector pWH1266, KAN^R, AMP^R, TET^R
A1S_0112::Tn	pLOFmini::Tn*10*:*gfp*:*kan* insertion in A1S_0112, KAN^R
A1S_0112::Tn(0112)	pLOFmini::Tn*10*:*gfp*:*kan* insertion in A1S_0112 containing pWH0112, KAN^R, AMP^R
A1S_0112::Tn(1266)	pLOFmini::Tn*10*:*gfp*:*kan* insertion in A1S_0112 containing shuttle vector pWH1266, KAN^R, AMP^R, TET^R
A1S_0115::Tn	pLOFmini::Tn*10*:*gfp*:*kan* insertion in A1S_0115, KAN^R
A1S_0115::Tn(0115)	pLOFmini::Tn*10*:*gfp*:*kan* insertion in A1S_0115 containing pWH0115, KAN^R, AMP^R
A1S_0115::Tn(1266)	pLOFmini::Tn*10*:*gfp*:*kan* insertion in A1S_0115 containing shuttle vector pWH1266, KAN^R, AMP^R, TET^R

[a] KAN^R, kanamycin resistance at 50 µg/mL; AMP^R, ampicillin resistance at 100 µg/mL; TET^R, tetracycline resistance at 12.5 µg/mL

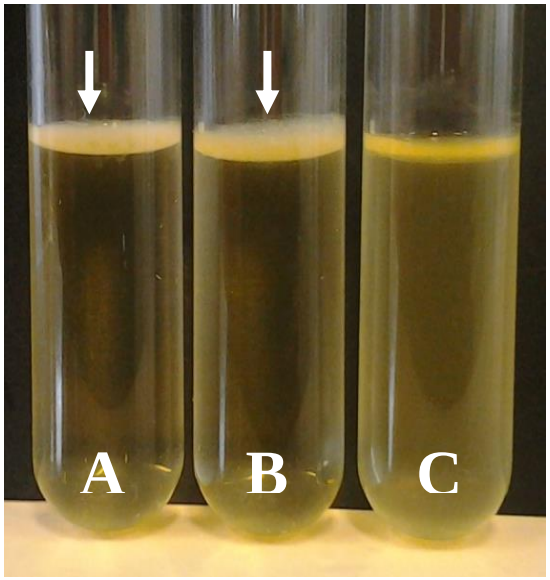

Figure 2.2: Pellicle formation by *A. baumannii* 17978hm WT, *cpdA*::Tn(0249) and *cpdA*::Tn(1266) strains

A. baumannii strains were grown in LB broth and analysed after a 72 hour incubation at 25°C in the absence of light. Pellicle material was assessed visually. (A) 17978hm WT strain and (B) *cpdA*::Tn(0249) complemented mutant strain showing developed pellicles at the interface between the liquid and air; and (C) *cpdA*::Tn(1266) mutant strain negative for pellicle formation. Arrows identify the pellicle material.

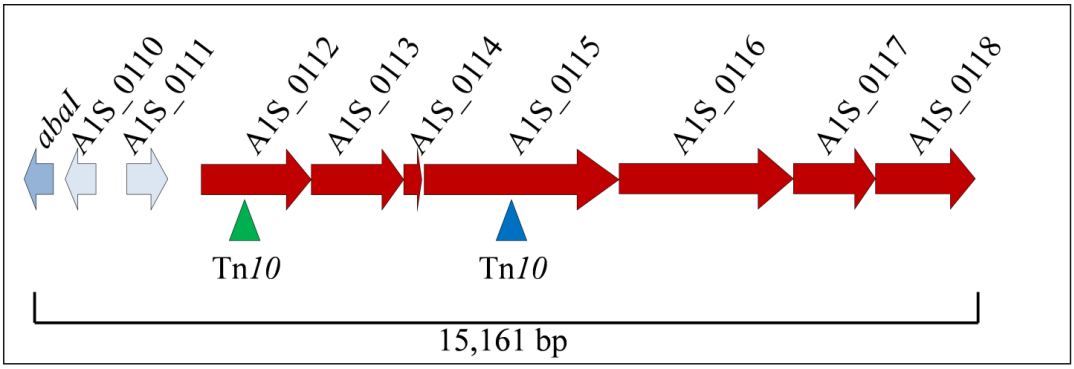

Figure 2.3: Operon with transposon insertion sites within A1S_0112 and A1S_0115 identified

The genetic organisation of the A1S_0112-0118 operon is shown with the arrows representing ORF and depict the direction of transcription. The location of the transposon pLOFmini::Tn*10*:*gfp*:*kan* insertions in A1S_0112 (green triangle) and A1S_0115 (blue triangle) are shown. Flanking genes illustrate the position of the operon within the chromosome adjacent to the quorum-sensing gene *abaI*, A1S_0110 hypothetical protein and A1S_0111 transcriptional regulator; the total size of the region shown is 15,161 bp in length.

Table 2.5: Fold change in gene expression of transposon mutant strains compared to the *A. baumannii* 17978hm WT strain

Strain	**A1S_0112**[ac]	**A1S_0115**[abc]	**A1S_0118**[bc]
cpdA::Tn	-2.8±0.21	ND	ND
cpdA::Tn(0249)	1.5±0.44	ND	ND
cpdA::Tn(1266)	-5.6±0.032	ND	ND
A1S_0112::Tn	NA	-335.46 ±1.42	-28.44± 1.33
A1S_0112::Tn(0112)	-0.49 ±1.39	-669.37 ±1.24	-51.63 ±1.70
A1S_0112::Tn(1266)	-171.25±1.68	-325.53 ±1.22	-85.43 ±1.46
A1S_0115::Tn	-1.14 ±1.59	NA	-83.29± 1.20
A1S_0115::Tn(0115)	-4.1 ±1.09	-1.16 ±1.63	-28.97± 1.54
A1S_0115::Tn(1266)	-0.99± 1.32	-347.29± 1.52	-72.50± 1.14

[a] NA, not applicable
[b] ND, not done
[c] Data from three biological replicates

transposon mutant strains showed comparable growth to the WT 17978hm strain (Figure 2.4), indicating that the loss of the pellicle is not due to a general growth defect. Since pellicle formation is only one type of biofilm, the ability to form a biofilm at the liquid-surface interface was also examined. The three transposon mutants were assessed for both their planktonic growth potential and their ability to form a biofilm on polypropylene (Figure 2.5 A, B). All transposon mutants showed an increase in planktonic growth compared to the 17978hm WT and the *cpdA*::Tn(0249) complemented derivative ($P < 0.001$) (Figure 2.5A). The transposon insertion mutants were able to form a significantly increased amount of biofilm in polypropylene tubes compared to the 17978hm WT strain (*cpdA*::Tn, A1S_0115::Tn and A1S_0112::Tn; $P < 0.05$, $P < 0.05$ and $P < 0.01$, respectively) (Figure 2.5B), while, the complemented *cpdA*::Tn(0249) mutant strain returned the phenotype to that of the 17978hm WT (Figure 2.6). Carriage of WT copies of A1S_0112 and A1S_0115 in their respective Tn*10* insertion mutant derivatives did not result in functional complementation (data not shown). The three pellicle deficient transposon mutants all displayed a >80 % reduction in cell surface hydrophobicity compared to the 17978hm WT strain, to essentially a hydrophilic nature (*cpdA*::Tn, A1S_0112::Tn and A1S_0115::Tn; $P < 0.001$, $P < 0.01$ and $P < 0.01$, respectively) (Figure 2.6). This indicates that hydrophobicity is affected when *cpdA*, A1S_0112 or A1S_0115 genes are insertionally inactivated. The presence of the WT *cpdA* gene in the *A. baumannii cpdA*::Tn(0249) derivative not only complemented the hydrophobicity character, but increased the HI to 60 % which is above the 17978hm WT strain ($P < 0.001$) (Figure 2.6); this would indicate that cAMP is involved in modulating cell surface hydrophobicity. The increase in hydrophobicity above the level seen with the 17978hm WT strain is likely due to a copy number effect of the WT *cpdA* determinant residing on the pWH1266 plasmid.

Traditionally, *A. baumannii* has been considered non-motile due to its lack of flagella; however, two forms of motility known as swarming and twitching have now been described in this species (Henrichsen 1975, Eijkelkamp *et al.* 2011b, Skiebe *et al.* 2012). While sliding motility in non-flagellated bacteria can occur by surfactant production (Stewart *et al.* 2009), twitching motility within *A. baumannii* is mediated by the extension and retraction of type IV pili as a form of

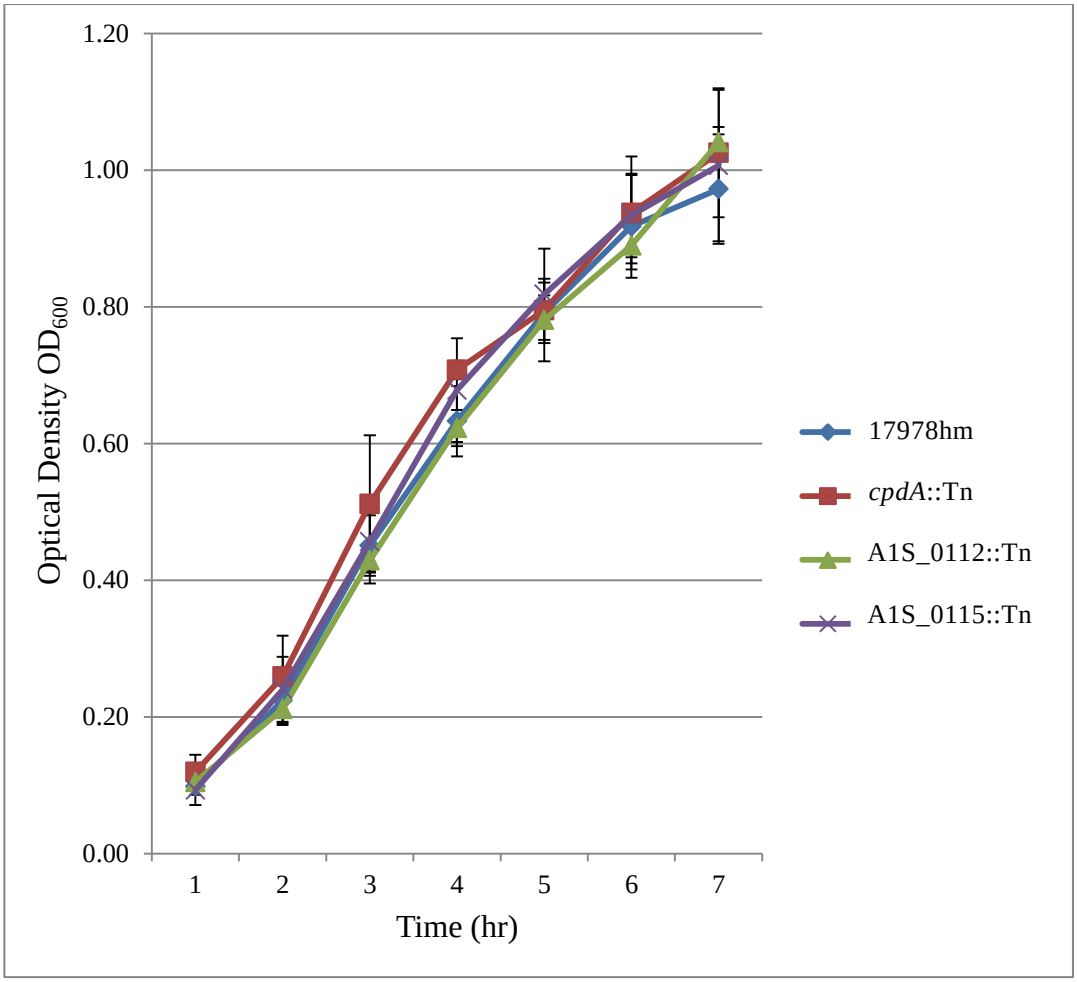

Figure 2.4: Bacterial cell growth of the *A. baumannii* 17978hm and *cpdA*::Tn, A1S_0112::Tn and A1S_0115::Tn Tn*10* insertion mutants

A. baumannii 17978hm transposon insertion mutants were assessed for growth in LB broth. Strains were subcultured 1:100 dilution into fresh LB broth; 200 µL samples were taken every hour and the OD_{600} determined spectroscopically. Bars indicate the standard deviation of three replicates.

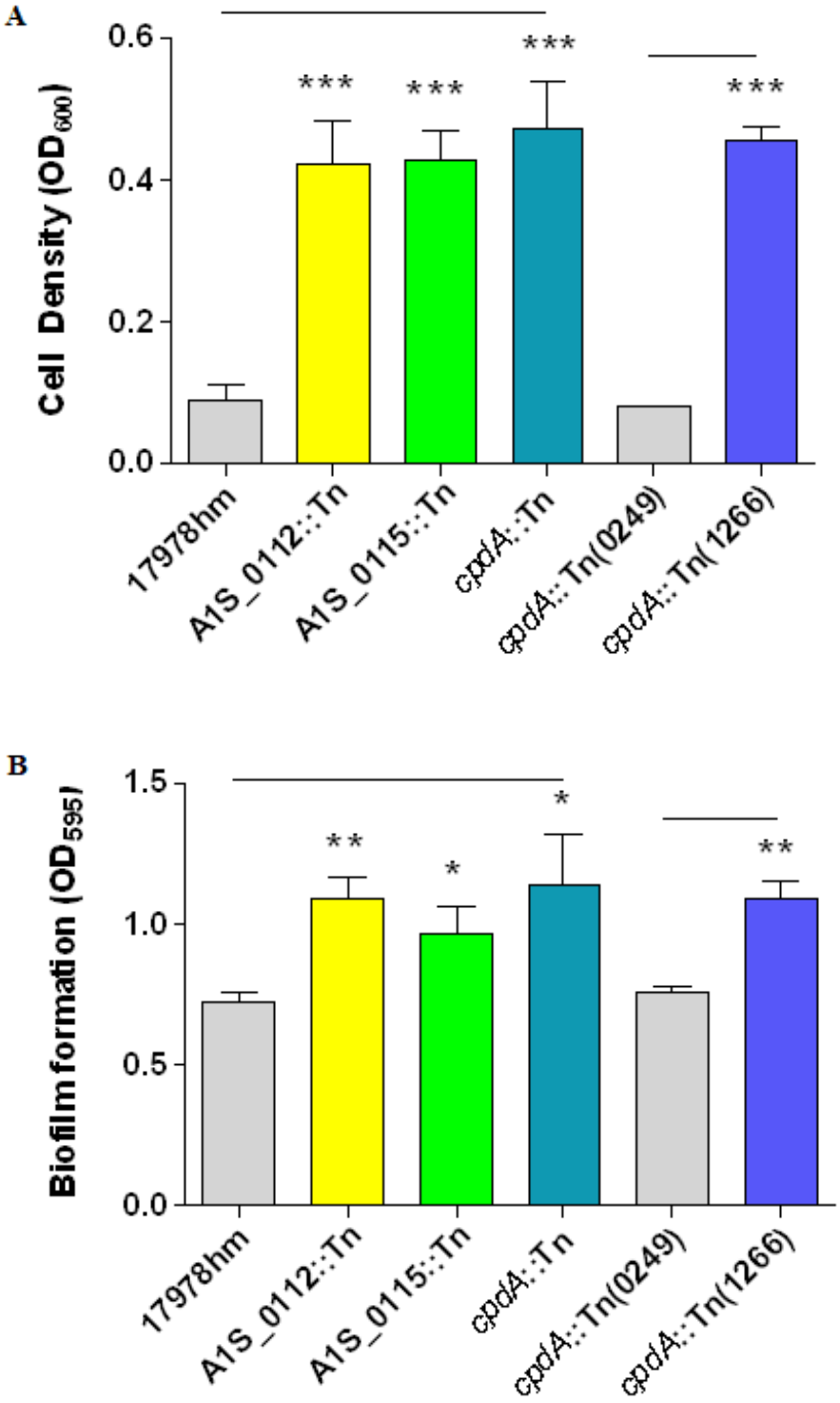
A
Cell Density (OD600)
0.6
0.4
0.2
0.0
***
***
***
***
17978hm
A1S_0112::Tn
A1S_0115::Tn
gpdA::Tn
gpdA::Tn(0249)
gpdA::Tn(1266)
B
Biofilm formation (OD595)
1.5
1.0
0.5
0.0
**
*
*
**
17978hm
A1S_0112::Tn
A1S_0115::Tn
gpdA::Tn
gpdA::Tn(0249)
gpdA::Tn(1266)

Figure 2.5: Planktonic growth and biofilm formation in polypropylene tubes of the *A. baumannii* 17978hm WT and *cpdA*::Tn, A1S_0112::Tn and A1S_0115::Tn Tn*10* insertion mutants

Cells were cultured in LB media without shaking at 37°C in polypropylene tubes for 72 hours. (A) Planktonic growth was assessed by removal of 1 mL of media and the optical density measured at OD_{600}. All three transposon insertion mutant strains showed a dramatic increase of planktonic growth; 4-fold greater than the 17978hm WT strain. Complementation of the *cdpA* mutation in the *cpdA*::Tn(0249) strain returned the phenotype to WT levels. (B) The level of biofilm produced was assessed by crystal violet staining. Transposon insertion mutant strains had an increased biomass of the surface/liquid biofilm by approximalty 30 % compared to that of the 17978hm WT. The *cpdA*::Tn(0249) mutant strain that contains a WT copy of the gene, restored the biofilm phenotype to that of the 17978hm WT. Bars indicate the standard deviation of three replicates. *** $P < 0.001$, ** $P < 0.01$ and * $P < 0.05$ as determined by a student *t*-test.

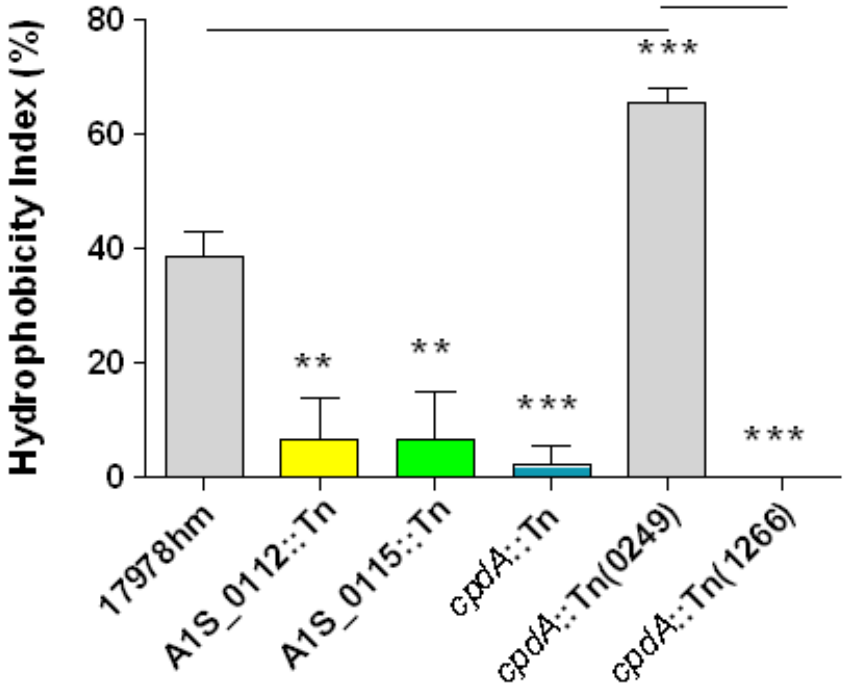

Figure 2.6: Hydrophobicity of *A. baumannii* 17978hm WT and *cpdA*::Tn, A1S_0112::Tn and A1S_0115::Tn Tn*10* insertion mutants

Hydrophobicity results were obtained by assessing the bacterial cell affiliation to xylene. The optical density of the cell suspension before (OD_{inital}) and after (OD_{final}) the addition of xylene was measured at 600 nm. All the transposon insertion mutant strains have reduced cell surface hydrophobicity compared to the 17978hm WT strain. The *cpdA*::Tn(0249) mutant strain with a WT copy of *cpdA* has a hydrophobicity greater than the 17978hm WT strain. Bars indicate the standard deviation of three replicates. *** $P < 0.001$ and ** $P < 0.01$ as determined by a student *t*-test.

surface translocation (Roca *et al.* 2012). Previously, the *A. baumannii* strain 17978hm was shown to be motile on LB media containing 0.25 % agar (Eijkelkamp *et al.* 2011b). Therefore, these conditions were applied to examine the motility phenotypes of the three pellicle-deficient transposon mutant strains. The A1S_0112::Tn and A1S_0115::Tn mutant strains proved to be non-motile as they only grew at the initial inoculum site on the agar plate (Figure 2.7). The A1S_0112::Tn and A1S_0115::Tn mutant strains harbouring either a WT copy of A1S_0112 or A1S_0115 or an empty vector pWH1266 also gave a negative result (Figure 2.7). Our data corroborated the findings by Clemmer *et al.* (2011) that the A1S_0112-0118 operon is required for motility, as insertions within this operon were found to be non-motile (Figure 2.7). However, the loss of motility seen in the transposon mutant strains is not universal because the *cpdA*::Tn variant remained motile despite presenting a visually different motility pattern compared to the 17978hm WT strain (Figure 2.7). The *cpdA*::Tn and *cpdA*::Tn(1266) strains presented a spoke like motility pattern, whereas the WT strain formed an even surface film of motile cells. The *cpdA*::Tn(0249) mutant strain returned the motility phenotype to that of the 17978hm WT covering the 0.25 % agar plate with motile bacteria cells (Figure 2.7). As such, motility was not substantially affected; however the manner by which the bacterial cells exercised their motility phenotype in the *cpdA*::Tn strain was altered. This research demonstrate that all pellicle forming strains including those that form a weak surface film are motile. Additionally, when the pellicle is disrupted there is either an alteration in the motile phenotype as seen in the *cpdA*::Tn mutant or complete abolishment of the motile phenotype.

Bacterial adherence is a critical virulence factor and aids in host and surface colonisation. The adherence of the *A. baumannii* mutant strains to human lung epithelial cells (A549) was assessed; all three transposon insertion strains had adherence capabilities that were not significantly different to that of the 17978hm WT strain (data not shown). This suggests that the mechanisms used by *A. baumannii* for pellicle formation are not essential for adherence to A549 human epithelial cells.

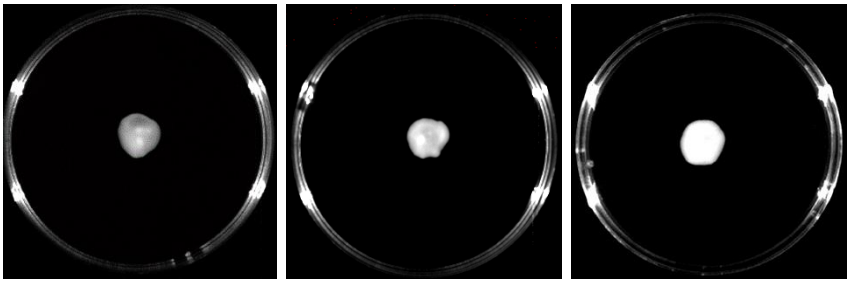

A1S_0115::Tn A1S_0115::Tn(1266) A1S_0115::Tn(0115)

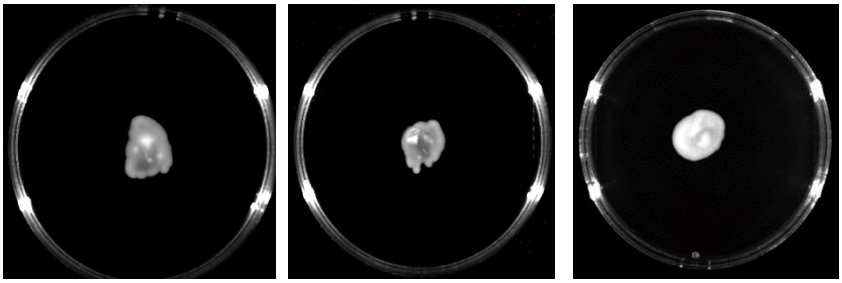

A1S_0112::Tn A1S_0112::Tn(1266) A1S_0112::Tn(0112)

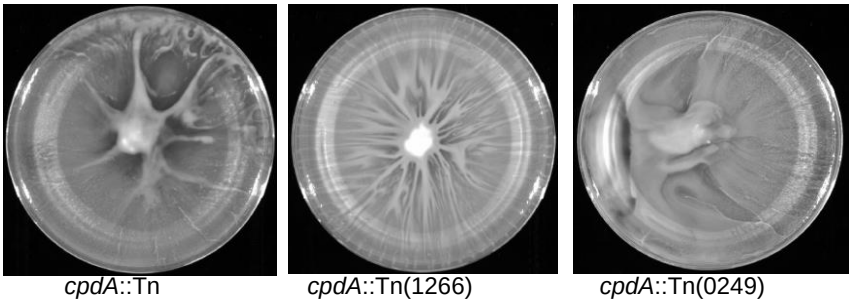

cpdA::Tn *cpdA*::Tn(1266) *cpdA*::Tn(0249)

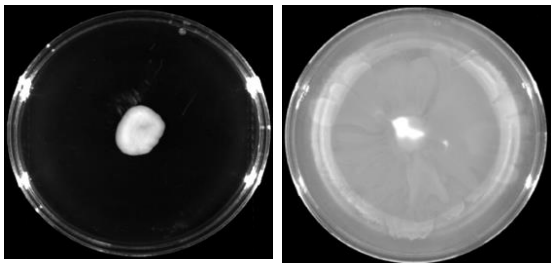

ATCC 17978 17978hm

Figure 2.7: Motility of *A. baumannii* ATCC 17978, 17978hm and transposon insertion mutants *cpdA*::Tn, A1S_0112::Tn and A1S_0115::Tn

An overnight culture of bacterial cells were used to inoculate LB media containing 0.25 % agar; plates were grown overnight at 37°C. The ΔA1S_0115, A1S_0115::Tn(0115) and A1S_0115::Tn(1266) transposon mutant strains and the A1S_0112::Tn, A1S_0112::Tn(0112) and A1S_0112::Tn(1266) transposon mutant strains only show growth at the initial inoculum site at the centre of the plate giving a non-motile phenotype. However, the *cpdA*::Tn, *cpdA*::Tn(0249) and *cpdA*::Tn(1266) transposon mutant strains retained motility. The complemented strain *cpdA*::Tn(0249) displayed a motility pattern almost identical to the 17978hm WT, whereas *cpdA*::Tn and *cpdA*::Tn(1266) displayed a "spoke-like" motility pattern. ATCC 17978 is included as a control displaying a non-motile phenotype

The levels of cAMP in the *cpdA*::Tn mutant strain are significantly increased compared to the 17978hm WT strain

The maintenance of intracellular cAMP levels is largely a result of controlling *cpdA* expression (McDonough *et al.* 2012). Therefore, if *cpdA* is inactivated, cAMP levels are expected to increase in the bacterial cell. Quantification of cAMP levels was achieved using a cyclic nucleotide XP enzymatic immunoassay kit. The *cpdA*::Tn mutant strain was found to have a level of cAMP approximately 24-fold greater than in the 17978hm WT strain (0.5 nM and 12 nM, respectively) ($P < 0.001$) (Figure 2.8). This confirmed that *cpdA* is involved in cAMP homeostasis within the cell and that the disruption of this gene dramatically affects the accumulation of this secondary signalling molecule. Examination of cAMP levels in strains *cpdA*::Tn(0249) and *cpdA*::Tn(1266) showed that the phenotype could be specifically attributed to the inactivation of *cpdA* (Figure 2.8).

2.5.5 Transcriptional profiling of *A. baumannii* 17978hm compared to the *cpdA*::Tn mutant strain under motility conditions

To assess the association between pellicle formation and motility, qRT-PCR was undertaken on the *A. baumannii* 17978hm parent and *cpdA*::Tn transposon mutant strain grown under previously identified motility conditions, i.e. on semi-solid LB agar (Eijkelkamp *et al.* 2013). Analysis of the operon A1S_0112-0118 (Figure 2.3) was undertaken by quantifying transcription of the A1S_0112 gene, the first gene in the operon. In the *cpdA*::Tn strain, the level of transcription of A1S_0112 was 2.8-fold down-regulated compared to the 17978hm WT (Table 2.5). This indicated that CpdA via cAMP plays a role, either directly or indirectly, in regulation of the A1S_0112-0118 operon. This potential regulatory role of CpdA and cAMP on the A1S_0112-0118 operon could explain the altered motility phenotype seen in the Δ*cpdA* mutant strain, possibly due to alteration in the production of a biosurfactant or through another unknown mechanism(s). The A1S_0112-0118 operon described above has previously been shown to be activated by quorum-sensing signals in the form of homoserine lactone (*abaI*, A1S_0109) (Clemmer *et al.* 2011). Furthermore, Saroj and Rather (2013) have shown that down-regulation of *abaI* led to a reduction in motility in *A. baumannii* strain M2 (Carruthers *et al.* 2013a, Saroj *et al.* 2013). Therefore, to examine whether insertional inactivation of *cpdA* in

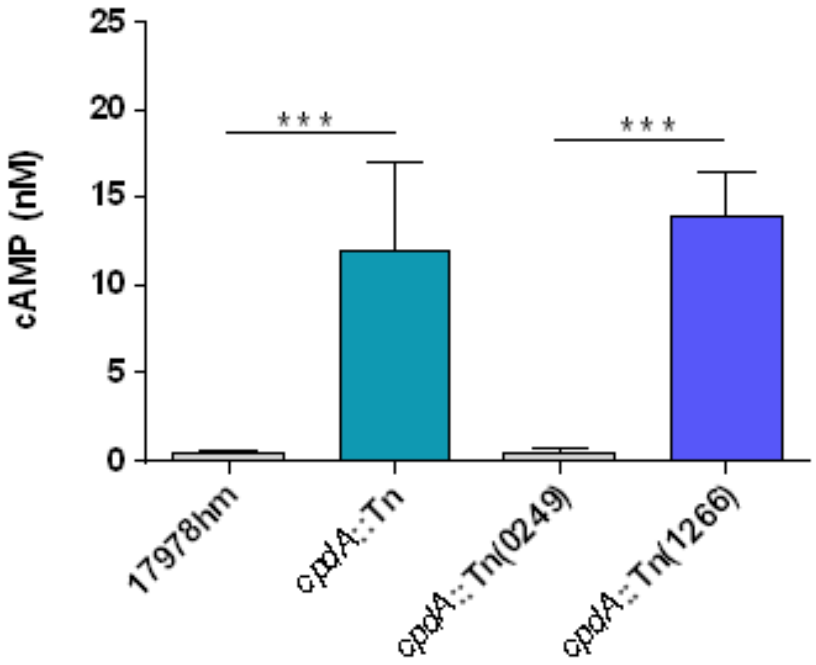

Figure 2.8: Determination of intracellular cAMP levels in the *A. baumannii* 17978hm and *cpdA*::Tn mutant strains

Bacterial cells were grown to an OD_{600} of 0.7, disrupted and cAMP levels determined using the Cyclic Nucleotide XP Enzymatic Immunoassay kit. The amount of cAMP is given in nM representing a sample corresponding to 1 mg of total cellular protein. Bars indicate the standard deviation of three replicates**.** The *cpdA*::Tn transposon mutant had 12mM of cAMP compared to the 17978hm WT strain which had 0.5mM of cAMP within the cell. The *cpdA*::Tn(0249) complemented mutant strain returned the cAMP levels to that of the 17978hm WT strain. The *cpdA*::Tn mutant strain harbouring the empty vector pWH1266 had no effect on the cAMP levels. *** $P < 0.001$ as determined by one-way ANOVA.

the *cpdA*::Tn mutant had a regulatory effect on the quorum-sensing gene *abaI* when grown on motility media, the levels of transcription of *abaI* using qRT-PCR were assessed. The results revealed that, despite the altered motility phenotype of the derivative, *abaI* is expressed at a level comparable to the 17978hm WT strain (~1.2-fold increase). This suggests that the A1S_0112-0118 operon is regulated independently by two different factors; quorum-sensing (AbaI) and cAMP. Levels of cAMP act as one of the major signalling molecules within the cell and have been show to regulate numerous genes in other bacterial species such as *P. aeruginosa* and *E. coli*, possibly through activation of Vfr (Fuchs *et al.* 2010a). In *P. aeruginosa vfr* is auto-regulated and upon inactivation of *cpdA*, *vfr* expression increases by 12-fold (Fuchs *et al.* 2010a, Fuchs *et al.* 2010b). This possibility was investigated in our *cpdA*::Tn mutant strain by examining the transcript of the putative *vfr* gene (A1S_1182). The qRT-PCR results showed a 1.7-fold decrease in *vfr* expression in the Δ*cpdA* mutant strain compared to the 17978hm WT strain, which, by a student *t*-test, was determined to be statistically insignificant. Thus, although a 1.7-fold reduction in *vfr* transcription was observed it is not known whether cAMP and Vfr work in concert in *A. baumannii*.

2.5.6 Whole transcriptome analysis of the *A. baumannii* 17978hm WT strain compared to the *cpdA*::Tn mutant strain

Alterations in the level of intracellular cAMP is known to affect a plethora of phenotypes, including alterations in metabolic processes, biofilm formation and cell surface hydrophobicity (McDonough *et al.* 2012). Therefore, RNA sequencing was used to investigate the transcriptome of the *cpdA*::Tn mutant grown in MH broth, in order to assess the impact that high levels of cAMP have within the bacterial cell. Transcriptome sequencing revealed that many genes were differentially expressed in the *cpdA*::Tn mutant compared to the 17978hm parent (Figure 2.9). Of the approximately 3400 annotated genes in ATCC 17978hm parent strain, 184 genes were more than 2-fold up-regulated and 494 genes were more than 2-fold down-regulated (Figure 2.9). The most highly up-regulated gene was identified as an alcohol dehydrogenase (A1S_1274, showed a 34-fold increase in expression) correlated with oxidation of carbon sources; which is important for metabolism, inferring a connection between increased cAMP levels within the cell and increased metabolism (Figure 2.9).

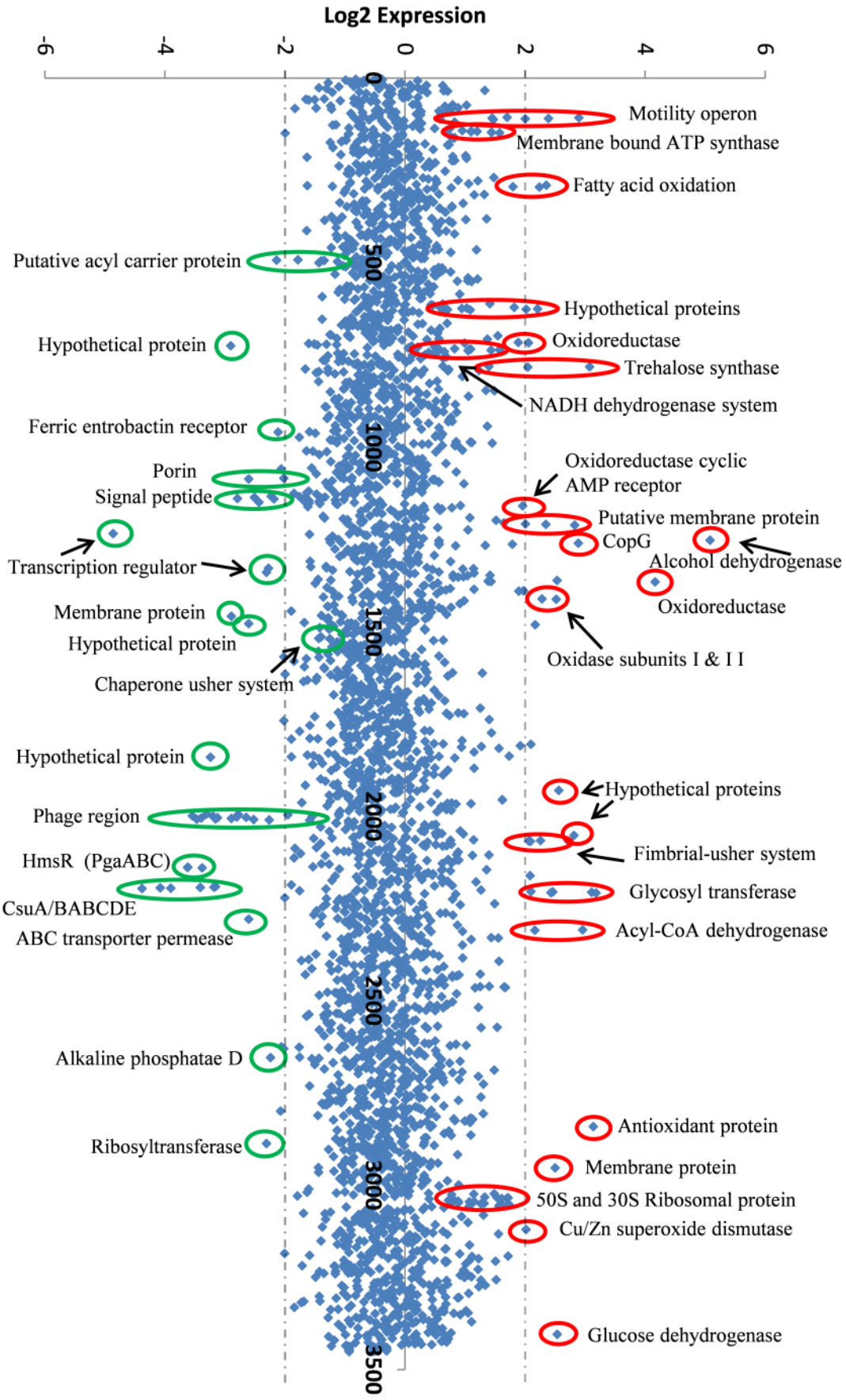
Log2 Expression
-6
-4
-2
0
2
4
6
0
500
1000
1500
2000
2500
3000
3500
Motility operon
Membrane bound ATP synthase
Fatty acid oxidation
Putative acyl carrier protein
Hypothetical proteins
Hypothetical protein
Oxidoreductase
Trehalose synthase
NADH dehydrogenase system
Ferric entrobactin receptor
Oxidoreductase cyclic
AMP receptor
Porin
Signal peptide
Putative membrane protein
CopG
Alcohol dehydrogenase
Transcription regulator
Oxidoreductase
Membrane protein
Hypothetical protein
Oxidase subunits I & I I
Chaperone usher system
Hypothetical protein
Hypothetical proteins
Phage region
Fimbrial-usher system
HmsR (PgaABC)
Glycosyl transferase
CsuA/BABCDE
Acyl-CoA dehydrogenase
ABC transporter permease
Alkaline phosphatae D
Antioxidant protein
Ribosyltransferase
Membrane protein
50S and 30S Ribosomal protein
Cu/Zn superoxide dismutase
Glucose dehydrogenase

Figure 2.9: HiSeq analysis of the *A. baumannii* 17978hm strain compared to the *cpdA*::Tn mutant strain

Comparative whole transcriptome analysis was undertaken on the 17978hm and *cpdA*::Tn strains using the Illumina platform. Sequence reads were mapped to the reference ATCC 17978 genome and the differential gene expression calculated. Diamond markers indicate the differential expression levels of all predicted ORF of the ATCC 17978 genome and are sorted on the x axis according to the locus tag. Changes of 2-fold or more in gene expression were considered significant, up-regulated genes are identified in red and down-regulated genes in green. Dashed lines indicate 4-fold (log_2=2) of differences in expression. Genes of particular interest are circled, many of which are discussed in the body of the text.

Variations in the expression of multiple potential transcriptional regulators were observed; this may be due to the significant alterations that cAMP levels have on the general metabolism of the cell. The greatest down-regulated gene was a putative transcriptional regulator (A1S_1256) showing a 29-fold decrease in expression. This putative transcriptional regulator (A1S_1256) is upstream of a MFS membrane transport protein facilitating movement across cell membranes. A number of the genes down-regulated in the *cpdA*::Tn mutant include genes encoding phage-related proteins (A1S_2021-2033), putative acyl carrier proteins, ferric enterobactin receptors, porins, signal peptides, membrane proteins and numerous hypothetical ORFs with no known function (Figure 2.9). Genes of particular interest in this study that were down-regulated include the CsuA/BABCDE system (A1S_2213-2218) (9 to 20-fold), the *hms* operon which consists of three genes designated A1S_2160 to A1S_2162) (10 to12-fold), and a chaperone usher system (A1S_1507-1510) (2-fold). Proteins encoded by the *csu* cluster and chaperone usher system have been identified as playing a role in the formation of pellicles and biofilms (Vallet *et al.* 2001, Tomaras *et al.* 2003, Eijkelkamp *et al.* 2011b, Martí *et al.* 2011a, McQueary *et al.* 2011, Eijkelkamp *et al.* 2014, Nait Chabane *et al.* 2014). Interestingly, a single polynucleotide polymorphism leading to truncation of the *csuB* gene potentially inactivating this operon has been identified within ATCC 17978 (Martí *et al.* 2011a, McQueary *et al.* 2011, Eijkelkamp *et al.* 2014). Within the *hms* operon two proteins (A1S_2160 and A1S_2161) share an average of 44 % identity with the PgaBC proteins (A1S_0938-0939), the third protein within Hms (A1S_2162) has been designated as a biofilm synthesis protein and shares no homology to the Pga proteins in *A. baumannii* ATCC 17978. The Pga system has previously been identified as being important in biofilm formation (Choi *et al.* 2009). Interestingly, a recent paper by Nait Chabane *et al*. (2014) found that *csuA/BABCDE* and *pgaABCD* genes and the chaperone usher system described above, are overrepresented within *A. baumannii* strains displaying a pellicle phenotype. This suggests that Hms and the chaperone usher pilus proteins could be key components in the formation of the pellicle matrix.

Numerous genes which were up-regulated encode proteins involved in oxidative phosphorylation (Figure 2.9). In particular, these include those encoding ubiquinol oxidase subunit I and II (A1S_1434 and A1S_1433) which are 5.7-fold and 4.9-fold

up-regulated, respectively. Other genes involved in oxidative phosphorylation include the NADH dehydrogenase complex (A1S_0762-0764) also up-regulated (Figure 2.9) and the ATP synthetase complex (A1S_0148-0156). One of the most highly up-regulated genes (A1S_1387) is an oxidoreductase (18-fold); this class of enzymes is often involved in the FAD to $FADH_2$ conversion, where $FADH_2$ plays a major role in oxidative phosphorylation. Therefore, many of the up-regulated genes are involved in the energy, and by extension, the metabolic status of the cell which is not surprising given the central role cAMP plays in cell metabolism.

Other genes of interest which were significantly up-regulated are those involved in 50S and 30S ribosome assembly. The potential role of these up-regulated ribosomal proteins maybe in the assembly of 100S ribosomes, as these are required for cells to survive long term nutrient stress in situations where glucose is low and cAMP is high (Wada *et al.* 2000). Other up-regulated genes including those involved in fatty acid oxidation, trehalose synthase, membrane proteins, dehydrogenase proteins and a number of proteins which are annotated as hypothetical ORFs.

Expression of a small operon consisting of four genes (A1S_2088-2091) was increased 4-fold. Proteins encoded by this region have been recently been found in extracted pellicle material (Nait Chabane *et al.* 2014). Since, the *cpdA*::Tn strain is not capable of pellicle production it would seem unlikely that the A1S_2088-2091 operon is involved in this phenotype, however, *cpdA*::Tn does show an increase in biofilm formation compared to the 17978hm WT strain and as such this operon may contribute to liquid surface biofilm production.

The previously described motility operon A1S_0112-0118 (Clemmer *et al.* 2011) is up-regulated approximately 3.8-fold in the *cpdA*::Tn mutant transcriptome, which is in contrast to RT-PCR data (Table 2.5). These RT-PCR studies were conducted on motility agar to look at the influence of motility on the change in transcription of this operon. On motility agar both cAMP and quorum-sensing may play a role in the control of this operon, however in liquid culture grown to mid-log phase used for the RNA-sequence analysis, cAMP appears to be solely responsible for the regulation of A1S_0112-0118.

2.6 Conclusion

This report has shown that pellicle formation is a phenotypic trait seen in a limited number of *A. baumannii* strains. For the first time, the secondary signalling molecule cAMP has been shown to play a critical role in pellicle formation as well as motility in *A. baumannii.* Additionally, this study has shown that insertions in *cpdA*, A1S_0112 and A1S_0115 completely abolish pellicle formation. Furthermore, transcriptional analyses identified that cAMP effects the expression of the A1S_0112-0118 operon essential for motility. Thereby, altering the migration pattern seen in the *cpdA*::Tn mutant strain when grown on semi-sold agar. Additionally, insertions in the A1S_0112-0118 operon in the A1S_0112 and A1S_0115 regions resulted in a non-motile phenotype. It is therefore speculated that the pellicle and motility phenotypes of *A. baumannii* are linked via the expression of cAMP and the A1S_0112-0118 operon. Increased cell surface hydrophobicity was identified as a partial indicator of pellicle formation ability in the clinical strains tested herein. Whole transcriptome analysis has identified an abundance of ORFs affected by the increase in cAMP within the *cpdA*::Tn mutant. A number of these correlate with genes previously known to be involved in pellicle formation including the *hms* locus and a chaperone usher system as well as the A1S_0112-0118 region identified in this study. Considering the importance of pellicle formation in the persistence and transmission of numerous bacterial species, this study has contributed to our understanding of the regulatory mechanisms behind these significant virulence traits in *A. baumannii*.

CHAPTER 3 The StkRS two-component system influences colistin resistance in *A. baumannii*

Declaration for thesis chapter three

Declaration by candidate

In chapter three the nature and extent of my contribution to the work was the following:

Nature of contribution	**Extent of contribution**
Experimental design, performance of experiments, writing, editing and revision of manuscript	80 %

The following co-authors' contributed to the work.

Name	**Nature of contribution**	**Extent of contribution**
Uwe Stroeher	Experimental design, editing and revision of manuscript	10 %
Melissa Brown	Experimental design, editing and revision of manuscript	10 %

The undersigned hereby certify the above declaration correctly reflects the nature and extent of the candidates and co-authors contribution to this work

Candidate's Date

Signature 2019

Supervisor's Date

Signature 2019

.

3.1 Preface

This chapter is to be submitted for publication in the journal Antimicrobial Agents and Chemotherapy as **Giles. S. K., Stroeher. U. H. and Brown. M. H.** (2019) The StkRS two-component system influences colistin resistance in *Acinetobacter baumannii*.

3.2 Abstract

A. baumannii is an MDR opportunistic human pathogen, responsible for numerous severe infections. Due to its severity, polymyxin antibiotics have re-emerged to treat these infections. This project, the mechanisms adopted by the *A. baumannii* 04117201 strain associated with the TCSTS StkRS to resist polymyxins were investigated. The *stkR* RR deletion mutant Δ*stkR* was generated using homologous recombination replacing the RR gene with an ERY^R cartridge. Assessment by minimum inhibitory concentration (MIC) of the Δ*stkR* mutant strain compared with the 04117201 WT strain, revealed a 2-fold increase in resistance to the clinically relevant polymyxins, CST and PMB. Additionally, *in vitro* investigations revealed an increase in cell surface hydrophobicity of the Δ*stkR* mutant compared with the 04117201 WT strain; however, this trend was reversed when the strains were exposed to CST. Transmission electron microscope (TEM) investigation of the bacterial cell surface after CST treatment identified membrane corrugation and perturbation of the 04117201 WT and Δ*stkR* mutant strains. Silver staining of the lipooligosaccharide excluded the complete loss of lipooligosaccharide as a means of CST resistance. Finally, qRT-PCR of the *pmrCAB* operon identified a significant up-regulation of the *pmrCAB* genes in the Δ*stkR* mutant strain compared to its parent. In summary these data demonstrate a relationship between the increase in CST resistance exhibited by the Δ*stkR* mutant strain and the StkRS TCSTS. Additionally, the TEM results suggest an envelope stress response affected by the StkRS two-component system.

3.3 Introduction

A. baumannii is a Gram-negative nosocomial opportunistic pathogen that causes severe infections worldwide. Pandemic outbreaks of *A. baumannii* are increasing in number and severity due to its MDR and pandrug-resistant nature (Chusri *et al.* 2015, Haag *et al.* 2016). *A. baumannii* has a number of systems by which the bacteria can

cause disease and circumvent antibiotic treatments. These systems are postulated to be regulated by a plethora of genetic mechanisms (Carruthers *et al.* 2013b, Fiester *et al.* 2015, Srinivasan *et al.* 2015). The TCSTS is one such mechanism used by *A. baumannii* to regulate complex functions within the bacterial cell (Gaddy *et al.* 2009b).

A typical TCSTS consists of a membrane-bound HK and a cytosolic RR. When a signal is received by the HK, the protein dimerises and is autophosphorylated at a conserved His residue. The phosphate molecule activates its cognate RR protein by binding to the conserved Asp residue in the N-terminal region (Adams *et al.* 2009, Mejean 2016). RR activation leads to a conformational change in the C-terminal or variable region of the RR protein (Capra *et al.* 2012), this allows for stimulation or repression of genes or regions of DNA causing downstream effects on cellular processes (Richmond *et al.* 2016, Tiwari *et al.* 2017).

TCSTSs have been shown to regulate a multitude of important virulence functions such as adhesion pili, surface polysaccharides, membrane proteins, capsule production, efflux pumps and type IV pili (Lazar Adler *et al.* 2016, Wessels 2016, Breland *et al.* 2017, Tiwari *et al.* 2017). TCSTS are also associated with alterations in antibiogram profiles; for example, in *A. baumannii* the AdeRS system regulates an efflux pump contributing to antibiotic resistance. Adding to the complexity of TCSTS within pathogenic bacteria, the TCSTS GigAB regulates biofilm formation in *P. aeruginosa* and antibiotic resistance in *A. baumannii* contributing to the diversity of TCSTS (Richmond *et al.* 2016, Gebhardt *et al.* 2017). Finally, the PmrAB TCSTS system in *A. baumannii* is linked to increased polymyxin resistance. Specifically mutations in *pmrA, pmrB* and/or *pmrC* have resulted in up-regulation of the *pmrCAB* genes leading to modification of lipid A by the addition of pEtN and/or galactosamine (GalN) and subsequent resistance to polymyxins (Park *et al.* 2011, Chin *et al.* 2015, Quesada *et al.* 2015, Girardello *et al.* 2017).

Due to the MDR nature of *A. baumannii*, patients presenting with these infections commonly rely on “last resort” antibiotics such as the polymyxin class of drugs. The polymyxin CST is a cationic peptide composed of a cyclic heptapeptide covalently attached to a fatty acyl chain (Evans *et al.* 1999, Trimble *et al.* 2016). CST is bactericidal with positively charged α,ɣ-diamonobutyric acid residues which

interact by attaching and displacing the magnesium and calcium divalent cations from the negatively-charged phosphate groups of lipid A which stabilises the lipooligosaccharide (LOS) or lipopolysaccharide (LPS) in the outer membrane (Da Silva *et al.* 2017, Bakthavatchalam *et al.* 2018). The major component of the outer leaflet of the outer membrane, where CST affects the permeability, is known in most bacteria as LPS. LPS has a general structure with a conserved lipid A, a core oligosaccharide and a highly variable O-antigen sugar structure (Girardello *et al.* 2017). The periplasmic LPS is anchored to the outer membrane by lipid A which is attached to the core oligosaccharide and variable O-antigen region extending outwards from the cell surface. However interestingly, *A. baumannii* is similar to *Neisseria* and *Campylobacter*, as it appears to lack a dedicated O-antigen ligase and does not attach an O-antigen to the lipid A core, therefore producing LOS not LPS (Weber *et al.* 2015a, Boll *et al.* 2016, Wei *et al.* 2017). Therefore displacement of the magnesium and calcium divalent cations increases the permeability of the outer membrane causing perturbation and surface corrugation. This can result in its collapse and leakage of the cellular content, a phenomenon known as blebbing (Hancock 1997, Falagas *et al.* 2010).

Three main mechanisms for CST resistance have been identified in *A. baumannii*. One involves the complete loss of the lipid A portion of the LOS, which correlates with mutations in *lpxA*, *lpxC, lpxD* and *lpsB* (Moffatt *et al.* 2010, Da Silva *et al.* 2017, Carretero-Ledesma *et al.* 2018). The second is modification of LOS by the addition of pEtN, achieved through two distinct pathways; one requires *pmrC* (Beceiro *et al.* 2011, Jones *et al.* 2017, Bakthavatchalam *et al.* 2018, Jaidane *et al.* 2018) and the other involved disruption of the HNS regulatory protein through an insertion sequence element (IS*Aba125*), that resulted in increased expression of *eptA* which encodes a second pEtN transferase (Deveson Lucas *et al.* 2018). The third mechanism is also a modification of LOS but is due to the addition of GalN; this correlates to mutations in the *pmrB* determinant of the PmrAB TCSTS (Chin *et al.* 2015). The increase in pEtN and GalN reduces the net charge of the LOS, thereby reducing its affinity to polymyxins (Chin *et al.* 2015, Girardello *et al.* 2017).

This chapter aimed to characterise a previously unknown TCSTS and determine its regulatory role. Through a series of phenotypical investigations, the TCSTS termed StkRS, was identified in the virulent clinical *A. baumannii* 04117201 strain.

Phenotypic examination of a constructed 04117201 Δ*stkR* mutant showed an increase in resistance to the polymyxins CST and PMB. As such, the mechanism for CST resistance in *A. baumannii* 04117201 was investigated by assessing lipid A loss and LOS modification. Further analysis of the Δ*stkR* mutant strain discovered significant alterations in the cell surface hydrophobicity, identifying interconnections between cell surface hydrophobicity and LOS modification. These associations further deepen our understanding of the transcriptional regulation leading to physiological changes in this significantly problematic pathogen.

3.4 Materials and Methods

3.4.1 Bacterial strains, and media

The clinical *A. baumannii* bacterial strains used and cultured in this study have been described previously (Giles *et al.* 2015). For maintenance, conjugation, cloning, and replicating plasmids, *E. coli* DH5α, SM10, or JM109 cells were used (Hanahan 1983, Simon *et al.* 1983, Yanisch-Perron *et al.* 1985). The *A. baumannii* strain 04117201 belongs to the international clone type II and was obtained from a tracheal aspirate sample at Flinders Private Hospital, SA, Australia (Eijkelkamp *et al.* 2011a).

3.4.2 Eukaryotic cell adherence assay

The adherence of *A. baumannii* cells to A549 human type 2 pneumocytes was investigated as previously (Giles *et al.* 2015). The data collected for the adherence assays were obtained from three replicate experiments and represent data points from each experiment in quadruplicate wells.

3.4.3 MIC and disk diffusion susceptibility

The MIC of antimicrobial compounds were determined using standard methods, as previously described (Wiegand *et al.* 2008). In brief, microtitre trays containing a 2-fold dilution series of the compound of interest were prepared and cultures added 1:1 in MH broth before being incubated overnight at 37°C with (shaking) . Bacterial growth was examined by absorbance at OD_{600} using a Multiskan EX (Adelab Scientific, SA, Australia). The standard agar disc diffusion technique was performed on 1 % MH agar with bacterial strains diluted to 0.5 McFarland unit. Results of the Kirby-Bauer disc diffusion were evaluated according to the Clinical and Laboratory Standards Institute guidelines (CLSI 2006, CLSI 2007).

3.4.4 Deletion replacement mutant construction by homologous recombination

Construction of a *stkR*-inactivated derivative of *A. baumannii* 04117201 was undertaken by homologous recombination. In brief, DNA fragments corresponding to 1.2 kb upstream and 1 kb downstream of *stkR* were PCR amplified using VELOCITY^{TM} DNA polymerase (Bioline, NSW, Australia) and specific oligonucleotides designed in NetPrimer (www.premiersoft.com) (Table 3.1). The cycling conditions used were 2 minutes at 94°C, followed by 30 cycles of 45 seconds at 94°C, 45 seconds at 60°C, and 90 seconds at 72°C. This was followed by a final extension of 10 minutes at 72°C. PCR products of the appropriate size were cloned into the suicide vector pEX18Tc via *Xba*I, *Bam*HI, or *Sac*I restriction sites and transformed into *E. coli* DH5α cells (Adams *et al.* 2018). Following sequence confirmation, pEX18Tc clones were electroporated into fresh electrocompetent *A. baumannii* 04117201 bacterial cells (Eijkelkamp *et al.* 2013).

3.4.5 Cell surface hydrophobicity tests

Cell surface hydrophobicity was examined as described previously (Eijkelkamp *et al.* 2013, Giles *et al.* 2015). The OD_{600} of the cell suspension was determined before ($OD_{initial}$) and after (OD_{final}) the addition of xylene. The HI was calculated as $(OD_{initial} - OD_{final} / OD_{initial}) \times 100$. Quantitative data were collected from three replicates.

3.4.6 TEM

TEM was undertaken as previously described (Gui *et al.* 2014) with the following modifications. *A. baumannii* cells in log phase were treated for 1 hour at 37°C (shaking) with 0, 3, or 12 µg/mL CST. Following incubation, MilliQ (MQ) washed cells, were fixed in 100 mM phosphate buffer pH 7.0 with 2.5 % glutaraldehyde, for 24 hours at room temperature. To postfixed cells, 100 mM phosphate buffer pH 7.0 with 1 % osmium tetroxide was added and the samples left

Table 3.1: Oligonucleotides used for cloning, sequencing and qRT-PCR

Name	Forward Primer (5' – 3')	Reverse Primer (5' -3')
Cloning		
stkR flanking UP	GAGATCTAGACCGCACTACGTTCGTACCGAC	GAGAGGATCCCGCCTGTTCAAGCTGTTC
stkR flanking Down	GAGAGGTACCCAGACTCACTGCTAAAAATAG	GAGAGAGCTCGCTTCAGCCATATAGCTTC
ERY^R	GAGAGGATCCCTTAAGAGTGTGTTGATAGTGC	GAGAGGATCCAGAATTATTTCCTCCCG
Sequencing		
Up flanking region	GGAGATAAGTTGGGCTTGGTG	CCAATCTCTACTCCTGTTTC
Down flanking region	CTAATGCCTATGTTACTAAG	GAGGAATTCATTGTGAATATTC
pEX18Tc	CCTCTTCGCTATTACGCCAG	GTTGTGTGGAATTGTGAGCG
ERY^R cartridge	CTTAAGAGTGTGTTGATAGTGC	AGAATTATTTCCTCCCG
stkR	ACGGTTAATTCATAAGCAATGAGT	GTGAAACTCTTGCACCAAACT
PmrA1.2	CCCATGTAAACTAAAGCGAGCC	CATCGACTTCTTGAAGTGCAACC
PmrA1F	GGACATGTTGCACTCTTG	
PmrA3F	GCAGCAACACCAGTATTA	
PmrB3.4	GGGCACCTCAATTTTCAGTGTC	GCTGAATACGCGCCAAACC
PmrB5.6	GCCGATGCTGCTCATGAATT	TTGGGCGCAAATGATGC
PmrB1F	GGTCAACTTGGCTATGCA	
PmrB2F	GAAGATAGCGGTGCAGGA	

PmrC1PCR	GGCTAAATATAGTTTCTAATAACG	CGACACGGTTTTGTAATTGA
PmrC2seq	GTCACTCACGCTGCTGAATT	CCGCTGTTGCCGTACCGC

Table 3.1: Continued

FpmrC3seq	GGGTATGCAAAAATACG	
FpmrC4seq	CGTCCACGTTTGATTGTTTT	
FpmrC5seq	GGTGTCATTATTTCACCCGA	
qRT-PCR		
16 S	CAGCTCGTGTCGTGAGATGT	CGTAAGGGCCATGATGACTT
pmrA	GAGGTGGAATGGGTCAAT	GGTCTGCTTTAAAACTTGC
pmrB	GGTTGCACTTCAAGAAGTC	TAAACAGATCTTCTTCGTGG
pmrC	CCATATTTTGGAGTAAAGGC	TTTTGGCAGTCCATTTCC
*gap*DH A1S_2501	CAACACTGGTAAATGGCGTG	ACAACGTTTTTCATTTCGCC

for 1 hour at 4°C. Samples were dehydrated in an ethanol series and embedded in 1 mL EMbed 812/Araldite 502 resin (Emgrid, SA, Australia), before cutting with a diamond knife (Diatome) and microtome (Leica EM UC6 Ultramicrotome) and being examined using a TEM (FEI Tecnai G2 Spirit). A magnification of 60,000 × was used for presentation of figures and a magnification of 11,500 × was used for determination of blebs per cell.

3.4.7 SDS-PAGE and LOS silver staining

SDS-PAGE and LOS silver staining was performed as previously described (Tsai *et al.* 1982, Fomsgaard *et al.* 1990) with the following modifications. A 10 mL overnight culture grown in LB was re-suspended in 50 µL lysis buffer (SDS, ß-mercaptoethanol, bromophenol blue and Tris-HCL pH 6.8 in MQ) and heated to 95°C for 3 minutes. An aliquot of 10 µL of Proteinase K (10 mM) was added to samples which were then resolved on a 15 % SDS-PAGE gel. Gels were fixed overnight fusing 40 % ethanol/5 % glacial acetic acid, followed by oxidation for 5 minutes (shaking) in 40 % ethanol/ 5 % glacial acetic acid, containing 0.007 g of periodic acid per mL. Gels were washed 4 times at 30 minutes intervals with MQ water. Gels were stained for 10 minutes (shaking) in 115 mL MQ containing 24 % of a 0.1 M NaOH solution, 1.7 % of a concentrated NH_4OH solution and 4.3 % of 20 % $AgNO_3$. Gels were washed with 3 changes of MQ water for 30 minutes, and developed using pre-warmed 1000 mL MQ containing 5 % citric acid and 0.05 % of 37 % formaldehyde solution. The development of colour was stopped using 1000 mL MQ containing 2 % glacial acetic acid.

3.4.8 RNA isolation

RNA was extracted as previously described in Chapter two (Giles *et al.* 2015) with the following modifications. Cells were grown in MH broth (Oxoid, ThermoFisher, SA, Australia) to an OD_{600} of 0.6 and treated for 1 hour with CST at 3 µg/mL. Cell where harvested by centrifugation (13,000 x *g* for 2 minutes at 4ºC), lysed in 1 mL of TRIzol ® reagent (Invitrogen, Australia) and 200 µL of chloroform added. Phases were separated by centrifugation (13,000 x *g* for 15 minutes at 4ºC) and total RNA extracted using the RNA Mini Kit II (Bioline, Australia) following the manufacturer's recommendations and DNaseI treated.

3.4.9 qRT-PCR

The iScript reverse-transcriptase cDNA synthesis kit (Bio-Rad, Australia) was used to synthesise cDNA following the manufacturer's recommendations. qRT-PCR was performed using iTaq^{TM} Universal SYBR$^{®}$ green supermix (Bio-Rad, Australia) in conjunction with a Rotor-Gene Q (Qiagen, VIC, Australia) with oligonucleotides designed in NetPrimer (www.premiersoft.com) (Table 3.1). A typical qRT-PCR run was 2 minutes at 95°C followed by 40 cycles of 10 seconds at 95°C, 15 seconds at 60°C, and 20 seconds at 72°C (Brazma *et al.* 2001). Transcriptional differences were calculated using the $\Delta\Delta C_t$ method (Livak *et al.* 2001) and the 16S rRNA (A1S_r01) and *gap*DH (A1S_2501) transcription levels were used as a reference.

3.4.10 Statistical analysis

The Graphpad Prism 7.0 (La Jolla, CA, United States of America) statistical package was used to analyse the results where appropriate. Assessments of skewness, kurtosis and the Shapiro–Wilk normality test (Samuels *et al.* 2012) were undertaken on all measures, and parametric or non-parametric tests for analysis of virulence were applied as needed.

3.4.11 Accession number

The DNA sequences of the TCSTS StkRS of *A. baumannii* 04117201 have been submitted to Genbank ID 2135660.

3.5 Results

3.5.1 Selection of a virulent *A. baumannii* strain

To select an *A. baumannii* strain with a high virulence potential, a number of known virulence-associated traits were examined in our collection of 54 clinical *A. baumannii* strains. From our previous analysis of biofilm-forming ability of these strains 11 that exhibited a higher level of biofilm formation were chosen for further examination (Eijkelkamp *et al.* 2011b). These 11 strains were assessed for their cell adherence ability, as it is the initial step in a disease state (Section 1.5.2) and antibiotic resistance (Brossard *et al.* 2012). Incubation with human A549 pneumocytes showed that the *A. baumannii* strain 04117201 was significantly more adherent than the well characterised strain ATCC 17978 ($P < 0.001$), and more adherent than the other clinical strains tested (Figure 3.1). Antimicrobial resistance

screening of the 11 clinical strains demonstrated that although *A. baumannii* 04117201 is highly resistant to many of the compounds tested, it is sensitive to ERY (Table 3.2), allowing for ERY to be used as a selection marker to generate mutants.

3.5.2 Construction of an *A. baumannii* Δ*stkR* derivative

To identify the complement of TCSTS in the *A. baumannii* strain 04117201, it was subjected to whole genomic sequencing by Illumina HiSeq (Wellcome Trust Sanger Institute) and assembled using Velvet 1.2.03 (Nigro *et al.* 2019). From this analysis 29 TCSTS were identified, two of which presented as orphan RR proteins and one hybrid kinase. Of these TCSTSs, the open reading frame ORF_839 in the *A. baumannii* 04117201 WT strain was named herein as the StkRS system and chosen for further investigation as it is absence from the avirulent *A. baumannii* SDF strain (Fournier *et al.* 2006). Investigation of the *stkR* RR and its predicted gene product places it in the LuxR family of RRs (Santos *et al.* 2012) as it possesses a conserved C-terminal helix-turn-helix (HTH) motif. In *A. baumannii* 04117201 the StkR RR is partnered with a hybrid HK sensor ORF_838 (StkS). This protein exhibits homology to the HTH motif of GerE in *B. subtilis* which is involved in sporulation (Baccigalupi *et al.* 2004). An *A. baumannii* 04117201 *stkR* RR deletion derivative (Δ*stkR*) was constructed by homologous recombination, inactivating the TCSTS through insertion of an ERY^R cassette into *stkR* (Fournier *et al.* 2006).

To assess if inactivation of *stkR* affected cells viability, the growth of the Δ*stkR* mutant strain was compared to the 04117201 WT in multiple media including; MH, M9 minimal media (M9), lung media (Palmer *et al.* 2007), and whole sheep blood (Figure 3.2). Interestingly the Δ*stkR* mutant grew significantly quicker in blood at the 4 hour time point, potentially indicating an increased resistance to various pressures in blood for example resistance to complement proteins. Additionally, growth in M9 identified a slight lag of the Δ*stkR* mutant compared to the 04117201 WT strain, suggesting the RR deletion may have an effect on the use of different carbon sources.

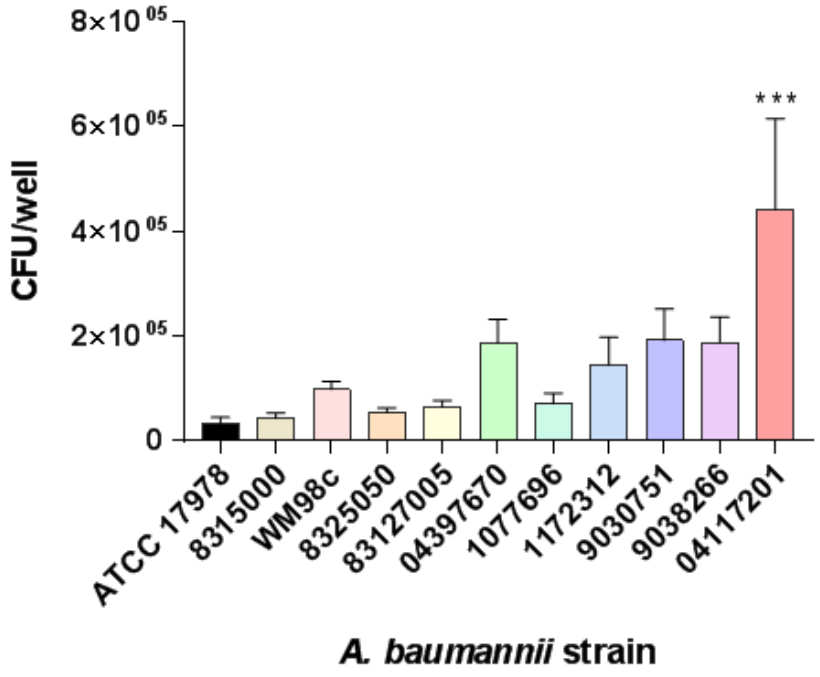

Figure 3.1: Cell adherence capacity of *A. baumannii* strains to A549 pneumocytes

The cell adherence capacity of 11 *A. baumannii* strains were examined after exposure to A549 cells. Bars indicate the standard error of three replicates. Analysis by skewness, kurtosis and the Shapiro–Wilk normality test were undertaken. *** $P <$ 0.001 as determined by an analysis of variance test, between ATCC 17978 and the clinical strains.

Table 3.2: Antimicrobial resistance profiles of the selected *A. baumannii* clinical strains

	***A. baumannii* strain**										
Compound[abc]	**ATCC 17978**	**04117201**	**1172312**	**WM98c**	**08315000**	**04397670**	**9030751**	**1077697**	**9038266**	**08325850**	**083217005**
AMP	250	>500	>500	250	>500	>500	>500	>500	>500	>500	>500
CIP	3.25	30	30	3.25	>240	60	60	60	60	>240	>240
CST	4	8	8	16	8	8	32	32	16	4	4
ERY	S	S	S	S	R	S	S	I	S	I	R
GEN	32	500	500	16	125	250	125	125	250	125	125
H_2O_2[d]	125	250	250	500	250	125	250	250	250	125	250
KAN	R	R	R	S	S	R	R	S	R	S	R
PMB	8	16	16	16	8	16	32	32	8	8	8
RIF	8	8	8	8	>64	4	4	4	4	4	4
TEL	0.93	1.87	1.87	1.87	3.75	3.75	1.87	1.87	3.75	3.75	3.75
TET	S	R	R	I	R	I	R	I	R	R	R

[a] AMP, ampicillin; CIP, ciprofloxacin; CST, colistin; ERY, erythromycin; GEN, gentamicin; H_2O_2, hydrogen peroxide; KAN, kanamycin; PMB, polymyxin B; RIF, rifampicin; TEL, tellurite; TET, tetracycline

[b] R, Resistance; I, Intermediate; S, Susceptible; determined by Kirby Bauer against the CLSI standards

[c] amounts presented in μg/mL.

[d] amounts presented in nM.

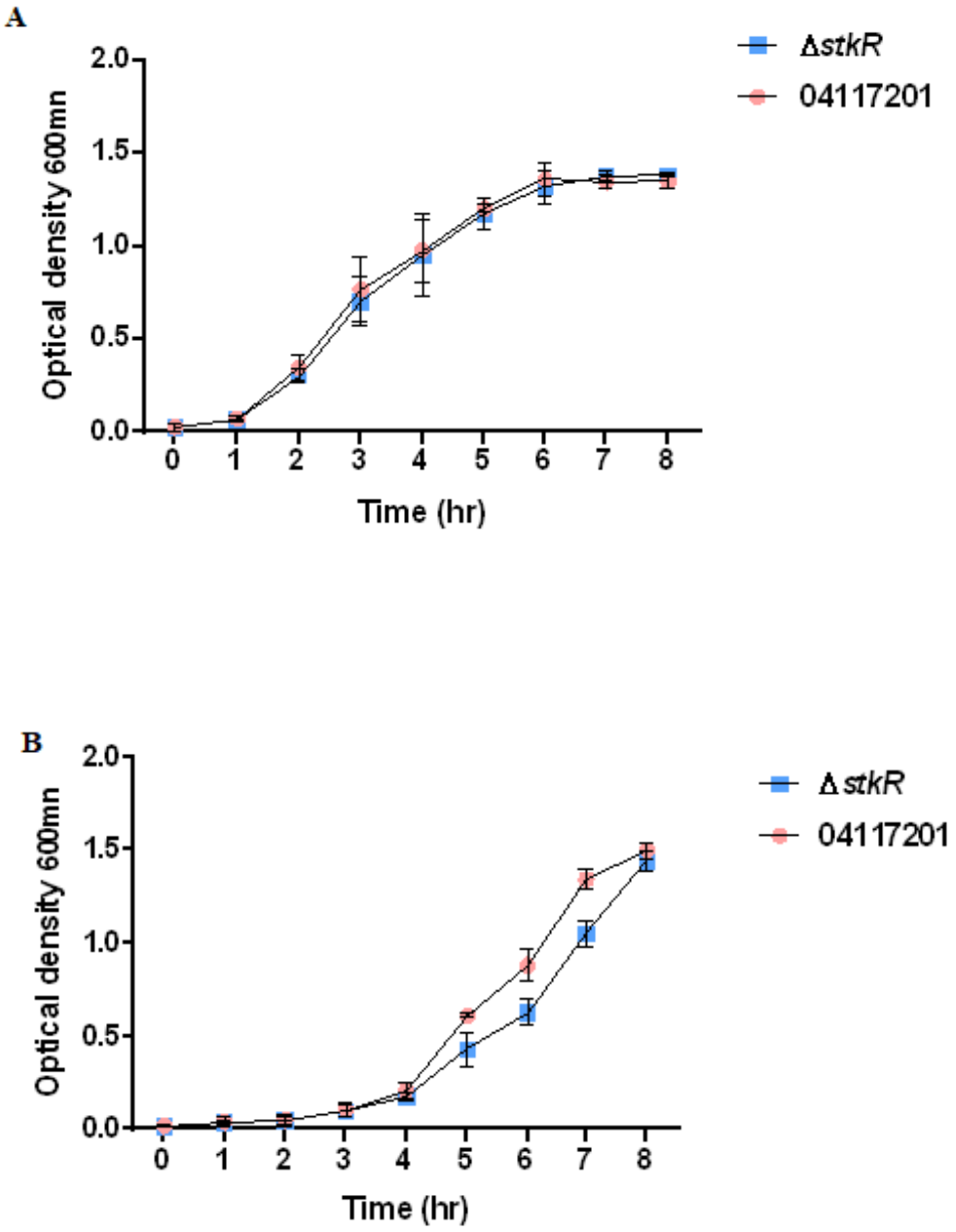
A
Optical density 600mn
2.0
1.5
1.0
0.5
0.0
0
1
2
3
4
5
6
7
8
Time (hr)
ΔstkR
04117201
B
Optical density 600mn
2.0
1.5
1.0
0.5
0.0
0
1
2
3
4
5
6
7
8
Time (hr)
ΔstkR
04117201

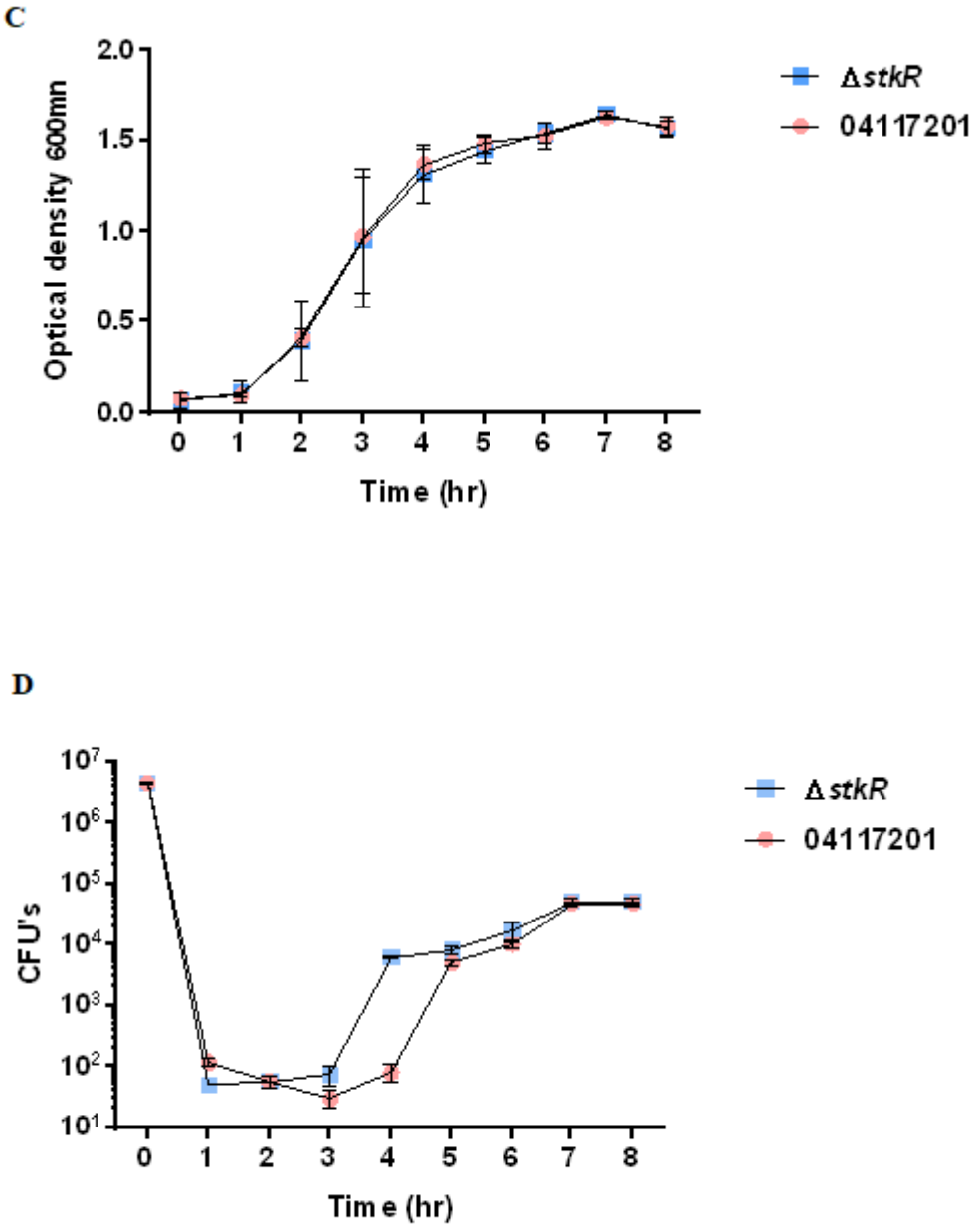

Figure 3.2: Growth analysis of the *A. baumannii* 04117201 WT and Δ*stkR* mutant strains

A. baumannii strains, 04117201 WT (pink circle) and Δ*stkR* mutant (blue square) were assessed for growth in a variety of media. Overnight bacterial cultures were used to inoculate 10 mL of media, samples of bacterial cells were taken every hour and growth levels determined spectroscopically at OD_{600} or by CFU plate count. Cells were grown in four different media; (A) MH, (B) M9, (C) lung, and (D) sheep blood. Bars represent the standard deviation of three replicates.

3.5.3 Antimicrobial resistance profiles of *A. baumannii* 04117201 and the Δ*stkR* mutant

As TCSTSs are known for regulating a variety of factors that influence antibiotic resistance, the 04117201 parent and Δ*stkR* derivative were assessed by MIC analysis for their ability to resist a variety of compounds including commonly used antibiotics and antimicrobials (Table 3.3). Of the 16 compounds tested, the MIC only altered for six compounds for the Δ*stkR* mutant strain when compared to the 04117201 parent. Exposure to CST and PMB, both cationic antimicrobial compounds, produced a 2-fold increase in resistance of the Δ*stkR* mutant. There was a marginal increase in resistance levels for Δ*stkR* for CHL, chlorhexidine (CHX), rifampicin (RIF) and KAN (Table 3.3).

3.5.4 Cell surface hydrophobicity after treatment with a sub-MIC level of CST

The antibiotic CST acts by attaching and displacing magnesium and calcium cations that act to stabilise the LOS in the *A. baumannii* cellular membrane (Sepahvand *et al.* 2017). Cell surface hydrophobicity is known to influence the affinity of CST (Moffatt *et al.* 2010). Since, a difference in resistance to CST was observed when *stkR* was inactivated, cell surface hydrophobicity of the Δ*stkR* mutant strain was compared with the 04117201 parent (Rosenberg *et al.* 1983, Eijkelkamp *et al.* 2013). The Δ*stkR* mutant strain was found to have an increased cell surface hydrophobicity index compared with the 04117201 parent when not exposed to CST ($P < 0.001$; Figure 3.3). However, when both strains were exposed to sub-MIC levels of CST, the Δ*stkR* mutant showed a significant decrease in cell surface hydrophobicity ($P < 0.01$; Figure 3.3) compared to the 04117201 WT strain. Additionally, CST exposure decreased cell surface hydrophobicity of the 04117201 WT strain ($P < 0.01$; Figure 3.3) however, this was less marked when compared to the Δ*stkR* mutant.

Table 3.3: Antimicrobial resistance profile of the *A. baumannii* 04117201 WT and Δ*stkR* mutant strains

	***A. baumannii* strain**		
Compound[abc]	**WT**	**Δ*stkR***	**Antibiotic family group**
AMK	10	10	Aminoglycoside
AMP	>500	>500	ß-lactam
CHL	5	8	Amphenicol
CHX	10	15	Chlorobenzenes
CIP	30	30	Carboxyl fluoroquinoline
CST	8	16	Polymyxin
GEN	500	500	Aminoglycoside
KAN	3000	>3000	Aminoglycoside
NAL	1250	1250	Quinolone
NOV	31	31	Aminocoumaria
PEN	125	125	Phenol ether
PMB	16	32	Polymyxin
RIF	4	6	Ansamycins
STR	>300	>300	Aminoglycoside
TEL	1.87	1.87	Metal
TRI	0.15–0.65	0.31–0.65	Diphenyl ether
TX	64	64	Nonionic surfactant

[a] AMK, amikacin; AMP, ampicillin; CHL, chloramphenicol; CHX chlorhexidine; CIP, ciprofloxacin; CST, colistin; GEN, gentamicin; KAN, kanamycin; NAL, nalidixic acid; NOV, novobiocin; PEN, pentamidine; PMB, polymyxin; RIF, rifampicin; STR, streptomycin; TEL, tellurite; TRI, triclosan; TX, triton X100.

[b] amounts presented in μg/mL

[c] All strain were grown in MH media

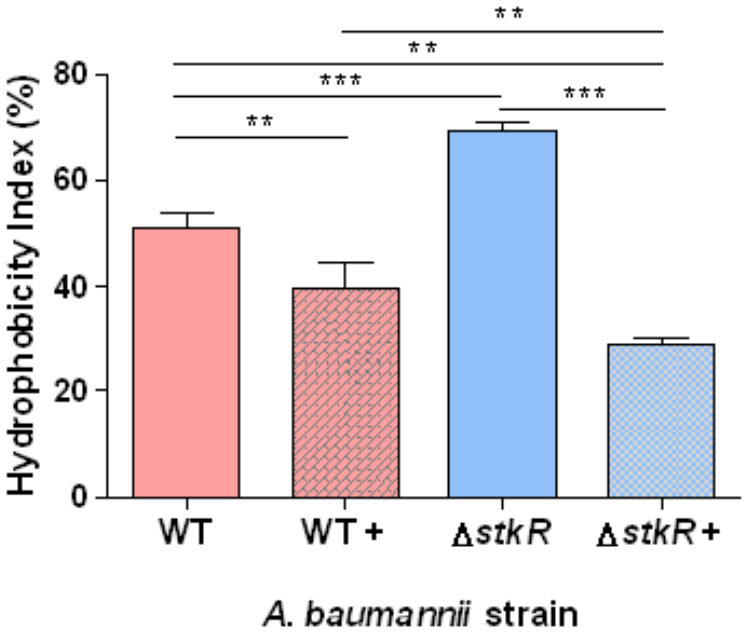

Figure 3.3: Cell surface hydrophobicity of the *A. baumannii* 04117201 WT and Δ*stkR* strains with / without CST treatment

Cell surface hydrophobicity was examined using the microbial adhesion to hydrocarbons (MATH) test (Rosenberg *et al.* 1983, Eijkelkamp *et al.* 2013). *A. baumannii* 04117201 WT and Δ*stkR* strains were tested either before or after exposure to 3 μg/mL of CST (+). Bars represent the standard deviation of three replicates. A Kruskal–Wallis test was performed to compare the means of the WT and Δ*stkR* cells with and without CST exposure. *** $P < 0.001$, ** $P < 0.01$ as established by an analysis of variance test.

3.5.5 Visualising the effects of CST treatment on the bacterial cell envelope

Since the mode of action of CST is disruption of the outer membrane, changes in the bacterial cell surface were assessed by TEM after CST treatment. Initial TEM analysis of the *A. baumannii* 04117201 and Δ*stkR* strains revealed a normal bacterial cell outer membrane (Figure 3.4; A, B). However, exposed to sub-MIC levels of CST (3 μg/mL) produced membrane surface protrusions in the 04117201 WT but not in the Δ*stkR* strain (Figure 3.4; C, D). The number of protruding events per bacterial cell known as blebs/cell (Alves *et al.* 2010, Girardello *et al.* 2017) were determined for both strains after treatment with 3 μg/mL CST. A total of 30 independent fields, including a minimum of 10 cells per field of view, spanning three different slides, were used to count blebs/cells. A significant increase in the number of blebs/cell in the 04117201 WT strain compared to the Δ*stkR* mutant could be observed at 2.5±0.3 blebs/cell vs 0.7±0.05 blebs/cell, respectively ($P < 0.0001$). Assessments of skewness, kurtosis and the Shapiro–Wilk normality test followed by an analysis of variance were used to assess significance. Treatment of the cells with a higher concentration of CST (12 μg/mL) resulted in both strains exhibiting extensive membrane perturbation leading to a breakdown of the bacterial cell wall with partially disintegrated cells (Figure 3.4; E, F).

3.5.6 Visualisation of the LOS of *A. baumannii* 04117201 and the Δ*stkR* derivative

A. baumannii acquires resistance to CST by three known mechanisms that affect the lipid A portion of the LOS. This is through either the complete loss of lipid A (Moffatt *et al.* 2010) or modifications by either GalN and/or pEtN (Arroyo *et al.* 2011, Chin *et al.* 2015) as described previously. To determine if lipid A was present or had undergone a significant modification, silver staining of the LOS was performed (Figure 3.5). Analysis by silver stained sodium dodecyl sulphate polyacrylamide gel electrophoresis (SDS-PAGE) identified a comparable lipid A profile between these strains (Figure 3.5).

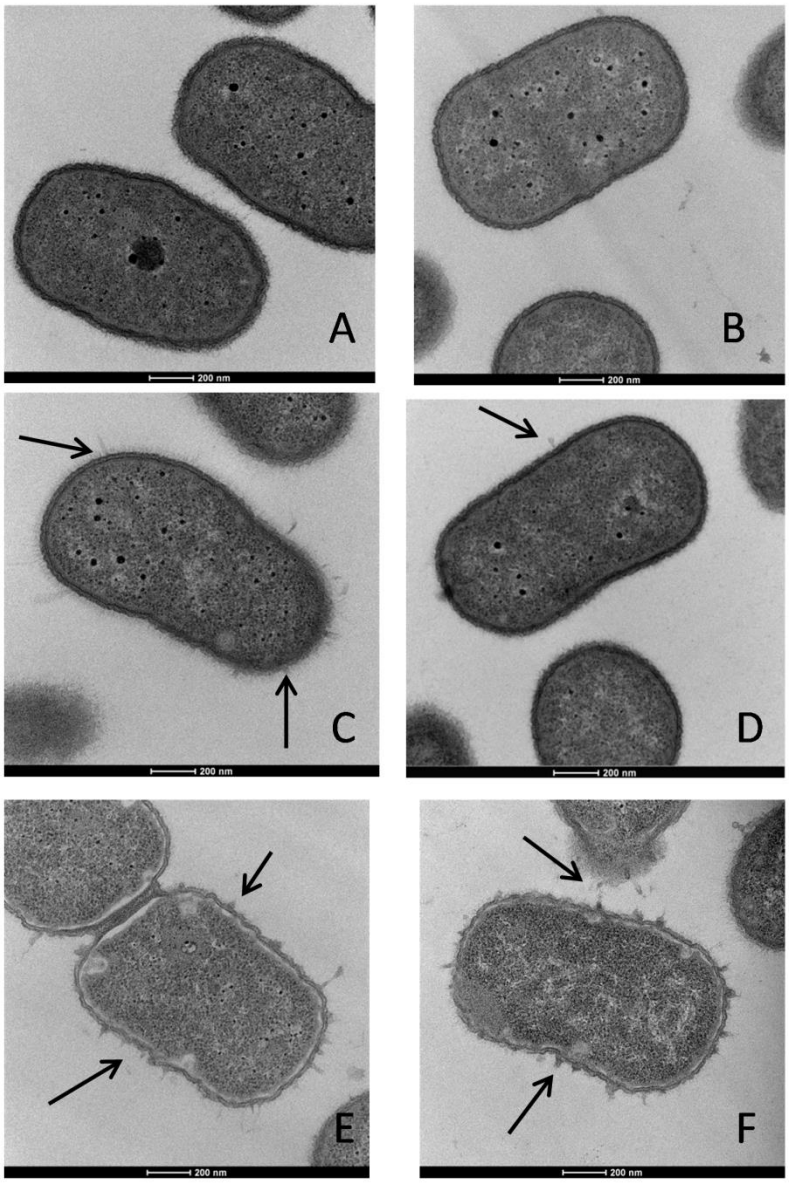

Figure 3.4: Membrane perturbation of the *A. baumannii* 04117201 and and Δ*stkR* strains with CST treatment

A. baumannii 04117201 and Δ*stkR* mutant cells were subjected to sub-MIC levels of CST (3 μg/mL and 12 μg/mL) and cross-sections were examined by TEM (60,000 × magnification); 200 nm scale is shown at the bottom of the image in white. Images are of (A) 04117201 WT, (B) Δ*sktR* mutant, (C) 04117201 WT after exposure to 3 μg/mL CST, (D) Δ*stkR* mutant after exposure to 3 μg/mL CST, (E) 04117201 WT after exposure to 12 μg/mL CST, and (F) *stkR* mutant after exposure to 12 μg/mL CST. The images are representative of data obtained; arrows show membrane perturbation and/or leakage of the cell contents.

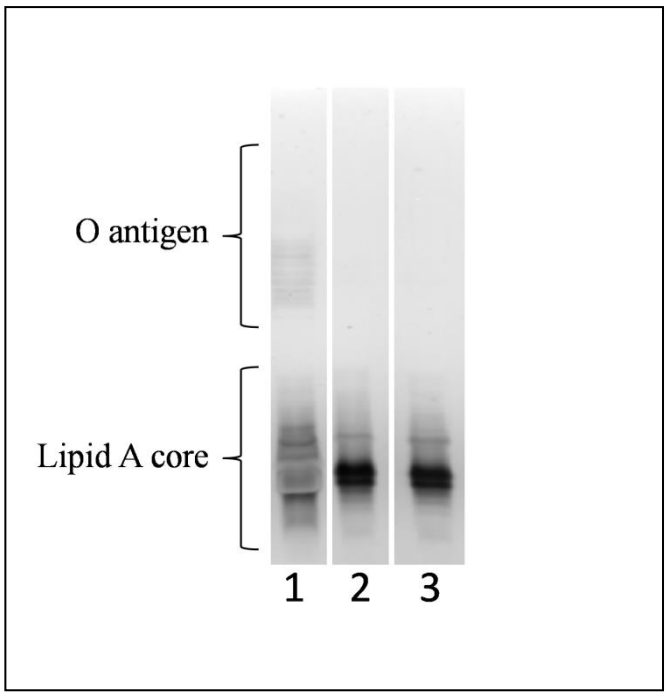

Figure 3.5: LOS analysis of the *A. baumannii* 04117201 WT and Δ*stkR* mutant strains

Whole cell lysates prepared from *A. baumannii* 04117201 and Δ*stkR* mutant cells were resolved on a 15 % polyacrylamide gel before silver staining. Lane 1 is a *P. aeruginosa* PA01 sample used as a positive control to visualise the lipid A and O-antigen components; Lane 2 is *A. baumannii* 0411720, and Lane 3 is *A. baumannii* Δ*stkR*. Brackets identify the lipid A core and O-antigen regions.

3.5.7 qRT-PCR analysis of *pmrCAB* in the *A. baumannii* 04117201 and Δ*stkR* mutant strains treated with a sub-MIC concentration of CST

The PmrAB TCSTS is known to regulate *pmrC* whose product is responsible for lipid A modification by the addition of pEtN, leading to an increase in CST resistance as previously described (Arroyo *et al.* 2011). Therefore, to investigate if this system played a role in the observations here, the expression of *pmrCAB* was analysed. Gene expression was analysed using qRT-PCR with RNA isolated from *A. baumannii* 04117201 and Δ*stkR* cells post treatment with 3 μg/mL of CST. An increase in transcription of the *pmrCAB* operon in the Δ*stkR* mutant compared to the 04117201 WT strain when exposed to sub-MIC of CST was observed; *pmrA* by 6.63-fold ($P < 0.02$), *pmrB* by 8.22-fold ($P < 0.0001$) and *pmrC* by17.63-fold ($P < 0.0003$). Increased transcription of *pmrCAB* can also be related to point mutants in the *pmrCAB* genes. Sequencing analysis was therefore undertaken on the Δ*stkR* mutant strain to determine if there were any point mutations in the *pmrCAB* genes. However, analysis of the DNA sequence of the 3.6 kb region encompassing the *pmrCAB* operon did not identify any point mutants in this region in the Δ*stkR* mutant strain (data not shown).

3.6 Discussion

A. baumannii have the ability to cause disease through a number of mechanisms, including adhering to biotic surfaces and resisting antimicrobial therapies, both essential mechanisms required to persist in a host (McQueary *et al.* 2011, Richmond *et al.* 2016). As such this work was initiated by identifying a potential highly virulent strain to investigate the virulence potential of *A. baumannii*. Examination of 11 clinical strains identified *A. baumannii* strain 04117201 as being the most adherent to A549 human pneumocytes (Figure 3.1). Additionally, examination of the antimicrobial resistance profiles of our collection of *A. baumannii* stains revealed that 04117201 is resistant to a wide range of compounds (Table 3.2). These findings, together with the demonstrated ability of the 04117201 to form a strong biofilm (Eijkelkamp *et al.* 2011b), resulted in the selection of this strain as the candidate to examine in detail potential virulence characteristics.

TCSTSs are involved in regulating a variety of virulence traits including antibiotic resistance, biofilm formation, and adhesion to eukaryotic cells as described

previously. Sequencing of the *A. baumannii* 04117201 strain genome revealed that this strain contains five TCSTS that are absent in the avirulent *A. baumannii* strain SDF. Therefore, any or all of these five TCSTS potentially correlate to the increased virulence potential, e.g., cell adherence and antimicrobial resistance exhibited by the 04117201 strain. As such, the TCSTS we termed StkRS was chosen for analysis through genetic manipulation by replacing the *stkR* RR with an ERY^R cassette giving rise to the *A. baumannii* Δ*stkR* mutant strain.

Comparison of the antimicrobial resistance profile of the resulting Δ*stkR* mutant strain compared to its parent showed this mutation caused a 2-fold increase in resistance to the polymyxins, CST and PMB, as well as minor increases in resistance to CHL, KAN and RIF (Table 3.3). The mechanism by which StkRS influences polymyxin resistance is currently unknown, however previous studies have found that *A. baumannii* strains lacking LOS are CST resistant and show a reduction in cell surface hydrophobicity (Soon *et al.* 2012). Therefore, alterations in cell surface hydrophobicity were examined to see if it also played a role in the modification in resistance seen in this mutant strain. The Δ*stkR* mutant strain displayed a significant decrease in cell surface hydrophobicity compared to the WT strain when exposed to CST at subinhibitory concentrations (Figure 3.3); these data demonstrate the ability of the Δ*stkR* mutant strain to respond under this particular stress by altering its bacterial cell surface. These results are similar to the study described previously, undertaken by Soon *et al* (2012), connecting the lack of LOS or herein, the significant decrease in LOS as seen in the Δ*stkR* mutant strain to a reduced ability of CST to bind to the membrane therefore increasing CST resistance.

TEM analyses of 04117201 and Δ*stkR* cells after CST treatment identified varying levels of membrane perforation, partially disintegrated cells and sometimes complete cellular lysis. The results are comparable to other studies investigating the effect of CST on the membrane (Mohamed *et al.* 2016, Girardello *et al.* 2017). Here, under sub-MIC CST treatment *A. baumannii* 04117201 displayed a significant increase in membrane perturbation/protrusion known as blebbing events compared to the Δ*stkR* mutant (Figure 3.4), indicating envelope disruption and the collapse of the outer membrane. This may be related to the decrease in cell surface hydrophobicity exhibited by the Δ*stkR* strain under CST treatment, since dramatic decreases in cell

surface hydrophobicity are related to CST resistance (Moffatt *et al.* 2010, Da Silva *et al.* 2017, Carretero-Ledesma *et al.* 2018). As silver staining of a whole cell lysate prepared from 04117201 and Δ*stkR* cells showed a comparable lipid A profile, the observed increase in CST resistance is not due to loss or gross modification of lipid A (Henry *et al.* 2012).

In other Gram-negative pathogens, such as *Salmonella enterica* and *Klebsiella pneumoniae*, *pmrCAB* is regulated by other TCSTSs. In these cases, the PhoPQ TCSTS leads to the activation of a small polypeptide known as PmrD, which binds to PmrA and stabilises it in its phosphorylated state, resulting in a concomitant increase in *pmrC* transcription (Gunn 2008, Cheng *et al.* 2010, Wand *et al.* 2016). Examination of available *Acinetobacter* genomes including the *A. baumannii* 04117201 strain failed to find a *pmrD* homologue . However, cross-regulation of *pmrCAB* is not limited to interactions with the PhoPQ system but can be further complicated by another TCSTS in *S. enterica* (designated *preAB*) (Merighi *et al.* 2009). This PreAB is similar to the *qseBC* system found in *E. coli* and appears to influence expression of *pmrCAB* as well, confirming that the *pmrCAB* system can be regulated by a number of TCSTS. Interestingly, a study in *S. enterica* of deletions or insertions in the PreB HK led to up-regulation of the *pmrCAB* system, but there was no concurrent increase in CST resistance, possibly because *pmrD* is not involved (Merighi *et al.* 2006).

Previous studies have also shown that increased decoration of lipid A results in CST resistance, and also commonly involves the PmrAB TCSTS. Increased transcription of the transferase *pmrC,* which can occur by mutations in the *pmrCAB* operon leads to the addition of pEtN to lipid A (Beceiro *et al.* 2011). However, sequence analysis did not identify any such mutations in the *pmrCAB* operon in the *A. baumannii* Δ*stkR* mutant strain suggesting an alternate mechanism causing up-regulation of the *pmrCAB* operon.

Another mechanism appears to work alongside but independently of the addition of pEtN. Chin *et al* (2015), using mass spectrophotometer analysis of a CST-resistant *A. baumannii* strain, identified decorations of the lipid A structure with both pEtN and GalN. The *pmrB* determinant regulates NaxD deacetylase which is involved in the addition of GalN to lipid A; when deleted, a CST-sensitive phenotype is

produced (Beceiro *et al.* 2011, Chin *et al.* 2015, Liu *et al.* 2016, Deveson Lucas *et al.* 2018). Examination of the *pmrCAB* operon using qRT-PCR revealed that the level of *pmrA*, *pmrB* and *pmrC* increased significantly in the Δ*stkR* mutant compared to the 04117201 WT strain when exposed to CST. As such there could be an addition of pEtN to the lipid A components of the cell and possibly accompanied by the addition of GalN when the bacterial cell is exposed to CST. The data presented here demonstrates that the PmrAB TCSTS may be contributing to CST resistance which could occur through the addition of pEtN and GalN. Additionally, the StkRS TCSTS is a contributing regulator of the PmrAB system. These results collectively display a probable reason for the CST resistance seen of the Δ*stkR* mutant strain.

Interestingly, a decrease in fitness was also identified for the Δ*stkR* mutant compared to the 04117201 WT strain when grown in M9 medium (Figure 3.2, B); a slight lag can be seen at the time points 6 and 7 hour time points. These observations are in contrast to Jones *et al* (2017), where the increased CST resistance resulted in a decreased survival rate when exposed to hydrogen peroxide (H_2O_2).

This is the first study to describe the novel TCSTS StkRS identified in the clinically relevant *A. baumannii* strain 04117201. These data have demonstrated that the increase in CST resistance seen for the Δ*stkR* mutant strain is not due to the loss of lipid A. However, it appears to be due to increased transcription of the *pmrCAB* operon. Additionally, cell surface hydrophobicity changes are apparent in the Δ*stkR* mutant and 04117201 WT strains after CST treatment, which correlates to the proposed addition of pEtN and GalN in the LOS of the *A. baumannii* strains. These data demonstrate that the deletion of *stkR* promotes for up-regulation of *pmrCAB* and a decrease in cell surface hydrophobicity, increasing CST resistance. CST represents a “last resort” antibiotic used for the treatment of severe *A. baumannii* infections, and understanding the resistance mechanisms to this clinically important compound is vital for its continued application. Additionally, as TCSTS are attractive drug targets, understanding their interconnected regulation is imperative for future development.

CHAPTER 4 *A. baumannii* virulence factors and the host immune response influences bacterial morbidity and mortality in a murine pneumonia infection model

Declaration for thesis chapter four

Declaration by candidate

In chapter four the nature and extent of my contribution to the work was the following:

Nature of contribution	**Extent of contribution**
Experimental design, performance of experiments, writing, editing and revision of manuscript	70 %

The following co-authors contributed to the work.

Name	**Nature of contribution**	**Extent of contribution**
Uwe Stroeher	Experimental design, performance of experiment (assisted with the *in vivo* model) editing and revision of manuscript	15 %
Shashikanth Marri	Performance of experiment (alignment of the RNA HiSeq strands against 04117201 *A. baumannii*)	5 %
Melissa Brown	Experimental design, editing and revision of manuscript	10 %

The undersigned hereby certify the above declaration correctly reflects the nature and extent of the candidates and co-authors contribution to this work.

Candidate's Date

Signature 2019

Supervisor's Date

Signature 2019

4.1 Preface

This chapter is to be submitted for publication in the journal mBio as **Giles, S. K, Stroeher, U. H, Marri, S., and Brown, M. H.** (2020) *Acinetobacter baumannii* virulence factors and the host immune response influences bacterial morbidity and mortality in a murine pneumonia infection model.

4.2 Abstract

MDR *A. baumannii* is of major global concern causing pneumonia, bacteraemia and septicaemia with mortality rates exceeding 70 % (Seifert *et al.* 1995, Fagon *et al.* 1996, Makris *et al.* 2018). Therefore, to examine this bacterium, in relation to virulence the novel TCSTS StkRS in the clinical *A. baumannii* 04117201 strain was investigated. An *A. baumannii* Δ*stkR* derivative was constructed from the *A. baumannii* 04117201 WT strain by deletion of the *stkR* response regulator gene and analysed. Comparative transcriptomic analyses were undertaken of the Δ*stkR* mutant against the 04117201 parent strain with RNA isolated from cells grown in four different media, chosen to represent four growth conditions. Firstly, M9 media representing the numerous hospital surfaces with a minimal nutrient and carbon sources, secondly lung media mimicking a pneumonia infection, thirdly whole blood representing septicaemia and lastly, Mueller Hinton (MH) media commonly used within the laboratory. . Numerous expression changes in the Δ*stkR* transcriptome were observed when grown in lung and M9 media over one thousand genes had an altered expression compared to the parent strain; interestingly in the blood and MH media there were minimal changes in transcription. *In vitro* assessment of the Δ*stkR* mutant identified an increased bacterial cell adherence to A549 human pneumocytes cells, enhanced survival under human serum stress and increased survival in a macrophage-mediated killing assay, in addition to an increased bacterial load in the lungs, blood and spleen in an intranasal murine model. Using an Antibacterial RT^2-PCR profiler array the innate immune response was examined in the lungs from inoculated mice. Infection with the 04117201 WT strain resulted in the differential expression of 75 genes (24 up- and 51 down-regulated more than 2-fold) compared to the naïve lung. In comparison, infection with the Δ*stkR* mutant strain modulated the expression of 66 genes (23 up- and 43 down-regulated more than 2-fold). This implies that removal of *stkR* dampens the innate immune response consequently leading to a larger bacterial load in the mouse. Taken together, this research has

identified that deletion of the *stkR* response regulator gene in *A. baumannii* 04117201 affects multiple factors that influence the virulence capacity and subsequently the disease progress of this organism.

4.3 Introduction

A. baumannii is most commonly found as a hospital-acquired pathogen infecting immune-compromised patients, but is also being reported more frequently in the wider community (Peleg *et al.* 2008, Fang *et al.* 2016, Ziolkowski *et al.* 2018). Severe infections such as ventilator-acquired pneumonia and bacteraemia potentially causing septicaemia and open-wound infections are instances where *A. baumannii* can commonly be identified (Dijkshoorn *et al.* 2007, Peleg *et al.* 2012). Of particular concern is the high mortality rate (between 55 % and 80 %) and the ability of *A. baumannii* to occupy various niches and withstand environmental pressures in the hospital as well as within a host. To survive, it must be able to respond to environmental changes and stressors by, for example, switching on efflux pumps in the presence of antibiotics or biocides This can include resistance to desiccation, cleaning regimes (e.g. disinfectants), antibiotics, and the host's immune response (e.g. macrophage phagocytosis) (Guo *et al.* 2016, Warner *et al.* 2016). Although many of the virulence factors of *A. baumannii* are known and are being examined, the regulatory mechanisms of these factors are only now being understood. One type of regulatory mechanism used by *A. baumannii* is the two-component signal transduction system (TCSTS) (Kroger *et al.* 2016), which allow a bacterium to sense and quickly adapt to its environment. TCSTS are comprised of two proteins: a membrane-bound histidine kinase (HK) and an intracellular cytoplasmic-located response regulator (RR). The HK receives a signal and undergoes a conformational change; this change results in phosphorylation of a conserved histidine residue and the phosphoryl group is subsequently transferred to an aspartate residue on the cognate RR. The RR then undergoes a conformational change, enabling it to act upon downstream genetic elements to modulate their transcription.

Numerous TCSTSs regulate a variety of mechanisms across bacterial species. For example, in *A baumannii*, the AdeRS TCSTS activates the multidrug efflux pump AdeABC (Marchand *et al.* 2004), the PmrAB TCSTS regulates genes associated with alterations in lipid A (Chen *et al.* 2013), and the EnvZ/OmpR TCSTS

is involved in the regulation of genes that respond to changes in osmolarity (Cai *et al.* 2002). TCSTSs can regulate the bacterial cell surface properties that alter adherence to biotic or abiotic surfaces and can lead to the formation of biofilms (Casino *et al.* 2010, Russo *et al.* 2016). TCSTSs have also been associated with virulence potential in aiding the bacteria (via different mechanisms) to survive or subvert macrophage cells and other cells of the immune system (Alves *et al.* 2017, Huang *et al.* 2017); this allows for an increased disease state and is an import factor in the prevalence of *A. baumannii* strains.

The innate immune system uses a large variety of genes to induce a response to an infection. The first line of defence commonly involves cytokines and chemokines e.g. IL6, which recruits phagocytic cells like neutrophils to the site of infection (van Faassen *et al.* 2007). To evade the immune response, *A. baumannii* have developed mechanisms that can reduce early neutrophil recruitment leading to higher persistence and therefore a disease state of the host (Dikshit *et al.* 2018). Neutrophils can kill bacteria using neutrophil extracellular traps (NETs). Recently, *A. baumannii* was discovered to inhibit NET formation by suppressing the adhesion of the neutrophils, thereby prolonging bacterial persistence (Kamoshida *et al.* 2018). The immune response against *A. baumannii*, and other infectious bacteria, also relies on the Toll-like receptor 4 pathways and CD14 as they both play a critical role in sensing LPS and LOS (Knapp *et al.* 2006). Bacteria like *E. coli* and *Brucella melitensis* interfere with the Toll /interleukin-1 receptor by secreting homologues, disrupting its function (Cirl *et al.* 2008).

This study aimed to identify what impact the StkRS TCSTS has on the virulence potential of the clinical *A. baumannii* strain 04117201. The hypothesis states that deletion of the *stkR* RR gene in the 04117201 WT strain will increase virulence of the Δ*stkR* mutant strain. The 04117201 WT and the generated Δ*stkR* mutant strain from unpublished data, were examined for several virulence traits, both *in vitro* and *in vivo*, assessment found an enhancement of the pathogenic potential of the Δ*stkR* mutant compared to the 04117201 WT strain.

4.4 Materials and Methods

4.4.1 Bacterial strains, media and growth conditions

The clinical *A. baumannii* bacterial strains used and cultured in this study have been described previously (Giles *et al.* 2015). For maintenance, conjugation, cloning, and replicating plasmids, *E. coli* DH5α, SM10, or JM109 cells were used (Hanahan 1983, Simon *et al.* 1983, Yanisch-Perron *et al.* 1985). The *A. baumannii* strain 04117201 belongs to the international clone type II and was obtained from a tracheal aspirate sample at Flinders Private Hospital, SA, Australia (Eijkelkamp *et al.* 2011a).

4.4.2 Statistical analysis

The Graphpad Prism 7.01 (La Jolla, United States of America) statistical package was used to analyse the results of all experiments. Assessments of skewness, kurtosis, and the Shapiro-Wilk normality test (Samuels *et al.* 2012) were undertaken on all measures and non-parametric tests were used as needed. Analyses of the *in vitro* and *in vivo* models were performed using a Student's *t*-test. A Contingency test (chi squared) was used to present the mouse mortality results. A probability, $P \leq 0.05$ was considered statistically significant (* $P < 0.05$; ** $P < 0.001$; and *** $P < 0.0005$).

4.4.3 Deletion replacement mutant construction by homologous recombination

Construction of a *stkR*-inactivated derivative of *A. baumannii* 04117201 was undertaken by homologous recombination. In brief, DNA fragments corresponding to 1.2 kb upstream and 1 kb downstream of *stkR* were PCR amplified using VELOCITY^{TM} DNA polymerase (Bioline, NSW, Australia) and specific oligonucleotides designed in NetPrimer (www.premiersoft.com) (Table 3.1). The cycling conditions used were 2 minutes at 94°C, followed by 30 cycles of 45 seconds at 94°C, 45 seconds at 60°C, and 90 seconds at 72°C. This was followed by a final extension of 10 minutes at 72°C. PCR products of the appropriate size were cloned into the suicide vector pEX18Tc via *Xba*I, *Bam*HI, or *Sac*I restriction sites and transformed into *E. coli* DH5α cells (Adams *et al.* 2018). Following sequence confirmation, pEX18Tc clones were electroporated into fresh electrocompetent *A. baumannii* 04117201 bacterial cells (Eijkelkamp *et al.* 2013).

4.4.4 Eukaryotic cell adherence and invasion assay

The adherence of *A. baumannii* cell to A549 human type 2 pneumocytes was investigated as previously described (Giles *et al.* 2015) with the following modifications. When assessing bacterial invasion, cells were treated with 400 μg/mL of amikacin (AMK) for 1 hour at 37°C. Cells were washed with 10 mL of sterile MilliQ. Washed cell monolayers were detached from the plate by treating with 100 μL of 0.25 % trypsin in PBS. The eukaryotic cells were subsequently lysed by the addition of 400 μL of 0.025 % Triton X-100. Serial 10-fold dilutions were spread plated onto LB agar to determine the number of CFU of adherent bacteria per well. The data collected for the adherence assays were obtained from three replicates and represent data points from each experiment in quadruplicate wells. Serum survival assay

Serum sensitivity assay was adapted from (Kim *et al.* 2009). In short, cells were grown to an OD_{600} = 0.6 in MH media at 37°C. Cells were then incubated with PBS, 40 % human serum or 40 % heat-inactivated human serum at 37°C for 2 hours with shaking. Bacteria were serially diluted and plated to determine the CFUs. Data was collected from three replicates.

4.4.5 Macrophage cell survival assay

Survival under macrophage pressure was investigated using the method of (Qiu *et al.* 2012) with the following modifications. Macrophage J774.2 cell lines were grown in Dulbecco's Modified Eagle media (Invitrogen, Australia) with 10% fetal bovine serum (Bovogen, Australia). Washed J774.2 monolayers in 24-well tissue culture plates were infected with bacterial inoculums containing ~1×10^7 CFU and spun at 1200 x *g* for 2 minutes. Wells were washed in PBS following a 2-hour infection at 37°C, and treated with 400 μg/mL of AMK for 1 hour at 37°C. The monolayers were washed with PBS; 10-fold dilutions were spread plated onto LB agar to determine the number of surviving CFU per well. The collated data are from three replicates and represent the data points from each experiment in quadruplicate wells.

4.4.6 *In vivo* mouse infection model

Female BL/6 mice aged 4 to 6 weeks were housed under pathogen-free conditions. Antibiotic-free pelleted food and autoclaved water were provided. Infection assays were performed intranasally, with approximately 5.0×10^8 CFU in 50 µl of PBS in groups of 15 mice per bacterial strain tested. Mice were euthanised at 24 hours post infection. After a pleural wash with PBS, the thoracic cavity was exposed and blood was collected by puncture of the right ventricle. Following blood collection, the pulmonary circulation was perfused with saline before the lung and spleen were separately excised into 1.5 mL of ice-cold PBS, weighed, and homogenised by a miller machine (FastPrep®24™ 5G, MP Biomedicals, Germany). The CFU of each strain was defined as CFU/mL of blood or CFU/whole lung or spleen after serial dilutions on to LB plates. All experiments involving mice were approved by the Animal Ethics Committee of Flinders University (851/13).

4.4.7 Bacterial and eukaryotic RNA isolation

RNA was extracted as described in Chapter two (Giles *et al.* 2015) with the following modifications. To measure transcriptional levels for either qRT-PCR or HiSeq RNA transcriptome analysis (conducted by SA Pathology; Central Adelaide Local Health Network); bacterial cells were harvested from MH broth, M9 media, blood or lung media at OD_{600} of 0.6, pelleted by centrifugation 8,000 × *g* at 4°C for 5 minutes and then lysed using TRIzol reagent (Life Technologies, Australia) and 200 µL of chloroform. When extracting lung material, the lung was lysed with 2 mL of TRIzol reagent (Life Technologies, Australia) and 600 µL of chloroform. From the aqueous phase total RNA was extracted using the RNA Mini Kit II (Bioline, Australia) following the manufacturer's instructions. Samples were cleaned using the RNasey® Min Elute™ Cleanup kit (Qiagen, Australia) and the purity and quantity of total RNA determined by measuring the $OD_{260/280}$ ratio (NanoDrop1000, Thermo Scientific, Australia). Triplicate bacterial samples were pooled and sent to SA Pathology for ribosomal RNA reduction using an Epicentre Ribo-Zero kit before RNA library bar-coding was undertaken. Samples were run on the Illumina HiSeq platform (1 × 50 bp single reads). For RT-PCR, samples were treated with DNaseI (Promega, United States of America) following the manufacturer's instructions.

4.4.8 Mouse immune investigation using the Antibacterial RT^2-PCR profiler array

The Antibacterial RT^2-PCR profiler array was used to determine the mouse immune response post infection. Total RNA extracted from homogenised mouse lung was used together with the RT^2 First Strand kit and SYBR green RT-PCR Master Mix to inoculate a 84-well format Antibacterial RT^2-PCR profiler array (Cat#PAMM-148ZD) (Qiagen, USA). Sample preparation and cycle times were performed according to the Antibacterial RT^2-PCR array protocol using a CFX96 instrument (Bio-Rad, Australia). The C_t values were normalised using the *gapDH* housekeeping gene and $\Delta\Delta C_t$ values were calculated (Livak *et al.* 2001).

4.4.9 Cytoscape mapping

The Cytoscape network program was used to present the Antibacterial RT^2-PCR profiler array data. The cDNA $\Delta\Delta C_t$ expression values were submitted to the InnateBD pathway program (http://www.innatedb.com) and the 84 genes of the array were found to form 465 pathways. The network was analysed for betweenness and centrality. The importance of the gene is demonstrated by color: up-regulated is shown in green; down-regulation is shown in red.

4.4.10 Bioinformatics analysis

The quality of the cDNA reads obtained from the HiSeq was checked using Fastqc (http://www.bioinformatics.babraham.ac.uk/projects/fastqc/). Reads were subsequently mapped to the reference genome using the bowtie aligner (http://bowtie-bio.sourceforge.net/index.shtml). Approximately 95 % of the reads mapped to the 04117201 genome, of which 83 % mapped to the coding regions. To determine changes in gene expression, the number of reads obtained for each ORF was normalised using reads per kb of transcript per million reads mapped.

4.4.11 qRT-PCR

The iScript reverse-transcriptase cDNA synthesis kit (Bio-Rad laboratories Inc) was used to synthesise cDNA following the manufacturer's instructions. qRT-PCR was conducted using iTaq™ Universal SYBR® green super mix (Bio-Rad, Australia) in conjunction with a Rotor-Gene Q (Qiagen, USA). A typical qRT-PCR run was as follows: 1 minute at 95°C, 40 cycles of 10 seconds at 95°C, 15 seconds at 55°C, and

20 seconds at 72°C (Brazma *et al.* 2001). Transcriptional differences were calculated using the $\Delta\Delta C_t$ method (Livak *et al.* 2001). The 16S rRNA (A1S_r01) and *gapDH* (A1S_2501) transcription levels were used as a reference.

4.5 Results

4.5.1 Adherence capabilities of the *A. baumannii* 04117201 WT and Δ*stkR* mutant strains to A549 epithelial cells

As stated previously, since *A. baumannii* commonly enters in a host via respiratory pathways, the initial infection is in the lungs, which requires the bacteria to adhere to biotic cells. *A. baumannii* 04117201 WT and Δ*stkR* mutant strains [previously constructed as described (Section 3.4.2)] were investigated for their ability to adhere to A549 human pneumocytes cells. Interestingly, the Δ*stkR* mutant showed a 2.2-fold increase in adherence to the A549 monolayer compared with the parent strain (Figure 4.1, $P < 0.01$). Due to the increase observed in cell adherence, an invasion assay was also performed. The invasion model enumerates internalised bacteria to identify whether the bacteria are intracellular. No significant change in the number of bacteria invading the epithelial cells between the two strain was seen ($P > 0.05$) (data not shown).

4.5.2 Survival in human serum complement of *A. baumannii* 04117201 WT cells compared to the Δ*stkR* mutant

The first line of defence to a bacterial infection usually involves the innate host immune response. This includes a number of proteins and cells (Garcia-Patino *et al.* 2017) and one that plays a critical role is the complement system found in the serum fraction of blood (Chamoun *et al.* 2018). One action of the complement system is performed via the membrane attack complex that creates a pore in the bacterial cell causing cell death. To assess the *A. baumannii* 04117201 and the ΔstkR derivative for their ability to withstand the complement system, the bacterial cells were incubated with normal human serum and the bacteria enumerated. The Δ*stkR* mutant strain showed an approximate 20 % increase in survival compared with the 04117201 WT strain (Figure 4.2, $P < 0.0001$), demonstrating the Δ*stkR* mutant strain has an increased ability to within stand complement killing.

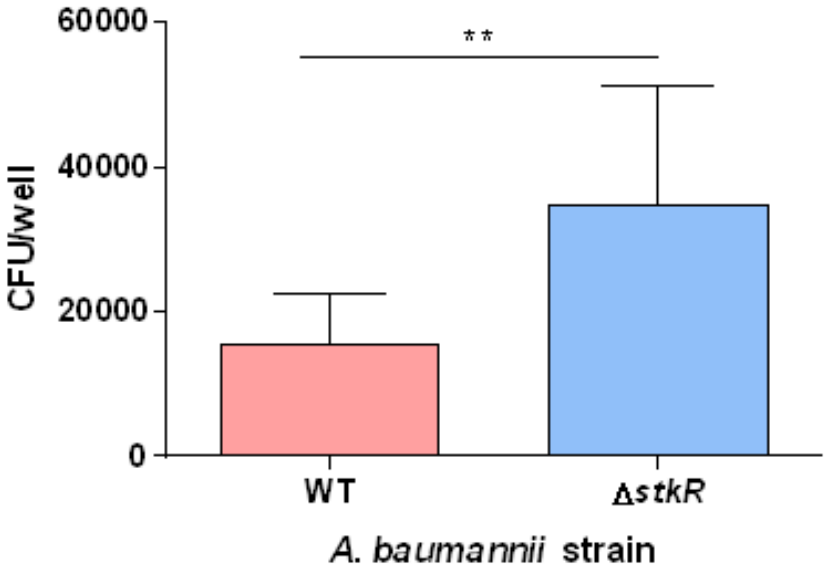

Figure 4.1: Cell adherence capacity of the *A. baumannii* 04117201 WT and Δ*stkR* mutant strains to A549 pneumocytes

The cell adherence capacity of the *A. baumannii* 04117201 WT and Δ*stkR* mutant strains were assessed. Bacterial cells were grown to a concentration of 1x10^7 CFU in MH, resuspended in DMEM and exposed to A549 pneumocytes four 4 hours, before bacterial cells were washed and enumerated. Adherent cells are presented as CFU/well. Bars indicate the standard error of three replicates. ** $P < 0.01$ as determined by an analysis of a parametric Student *t* test.

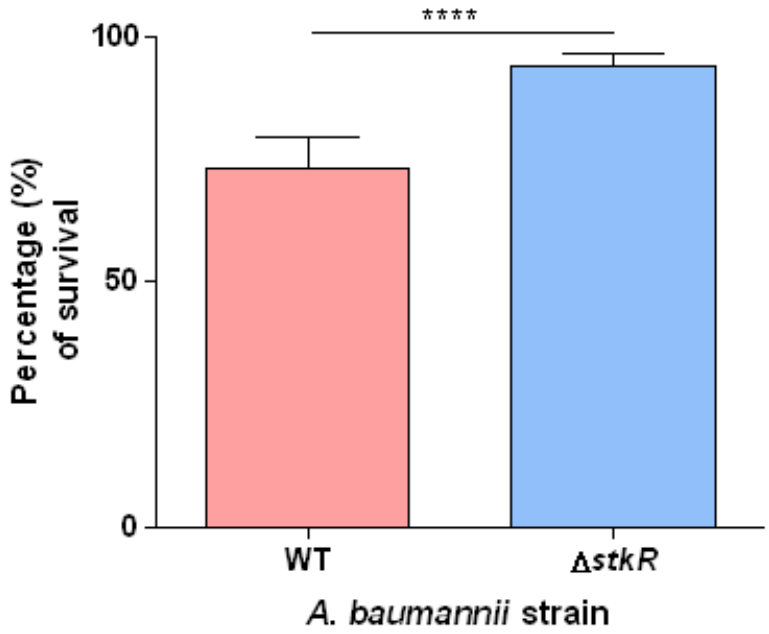

Figure 4.2: Survival of *A. baumannii* 04117201 WT and Δ*stkR* mutant strains in human serum

Survival of *A. baumannii* 04117201 and Δ*stkR* cells were examined. Bacteria were grown to a concentration of ~1x10^7 CFU in MH, resuspended in PBS and exposed to human serum for 2 hours. Following treatment with 400 µg/mL of AMK for 1 hour, monolayers were washed and enumerated. The number of bacterial cells post exposure is presented as percentage of survival. Bars indicate the standard error of three replicates. **** $P < 0.0001$ as determined by an analysis of a parametric Student *t* test.

4.5.3 Survival under J774.2 mouse macrophage stress of the *A. baumannii* 04117201 WT compared to the Δ*stkR* mutant strain

Macrophages and other phagocyte cells represent a major host defense system (Jun *et al.* 2013). Therefore, the ability of a bacterial cell to withstand phagocytosis dramatically increases its chance of persisting within a host. To investigate survival of the 04117201 WT and Δ*stkR* mutant strains, the bacterial cells were exposed to a monolayer of a J774.2 mouse macrophage cells. Enumeration of bacteria that survived phagocyte engulfment revealed a 3.3-fold increased survival rate of the Δ*stkR* mutant strain compared to the 04117201 WT strain (Figure 4.3, $P < 0.001$).

4.5.4 Infection capabilities of the *A. baumannii* 04117201 WT and Δ*stkR* mutant strains in a murine model

As an increase in the virulence potential of the Δ*stkR* mutant strain in a number of *in vitro* assays was identified, further investigation was undertaken to test if this trait is replicated in an *in vivo* mouse model. As such, C57/BL6 4 to 6 week-old female mice were used to assess the *in vivo* attributes of the 04117201 WT and Δ*stkR* mutant strains. Mice were challenged with bacterial cells introduced intranasally to mimic a pneumonia infection. A significant increase in the bacterial cell load of the Δ*stkR* mutant strain compared with the 04117201 WT strain was identified: 15-fold in the lung (Figure 4.4A, $P < 0.001$); 7-fold in the spleen (Figure 4.4B, $P < 0.01$), and 4-fold in the blood (Figure 4.4C, $P < 0.01$). Further assessment by a contingency test identified an increase in the number of mice that died due to the infection. The incidence of death increased from 3 % for mice infected with the 04117201 WT strain to 30 % for mice infected with the Δ*stkR* mutant strain (chi-square test $P < 0.01$).

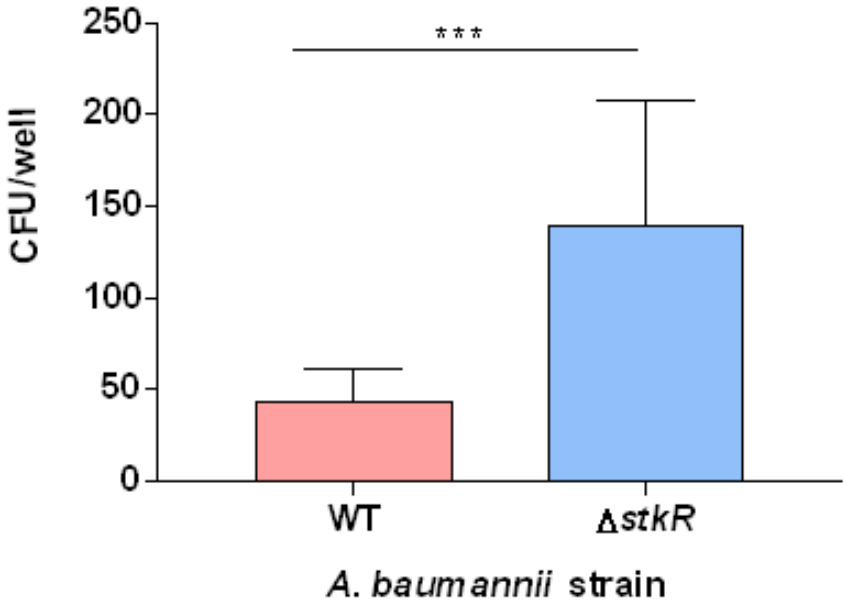

Figure 4.3: Bacterial cell survival of the *A. baumannii* 04117201 WT and Δ*stkR* mutant strains in J774.2 macrophages

A. baumannii 04117201 and the Δ*stkR* derivative were assessed for phagocytosic survival. Bacteria were grown to a concentration of ~1x10^7 CFU in MH, resuspended in DMEM and incubated with J774.2 mouse macrophage cells for 2 hours. Following treatment with 400 µg/mL of AMK for 1 hour, monolayers were washed and enumerated. The number of bacterial cells post exposure are presented as CFU/well. Bars indicate the standard error of three replicates. *** $P < 0.001$ as determined by an analysis of a parametric Student *t* test.

(A)

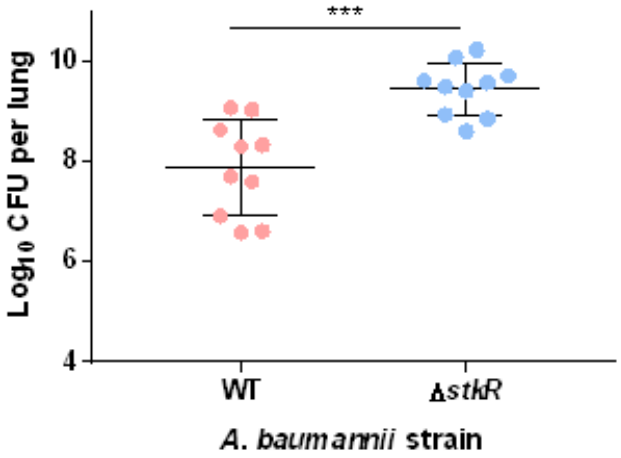
***
Log10 CFU per lung
10
8
6
4
WT
ΔstkR
A. baumannii strain

(B)

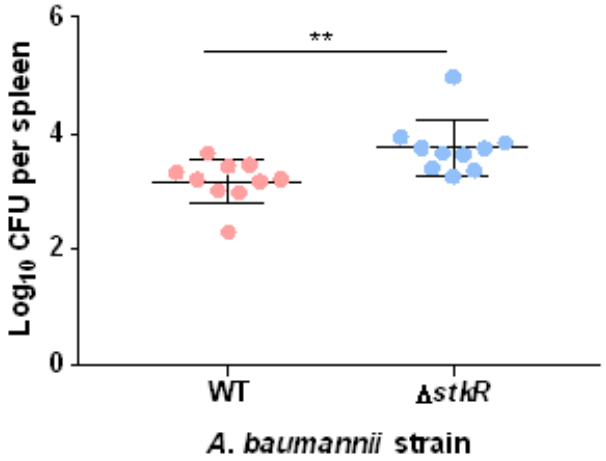
**
Log10 CFU per spleen
6
4
2
0
WT
ΔstkR
A. baumannii strain

(C)

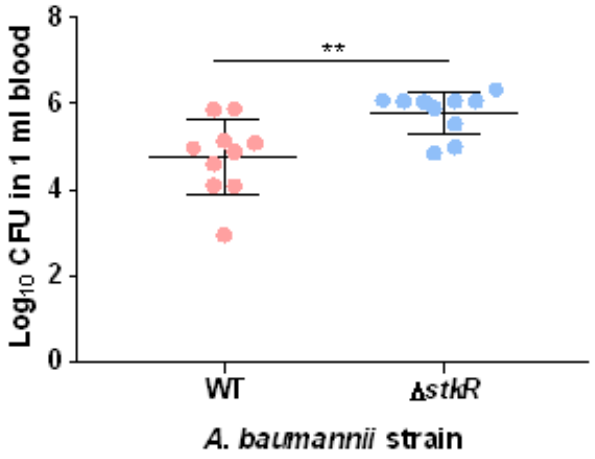
**
Log10 CFU in 1 ml blood
8
6
4
2
0
WT
ΔstkR
A. baumannii strain

Figure 4.4: Bacterial cell load of the *A. baumannii* 04117201 WT and Δ*stkR* mutant strains in mouse tissue and blood post infection

The *A. baumannii* 04117201 WT and Δ*stkR* strains were examined in a murine model. Bacterial cells were grown to a concentration of ~5x10^8 CFU in MH, resuspended in PBS and injected intranasally into C57/BL6 4 to 6 week-old female mice. Mice were euthanised at 24 hours post infection. Post infection murine tissue and blood were collected and the bacterial cells enumerated, with CFU determined by plating. (A) Log_{10} CFU per total mouse lung; (B) Log_{10} CFU per total mouse spleen; (C) Log_{10} CFU in 1 mL of mouse blood. Circles indicate individual animals, lines represent media values of bacterial burden of ten biological replicates. *** $P < 0.001$, ** $P < 0.01$ as determined by an analysis of a nonparametric Student *t* test.

4.5.5 Investigation of the murine immune transcriptional response post infection with *A. baumannii* 04117201 and Δ*stkR* derivative

Despite recent research examining *A. baumannii* infections, the details of how the immune system responds to this pathogen have largely been ignored. Here, genes involved in the mouse innate immune response were investigated by RT-PCR using RNA isolated from mice infected with either 04117201 or Δ*stkR* cells. The Antibacterial RT^2-PCR Profiler array assesses 84 genes that have been suggested to be involved in the mouse innate immune response including genes involved in chemokine and cytokine production and cell apoptosis (J. Wang *et al.* 2019). Analysis of the RT-PCR results identified 75 genes that were at least 2-fold differentially expressed (24 up-regulated and 51 down-regulated) when infected with *A. baumannii* 04117201 cells compared with a naïve lung (no infection). Interestingly, when the mouse lung is infected with the 04117201 Δ*stkR* variant the innate immune response is reduced with only 66 differentially expressed genes (23 up-regulated and 43 down-regulated) compared with a naïve lung. As seen in Table 4.1, 15 genes have changed in expression due to the infection of either the 04117201 WT or the Δ*stkR* mutant strains; these include Ifnb1, Tlr6 and Tlr9, Irf5, Ticam2, Irak3, Ripk2, Tnfrsf1a, Pycard, Rela, Map2k3, Ripk1, Nlrp1a, Il12a, and Crp. The most up-regulated of the host's immune genes, in response to both the 04117201 WT and Δ*stkR* mutant strains infection, were the chemokines Cxcl3, Cxcl4, Ccl3, Cxcl1, Ccl5, then the Tnf, and interleukin genes Il5, Il1b, followed by Camp, Slc11a1, Lcn2, Mefv, Slpi, Nlrp3, and Cd14 (Table 4.1). The most noticeable reduction in transcription was Cxcl3 by 2,030-fold following the 04117201 WT strain infection and 1,324-fold following Δ*stkR* mutant strain infection; this reduced response was mirrored to varying degrees by Ccl4, Ccl3, Cxcl1, and Ccl5.

To visualise the murine innate immune response after infection by *A. baumannii* 04117201 WT and the Δ*stkR* derivative, the immune response data was assessed by pathway analysis allowing for the identification of 465 distinct pathways (Figure 4.5; A, B). The connections were assessed for betweenness and centrality, where the size of the node (coloured circles) is directly related to number of connections and is described as a hub.

Table 4.1: The mouse innate immune response to infection with either *A. baumannii* 04117201 WT or Δ*stkR* strains

Name of gene	Symbol	Fold change Δ*stkR*[a]	*P*-value	Fold change WT[a]	*P*-value
Chemokine (C-X-X motif) ligand 3	Cxcl3	1324.58	0.01	2030.76	0.00
Chemokine (C-C motif) ligand 4	Ccl4	240.33	0.02	261.84	0.01
Tumor necrosis factor	Tnf	208.04	0.13	145.12	0.01
Chemokine (C-C motif) ligand 3	Ccl3	191.34	0.23	237.85	0.05
Interleukin 6	Il6	129.72	0.01	358.51	0.00
Chemokine (C-X-X motif) ligand 1	Cxcl1	101.66	0.15	211.46	0.12
Interleukin 1 beta	Il1b	63.38	0.06	67.94	0.00
Cathelicidin antimicrobial petide	Camp	46.38	0.26	55.83	0.20
Solute carrier family 11 (proton-coupled divalent metal ion transporters), member 1	Slc11a1	28.20	0.02	23.48	0.00
Lipocalin 2	Lcn2	20.95	0.00	18.79	0.00
Mediterranean fever	Mefv	14.47	0.00	38.81	0.00
Chemokine (C-C motif) ligand 5	Ccl5	14.30	0.01	16.73	0.00
Secretory leukocyte peptidase inhibitor	Slpi	13.83	0.00	16.61	0.00
NLR family, pyrin domain containing 3	Nlrp3	11.49	0.08	27.10	0.03

Table 4.1: Continued

Name of gene	Symbol	Fold change Δ*stkR*[a]	*P*-value	Fold change WT[a]	*P*-value
CD14 antigen	Cd14	11.09	0.26	10.85	0.84
Toll-like receptor 2	Tlr2	4.88	0.56	3.73	0.57
Interferon regulatory factor 7	Irf7	4.74	0.03	3.03	0.01
Z-DNA binding protein 1	Zbp1	4.03	0.00	2.46	0.00
Nucleotide-binding oligomerisation domain containing 2	Nod2	2.85	0.23	3.75	0.05
Nuclear factor of kappa light polypeptide gene enhancer in B-cell inhibitor, alpha	Nfkbia	2.76	0.01	2.82	0.01
Interferon beta 1, fibroblast	Ifnb1	2.34	0.00	1.65	0.00
Baculoviral IAP repeat-containing 3	Birc3	2.27	0.23	2.60	0.05
Toll-like receptor 6	Tlr6	2.06	0.18	-1.05	0.69
Myeloid differentiation primary response gene 88	Myd88	1.99	0.00	1.90	0.01
Interferon regulatory factor 5	Irf5	1.92	0.23	2.06	0.03
Toll-like receptor adaptor molecule 2	Ticam2	1.85	0.14	-10.66	0.29
Toll-like receptor 1	Tlr1	1.73	0.06	1.03	0.00
Lactotransferrin	Ltf	1.68	0.01	1.24	0.01

Table 4.1: Continued

Name of gene	Symbol	Fold change Δ*stkR*[a]	*P*-value	Fold change WT[a]	*P*-value
Interleukin-1 receptor-associated kinase 3	Irak3	1.66	0.01	2.32	0.00
Toll-like receptor 9	Tlr9	1.56	0.02	3.91	0.00
Receptor (TNFRSF)-interacting serine-threonine kinase 2	Ripk2	1.04	0.47	-2.07	0.14
Proline-serine-theronine phosphate-interacting protein 1	Pstpip1	-1.27	0.36	-1.19	0.23
Tumor necrosis factor receptor superfamily, member 1a	Tnfrsf1a	-1.33	0.00	-2.44	0.02
PYD and CARD domain containing	Pycard	-1.49	0.02	-2.66	0.01
Mitogen-activated protein kinase kinase 1	Map2k1	-1.51	0.04	-1.15	0.00
V-rel reticuloendotheliosis viral oncogene homolog A (avian)	Rela	-1.54	0.00	-3.11	0.00
Cathepsin G	Ctsg	-1.56	0.17	-1.94	0.36
Mitogen-activated protein kinase kinase 3	Map2k3	-1.60	0.03	-2.03	0.02
Receptor (TNFRSF)-interacting serine-threonine kinase 1	Ripk1	-1.60	0.03	-2.34	0.00
NLR family, pyrin domain containing 1A	Nlrp1a	-1.66	0.09	-4.10	0.18
Interleukin 12A	Il12a	-1.86	0.26	-19.30	0.02
Bactericidal permeability increasing protein	Bpi	-2.01	0.02	-3.55	0.00
Deleted in malignant brain tumors 1	Dmbt1	-2.01	0.00	-3.55	0.00

Table 4.1: Continued

Name of gene	Symbol	Fold change Δ*stkR*[a]	*P*-value	Fold change WT[a]	*P*-value
Interferon alpha 9	Ifna9	-2.01	0.00	-3.55	0.00
NLR family, CARD domain containing 4	Nlrc4	-2.01	0.03	-3.55	0.00
NLR family, apoptosis inhibitory protein 1	Naip 1	-2.01	0.01	-3.55	0.00
Nuclear factor of kappa light polypeptide gene enhancer in B-cell 1, p105	Nfkb1	-2.02	0.01	-2.84	0.00
Caspase1	Casp1	-2.25	0.06	-2.11	0.00
Mitogen-activated protein kinase kinase 4	Map2k4	-2.29	0.13	-5.99	0.06
C-reactive protein, pentraxin-related	Crp	-2.49	0.11	-1.35	0.08
Proteinase 3	Prtn3	-2.62	0.23	-4.92	0.05
Conserved helix-loop-helix ubiquitous kinase	Chuk	-2.79	0.05	-3.20	0.01
Toll-like receptor 4	Tlr4	-2.82	0.09	-5.29	0.03
Toll-like receptor adaptor molecule 1	Ticam1	-2.98	0.23	-9.87	0.05
Nucleotide-binding oligomerisation domain containing 1	Nod1	-3.00	0.55	-6.75	0.08
SGT1, suppressor of G2 allele of SKP1 (s. Cerevisiae)	Sugt1	-3.01	0.06	-6.35	0.01
Toll-interleukin 1 receptor (TIR) domain-containing adaptor protein	Tirap	-3.05	0.03	-3.09	0.00
RAS-related C3 botulinum substrate 1	Rac1	-3.24	0.19	-5.74	0.10

Table 4.1: Continued

Name of gene	Symbol	Fold change Δ*stkR*[a]	*P*-value	Fold change WT[a]	*P*-value
Toll interacting protein	Tollip	-3.43	0.04	-5.25	0.00
Lymhocyte antigen 96	Ly96	-3.45	0.33	-3.53	0.04
heat shock protein 90, alpha (cytosolic), class A member 1	Hsp90aa1	-4.04	0.66	-6.29	0.74
Caspase8	Casp8	-5.06	0.52	-6.35	0.08
Interleukin-1 receptor-associated kinase 1	Irak1	-5.07	0.01	-8.08	0.00
Inhibitor of kappaB kinase beta	ikbkb	-5.30	0.21	-6.23	0.02
Mitogen-activated protein kinase kinase kinase 7	Map3k7	-5.76	0.10	-8.93	0.01
Myeloperoxidase	Mpo	-5.91	0.94	-10.43	0.11
Mitogen-activated protein kinase 8	Mapk8	-6.77	0.03	-3.73	0.03
Thymoma viral proto-oncogene 1	Akt1	-7.02	0.00	-14.38	0.00
Lipopolysaccharide binding protein	Lbp	-7.31	0.06	-29.26	0.00
Jun oncogene	Jun	-7.64	0.39	-5.84	0.06
Mitogen-activated protein kinase 1	Mapk1	-7.81	0.77	-9.97	0.12
X-linked inhibitor of apoptosis	Xiap	-8.36	0.08	-14.49	0.01
Interleukin 18	Il18	-8.70	0.79	-10.35	0.99

Table 4.1: Continued

Name of gene	Symbol	Fold change Δ*stkR*[a]	*P*-value	Fold change WT[a]	*P*-value
Interleukin 12B	Il12b	-8.85	0.06	-5.09	0.08
Fas (TNFRSF6)-associated via death domain	Fadd	-9.92	0.06	-254.80	0.05
Lysozyme 2	Lyz2	-10.38	0.04	-34.50	0.00
Mitogen-activated protein kinase 14	Mapk14	-10.53	0.59	-39.58	0.97
Mitogen-activated protein kinase 3	Mapk3	-17.96	0.67	-36.58	0.30
Phosphatidylinositol 3-kinase, catalytic, alpha polypeptide	Pik3ca	-19.32	0.00	-25.15	0.00
Serum amyloid P-component	Apcs	-19.47	0.63	-34.37	0.07
Toll-like receptor 5	Tlr5	-42.43	0.01	-221.06	0.00
Caspase recruitment domain family, member 9	Card9	-51.17	0.03	-164.15	0.20
Tnf receptor-associated factor6	Traf6	-107.35	0.01	-20.35	0.00
Caspase recruitment domain family, member 6	Card6	-128.57	0.01	-199.94	0.08

[a] C_t values were normalised using the *gapDH* housekeeping gene and $\Delta\Delta C_t$ values were calculated against the naïve infected mouse give fold change gene expression for Δ*stkR* or WT infected lung tissue.

Figure 4.5 clearly demonstrates the modulation of genes in response to infection by either strain. A number of chemokines and cytokines are up-regulated in both data sets and genes involved in apoptosis, including Fadd, Fas, and Tnf, are differentially regulated showing increased apoptosis of the mouse lung tissue with infected with the WT strain. The largest hub in both the 04117201 WT and Δ*stkR* mutant strains systems was identified as RelA, a gene involved in a wide variety of processes including inflammation and apoptosis (Lawrence 2009, Chalmers *et al.* 2019).

4.5.6 Transcriptome analysis of the *A. baumannii* 04117201 WT and Δ*stkR* strains grown in MH media

The transcriptomic profile of *A. baumannii* 04117201 and its corresponding Δ*stkR* derivative was assessed from cells grown in MH media to determine the influence that removal of *stkR* has on gene expression. MH is a nutrient rich standard media used within the lab to grow bacteria as such forms a comparable baseline for this investigation. The relative $\log_2$ expression and annotation was analysed (Figure 4.6), additionally, a list of the altered gene expression was produced (Appendix B). As shown in Figure 4.6, a number of genes were differentially expressed in the Δ*stkR* mutant compared to the it's parent. Fourteen genes were up-regulated and 64 genes down-regulated, giving a total of 78 genes whose expression changed 2-fold or more. Up-regulated genes include NADP-specific glutamate (which is a cofactor in the synthesis of urea), butyryl-CoA dehydrogenase (involved in metabolic pathways such as fatty acid metabolism), Aspartate amino transferase (an enzyme that catalyses the reversible transfer of an α-amino group). The GroL and GroES chaperone protein binding system which are associated with biofilm formation (Lemos *et al.* 2007) were also up-regulated. Furthermore a multidrug translocase protein identified as being related to CHL resistance in *A. baumannii* strains was up-regulated (Wang *et al.* 2014). Lastly, a transferase protein (which is potentially involved in substrate binding) (Kuhn *et al.* 2013) and a number of hypothetical proteins were up-regulated. Genes that were down-regulated due to inactivation *stkR* strain include *dnak* (1.9-fold) which is associated with biofilm formation and has been shown to be correlated with the increased expression of the GroEL chaperone binding protein which is listed above as up-regulated.

(A)

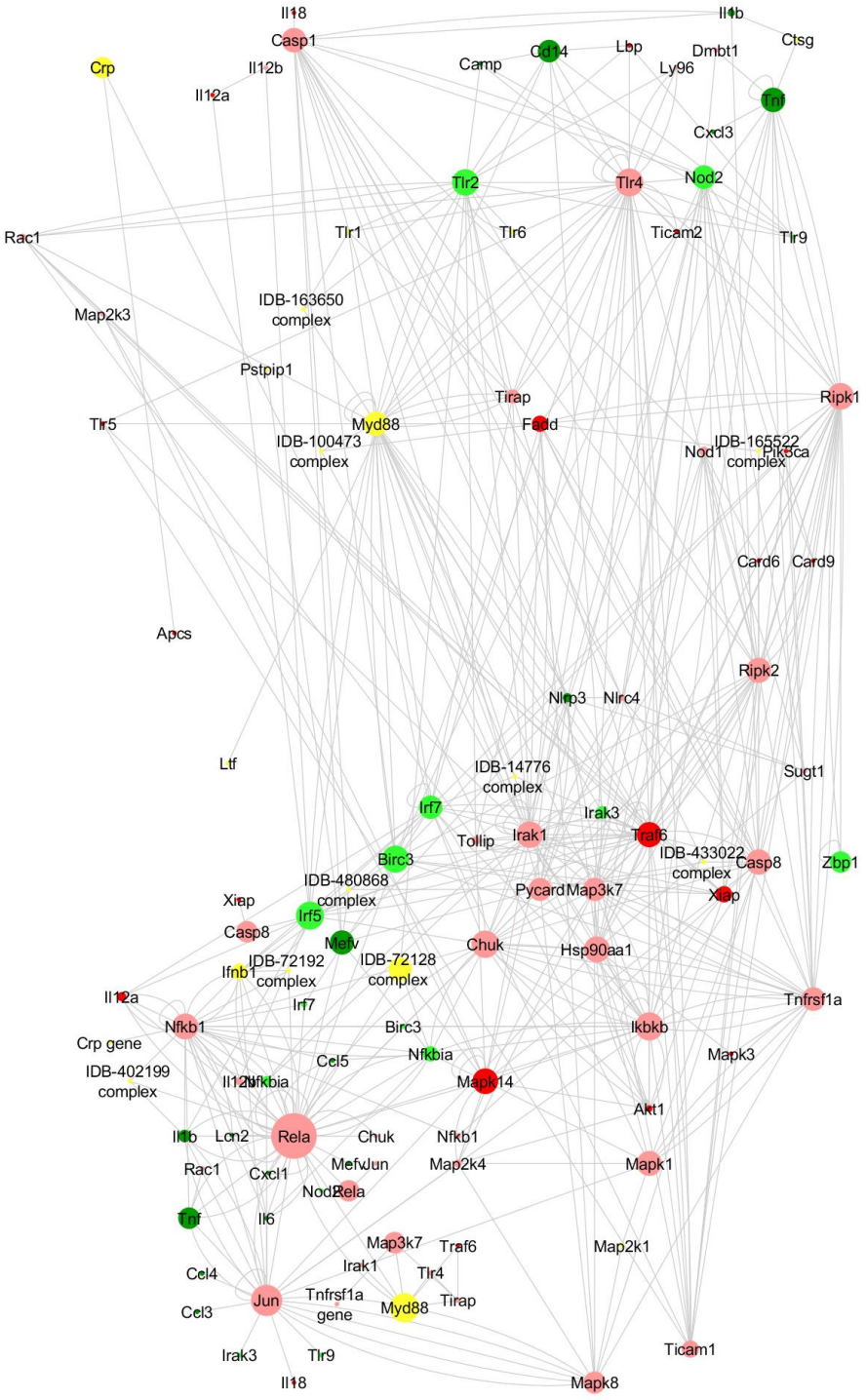
Il18
Il1b
Casp1
Ctsg
Cd14
Lbp
Dmbt1
Crp
Camp
Ly96
Il12b
Il12a
Tnf
Cxcl3
Tlr2
Tlr4
Nod2
Rac1
Tlr1
Tlr6
Ticam2
Tlr9
IDB-163650 complex
Map2k3
Pstpip1
Tirap
Ripk1
Tlr5
Myd88
Fadd
IDB-100473 complex
Nod1
IDB-165522 complex
Pik3ca
Card6
Card9
Apcs
Ripk2
Nlrp3
Nlrc4
Ltf
IDB-14776 complex
Sugt1
Irf7
Irak3
Tollip
Irak1
Traf6
Birc3
IDB-433022 complex
Casp8
Zbp1
IDB-480868 complex
Pycard
Map3k7
Xiap
Irf5
Casp8
Chuk
Hsp90aa1
IDB-72192 complex
IDB-72128 complex
Ifnb1
Il12a
Irf7
Tnfrsf1a
Nfkb1
Birc3
Ikbkb
Crp gene
Nfkbia
Mapk3
Cel5
IDB-402199 complex
Mapk14
Akt1
Il1b
Lcn2
Rela
Chuk
Nfkb1
Rac1
Cxcl1
Map2k4
Mapk1
Rela
Tnf
Il6
Map3k7
Traf6
Map2k1
Irak1
Cel4
Tlr4
Jun
Tnfrsf1a gene
Tirap
Cel3
Myd88
Ticam1
Irak3
Tlr9
Il18
Mapk8

(B)

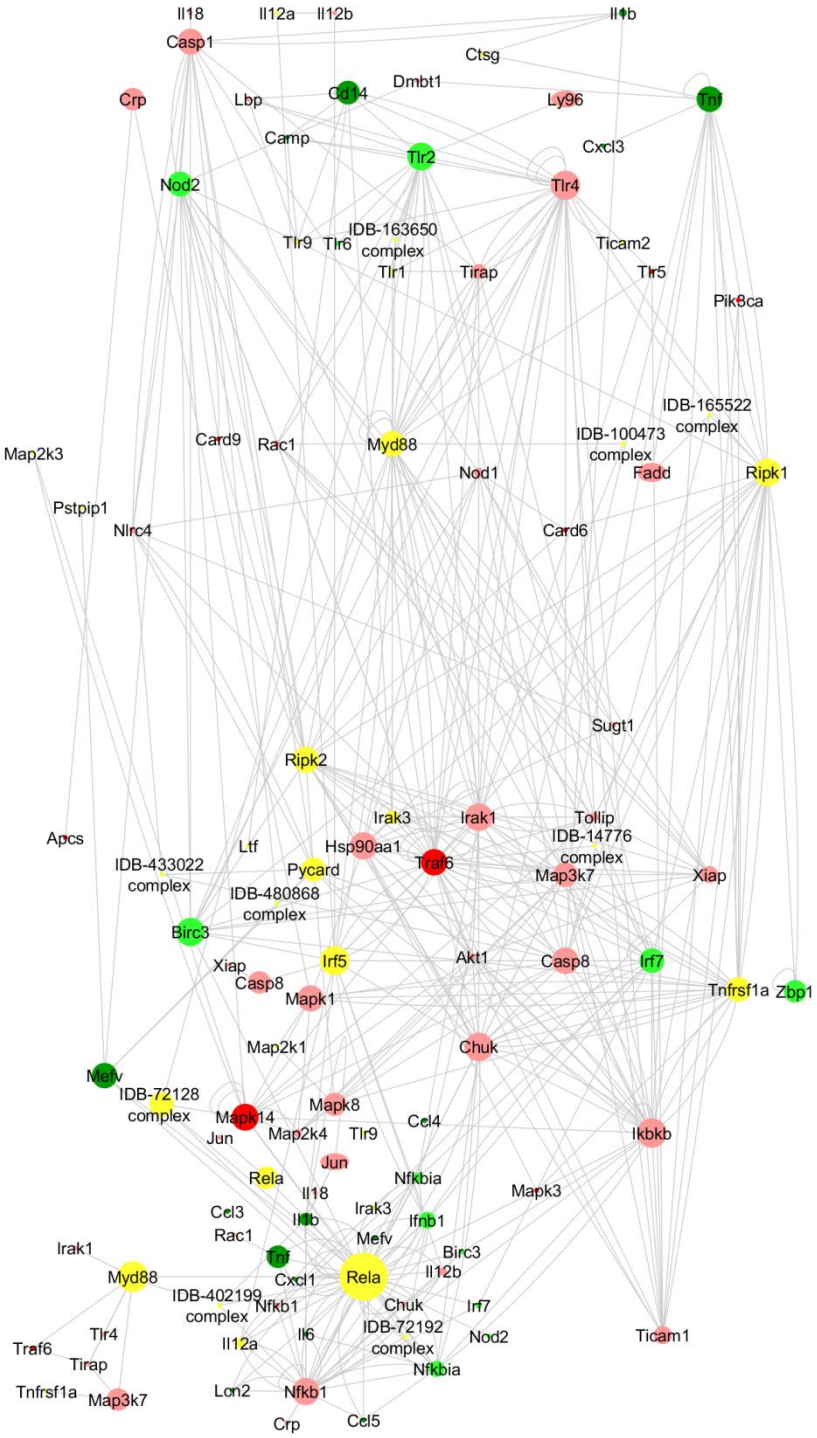
Il18
Il12a
Il12b
Il1b
Casp1
Ctsg
Dmbt1
Crp
Lbp
Cd14
Ly96
Tnf
Camp
Cxcl3
Tlr2
Nod2
Tlr4
Tlr9
Tlr6
IDB-163650 complex
Tlr1
Ticam2
Tirap
Tlr5
Pik3ca
IDB-165522 complex
Map2k3
Card9
Rac1
Myd88
IDB-100473 complex
Nod1
Fadd
Ripk1
Pstpip1
Nlrc4
Card6
Sugt1
Ripk2
Irak3
Irak1
Tollip
Apcs
Ltf
Hsp90aa1
IDB-14776 complex
IDB-433022 complex
Pycard
Traf6
Map3k7
Xiap
IDB-480868 complex
Birc3
Xiap
Irf5
Akt1
Casp8
Irf7
Casp8
Mapk1
Tnfrsf1a
Zbp1
Map2k1
Chuk
Mefv
IDB-72128 complex
Mapk8
Mapk14
Cel4
Jun
Map2k4
Tlr9
Ikbkb
Jun
Rela
Nfkbia
Il18
Mapk3
Cel3
Il1b
Irak3
Ifnb1
Rac1
Mefv
Irak1
Tnf
Birc3
Myd88
Cxcl1
Rela
Il12b
IDB-402199 complex
Nfkb1
Chuk
Irf7
Tlr4
Il6
IDB-72192 complex
Nod2
Ticam1
Traf6
Il12a
Tirap
Nfkbia
Tnfrsf1a
Map3k7
Lcn2
Nfkb1
Crp
Cel5

Figure 4.5: Cytoscape analysis of the murine innate immune response after infection with *A. baumannii* 04117201 WT and Δ*stkR* mutant cells compared to a naïve lung

The innate immune response of the mouse lung 24 hours post infection was assessed. RNA was extracted from murine tissue after infection with either the 04117201 WT or Δ*stkR* mutant strains. RNA samples were analysed using the Antibacterial RT^2 PCR profiler array (Qiagen). Triplicate arrays were pooled and transcriptional fold changes were calculated against arrays performed with RNA isolated from naïve lungs. The immune response data was assessed by pathway analysis using the Innate BD website (https://www.innatedb.com/) and Cytoscape (https://cytoscape.org) identified 465 distinct pathways. The connections were assessed for betweenness and centrality, where the size of the node (coloured circles) is directly related to the number of connections. The green coloured nodes represent an increase gene expression; dark green >10-fold and light green 10- to 2-fold. In contrast, a decrease in gene expression is represented by red >10-fold and pink 10- to 2-fold; yellow nodes represent genes with less than 2-fold change in expression.

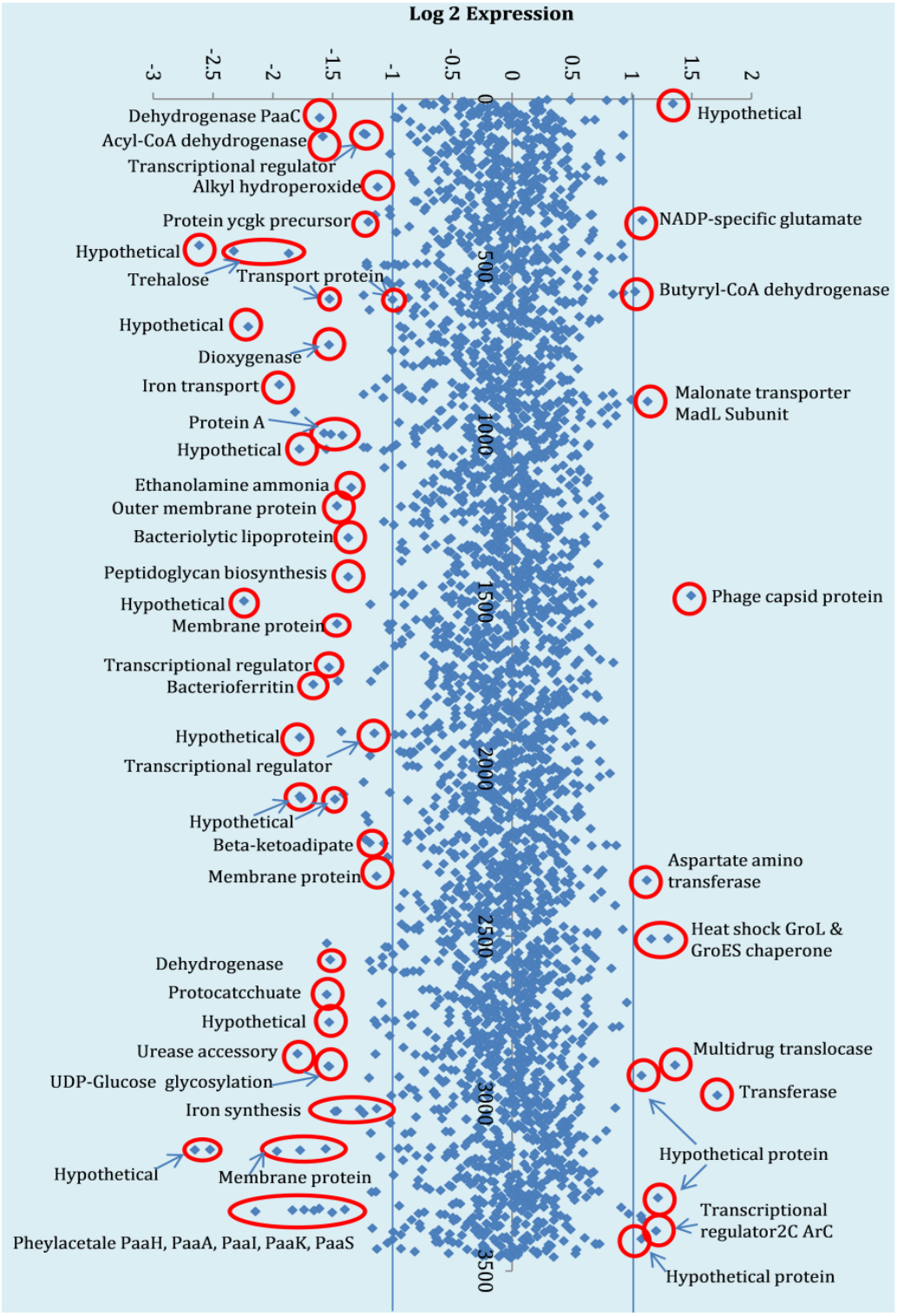
Log 2 Expression
-3
-2.5
-2
-1.5
-1
-0.5
0
0.5
1
1.5
2
0
500
1000
1500
2000
2500
3000
3500
Dehydrogenase PaaC
Acyl-CoA dehydrogenase
Transcriptional regulator
Alkyl hydroperoxide
Protein ycgk precursor
Hypothetical
Trehalose
Transport protein
Hypothetical
Dioxygenase
Iron transport
Protein A
Hypothetical
Ethanolamine ammonia
Outer membrane protein
Bacteriolytic lipoprotein
Peptidoglycan biosynthesis
Hypothetical
Membrane protein
Transcriptional regulator
Bacterioferritin
Hypothetical
Transcriptional regulator
Hypothetical
Beta-ketoadipate
Membrane protein
Dehydrogenase
Protocatcchuate
Hypothetical
Urease accessory
UDP-Glucose glycosylation
Iron synthesis
Hypothetical
Membrane protein
Pheylacetale PaaH, PaaA, PaaI, PaaK, PaaS
Hypothetical
NADP-specific glutamate
Butyryl-CoA dehydrogenase
Malonate transporter MadL Subunit
Phage capsid protein
Aspartate amino transferase
Heat shock GroL & GroES chaperone
Multidrug translocase
Transferase
Hypothetical protein
Transcriptional regulator2C ArC
Hypothetical protein

Figure 4.6: Whole transcriptome analysis of the *A. baumannii* 04117201 WT and Δ*stkR* mutant strains in MH media

Comparative whole transcriptome analysis of the *A. baumannii* 04117201 WT and Δ*stkR* mutant strains using the Illumina platform from RNA isolated when grown in MH media. Sequence reads were mapped to the reference 04117201 WT genome and the differential gene expression calculated. Diamond markers indicate the differential expression levels of all predicted ORFs of the 04117201 WT genome and are sorted on the x axis according to the locus tag. Changes of 1 or more Log 2 in gene expression were considered significant. Genes of interest are circled, many of which are discussed in the body of the text and listed in Appendix B .

The *dnak* gene is down-regulated (1.9-fold) and the *groEL* gene up-regulation (2.4-fold) (Lemos *et al.* 2007). Down-regulation of the UDP-glucose glycosylation determinant is potentially correlated with capsule production (Cardoso *et al.* 2010). The trehalose operon is shown to be down-regulated (5 and 3.6-fold) (also known as disaccharides) has been associated with increased resistance to desiccation and temperature change (Avonce *et al.* 2006, Park *et al.* 2016). In addition, down-regulation of the *paaA* operon between (2.6 and 4.4-fold) has been found to be associated with surface proteins and antigens (Tamura *et al.* 2004). Finally, a number of outer membrane and membrane proteins, transcriptional regulators, iron transport, and peptidoglycan biosynthesis are down-regulated. The majority of the genes mentioned above affect the membrane of the bacterial cell and are potentially related to the phenotypic changes seen in the Δ*stkR* mutant strain.

4.5.7 Transcriptome analysis of the *A. baumannii* 04117201 WT and Δ*stkR* mutant strains grown in lung media

To infect a host and cause disease bacteria need to exist in a variety of host environments. This can include the skin (externally on a host) and the lungs, blood, and tissues (internally in a host). To mimic pneumonia, investigation of *A. baumannii* 04117201 and the impact of *stkR* inactivation was undertaken on cells grown in lung media. Whole transcriptome analysis identified numerous differentially expressed genes in the Δ*stkR* mutant strain when compared its parent. Over 700 genes were up-regulated and 464 genes down-regulated, giving a total of 1,165 genes whose expression changed by 2-fold or more (Figure 4.7 and Appendix C). The up-regulated genes included a large number of iron up-take systems essential for survival within a host (Eijkelkamp *et al.* 2011a). This list includes iron membrane, outermembrane family receptors, TonB dependant outer membrane receptor and acquisition genes, ferrochrome-iron receptor, siderophore biosynthesis, ferrous iron transport, and the three major iron up-take systems previously described (Eijkelkamp *et al.* 2011a). Genes involved in zinc homeostasis included the L31 zinc independent proteins (Nairn *et al.* 2016) for acquisition, storage, and general homeostasis. Interestingly, the *paaA* operon that is potentially involved in surface proteins (Tamura *et al.* 2004) were found to be up-regulated between (2.9 to 28.9-fold) in the lung media,

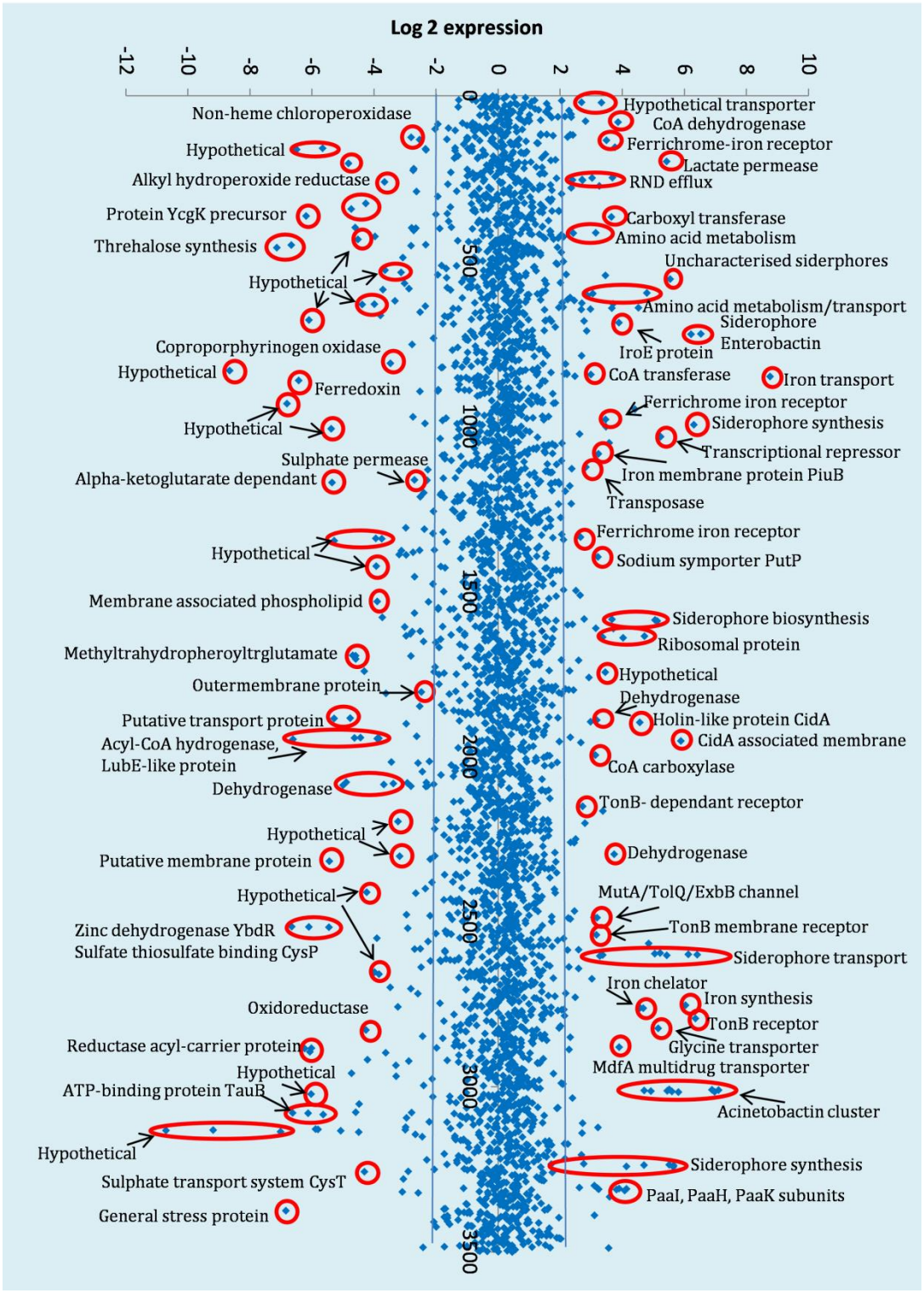
Log 2 expression
-12
-10
-8
-6
-4
-2
0
2
4
6
8
10
0
500
1000
1500
2000
2500
3000
3500
Non-heme chloroperoxidase
Hypothetical
Alkyl hydroperoxide reductase
Protein YcgK precursor
Threhalose synthesis
Hypothetical
Coproporphyrinogen oxidase
Hypothetical
Ferredoxin
Hypothetical
Sulphate permease
Alpha-ketoglutarate dependant
Hypothetical
Membrane associated phospholipid
Methyltrahydropheroyltrglutamate
Outermembrane protein
Putative transport protein
Acyl-CoA hydrogenase,
LubE-like protein
Dehydrogenase
Hypothetical
Putative membrane protein
Hypothetical
Zinc dehydrogenase YbdR
Sulfate thiosulfate binding CysP
Oxidoreductase
Reductase acyl-carrier protein
Hypothetical
ATP-binding protein TauB
Hypothetical
Sulphate transport system CysT
General stress protein
Hypothetical transporter
CoA dehydrogenase
Ferrichrome-iron receptor
Lactate permease
RND efflux
Carboxyl transferase
Amino acid metabolism
Uncharacterised siderphores
Amino acid metabolism/transport
Siderophore
IroE protein
Enterobactin
CoA transferase
Iron transport
Ferrichrome iron receptor
Siderophore synthesis
Transcriptional repressor
Iron membrane protein PiuB
Transposase
Ferrichrome iron receptor
Sodium symporter PutP
Siderophore biosynthesis
Ribosomal protein
Hypothetical
Dehydrogenase
Holin-like protein CidA
CidA associated membrane
CoA carboxylase
TonB- dependant receptor
Dehydrogenase
MutA/TolQ/ExbB channel
TonB membrane receptor
Siderophore transport
Iron chelator
Iron synthesis
TonB receptor
Glycine transporter
MdfA multidrug transporter
Acinetobactin cluster
Siderophore synthesis
PaaI, PaaH, PaaK subunits

Figure 4.7: Whole transcriptome analysis of the *A. baumannii* 04117201 WT and Δ*stkR* mutant strains in lung media

Comparative whole transcriptome analysis on the *A. baumannii* 04117201 WT and Δ*stkR* strains using the Illumina platform from RNA isolated when grown in lung media. Sequence reads were mapped to the reference 04117201 WT genome and the differential gene expression calculated. Diamond markers indicate the differential expression levels of all predicted open reading frames of the 04117201 WT genome and are sorted on the x axis according to the locus tag. Changes of 1 or more Log 2 in gene expression were considered significant. Genes of particular interest are circled, many of which are discussed in the body of the text and listed in Appendix C.

which is the opposite to what was found in the MH media (Fig 4.6). The membrane-associated proteins CidA and CidB, which have been found to contribute to biofilm formation (Ranjit *et al.* 2011) and involved in biofilm formation, were also up-regulated. Other up-regulated genes included genes involved in lipid metabolism, dehydrogenases, amino acid, carbohydrate metabolism and hypothetical proteins. Down-regulated genes that were identified included transcriptional regulators involved in vast array of mechanisms. Interestingly, the trehalose synthesis operon was significantly down-regulated by 101 and 140-fold similar to what was identified in the MH media analysis. Furthermore, a number of putative membrane and transport proteins, outermembrane proteins and membrane-associated phospholipids, all of which are potentially involved in capsule production and the LOS components of the membrane potentially contributing to cell adherence and antimicrobial resistance. Hypothetical proteins and a general stress protein were also down-regulated.

4.5.8 Transcriptome analysis of the *A. baumannii* 04117201 WT and Δ*stkR* mutant strains grown in M9 media

A. baumannii is able to survive on a variety of surfaces within the hospital environment including bed railings, walls and other inanimate objects which are limited in nutrients and carbon sources. To investigate this ability the *A. baumannii* 04117201 WT and Δ*stkR* mutant strains were grown in the minimal media M9 mimicking this niche. Whole transcriptome analysis identified large collections of differentially expressed genes of the Δ*stkR* mutant when compared to the 04117201 WT strain. In total 930 genes were up-regulated and 246 genes were down-regulated, giving a total of 1,176 genes expression changed by 2-fold or more (Figure 4.8 and Appendix D. Up-regulated genes were very similar to those found in the lung media analysis; these included a number of hypothetical proteins, the iron up-take systems (PuiB) up-regulated by 13-fold and the iron membrane OMR family receptors up-regulated between 7 and 11-fold, the TonB dependent outer membrane receptor which is up-regulated by 50-fold, ferrichrome-iron receptor up-regulated by 20-fold and the siderophore iron chelate operon up-regulated between 57 and 859-fold and the TonB dependant iron acquisition operon up-regulated between 8.9 and 416-fold (Eijkelkamp *et al.* 2011a).

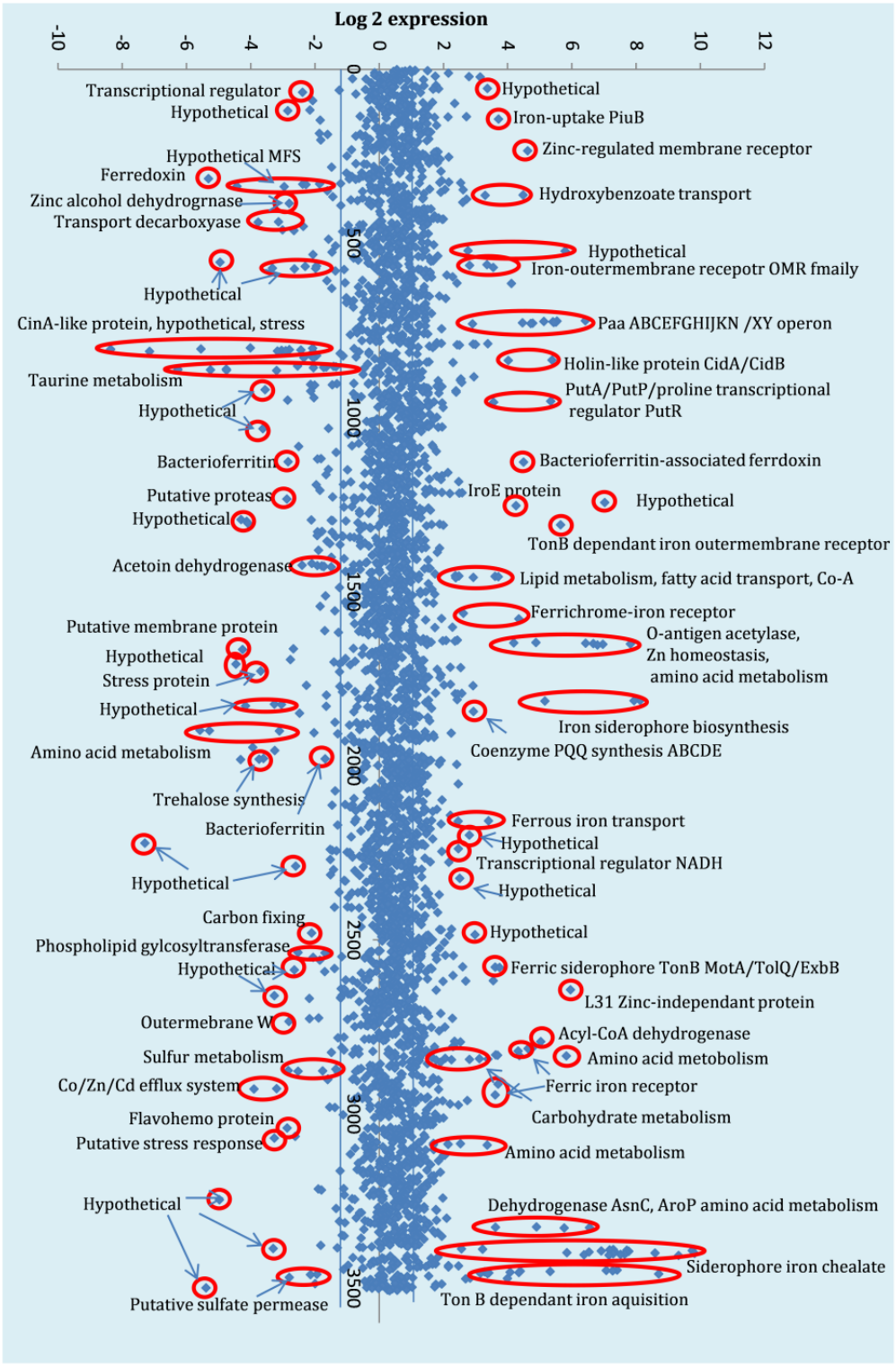
Log 2 expression
-10
-8
-6
-4
-2
0
2
4
6
8
10
12
0
500
1000
1500
2000
2500
3000
3500
Transcriptional regulator
Hypothetical
Hypothetical MFS
Ferredoxin
Zinc alcohol dehydrogrnase
Transport decarboxyase
Hypothetical
CinA-like protein, hypothetical, stress
Taurine metabolism
Hypothetical
Bacterioferritin
Putative proteas
Hypothetical
Acetoin dehydrogenase
Putative membrane protein
Hypothetical
Stress protein
Hypothetical
Amino acid metabolism
Trehalose synthesis
Bacterioferritin
Hypothetical
Carbon fixing
Phospholipid gylcosyltransferase
Hypothetical
Outermebrane W
Sulfur metabolism
Co/Zn/Cd efflux system
Flavohemo protein
Putative stress response
Hypothetical
Putative sulfate permease
Hypothetical
Iron-uptake PiuB
Zinc-regulated membrane receptor
Hydroxybenzoate transport
Hypothetical
Iron-outermembrane recepotr OMR fmaily
Paa ABCEFGHIJKN /XY operon
Holin-like protein CidA/CidB
PutA/PutP/proline transcriptional regulator PutR
Bacterioferritin-associated ferrdoxin
IroE protein
Hypothetical
TonB dependant iron outermembrane receptor
Lipid metabolism, fatty acid transport, Co-A
Ferrichrome-iron receptor
O-antigen acetylase, Zn homeostasis, amino acid metabolism
Iron siderophore biosynthesis
Coenzyme PQQ synthesis ABCDE
Ferrous iron transport
Hypothetical
Transcriptional regulator NADH
Hypothetical
Hypothetical
Ferric siderophore TonB MotA/TolQ/ExbB
L31 Zinc-independant protein
Acyl-CoA dehydrogenase
Amino acid metobolism
Ferric iron receptor
Carbohydrate metabolism
Amino acid metabolism
Dehydrogenase AsnC, AroP amino acid metabolism
Siderophore iron chealate
Ton B dependant iron aquisition

Figure 4.8: Whole transcriptome analysis of the *A. baumannii* 04117201 WT and Δ*stkR* mutant strains in M9 medium

Comparative whole transcriptome analysis on the *A. baumannii* 04117201 WT and Δ*stkR* mutant strains using the Illumina platform from RNA isolated when grown in M9 media. Sequence reads were mapped to the reference 04117201 WT genome and the differential gene expression calculated. Diamond markers indicate the differential expression levels of all predicted ORF of the 04117201 WT genome and are sorted on the x axis according to the locus tag. Changes of 1 or more Log 2 in gene expression were considered significant. Genes of interest are circled, many of which are discussed in the body of the text and listed in Appendix D.

Zinc genes included the zinc outermembrane receptor up-regulated by 24-fold and the L31 zinc independent proteins up-regulated by 62-fold, important in many cellular processes (Hantke 2001, Nairn *et al.* 2016). The *paaA* operon cluster that are involved in surface proteins (Tamura *et al.* 2004) were also found to be up-regulated between 2.3 and 85-fold, as were the membrane associated proteins CidA and CidB up-regulated by 41 and 16-fold (Ranjit *et al.* 2011). The up-regulated genes also included lipid metabolism, dehydrogenises, amino acid and carbohydrate metabolism again potentially affecting the LOS of the bacterial cell. The down-regulated genes identified in the M9 media were again similar to those found down-regulated in the lung media analysis; these included transcriptional regulation genes and various hypotheticals. The ferredoxin genes were down-regulated by 39-fold, zinc alcohol dehydrogenase genes down-regulated 6.9-fold as well as a CinA-like protein cluster of genes down-regulated between 4.2 and 328-fold which could be involved in decreasing the bacterial cells competence (Solomon *et al.* 1996). Additionally, the taurine metabolism operon was down-regulated between 26 and 76-fold, bacterioferritin involved in iron storage and metabolism was down-regulated 3.6-fold and the trehalose operon was down-regulated 13 and 19.9-fold. Amino acid metabolism was down-regulated 47-fold, and the phospholipid glycosyltransferase genes were down-regulated between 3.2 and 5.7-fold which are possibly involved with capsule and LOS production. The outer membrane W was down-regulated 7-fold, the sulfur metabolism operon was down-regulated between 2.4 and 7.1-fold and the Co/Zn/Cd efflux system was down-regulated by 9-fold.

4.5.9 Transcriptome analysis of the *A. baumannii* 04117201 WT and Δ*stkR* mutant strains grown in blood

Septicaemia is a serious disease state of *A. baumannii* where the bacterial cell enters the blood stream and can subsequently colonise various important organs. To investigate the regulatory differences between the *A. baumannii* 04117201 WT and Δ*stkR* mutant strains when grown in whole blood transcriptome analysis was undertaken. Transcriptome analysis identified a collection of differentially expressed genes of the Δ*stkR* mutant when compared to the 04117201 WT strain. A total of 16 up-regulated and 123 down-regulated genes, giving a 139 differentially expressed by 2-fold or more (Figure 4.9), a list was also generated of the altered genes see

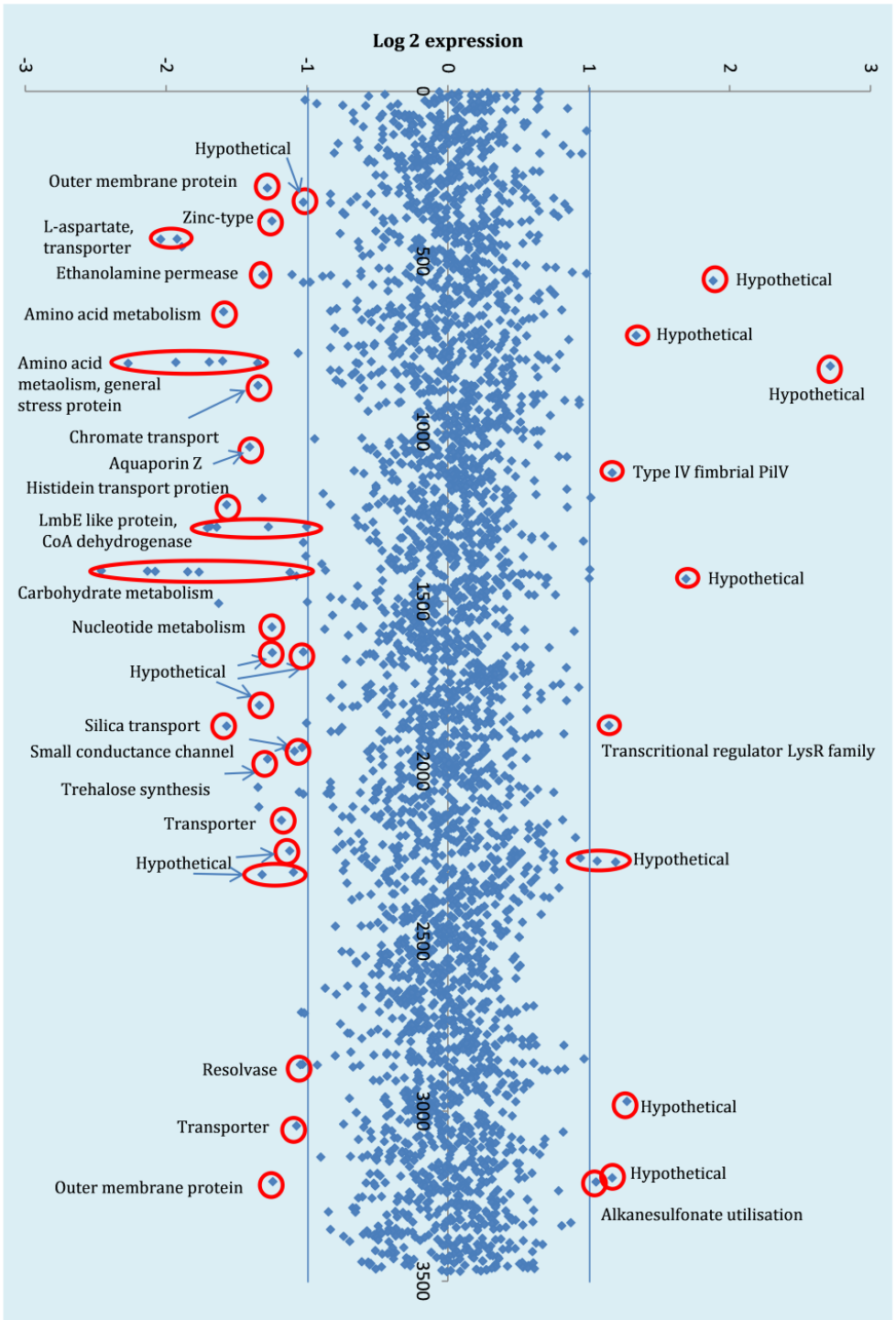
Log 2 expression
-3
-2
-1
0
1
2
3
0
500
1000
1500
2000
2500
3000
3500
Hypothetical
Outer membrane protein
Zinc-type
L-aspartate, transporter
Ethanolamine permease
Amino acid metabolism
Amino acid metaolism, general stress protein
Chromate transport
Aquaporin Z
Histidein transport protien
LmbE like protein, CoA dehydrogenase
Carbohydrate metabolism
Nucleotide metabolism
Hypothetical
Silica transport
Small conductance channel
Trehalose synthesis
Transporter
Hypothetical
Resolvase
Transporter
Outer membrane protein
Hypothetical
Hypothetical
Hypothetical
Type IV fimbrial PilV
Hypothetical
Transcritional regulator LysR family
Hypothetical
Hypothetical
Hypothetical
Alkanesulfonate utilisation

Figure 4.9: Whole transcriptome analysis of the *A. baumannii* 04117201 WT and Δ*stkR* mutant strains in blood

Comparative whole transcriptome analysis on the *A. baumannii* 04117201 WT and Δ*stkR* mutant strains using the Illumina platform from RNA isolated when grown in blood. Sequence reads were mapped to the reference 04117201 WT genome and the differential gene expression calculated. Diamond markers indicate the differential expression levels of all predicted ORF of the 04117201 WT genome and are sorted on the x axis according to the locus tag. Changes of 1 or more Log 2 in gene expression were considered significant. Genes of interest are circled, many of which are discussed in the body of the text and listed in Appendix E

Appendix E. There are significantly less genes altered between the 04117201 WT and Δ*stkR* mutant strains when grown in blood compared to the lung media and M9 media investigations. Up-regulated genes included various hypothetical proteins, the Type IV fimbrial PilV up-regulated 2.2-fold, which is a trans membrane protein associated with secretion and a LysR transcriptional regulator up-regulated 2.2-fold involved in various cellular processes. Similar to the other transcription investigations but a significantly reduced number of changes. The down-regulated genes include outer membrane proteins down-regulated by 2.4-fold, zinc down-regulated 2.3-fold, ethanolamine permease down-regulated 2.1 and 2.4-fold, amino acid metabolism down-regulated 2-fold, and dehydrogenase genes down-regulated 2-fold. Silica transport down-regulated 2.9-fold, and other transport proteins were also down-regulated 2-fold. Additionally, only one of the trehalose synthesis genes were down-regulated 2.4-fold, the other did not changes in its regulation. The results presented here suggest that the *stkR* RR gene has a reduced impact on the bacterial strain when grown in blood when compared to the other media..

4.5.10 Transcriptional alterations of the *A. baumannii* strains when grown in different media

To aid in visualisation of the differences and similarities seen in the transcriptome for the 04117201 WT and Δ*stkR* mutant strains grown in different media, Venn diagrams were generated (Figure 4.10). In lung media the Δ*stkR* mutant showed 464 down-regulated genes and 701 up-regulated genes, in MH media the Δ*stkR* mutant strain showed 61 down-regulated genes and 14 up-regulated genes**,** in blood the Δ*stkR* mutant strain showed 123 down-regulated genes and 16 up-regulated genes, and in M9 media Δ*stkR* mutant strain showed 246 down-regulated genes and 930 up-regulated genes. As seen from these data, the lung and M9 media showed the greatest overall transcriptional changes of the Δ*stkR* mutant strain compared with the 04117201 WT strain. The blood and MH media showed minimal differences in transcription between the 04117201 WT and the Δ*stkR* mutant strains.

4.6 Discussion

This project has produced a significant amount of data identifying many genes that potentially contribute to the pathogenicity of the clinical *A. baumannii* strain 04117201 by analysing. Mutation by recombination of the RR gene *stkR* in the

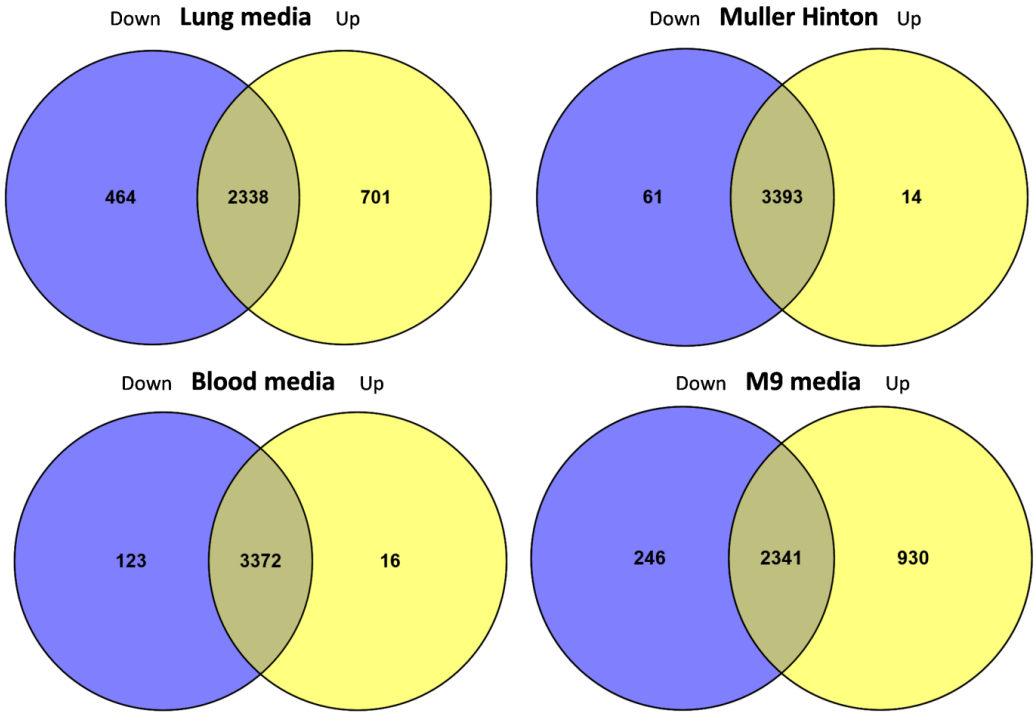

Figure 4.10: Venn diagram of the *A. baumannii* 04117201 WT strain compared to the Δ*stkR* mutant strain across four media

Whole transcriptome data was analysed using the Illumina platform and sequenced reads were mapped to the reference 04117201 WT genome; differential gene expression was then calculated. Venn diagrams were generated using the Venny 2.1 program http://bioinfogp.cnb.csic.es/tools/venny/. Up and down-regulated genes from RNA isolated from the 04117201 WT strain compared to the Δ*stkR* mutant strain grown in different media were used to generate the Venn diagrams.

04117201 WT *A. baumannii* strain, generated the Δ*stkR*. The Δ*stkR* mutant and the progenitor was assessed for potential virulence factors using *in vitro* and *in vivo* assays. Regulatory mechanisms like TCSTSs are used by bacteria to actively alter their response to a stimulus through the action of the HK and RR proteins (Chen *et al.* 2017). These systems have been reported to be involved in numerous biological processes.

4.6.1 Cell adherence and mouse model analysis of the *A. baumannii* 04117201 WT and Δ*stkR* mutant strain

The research described herein has demonstrated that the *A. baumannii* Δ*stkR* mutant can adhere to the surface of human epithelial A549 pneumocytes in greater numbers than the 04117201 WT strain. These data suggest that deletion of the RR in the StkRS system alters genes required for increased cell adherence. To further investigate this finding, the two strains were assessed in an *in vivo* model. Results obtained supported the *in vitro* data as the Δ*stkR* mutant strain had an increased bacterial load in the lung, blood, and spleen of the mouse compared with the 04117201 WT strain. This increase in adherence and bacterial load occurred alongside regulatory changes (Figures 4.6-4.9), which are hypothesised to be contributing factors in bacterial cell adherence regulated by the StkRS TCSTS.

4.6.2 Transcriptional analysis of the 04117201 WT and Δ*stkR* mutant in different media

Bacteria like *A. baumannii* have to survive in different ecological niches. This includes the blood, on hospital surfaces and human skin. Since bacteria change the expression of proteins based on the environment they inhabit it was expected that cells grown in different media would have differences in their transcriptome. Here, four different media were investigated. MH a rich nutrient media commonly used in laboratories to grow bacteria, lung media which is used to mimic a pneumonia infection, M9 media representing a minimal nutrient and carbon source environment like a hospital ventilator machine and whole blood to mimic septicaemia (Section 4.6.6-4.5.9). These four different media where chosen to provide a broad base of analysis across potential ecological niches that *A. baumannii* can survive in. The transcriptional changes observed in the four different media include changes in regulation of outer membrane structures such as the Type IV pili which have been

previously linked to motility, a phenotype correlated to adherence mechanisms (Mattick 2002, Eijkelkamp *et al.* 2011b, Giles *et al.* 2015). Trehalose synthesis which is implicated in osmotic stress and membrane stabilisation also a potential mechanism in adherence capabilities (Leslie *et al.* 1995, Avonce *et al.* 2006, Park *et al.* 2016). Furthermore, membrane-associated proteins, including the *paaA* operon, which is presumed to play a role in the attachment of bacteria to surfaces (Batisson *et al.* 2003) were also altered in expression. The *cidAB* genes involved in oxidative tolerance and virulence in bacteria (Ahn *et al.* 2016) and the *dnaK*, *groL*, and *groES* genes also affiliated with osmotic shock, biofilm formation, and membrane associated phospholipid genes (Jyot *et al.* 1999, Lemos *et al.* 2007, Marchenkov *et al.* 2018) were all altered in their expression. The above taken together provide a good basis for the altered *in vitro* phenotype seen of the Δ*stkR* mutant strain in relation to the increased adherence capabilities identified (Fig.4.1 and Fig.4.4).

Interestingly, an increase in transcription of iron acquisition and receptor genes in the Δ*stkR* mutant strain were identified in the lung and M9 media (Fig. 4.7 and Fig.4.8). The iron acquisition and receptor genes identified in Fig. 4.7 and 4.8 are postulated to contribute to an array of phenotypes, this includes increased cell adherence and bacterial cell survival within a host where there is a limited amount of iron and therefore an increased need for iron acquisition genes (Gaddy *et al.* 2012). These regulatory changes identified of the bacterial *A. baumannii* strains 04117201 WT and Δ*stkR* mutant when grown in lung and M9 media may be being replicated when grown in the *in vivo* models undertaken herein, demonstrating a plausible cause for the increased bacterial cell adherence and bacterial cell load of the Δ*stkR* mutant strain compared to the WT parent (Fig. 4.1 and 4.4). Intriguingly, genes such as OmpA (Choi *et al.* 2008, Gaddy *et al.* 2009b), Bap (Loehfelm *et al.* 2008), and pgaABCD or PNAG (Choi *et al.* 2009) that are traditionally known to be involved in adherence and biofilm formation were unchanged in transcription, adding to the novelty of the genes identified here.

4.6.3 Survival response of the *A. baumannii* 04117201 WT and Δ*stkR* mutant strains

Within a host system, bacteria are exposed to a variety of immune defence cells and it is unsurprising that a number of the differently regulated genes identified in

the lung and M9 media (Section 4.5.6 - 4.5.9) are associated with osmotic shock, commonly induced within neutrophils and macrophage cell to lyse bacterial cells.

In addition to the above, investigations into the mechanisms by which bacteria evade the host's immune system have also been conducted. Neutrophils and macrophage cells use a variety of mediators to induce killing, including nitric oxide, reactive oxygen, and phagolysosme-associated enzymes (Qiu *et al.* 2012, Weiss *et al.* 2015). The ability to withstand these mechanisms is an interesting virulence factor because it enables bacteria to become intracellular. This project demonstrated that deletion of the *stkR* gene resulted in an increased survival rate of the Δ*stkR* mutant compared to the 04117201 WT strain when exposed to J774.2 macrophage cells (Figure 4.3). Macrophage cells are known to participate in early inflammatory response and host defence against *A. baumannii* strains (Qiu *et al.* 2012). The observations made here imply that the Δ*stkR* mutant strain has an increased ability to withstand pressures while being actively phagocytosed by host immune cells. The increased survival of the Δ*stkR* mutant when exposed to macrophage cells and within the *in vivo* model is conceivably correlated to the altered regulation of these genes and others described previously (4.6.1 and 4.6.2).

In addition to withstanding phagocytosis, the Δ*stkR* mutant strain has an increased ability to resist the action of complement, another host defence system (Kim *et al.* 2009), where cascading proteins bind to the surface of a bacterial cell creating a pore and inducing lysis (Serna *et al.* 2016). Within *A. baumannii*, the *cipA* gene and OmpA together with multiple other membrane proteins have been identified as being involved in serum resistance (Kim *et al.* 2009, Koenigs *et al.* 2016). Interestingly, several transcriptional changes in outer membrane proteins including OmpW, TonB receptors, lipoproteins and OmpA precursors, ranging from a 3-fold decrease to an 84-fold increase were shown. These modifications are hypothesised to aid the increased serum resistance of the Δ*stkR* mutant.

Interestingly, the regulator IdeR in *Mycobacterium tuberculosis*, is involved in both iron acquisition and survival within macrophage cells (Gold *et al.* 2001), implying a link between the two phenotypes. As such, it is possible that there is a link within the Δ*stkR* mutant strain correlated with the increased expression of the iron acquisition gene and the increased bacterial load identified in the *in vivo* model.

These results are unlike others because *A. baumannii* is not traditionally known as an intracellular bacterium (Peleg *et al.* 2008); however, as new strains are identified and investigated, the capabilities of this pathogen are becoming known.

4.6.4 Investigation of the immune response of the host

Expression of virulence traits is essential for bacteria to infect a host and cause disease. Additionally, how the innate immune system responds to this infection also determines the disease progression. As such, this project investigated a collection of 84 immune genes involved in apoptosis, proinflammatory responses, cytokine and chemokine production. These data demonstrate that a lower response was induced by infection with the Δ*stkR* strain in comparison with the 04117201 WT strain. In particular, chemokines which work as chemoattractants are produced by the eukaryotic cell to recruit neutrophils to the site of infection (Breslow *et al.* 2011). The expression of the chemokines Cxcl3, Ccl4 and Ccl5 where statistically lower in the mouse lung when infected by the Δ*stkR* mutant strain compared to the WT parent (Table 4.1 $P < 0.01$, 0.02 and 0.01, respectively). Furthermore, as neutrophils are known to actively phagocytosis invading cells fighting infection therefore the recruitment of neutrophils post infection is postulated to be reduced in the mouse when infected with the Δ*stkR* mutant strain compared to the 04117201 WT strain. The implicated reduced presence of neutrophils within the lungs implies a cause for the rapid replication of the Δ*stkR* mutant strain and increased bacterial load identified.

In addition to the reduced activation of the chemokine response, several genes in the mouse lung exhibited differential expression when infected with the Δ*stkR* mutant strain compared to the 04117201 WT strain. These include: Fas and Traf6, which are associated with apoptosis (Micheau *et al.* 2003); Tlr5, Tlr4, Ticam1, and Ticam the Toll-like receptor pathways traditionally regulating inflammation in response to bacterial pathogens (Knapp *et al.* 2006, Wang *et al.* 2016, Chamoun *et al.* 2018); and CARD motifs, which are present on a number of proteins that also promote apoptosis. The interference in programmed cell death has the potential to increase the bacterial cell load in eukaryotic cells, thereby aiding the bacteria in their infection. These data describe the intrinsic ability of the Δ*stkR* mutant strain to survive within a host, multiply, cause disease, and evade the host immune response.

4.6.5 Conclusion

In summary, a strong association between the TCSTS StkRS and the pathogenicity of the *A. baumannii* 04117201 has been demonstrated. This research has shown that the Δ*stkR* mutant has an increased ability to survive macrophage pressures, resistant human serum and attach to pneumocytes cells. The Δ*stkR* mutant strain also invokes a decreased innate immune response postulated to be an important factor in the strain's ability to induce a disease state. Finally, deletion of the *stkR* gene resulted in vast and diverse alteration in transcription that subsequently increased the virulence capacity of the Δ*stkR* mutant strain compared to the 04117201 WT strain supporting these hypotheses.

CHAPTER 5 Discussion and final conclusions

5.1 Discussion and final conclusion

The dramatic increase of nosocomial *A. baumannii* infections combined with the increased rate of resistance to antibiotics has enhanced the importance of investigating the virulence mechanisms of this bacterium. The limited introduction of new antibiotic therapies means that *A. baumannii* remains a continuing threat to human health, increasing morbidity and mortality globally, particularly in immune-compromised patients. This body of work focused on investigating the virulence traits and the genetics responsible in aiding *A. baumannii* to persist in the hospital environment as well as the human host.

5.2 *A. baumannii* pellicle formation and associated mechanisms

The formation of a biofilm is a mechanism enabling bacteria to adhere to a variety of surfaces including eukaryotic cells. A biofilm provides protection inside and outside of a host, potentially increasing survival under an array of conditions including desiccation, and antimicrobial therapy including prolonged and life-long treatment and hospital cleaning regimes (Sections 1.5.2 – 1.5.2.3). A biofilm is generated through a number of stages (Figure 1.2), where a free-floating bacterial cell binds to a surface, multiplies and produces a comprehensive bio-structure involving a large collection of cells covered and embedded in exopolysaccharides, proteins and free floating DNA (Longo *et al.* 2014). There are two interfaces where a biofilm can be produced, the surface-liquid interface and the air-liquid interface (Kentache *et al.* 2017). The latter, known as a pellicle, has been extensively examined within this thesis and compared to the traditional biofilm, phenotypically, mechanically and genetically.

In Chapter two, a constant temperature of 25°C was required for adequate pellicle formation correlating with previous research that found limited pellicle formation at temperatures of 37°C (Martí *et al.* 2011a, Giles *et al.* 2015). Investigation of pellicle formation using polypropylene and glass tubes, representing different aspects of a hospital environment, in particular tubing, identified pellicle forming strains sporadically amongst our collection of 54 clinical strains (Section 2.5.1, Table 2.1, Figure 2.1). This confirmed that the pellicle trait is a rare occurrence in *A. baumannii* strains. In addition to identifying pellicle forming strains, alterations in cell surface hydrophobicity when exposed to xylene were investigated in the 54

clinical strain set. Interestingly a correlation between an increase in cell surface hydrophobicity and pellicle forming ability was identified. This discovery confirmed links in the literature seen between cell surface hydrophobicity and adherence capabilities (Pour *et al.* 2011). Further investigation of the pellicle forming strains focussed on motility (Eijkelkamp *et al.* 2011b). This research connected the three phenotypes, as the motile phenotype was displayed in all pellicle forming strains, significantly increasing our understanding of the interconnectedness of these three important characteristics.

To increase our understanding of the genetics involved in formation of the pellicle genetic assessment of the best pellicle former, the *A. baumannii* strain 17978hm, was undertaken. Generation of a transposon insertion bank, allowed for the identification of a number of key genetic elements required for pellicle formation; A1S_0115, A1S_0112 and A1S_0249 (*cpdA*) (Section 2.5.3). The three mutant strains A1S_0115::Tn, A1S_0112::Tn and *cpdA*::Tn that were generated were unable to form a pellicle. Intriguingly, these three mutants had altered cell surface hydrophobicity and motility, further substantiating the genetic interconnectedness of these three phenotypes. The A1S_0114 and A1S_0112 genes had been previously found to be associated with motility (Eijkelkamp *et al.* 2011b). However, the involvement of *cpdA* is a novel association with *A. baumannii* pellicle formation ability, cell surface hydrophobicity and motility, as little research has been conducted on the effects of cAMP in *A. baumannii*. However interestingly, research into the production of biofilms by *P. aeruginosa* has identified high levels of cAMP inhibiting biofilm formation, similar to what has been identified here (Almblad *et al.* 2019).

To understand the importance this secondary signalling molecule has on the three phenotypes, namely pellicle formation, cell surface hydrophobicity and motility, the *cpdA*::Tn strain was further investigated. The gene *cpdA* controls accumulation of cAMP, a global secondary signalling molecule, which is required for the function of multiple systems in a bacterial cell (Section 1.8). Determination of the intracellular concentration of cAMP, confirmed its significance in the formation of the pellicle, hydrophobicity and motility phenotypes seen in this *A. baumannii* strain (Section 2.5.3 - 2.5.5) (Nait Chabane *et al.* 2014, Kentache *et al.* 2017).

Interestingly, in *P. aeruginosa*, cyclic di-GMP, another secondary signally molecule which acts similarly to cAMP, has been identified as a central regulator involved in sessile formations of bacteria, specifically biofilm formation (Xu *et al.* 2016). In *P. aeruginosa*, cyclic di-GMP acts upon the SagS-HapZ system generating a biofilm state. Another example of this type of regulation involves the *Serratia marcescens* type I fimbriae-dependent biofilm, which is regulated by the cAMP-CRP complex and deletion of the *cpdS* gene encoding the cAMP-phosphodiesterase protein, results in defective biofilm formation and reduced fimbriae production (Kalivoda *et al.* 2013). These data pinpoint feasible interactions of the secondary signally molecule cAMP. Therefore, to look more closely at this, transcriptomic investigation of the generated *cpdA*::Tn mutant strain was undertaken. Transcriptomic investigation identified numerous alterations in the *cpdA*::Tn mutant profile compared to the 17978hm parent. The genes of interest include the chaperon usher pilus and the CsuA/BABCDA systems were both down-regulated, these systems having been previously identified as key components in pellicle formation (Nait Chabane *et al.* 2014, Kentache *et al.* 2017). From these data, it can be postulated that the cAMP secondary signalling molecule is regulating these required systems in the *cpdA*::Tn mutant and therefore altering the pellicle, cell surface hydrophobicity and motility phenotypes.

In summary, Chapter two identified a novel genetic element *cpdA* and its involvement in pellicle formation. Additionally the identification of a strong correlation between pellicle production, cell surface hydrophobicity and motility through cAMP has increased our understanding of the intricate formation of the pellicle and the interconnected regulation of these phenotypes.

5.3 *A. baumannii* StkRS TCSTS is associated with antibiotic resistance

The complexity and global regulation of TCSTSs has been demonstrated through a variety of TCSTS including the BfmSR system. As such, further research into the numerous unknown systems in *A. baumannii* is needed to identify and then understand the reach of these complex TCSTS. Moreover, the need for better equipped treatment regimes and targeted antibiotics has led researchers to investigate TCSTS, as they are possible targets for disruption (Section 1.7). Thus, Chapter three focused on the evaluation and identification of the highly virulent *A. baumannii*

strain 04117201, and the identification of an unknown TCSTS named in this study as StkRS.

The dramatic increase of antibiotic resistant strains seen through the past decade has generated alarm as to the increased occurrence of *A. baumannii* infections and their severity in the hospital environment (Ahmad *et al.* 2018). As current antibiotics are continuing to come up short against MDR and pandrug-resistant *A. baumannii* strains, investigation into the antibiotic resistance mechanisms used by *A. baumannii* is imperative. There are many mechanisms used by bacteria to resist antibiotics, these include efflux pumps, such as the RND complexes AdeABC, AdeFGH and AdeIJK. Another mechanism is the exchange and accumulation of mobile genetic elements like $bla_{OXA\text{-}143}$ which encodes resistance to beta-lactams. Furthermore, alterations in the cells surface capsule or the lipid A inner or outer core (Section 1.5), can reduce binding affiliation of antibiotics therefore increasing antibiotic resistance. The regulation of some of these mechanisms can be attributed to TCSTS (Section 1.6.1). For example, the BfmSR TCSTS system can modulate the *csuA/BABCDE* chaperone operon pili system, altering cell surface pili and biofilm formation ability. Importantly the formation of the biofilm is also correlated with antibiotic resistance as the biofilm structure itself can provide a barrier against antibiotics (Section 1.5.2.2). BfmSR also regulates resistance to carbapenems and CHL antibiotics. Furthermore, highlighting the global regulatory ability of TCSTS, the BfmSR is responsible for increased complement mediated bactericidal resistance through the OmpA protein (Section 1.6.1.5.2).

To identify an appropriate virulent *A. baumannii* strain a selection of virulence assays were undertaken on the collection of 54 clinical strains. These assays included assessments of biofilm formation, antibiotic resistance and adherence to A549 pneumocytes as these traits have been previously identified as important in survival and establishment of infection. These analyses identified *A. baumannii* 04117201 as the best candidate (Section 3.5.1); it displayed resistance to multiple antimicrobial agents, showed an ability to form a robust biofilm and was able to adhere to A549 pneumocytes (Table 3.2, Figure 3.1) (Eijkelkamp *et al.* 2011b), pointing to a potentially highly virulent strain. The aim of this chapter was to identify and characterise a TCSTS potentially involved in regulating factors that play a role in

virulence. As such, the genome of *A. baumannii* 04117201 genome was analysed for TCSTS that did not have homologues in the avirulent SDF strain. This allowed the identification of the TCSTS we designated StkRS that fulfilled these criteria. Genetic removal of the RR gene *stkR* by homologous recombination generated the Δ*stkR* mutant strain (Section 3.5.2)

To see if this TCSTS was involved in regulating antimicrobial resistance, analyses with a variety of clinically relevant antibiotics, including polymyxins, was undertaken. Antibiotic sensitivity profiling of the Δ*stkR* mutant (Section 3.5.3, Table 3.2) identified an increase in CST resistance compared to the 04117201 WT. CST is a polymyxin cationic peptide composed of a cyclic heptapeptide covalently attached to a fatty acyl chain (Section 3.3). CST functions by attaching and then displacing magnesium and calcium cations, in turn increasing the permeability of the outer membrane, that results in leakage of cellular contents (Hancock 1997, Falagas *et al.* 2010, Deveson Lucas *et al.* 2018, Jaidane *et al.* 2018). CST resistance is being more readily reported in the literature and as it constitutes resistance to what is known as a 'last resort' antibiotic, urgency is needed to investigate the different mechanisms used by bacteria to generate resistance to it. There are three mechanisms associated with increased polymyxin resistance identified to date in *A. baumannii*. One is the modification of lipid A by the addition of pEtN which can be achieved via two different pathways; the first is via PmrC which is associated with the PmrAB TCSTS, and the second is associated with HNS and pEtN. The second mechanism is modification of lipid A by the addition of GalN through NaxD which is by the *pmrB* gene, and the third is the complete loss of lipid A (Section 3.3). Investigation of the Δ*stkR* mutant strain eliminated the complete loss of lipid A as the mechanism for CST resistance (Carretero-Ledesma *et al.* 2018), as a silver stain of a PAGE showed no identifiable alterations in the lipid A component (Section 3.5.6). Therefore, further investigations to identify the genetic elements responsible for the observed resistance were undertaken. RT-PCR revealed a significant increase in transcription of the *pmrCAB* genes, suggesting decoration of the lipid A component with pEtN and/ or GalN (Section 3.5.7) providing the most probable reason for the increase in CST resistance seen in the Δ*stkR* mutant (Adams *et al.* 2009, Beceiro *et al.* 2011). An increase in expression of *pmrC* is traditionally correlated with point mutations in

pmrCAB itself, however sequencing did not reveal any mutations in the Δ*stkR* mutant strain (Section 3.5.7).

TCSTSs are able to regulate other systems by a process known as cross-talk between non-cognate pairs (Section 1.6.1.6). For example, the BfmSR system can be activated by another HK thereby inducing biofilm formation (Olson *et al.* 2012) (Section 1.6.1.5.2). Usually, *pmrC* is regulated by the PmrAB however evidence presented herein suggests that there is possible cross-talk between the PmrAB and StkRS systems acting upon *pmrC* (Section 3.5.7). This conjecture is also supported by studies undertaken in other species including *S. enterica* and *K. pneumoniae*, where the PhoPQ and PreAB TCSTS interact with the PmrAB TCSTS acting on *pmrC* (Section 3.6).

As stated previously, one of the mechanisms for CST resistance is the complete loss of the lipid A portion of LOS/LPS (Section 3.3). This commonly results in a significant decrease in the cell surface hydrophobicity of the strain, indicating a change in cell surface charge and decreasing CST binding affinity. Therefore, extrapolation of these data suggests that the cell surface hydrophobicity and lipid A are correlated in CST resistance. As such, the *A. baumannii* 04117201 WT and Δ*stkR* mutant strains were investigated for alterations in their cell surface hydrophobicity with/ without CST treatment (Section 3.5.4). Interestingly, the Δ*stkR* mutant strain presented an increased cell surface hydrophobicity when compared to its parent in standard growth conditions without CST treatment (Section 3.5.4, Figure 3.3). However, fascinatingly, the cell hydrophobicity of both strains decreased when exposed to CST at subinhibitory concentrations and was significantly ($P < 0.0005$) greater for the Δ*stkR* mutant than the 04117201 WT strain. These data, taken together with the transcriptional changes identified of the *pmrCAB* system in the Δ*stkR* mutant, present a correlation between cell surface hydrophobicity and the addition of pEtN and or GlaN to lipid A effecting CST resistance. These results are supported by others which have identified alterations in the hydrophobicity of the membrane when altering the concentrations of pEtN and or GlaN (Kim *et al.* 2016).

In conclusion, chapter three identified a highly virulent *A. baumannii* strain, containing a novel TCSTS named here as StkRS. When the *stkR* RR gene is deleted

there is an increase in CST resistance. Additionally, under CST treatment transcription of the *pmrCAB* operon increased and the cell surface hydrophobicity decreased for the Δ*stkR* mutant strain more in comparison to the 04117201 WT strain. These data collectively present a plausible reason for the CST resistance seen for the Δ*stkR* mutant as well as identifying an association between the StkRS TCSTS, the PmrAB TCSTS, and CST resistance. This research highlights the interconnectedness of TCSTS mechanisms in *A. baumannii*.

5.4 *A. baumannii* StkRS TCSTS is associated with virulence traits

The ability of *A. baumannii* to infect and persist in a human host is seen globally in the high morbidity and mortality rates of this bacterium. *A. baumannii* possesses multiple virulence factors as stated previously (Section 1.6, 1.7, 1.9 and 1.10) and these are important in the survival and infectivity of this bacterium. Subsequently, Chapter four focused on determining if the StkRS TCSTS identified in Chapter three plays a role in regulating these factors. The studies confirmed that StkRS TCSTS in 04117201 is associated with virulence traits as seen by the increase in antibiotic resistance through regulation of *pmrC* and alteration in cell surface hydrophobicity, extending the finding described in Chapter 3, namely increased cell adherence capability and biofilm formation.

A. baumannii is commonly identified as infecting the lungs and causing pneumonia (Section 1.1 – 1.4). Infection within a host generally begins with a bacterial cell arriving at the site, adhering and multiplying (Draughn *et al.* 2018). In *A. baumannii*, this can involve a variety of pili e.g. type IV and outer membrane proteins (Section 1.6). Being able to evade the immune system is another essential function allowing survival in a host. This can be accomplished by resisting osmotic pressures commonly caused by macrophage cells and resisting complement proteins within serum (Section 1.10). Thus, the 04117201 WT and Δ*stkR* derivative were investigated for adherence capabilities, macrophage survival, resistance to human serum and persistence within a mouse *in vivo* infection model. Results obtained identified a greater capacity of the Δ*stkR* mutant to adhere to A549 pneumocytes cells (Section 4.5.1). As stated, there are many mechanisms which can be utilised to increased cell adherence, for example Type IV pili are appendages non-covalently assembled on the membrane and are essential in a number of processes like motility,

biofilm formation and host cell adherence (Ronish *et al.* 2019). Type IV pili where identified as being up-regulated of the Δ*stkR* mutant compared to the parent 04117201 strain by approximately 2-fold in the blood, lung and M9 media. Potentially correlating to the increased cell adherence seen of the mutant strain. Other proteins like Bap essential for biofilm formation as well as adherence where not identified in any of the transcriptome analysis (Brossard *et al.* 2012) highlighting the novelty of the genes identified. Interestingly, the *paaA* operon genes, where identified as down-regulated when the Δ*stkR* mutant strain was grown in MH media but up-regulated significantly approximate 15-fold in the Δ*stkR* mutant when grown in lung and M9 media, the *paaA* operon genes are also correlated with cell adherence, suggesting that the Δ*stkR* mutant has an increased ability to adhere to surfaces when exposed to a lung or minimal media environment. In addition to the above a number of capsule proteins including carbohydrate metabolism genes and membrane associated phospholipid where found to be up-regulated in the Δ*stkR* strain when grown in the lung media adding to the complexity of the transcriptomic changes being undertaken of the bacterial strain and presenting a plausible foundation for the increased adherence seen of the Δ*stkR* mutant strain in the mouse lung (Batisson *et al.* 2003, Tamura *et al.* 2004).

To generate a complete view of the influence of the StkRS TCSTS resistance to complement killing by human serum proteins was assessed (Section 4.5.2). An increased ability to withstand complement mediated killing by human serum was identified for the Δ*stkR* mutant when compared to its parent. Evading and or resisting the attachment of these immune proteins within blood are essential for bacterial cells to cause disease within a host. Cell lysis is achieved through a step by step process which creates a pore releasing the cellular content (Section 1.10). There are a number of factors which can assist in resisting these proteins including extracellular polysaccharides, lipopolysaccharide, lipid A, the capsule and outer membrane proteins like OmpA (Pakharukova *et al.* 2018). Interestingly, the ability of the StkRS TCSTS to alter the lipid A component of the Δ*stkR* mutant strain in response to stimuli e.g. CST antibiotic has been identified and discussed in chapter three (Section 3.6). These results are similar to *Neisseria gonorrhoeae* were alteration in the lipid A component due to the loss of pEtN decreased resistance to complement killing as

well as resistance to polymyxin B, connecting these two phenotypes (Lewis *et al.* 2009).

An increased ability to survive challenge by macrophages was seen when the *stkR* gene was inactivated (Section 4.5.3). Macrophage survival for many pathogens (Section 1.10) is an important step in host colonisation. A number of genes are associated with increased survival under oxidative stress, including *cidAB* and *dnaK*; these genes are also associated within biofilm formation via membrane associated phospholipid genes (Section 4.6). Interestingly, the CST resistance seen in the Δ*stkR* strain can commonly result in a decrease in bacterial cell fitness, specifically related to a decrease in survival when exposed to H_2O_2 (Jones *et al.* 2017). However, this was not observed for the Δ*stkR* mutant strain, which is in contrast to Jones *et al* (2017), further identifying the novelty of the StkRS system.

In vitro assessments indicated that the StkRS TCSTS is involved in virulence. To confirm and extend this investigation utilising an *in vivo* murine model was undertaken. A significant increase in the bacterial cell load in the lung, spleen and blood of the Δ*stkR* mutant strain compared to the 04117201 WT strain was identified (Section 4.5.2 and 4.5.5). These data correlates with the increased ability to adhere to A549 cells identified for the Δ*stkR* mutant strain. The increased adherence of the Δ*stkR* mutant in the murine model also identifies and increased pathogenic potential of the mutant strain and its ability to withstand and evade the immune response which will be discussed further.

5.4.1 Deletion of the *stkR* RR gene leads to dramatic transcriptomic changes across a variety of media

To identify genetic regulatory mechanisms associated with the TCSTS StkRS, HiSeq transcriptomic analysis was undertaken of the two strains grown in different media used to mimic the different environments used in the *in vitro* and *in vivo* assays (Section 4.5.6 - 4.5.10). As expected, overall there are large transcriptional changes between the Δ*stkR* and 04117201 WT strain in all media. However this was most apparent in the lung and M9 media (Appendix B, C, D and E). The number of genes that changed in transcription of the Δ*stkR* mutant compared to the WT when grown in the lung gave a total of 701 up-regulated and 464 down-regulated; when

grown in M9 media resulted in 930 up-regulated and 246 down-regulated, whereas significantly lower transcriptomic changes were seen when grown in the blood resulting in only 16 up-regulated and 123 down-regulated of the Δ*stkR* mutant when compared to the WT strain. Finally, when the Δ*stkR* mutant was grown in MH media the resulting number of gene changing in their transcriptomic where only 14 up-regulated and 61 down-regulated genes when compared to the WT strain. The large significant number of genes that changed in transcription between the Δ*stkR* mutant and WT are suggestive that the *stkR* RR is a critical component in regulating mechanims of this *A. baumannii* bacterial strain 04117201.

5.4.1.1 Iron acquisition

Of the highly up-regulated genes identified when grown in the lung and M9 media, some were associated with iron acquisition, one particular outermembrane receptor giving an increase in transcription of 82-fold and 50-fold respectively, in the Δ*stkR* mutant strain compared to the WT. Iron acquisition being a necessary process for survival within the host suggesting a correlation between the deletion of the *stkR* gene and increased iron contributing to the increased bacterial load in the *in vivo* model (Gaddy *et al.* 2009b) as well as having been described as an important virulence factor in *A. baumannii* persistence. A large range of other iron acquisition genes including iron uptake genes gave increases of 9 and 13-fold in transcription in the lung and M9 media respectively; siderophore receptor genes gave increases of 12 and 11-fold transcription in the lung and M9 media respectively; ferric iron transport genes increased by 2.4 and 2.6-fold transcription in the lung and M9 media respectively; receptor genes increased by 6-fold in both the lung and M9 media and iron receptor genes increased by 11 and 20-fold in transcription in the lung and M9 media respectively. In addition to the above a siderophore biosynthesis gene cluster was up-regulated between 26-fold to 435-fold when grown in the lung media and between 57-fold to 904-fold when grown in M9 media (Dorsey *et al.* 2003b, Mihara *et al.* 2004, Zimbler *et al.* 2009). These data demonstrate a substantial link between the StkRS TCSTS and iron acquisition within the bacterial strain.

5.4.1.2 Capsule production

The capsule is a known important virulence trait contributing to a range of abilities including resistance to antibiotics e.g. CST, macrophage survival and human

serum resistance as identified in chapter three. Additionally, as described in chapter four, genes associated with biofilm formation including the Type IV pili (Mattick 2002), metabolic pathways such as fatty acid metabolism and glycosylation are connected with the production of capsule affecting the outer membrane, these were all identified as altered in transcription (Shashkov *et al.* 2015, Wessels 2016). Type IV pili like *pilO*, *fimT* and *pilV* were all up-regulated between 2 and 2.6-fold in Δ*stkR* mutant strain compared to the WT when grown in the lung media. Whereas, the Type IV pili *pilN* and *pilA* were up-regulated 2.6-fold in the Δ*stkR* mutant when grown in M9 media. Showing the bacterial strain responding differently when grown in different media.

Furthermore, the production of biosurfactants and glycosylation (Lees-Miller *et al.* 2013), glycosylation having also been reported in chapter four as significantly up-regulated in the Δ*stkR* mutant strain potentially altering the capsule layer of the strain. Additionally, biosurfactants can alter the polysaccharides surrounding the bacteria cell, leading to alterations in cell surface hydrophobicity, motility, and protection against the host immune response e.g. serum and phagocytosis (Prabhu *et al.* 2003, Wessels 2016). Fascinatingly, an aromatic amino acid AroP transport and biosynthesis genes were identified as highly up-regulated in the Δ*stkR* mutant strain 53-fold and 83-fold respectively, in the lung and M9 investigations.

Interestingly, trehalose synthesis also affects the outer membrane and therefore has been implicated in capsule production (Avonce *et al.* 2006, Park *et al.* 2016), and was significantly altered in its transcription across the different media. When the Δ*stkR* mutant was grown in MH media the trehalose genes were down-regulated by 5 and 3.6-fold compared to the WT strain. Whereas, when the strains where grown in the lung media the trehalose genes where significantly up-regulated by 101 and 140-fold; this was not repeated when the strain where grown in M9 or blood. The Δ*stkR* strain showed a down-regulation of the trehalose genes of 13 and 19-fold compared to the WT strain when grown in M9 media and when grown in blood only the first gene of the operon was altered in its transcription showing a down-regulation of 2-fold.

These data highlight the significant transcriptomic differences seen across the different media when the *stkR* RR gene is deleted in the *A. baumannii* 04117201 bacterial strain, and how the growth conditions can so dramatically alter the epigenetics of the bacterial cell. Taken together the transcriptional changes identified herein are most probably the genetic contributing factors leading to the increased virulence seen of the Δ*stkR* mutant compared to the 04117201 WT strain through capsule production, alteration of the lipid A components and pili formation.

5.4.2 Deletion of the *stkR* RR gene invokes a reduce innate immune response of the host

There are many factors which aid in the bacterial cell survival in a host, the majority of which have been described above. However, the ability of a bacterial strain to evade the host immune response is a key component of its survival (Section 1.10). Therefore, investigation of the ability of the two strains to evade the host immune response was undertaken. Analysis of the host (murine) immune response was conducted using an PCR-array assessing 84 immune genes specifically targeting genes believed to be affected by bacterial pathogens. Cytoscape modelling was used to present and elucidate effects on the mouse immune response between *A. baumannii* 04117201 and its derivative (Section 4.5.5) (Table 4.1 and Figure 4.5). Chemokines, the Toll-like receptor pathway and programmed cell apoptosis were identified as being significantly altered in their response to removal of *stkR* RR gene. The chemokines showed a reduction of up to 706-fold difference in transcription expression when the host was infected with the Δ*stkR* mutant compared to the WT strain. Additionally, other chemokine genes showed a reduction between 2 and 110-fold between the strains. These dramatic differences in the ability of the host to identify the Δ*stkR* mutant strain are postulated to be involved in the ability of the Δ*stkR* mutant strain to produce a much larger bacterial load as well as evade the immune response in the murine host.

Interestingly, *A. baumannii* is able to be identified by the Toll-like receptor 4 (Takeuchi *et al.* 2002) and CD14, which commonly leads to early recruitment of neutrophils in the host system when infected by this pathogen (de Breij *et al.* 2012). However, the expression of CD14 was unchanged between the two strain, and the toll-like receptor 4 gene was reduced in its expression by 2.8-fold when infected with

the Δ*stkR* mutant strain and 5.2-fold when infected with the WT strain. Again, these data could be a representative that this particular pathogen, 04117201 *A. baumannii* strain is able to slip past the innate immune response and cause an infection (Knapp *et al.* 2006).

Another indication of infection is the regulation of programmed cell death commonly by regulated in part by Fas (tumor necrosis factor receptor super family member 6 (TNFRSF6) (L. Wang *et al.* 2010). Interestingly, this gene was down-regulated in the host when infected by the Δ*stkR* mutant by 9.9-fold and significantly down-regulated in the host when infected by the WT strain by 254-fold. Fas is a type I transmembrane protein, which forms the death-inducing signalling complex (DISC). This is found on the surface of the cell and is an extrinsic pathway leading programmed cell death (Huang *et al.* 1996, Micheau *et al.* 2003).

A. baumannii has been shown to invoke a reduced response of inflammatory cytokines when compared to other *Acinetobacter sp.* like *Acinetobacter junii* in an infection (de Breij *et al.* 2010). Therefore, as removing *stkR* generated a reduced immune response in comparison to the 04117201 WT strain this reduced innate immune response could be significant in comparison to the rest of the *A. baumannii* strains and by extension other *Acinetobacter sp.* These results are consistent with experiments using immune deficient mice, where there is a noticeable reduction in production of cytokines, chemokines, tumour necrosis factor and chemoattractant proteins (Garcia-Patino *et al.* 2017). All of which have been identified as contributing to a reduced production of neutrophils to the site of infection, and therefore contributing to the increased bacterial load in the mouse.

In summary, the *in vitro* and *in vivo* investigations illuminated the breadth of the mechanism correlated to the StkRS TCSTS and demonstrated that this particular TCSTS is most likely responsible for altering the lipid A component and therefore capsule of the cell structure. Alterations of the cell surface is, as seen in the physiological and regulatory changes of the Δ*stkR* mutant leads to a dramatic increase of virulence potential, including the ability to evade the innate immune response and cause a significant bacterial cell load in a mouse model. These data have contributed significantly to the understanding of TCSTSs and their multiple effects and interconnectedness within bacterial cells.

5.5 Final conclusions

A. baumannii strains within this project were examined using a combination of phenotypic and molecular analyses. Multiple mechanisms and genes, important *A. baumannii* virulence traits, contribute to this significant human bacterium's ability to persist and persevere in the hospital environment and within a host. Generation of a mutant bank using a transposon insertion, allowed for examination and identification of the molecular link between pellicle formation and motility; via the secondary signalling molecule cAMP. Additionally, alterations in hydrophobicity were identified as important for pellicle formation. Investigation of a variety of *A. baumannii* strains including cell adherence, motility and biofilm formation identified a number of potentially highly pathogenic bacterial strains in our collection of 54. Evaluation of the strains identified the 04117201 strain as presenting a highly potential virulence as demonstrated in the *in vitro* assays undertaken herein. As such this *A. baumannii* strain 04117201 was investigated for its TCSTS and their presence in the avirulent strain SDF. Upon analysis it was identified that the StkRS TCSTS identified herein was not present in the SDF strain and therefore possibly related to the increased virulence potential seen of the 04117201 *A. baumannii* strain. A large scale transcriptomic analysis of bacteria grown in a variety of media linked with *in vitro*, *in vivo* and immune array studies highlighted the role of the *stkR* RR gene in *A. baumannii* 04117201.The significant studies undertaken herein have identified novel regulatory genes and as such have aided in increasing our understanding of this specie as well as contributed to the wider body of knowledge.

5.6 Future directions

Future research is required on the MDR *A. baumannii* pathogen as its high morbidity and mortality rates are a global concern. This thesis focused on antibiotic resistance and virulence capabilities. As such modification of the capsule and or lipid A has been identified herein as a contributing mechanism leading to the increased antibiotic resistance and increased virulence seen of the Δ*stkR* mutant strain compared to the 04117201 WT strain. To investigate the specific changes made of the lipid A component, the Δ*stkR* mutant and 04117201 WT strains would be chemically assessed using thin layer chromatography and tandem mass-spectrometry using electronspray ionization coupled to collision induced dissociation and

ultraviolet photodissociation. These assessments would identify the precise alterations in the lipid A component of the cell when exposed to CST. From these results specific identification of the chemical decoration of the lipid A component of the bacterial cell would confirm either pEtN and or GlaN as the main contributor to increased antibiotic resistance and virulence potential. LOS in *A. baumannii* as previously described (Section 3.3) has a general structure with a conserved lipid A and a core oligosaccharide. Identification of the precise decoration of the lipid A component with either pEtN or GlaN would be the first step in working towards identifying new structures to inhibit, with a focus on reducing the resistance to cationic antimicrobial peptides like CST.

Regulation of the *pmrCAB* operon is hypothesised in this study to be affected by the StkRS TCSTS (Section 3.5.7). This effect is suggested to be through cross-talk of non cognate pairs. To investigate the potential cross-talk between these two systems PmrAB and StkRS assessment using western blotting and gel shift assays would be undertaken to identifying binding sites and autophosphorylation to confirm or reject the hypothesis from chapter three (Siryaporn *et al.* 2010, Miyake *et al.* 2019). Upon identification of the regulatory mechanisms of these systems, if the hypothesis was not confirmed further investigation into identifying the intermediate acting upon the PmrAB system would be undertaken.

There are five TCSTS in the *A. baumannii* 04117201 strain that are not present in the avirulent SDF strain, investigation of these TCSTS is the initial step in gaining a greater understanding of the interconnectedness of these systems within a particular strain. These investigations would highlight and identify the particulars of each system and how they work individually as well as together. This research would not only assess the RR proteins within these systems but the HK proteins as well. Generating an array of RR and HK mutants as well as double mutants where the entire system is knocked out would be one avenue to peruse. The limitations to assessing the two-component systems in this manner is the time constraints, generating knock out mutants is a long winded process. Similar to the research presented in this thesis the research would focus on the virulence traits of the strain. This analysis would be undertaken by a number of assays, including cell adherence, resistance to serum, macrophage survival and antimicrobial resistance; and would

also include assessing pH stress and desiccation survival as these assays are also important in identifying virulence. In addition to the above, investigation into the interconnectedness of the TCSTS would be undertaken. This would focus on the phosphorylation of the HK and RR proteins at the His and Asp residues possibly using western blotting and gel shift assays, with the hope of identifying any potential cross-talk between the TCSTS.

As described previously Chapter 4 identified significant transcriptomic differences across the different media. It was suggested that these data are the genetic contributing factors leading to the increased virulence through capsule production and alteration of the lipid A components, pili formation and resistance to osmotic pressures of the *A. baumannii* strain analysed herein. As the production of capsule is a know virulence factor and without a capsule a bacterial strain is considered avirulent, further investigation into the specific genes contributing to the regulation and therefore production of the different capsule components would be a interesting area to continue investigating. Potentially leading to a greater understanding of the capsule and its role in virulence.

As *A. baumannii* is a rapidly emerging pathogen, new research into the disruption of these TCSTS could potentially provide an alternate avenue for patient treatment. Of particular interest is the ability to inhibit or remove the TCSTS within these bacterial strains, as these systems are not present in humans. One method that is continuing to generate advancement is CRISPR gene editing. Future research could use CRISPR to specifically target the TCSTS know for increasing virulence in these bacterial strain removing them from the bacterial genome and turning highly pathogenic bacteria in to avirulent strains easily removed from the body by the immune system potentially aided by antibiotics (Mangas *et al.* 2019, Y. Wang *et al.* 2019).

The future research suggested are steps in the right direction of understanding and potentially developing new means of combating this pathogen; however, the only way to know is to continue fundamental research.

APPENDICES

Appendix A: Characteristics of 54 clinical *A. baumannii* isolates

Isolate[def]	Pellicle plastic[a]	Pellicle glass[a]	Biofilm[b]	Hydrophobicity[c]	Motility Twitching	Motility Swarming	Source
ATCC 17978	Medium	Good	Low	Low	-	+	Meningitis
17987hm	Good	Good	Not tested	Low	Not tested	Not tested	Meningitis
6896168	0	0	Medium	0	-	-	Unknown
9028181	0	0	Medium	High	-	-	Pus
11986752	Low	Low	Good	High	+	-	Pus
2320495	Medium	Good	Good	High	+	+	Pus
4397670	0	0	Good	High	-	-	Unknown
WM98c	Medium	Good	Good	High	+	-	Unknown
WM97a	0	0	Good	High	-	-	Sputum
04145027	Good	Good	Medium	High	+	+	Vaginal
06345143	0	0	Medium	Low	-	-	Tracheal aspirate
05293224	0	0	Medium	0	+	-	Tracheal aspirate
04202856	0	0	Medium	High	-	-	Urine
D1279779	0	0	Medium	0	-	-	CA blood
ATCC 19606	0	0	Good	Low	-	-	Urine
AYE	0	Good	Medium	High	+	-	Urinary tract
6772166	0	0	Medium	0	+	-	Pus
6856775	0	0	Medium	0	+	-	Sputum
PW01c	0	0	Medium	0	+	-	Unknown

Appendix A

Isolate[def]	Pellicle plastic[a]	Pellicle glass[a]	Biofilm[b]	Hydrophobicity[c]	Twitching	Swarming	Source
WM98	0	0	Medium	Low	+	-	Wound
6877889	0	0	Medium	Low	+	-	Sputum
6870155	0	0	Low	Low	+	-	Sputum
AB0057	0	Good	Medium	0	+	-	Blood
6856390	0	0	Medium	0	-	-	Sputum
9137982	0	0	Medium	Low	-	-	Pus
6913054	0	0	Medium	0	-	-	Blood
1182468	0	0	Medium	0	-	-	Sputum
1182372	0	0	Medium	0	-	-	Sputum
11986751	0	0	Medium	0	-	-	Pus
9078336	0	0	Medium	0	-	-	Sputum
1182372	0	0	Medium	0	-	-	Sputum
1172312	0	0	Good	Low	-	-	Sputum
1077697	0	0	Good	Low	-	-	Sputum
9038266	0	0	Medium	Low	-	-	Sputum
9034499	0	0	Medium	Low	-	-	Sputum
1198673	-	-	-	-	-	-	Sputum
1279683	0	0	Medium	Low	-	-	Pus
9030751	0	0	Good	0	-	-	Pus
9030759	0	0	Medium	0	-	-	Sputum
RB02	0	0	Medium	0	-	-	Rectum
WM99a	0	0	Medium	Low	-	-	Unknown

Isolate[def]	Pellicle plastic[a]	Pellicle glass[a]	Biofilm[b]	Hydrophobicity[c]	Twitching	Swarming	Source
WM99a	0	0	Medium	Low	-	-	Unknown
RB02b	0	0	Medium	0	-	-	Sputum
WM00	0	0	Medium	0	-	-	Bronchial
PW01b	0	0	Medium	0	-	-	Unknown
RB01	0	0	Medium	0	-	-	Blood
RB02e	0	0	Medium	0	-	-	Rectum
RB02d1	0	0	Medium	0	-	-	Tracheal aspirate
PW01a	0	0	Medium	0	-	-	Unknown
08317005	0	0	Good	Low	+	-	Tracheal aspirate
08325850	0	0	Good	0	+	-	Tracheal aspirate
08315000	0	0	Good	0	-	-	Wound
4117201	0	0	Medium	Low	-	-	Tracheal aspirate
5299446	0	0	Medium	Low	-	-	Tracheal aspirate
6954775	0	0	Medium	0	-	-	Catheter
WM99c	0	0	Medium	0	-	-	Sputum
ACICU	0	0	Not tested	Low	-	-	Cerebrospinal fluid

[a] Pellicle - Good = > 0.5, medium = 0.2-0.5, low = < 0.2,
[b] Biofilm– Good = > 1.5, medium = 0.5 – 1.4, low = < 0.5,
[c] Hydrophobicity high > 45%, low < 45% zero = 0
[d] Purple = non-international clone type I or II,
[e] Green = international clone type I,
[f] Blue = international clone type II.

Appendix B: Gene expression of the Δ*stkR* mutant compared to the WT in MH media

Peg Number	Fold Change	Gene Name
Up regulated		
799	2.03	Butyryl-CoA dehydrogenase
840	3.28	Acyteltransferase
872	2.19	Malonate transporter MadL subunit
971	2.32	Hypothetical protein
1186	2.56	Multidrug translocase MdfA
1235	2.30	Transcriptional regulator AraC family
1341	2.10	Carbonic anhydrase
1385	2.12	NADP-specific glutamate dehydrogenase
1653	2.11	Hypothetical protein
2244	2.53	Hypothetical protein
2320	2.11	Hypothetical protein
2340	2.81	Phage capsid protein
2939	2.12	Isoleucyl-tRNA synthetase
3218	2.23	Heat shock protein 60 family co-chaperone GroES
3219	2.46	Heat shock protein 60 family chaperone GroEL
3343	2.18	Asp aminotransferase
Down regulated		
41	-2.36	5-nucleotidase SurE
150	-2.58	Bacteriolytic lipoprotein entericidin B
163	-2.06	Alkylphosphonate utilisation operon protein PhnA
206	-2.17	Alkyl hydroperoxide reductase subunit like protein
254	-2.11	Hypothetical protein
308	-2.36	Benzoate transport protein
311	-2.20	Benzoate dioxygenase beta subunit
340	-3.51	Hypothetical protein
341	-2.02	Hypothetical protein
390	-2.92	Uncharacterised zinc-type alcohol protein-
402	-2.36	Urea carboxylase-related ABC transporter protein
448	-2.68	L-Asp-beta-decarboxylase

Peg Number	Fold Change	Gene Name
471	-2.78	Hypothetical protein
473	-3.39	Hypothetical protein
500	-2.22	Transcriptional regulator LysR family
553	-2.53	Ethanolamine ammonia-lyase heavy chain
564	-2.20	Hypothetical protein
566	-2.02	Glutathione S-transferase family protein
571	-2.28	Hypothetical protein
582	-3.42	Hypothetical protein
584	-2.30	Protein ycgK precursor
669	-2.28	Transporter MFS superfamily
738	-2.26	Transporter MFS superfamily
742	-2.86	Phenylacetic acid degradation protein PaaN
743	-4.42	Phenylacetate-CoA oxygenase PaaG subunit
744	-3.33	Phenylacetate-CoA oxygenase PaaH subunit
745	-2.63	Phenylacetate-CoA oxygenase PaaI subunit
746	-3.15	Phenylacetate-CoA oxygenase PaaJ subunit
747	-3.57	Phenylacetate-CoA oxygenase/reductase PaaK
748	-3.05	Phenylacetate degradation enoyl-CoA PaaA
749	-3.05	Phenylacetate degradation enoyl-CoA PaaB
750	-3.04	3-hydroxyacyl-CoA dehydrogenase PaaC
822	-3.90	Hypothetical protein, putative exported protein
825	-5.75	Hypothetical protein
826	-6.28	Hypothetical protein
827	-3.41	CinA-like protein
829	-2.94	Catalase
830	-2.88	3-oxoacyl-[acyl-carrier protein] reductase
831	-2.89	Hypothetical protein
841	-2.01	ABC up-take transporter membrane protein
850	-2.75	Major membrane protein I
851	-2.00	Serine acetyltransferase
876	-3.42	Hypothetical protein
931	-2.10	Acyl-CoA dehydrogenase probable

Peg Number	Fold Change	Gene Name
945	-6.12	Hypothetical protein
1059	-2.58	Hypothetical protein
1083	-2.36	Transporter LysE family
1086	-2.33	Transcriptional regulator AraC family
1156	-3.16	Bacterioferritin associated ferredoxin
1321	-2.06	Hypothetical protein
1333	-2.18	Sulfatase modifying factor 1 precursor
1338	-2.03	TonB dependent receptor
1368	-2.20	Hypothetical protein
1369	-3.46	Urease accessory protein UreD
1412	-2.03	Hypothetical protein
1475	-2.10	Organosulfonate ABC transporter binding protein
1552	-2.33	Aromatic amino acid transport protein AroP
1576	-2.12	Coenzyme dependent methylene tetra
1629	-2.75	Salicylate hydroxylase
1686	-2.24	Glyoxalase family protein
1701	-2.19	Conserved putative membrane protein
1841	-2.88	Benzoate dioxygenase ferredoxin reductase
1850	-2.67	Hypothetical protein
1853	-2.85	Coenzyme PQQ synthesis protein A
1864	-2.02	Hypothetical protein
1926	-2.36	TcuC integral membrane protein
1937	-2.88	Transcriptional regulator TetR family
2017	-5.01	Trehalose-phosphate synthase [UDP-forming]
2018	-3.64	Trehalose-6-phosphate
2077	-2.05	Hypothetical protein
2103	-2.10	Hypothetical protein
2106	-3.42	Hypothetical protein
2107	-2.93	Putative bacteriophage protein
2108	-2.31	Putative bacteriophage protein
2109	-2.01	Putative bacteriophage protein
2113	-2.10	Putative bacteriophage protein

Peg Number	Fold Change	Gene Name
2121	-2.09	Putative bacteriophage protein
2124	-2.31	Hypothetical protein
2126	-2.05	Uncharacterised protein conserved in bacteria
2127	-2.32	Putative bacteriophage protein
2128	-2.32	Putative bacteriophage protein
2166	-2.27	Transcriptional regulator ArsR family
2234	-2.05	Hypothetical protein
2236	-4.72	Hypothetical protein
2260	-4.61	Hypothetical protein
2327	-2.29	Hypothetical protein
2330	-2.14	Hypothetical protein
2356	-2.26	Hypothetical protein
2357	-2.74	Hypothetical protein
2364	-2.27	L-arabonate dehydratase
2374	-2.28	Beta-ketoadipate enol-lactone hydrolase
2379	-2.33	Transcriptional regulator AraC family
2408	-2.92	Protocatechuate 4-dioxygenase beta chain
2453	-2.18	Hypothetical protein
2462	-2.00	Hypothetical protein
2537	-2.12	Transcriptional regulator TetR family
2845	-2.99	Acyl-CoA dehydrogenase short-chain specific
2854	-2.24	Acetyl-coenzyme A synthetase
2915	-2.10	Hypothetical protein
2931	-2.83	Alkanesulfonates binding protein
2972	-2.29	Hypothetical protein
3205	-2.05	Hypothetical protein
3260	-2.22	Hypothetical protein
3267	-2.07	Hypothetical protein
3269	-2.88	Hypothetical protein
3290	-2.09	Hypothetical protein
3318	-2.20	Sulfate transport system permease protein CysW
3319	-2.25	Sulfate transport system permease protein CysT

Peg Number	Fold Change	Gene Name
3402	-2.88	Pyruvate decarboxylase Indole-3-pyruvate
3433	-2.03	Hypothetical protein
3436	-2.65	Transcriptional regulator TetR family
3458	-2.04	Transcriptional regulator TetR family
3459	-2.08	Transcriptional regulator TetR family
3466	-2.18	Iron chelator utilisation protein
3470	-3.85	Iron transport protein
3471	-2.79	Iron compound ABC up-take transporter PiuC
3472	-2.75	Iron(III) dicitrate transport ATP binding FecE
3477	-2.41	Dihydroxybenzoate-AMP ligase
3479	-2.19	His decarboxylase
3529	-2.00	Uncharacterised siderophore biosynthesis protein
3530	-2.03	Monooxygenase
3540	-2.97	Siderophore synthetase small component
3581	-2.36	Hypothetical protein

Appendix C: Gene expression of the Δ*stkR* mutant compared to the WT in lung media

Peg Number	Fold Change	Gene Name
Up Regulated		
3	2.31	Hypothetical protein
4	2.22	Hypothetical protein
5	2.51	Hypothetical protein
13	11.02	Fimbrial protein precursor
22	3.69	RND efflux system outer membrane NodT family
23	8.17	RND multidrug efflux transporter protein
24	12.87	RND efflux system membrane fusion CmeA
50	2.20	Hypothetical protein
51	2.47	Hypothetical protein
52	2.16	Hypothetical protein
54	2.70	Hypothetical protein
56	2.54	Hypothetical protein
57	9.60	Hypothetical protein
58	4.26	Hypothetical protein
59	4.24	Hypothetical protein
74	2.37	LSU ribosomal protein L27p
75	2.55	LSU ribosomal protein L21p
93	2.68	Hypothetical protein
112	2.82	Undecaprenyl-diphosphatase
113	2.54	Phenylacetic acid degradation operon paaX
128	2.56	Protein A
129	2.36	Aspartyl-tRNA amidotransferase subunit B
130	2.23	Hypothetical protein
138	6.78	Sodium/alanine symporter family protein
139	3.28	Hypothetical protein
140	2.87	Hypothetical protein
145	9.41	Uncharacterised iron-regulated membrane PiuB
146	3.38	Integral membrane protein
151	2.89	N-succinyl-L L-diaminopimelate desuccinylase

Peg Number	Fold Change	Gene Name
163	4.58	Alkylphosphonate utilisation operon protein PhnA
178	2.73	GTP-binding protein TypA/BipA
179	4.52	Putative transporter
180	3.49	Ribosomal RNA small subunit methyltransferase
181	3.44	Lysine-specific permease
182	13.14	Protein RtcB
183	8.88	Hypothetical protein
198	2.33	Hypothetical protein
199	2.08	Serine protease
237	5.27	Zinc-regulated outer membrane receptor
240	2.65	Aspartyl-tRNA synthetase
241	2.08	Exopolysaccharide phosphotransferase
242	2.66	Hypothetical protein
243	4.42	Hypothetical protein
256	3.79	Hypothetical protein
257	3.04	S-adenosylmethionine:tRNA
258	2.07	Hypothetical protein
259	2.62	Conserved membrane protein LemA family
260	2.26	tRNA-guanine transglycosylase
261	2.74	Preprotein translocase subunit YajC
261	2.74	Preprotein translocase subunit YajC
262	3.63	Protein-export membrane protein SecD
263	2.64	Protein-export membrane protein SecF
270	2.04	Hypothetical protein putative signal peptide
271	2.69	tRNA methyltransferase
273	2.62	Hypothetical protein YajQ
274	3.10	Hypothetical protein
324	7.11	Fragment of transposase
328	3.70	Hypothetical protein
329	3.01	Cold shock protein CspG
330	4.32	Hypothetical protein
338	2.04	Hypothetical protein

Peg Number	Fold Change	Gene Name
339	3.40	Secretion activation protein
349	2.15	Putative ATP-binding component
350	2.52	HlyD family secretion protein
354	2.78	Putative O-methyltransferase protein
357	2.65	Hypothetical protein
366	10.07	4-hydroxybenzoate transporter
367	6.46	Hypothetical protein
369	2.12	Hypothetical protein
378	4.13	Hypothetical protein putative exported protein
409	2.53	Uncharacterised protein ImpF
410	2.59	Protein ImpG/VasA
411	2.40	Uncharacterised protein ImpH/VasB
422	2.51	Probable TM protein
428	2.39	Histone acetyltransferase and acetyltransferases
434	2.25	Putative ATP/GTP-binding protein
435	3.22	Transcriptional regulator GntR family
436	3.34	Hypothetical protein
437	3.09	Transcriptional regulator TetR family
439	2.89	CsuA
440	3.11	Sigma-fimbriae uncharacterised subunit
441	2.25	Sigma-fimbriae chaperone protein
454	2.66	Asp racemase
463	2.34	Methionine ABC transporter permease protein
464	2.80	Methionine ABC transporter ATP-binding protein
481	3.81	LSU ribosomal protein L9p
482	4.35	SSU ribosomal protein S18p zinc-independent
483	4.15	SSU ribosomal protein S6p
484	2.92	Heme O synthase farnesyltransferase CtaB
487	2.09	Cytochrome O ubiquinol oxidase subunit I
503	2.25	Methylase of polypeptide chain release factors
507	9.06	3-hydroxyacyl-CoA dehydrogenase
508	7.90	Butyryl-CoA dehydrogenase

Peg Number	Fold Change	Gene Name
509	2.37	Acyl-CoA synthetases AMP-acid ligases
513	2.16	Dihydroneopterin aldolase
514	2.90	Hydroxymethyldihydropteridine
526	2.94	Hypothetical protein
527	2.47	Aconitate hydratase dehydratase
530	2.90	Putative permease (MFS superfamily)
531	10.34	Hypothetical protein
532	26.31	Hypothetical protein
538	2.16	DNA-damage-inducible protein J
544	2.37	Integral membrane protein
547	2.13	UDP-2 3-diacylglucosamine hydrolase
548	2.37	Peptidyl-prolyl cis-trans isomerase PpiB
550	2.42	Hypothetical protein
551	2.55	Glutamine amidotransferase class-I
560	2.77	5-carboxymethyl-2-hydroxymuconate isomerase
561	2.18	Pputative transcriptional regulator (AraC family)
571	13.07	Hypothetical protein
573	6.50	Outer membrane receptor proteins Fe transport
580	12.08	Putative OMR family iron-siderophore precursor
585	3.34	ABC-type transport system ATPase component
587	2.41	Hypothetical protein
592	7.06	Benzoate transport protein
597	2.59	Hypothetical protein
602	2.08	Transcriptional regulator TetR family
603	3.18	Methyl viologen resistance protein smvA
610	3.17	Tyrosine phosphatase
611	2.43	UDP-N-acetylenolpyruvoylglucosamine reductase
622	2.15	Ribosomal-protein-S18p-alanine acetyltransferase
628	3.44	Tyrosyl-tRNA synthetase mitochondrial
629	8.14	Tyrosyl-tRNA synthetase mitochondrial
630	2.01	Hypothetical protein
638	2.19	Deoxyuridine 5'-triphosphate nucleotidohydrolase

Peg Number	Fold Change	Gene Name
646	2.43	Outer membrane lipoprotein YaeT
647	3.81	FUR regulation protein
660	2.19	Membrane fusion component MDRresistance
661	2.05	Inner membrane component MDRresistance
663	3.35	Putative ABC oligo/dipeptide transport
664	2.50	DNA-methyltransferase
665	2.77	Conserved hypothetical protein
672	3.21	Hypothetical protein
678	2.66	Malate:quinone oxidoreductase
689	5.57	YaeQ protein
693	2.69	Biofilm PGA synthesis auxiliary protein PgaD
695	2.61	PnuC-like transporter linked to homoserine kinase
711	2.66	L-Proline/Glycine betaine transporter ProP
715	2.82	Transcriptional regulator AraC family
719	3.34	Glycine cleavage system transcriptional activator
726	2.26	Phosphate transporter
727	2.19	D-serine dehydratase
731	2.06	Permease of the drug/metabolite transporter DMT
732	2.80	Predicted regulator PutR proline utilisation GntR
737	2.18	Transcriptional regulator AraC family
741	2.11	L-serine dehydratase
742	28.90	Phenylacetic acid degradation protein PaaN
743	16.92	Phenylacetate-CoA oxygenase PaaG subunit
744	17.62	Phenylacetate-CoA oxygenase PaaH subunit
745	14.94	Phenylacetate-CoA oxygenase PaaI subunit
746	14.08	Phenylacetate-CoA oxygenase PaaJ subunit
747	9.47	Phenylacetate-CoA oxygenase/reductase PaaK
748	9.14	Phenylacetate degradation hydratase PaaA
749	6.15	Phenylacetate degradation hydratase PaaB
750	5.11	3-hydroxyacyl-CoA dehydrogenase PaaC
751	3.12	Phenylacetic acid degradation PaaE ketothiolase
755	2.93	Phenylacetic acid degradation PaaD thioesterase

Peg Number	Fold Change	Gene Name
758	2.91	Retron-type reverse transcriptase
766	2.15	Hypothetical protein
778	2.69	Pca regulon regulatory protein PcaR
780	2.13	Probable transcriptional regulator
781	2.51	Ferric iron ABC transporter iron-binding protein
808	4.14	Indolepyruvate ferredoxin oxidoreductase
809	2.14	Transcriptional regulator
810	6.61	Hydroxymethylglutaryl-CoA lyase
811	8.80	Methylcrotonyl-CoA carboxylase biotin subunit
812	10.39	Methylglutaconyl-CoA hydratase
813	12.58	Methylcrotonyl-CoA carboxylase transferase
814	14.60	Isovaleryl-CoA dehydrogenase
815	7.62	Predicted transcriptional regulator LiuX
816	4.73	Acetoacetyl-CoA synthetase long-chain-fatty-acid
817	3.81	SAM-dependent methyltransferases
818	5.12	Putative protein (DcaP-like)
819	3.23	Lipolytic enzyme
820	2.07	Transcriptional regulator LysR family
835	4.89	Transporter LysE family
858	59.33	Holin-like protein CidA
859	23.71	CidA-associated membrane protein CidB
863	3.46	MFS permease
864	3.77	Hypothetical protein
874	2.42	Malonate utilisation transcriptional regulator
896	3.22	Arsenate reductase
897	2.32	Arsenical resistance operon repressor
898	2.69	Arsenical-resistance protein
908	4.19	L-asparaginase
909	2.40	Proton/glutamate &, Sodium/glutamate symport
914	3.33	Arginine exporter protein ArgO
918	2.11	Putative membrane protein
919	3.89	Putative membrane protein

Peg Number	Fold Change	Gene Name
924	2.87	Membrane protein
940	2.85	Hypothetical protein
941	3.84	Acyltransferase family protein
948	4.33	Cytosine/purine/uracil/thiamine/allantoin protein
953	4.11	Fimbrial adhesin precursor
954	2.15	Type 1 fimbriae anchoring protein FimD
955	2.81	P pilus assembly protein chaperone PapD
956	7.24	Fimbrial protein precursor
959	2.11	Biotin synthase
978	3.36	tRNA (uracil(54)-C5)-methyltransferase
980	37.73	Transcriptional repressor of PutA and PutP
982	2.89	PutR transcriptional activator of PutA and PutP
983	9.31	Proline/Na & PutP propionate/Na symporter
985	2.37	Glycine cleavage system H protein
989	3.56	Nucleoprotein/polynucleotide-associated enzyme
990	3.08	Conserved putative membrane protein.
991	3.56	Sodium/dicarboxylate symporter
993	2.24	Putative transcriptional regulator (TetR family)
994	3.36	Putative cytoplasmic protein
995	3.40	Maf/YceF/YhdE family protein
998	2.80	Hypothetical protein
1004	2.24	rRNA subunit methyltransferase GidB
1007	2.41	MotA/TolQ/ExbB proton channel family protein
1017	2.29	General secretion pathway protein I
1018	2.07	General secretion pathway protein J
1025	2.19	Cytidylate kinase
1026	3.01	SSU ribosomal protein S1p
1030	2.81	Hypothetical protein
1033	2.16	ATPase AFG1 family
1051	2.25	Transcription antitermination protein NusG
1052	2.86	LSU ribosomal protein L11p (L12e)
1053	2.97	LSU ribosomal protein L1p (L10Ae)

Peg Number	Fold Change	Gene Name
1054	4.01	LSU ribosomal protein L10p (P0)
1055	3.67	LSU ribosomal protein L7/L12 (P1/P2)
1093	2.18	Permease of the drug/metabolite transporter DMT
1096	2.07	Exonuclease putative
1102	6.18	Propionyl-CoA:succinyl-CoA transferase
1112	2.23	Conserved hypothetical, putative signal peptide
1116	2.14	Hypothetical protein
1125	4.33	Arginine permease RocE
1140	2.03	Type IV pilus biogenesis protein PilO
1156	10.96	Bacterioferritin-associated ferredoxin
1160	2.42	Guanylate kinase
1162	2.67	Type IV fimbrial biogenesis protein FimT
1163	2.30	Type IV fimbrial biogenesis protein PilV
1170	2.25	16S rRNA processing protein RimM
1171	2.74	tRNA (Guanine37-N1) methyltransferase
1172	3.04	LSU ribosomal protein L19p
1186	14.96	Multidrug translocase MdfA
1195	2.41	Hypothetical protein
1196	6.04	Arginine permease RocE
1199	2.72	Ortholog Bordetella pertussis BX470248 BP2475
1206	2.24	Di-/tripeptide transporter
1211	2.96	Hypothetical protein
1212	8.60	Hypothetical protein
1232	2.27	SSU ribosomal protein S2p (SAe)
1233	3.09	Translation elongation factor Ts
1234	2.84	Hypothetical protein
1236	3.02	AzlC family protein
1242	2.58	Hypothetical protein
1243	3.42	NADPH-dependent cyano-deazaguanine reductase
1244	5.02	ABC-type multidrug transport system
1245	5.32	ABC-type multidrug transport system ATPase c
1246	2.60	Hypothetical protein

Peg Number	Fold Change	Gene Name
1247	2.97	Exodeoxyribonuclease X
1272	21.29	Hypothetical protein
1281	14.87	IroE protein
1288	2.91	UPF0246 protein YaaA
1289	2.86	Hypothetical protein
1294	3.09	Hypothetical protein
1295	2.70	Cold shock protein CspA
1305	2.30	Amidophosphoribosyltransferase
1310	2.08	Transamidase GatB domain protein
1336	3.26	Rhomboid family protein
1337	2.85	NfuA Fe-S protein maturation
1338	82.18	TonB-dependent outer membrane receptor
1339	2.70	Hypothetical protein
1341	2.03	Carbonic anhydrase
1352	2.24	Rubredoxin
1354	3.06	Hypothetical protein
1355	2.14	Lysyl-tRNA synthetase (class II)
1361	2.67	Hypothetical protein
1365	5.02	Isocitrate lyas
1367	2.23	Hypothetical protein
1381	2.13	Adenylate kinase
1382	2.70	Hypothetical protein
1389	2.04	Tyrosyl-tRNA synthetase
1404	4.46	LSU ribosomal protein L34p
1405	3.81	Ribonuclease P protein component
1406	5.14	Protein YidD
1407	3.32	Membrane translocase component Yid long form
1409	2.01	Uncharacterised YaiN formaldehyde detox operon
1417	2.59	Glutathionylspermidine synthase group 1
1418	3.22	Hypothetical protein
1429	2.71	Hypothetical protein
1440	2.03	Transcription regulatory protein opdE

Peg Number	Fold Change	Gene Name
1449	2.31	Hypothetical protein
1463	5.49	beta-lactamase-like protein
1464	4.74	Oxidoreductase (flavoprotein)
1465	2.59	Cell division DivIC stabilises FtsL/ RasP cleavage
1482	2.17	Asp ammonia-lyase
1483	2.46	Hypothetical protein
1487	2.52	Acetyl-CoA C-acyltransferase
1488	4.12	Short chain fatty acids transporter
1489	6.05	Acetyl-CoA:acetoacetyl-CoA transferase beta
1490	7.95	Acetyl-CoA:acetoacetyl-CoA transferase alpha
1491	2.38	LysR family transcriptional regulator
1492	5.03	D-beta-hydroxybutyrate permease
1493	2.29	D-beta-hydroxybutyrate dehydrogenase
1497	2.36	Putative acetyltransferase
1520	2.05	PhaK-like protein
1534	2.05	Hypothetical protein
1540	3.70	Permease of the drug/metabolite transporter DMT
1541	2.42	LysR family transcriptional regulator STM3121
1567	4.04	33-36 kDa outer membrane protein
1570	6.05	Acetate permease ActP (cation/acetate symporter)
1571	4.72	Putative membrane protein clustering with ActP
1597	6.53	Ferrichrome-iron receptor
1598	3.33	Probable TM protein
1612	2.78	Hypothetical protein
1613	11.05	Ferrichrome-iron receptor
1614	2.18	Orotate phosphoribosyltransferase
1628	2.24	Nucleoside-binding outer membrane protein
1637	2.76	Hypothetical protein
1638	2.72	Hypothetical protein
1653	3.90	Hypothetical protein
1665	2.44	Transcription termination protein NusB
1673	3.23	Formiminoglutamase

Peg Number	Fold Change	Gene Name
1674	4.88	Imidazolonepropionase
1675	3.11	His transport protein (permease)
1676	5.37	His ammonia-lyase
1677	8.86	Urocanate hydratase
1678	4.09	Conserved hypothetical protein
1679	3.24	His utilisation repressor
1680	2.48	O-antigen acetylase
1681	9.72	Putative metal chaperone, Zn homeostasis GTPase
1682	10.35	Hypothetical protein
1683	43.33	Aromatic amino acid transport protein AroP
1684	70.12	Fumarylacetoacetase
1685	85.45	Maleylacetoacetate isomerase, transferase
1686	33.13	Glyoxalase family protein
1687	2.15	Transcriptional regulator IclR family
1688	37.36	4-hydroxyphenylpyruvate dioxygenase
1695	2.14	Phosphoribosylaminoimidazole synthase
1704	2.30	A/G-specific adenine glycosylase
1706	2.05	Hypothetical protein
1730	2.14	Ribosomal RNA subunit methyltransferase B
1749	2.18	Glutaredoxin-related protein
1750	3.18	Hypothetical protein
1753	4.87	Branched-chain amino acid transport system
1754	2.96	Hypothetical protein
1759	2.94	PTS system fructose-specific IIB component
1762	2.71	Hypothetical protein
1767	3.59	Sulfate permease
1780	3.09	Regulatory protein RecX
1781	2.53	TPR repeat, putative periplasmic, domain
1782	2.84	Acyl, UDP-acetylglucosamine O-acyltransferase
1783	3.38	3R-hydroxymyristoyl carrier protein dehydratase
1784	2.12	UDP-hydroxymyristoyl acyltransferase
1799	2.12	Hypothetical protein

Peg Number	Fold Change	Gene Name
1803	3.14	Hypothetical protein
1804	4.95	Hypothetical protein
1811	2.19	tRNA 2-thiouridine synthesising protein E
1828	5.13	3-dehydroquinate dehydratase II
1829	3.86	Biotin carboxyl carrier protein
1830	3.42	Biotin carboxylase of acetyl-CoA carboxylase
1832	2.41	Nucleoside:H+ symporter: MFS
1847	2.15	Molybdenum transport ATP-binding ModC
1848	92.73	Dehydrogenase siderophore
1849	74.52	Isochorismatase of siderophore biosynthesis
1850	11.15	Hypothetical protein
1880	11.27	Ferrichrome iron receptor
1888	2.39	ATP phosphoribosyltransferase
1891	2.02	Para-aminobenzoate synthase aminase component
1906	2.01	Ribulose-phosphate 3-epimerase
1907	2.46	Putative hydrolase
1937	2.01	Transcriptional regulator TetR family
1942	3.20	Hypothetical protein
1947	2.12	Hypothetical protein
1964	2.11	Heme-regulated two-component RR
1987	2.04	1-aminocyclopropane-1-carboxylate deaminase
1996	2.47	5'-methylthioadenosine nucleosidase
2009	2.19	Biotin-protein ligase / Biotin operon repressor
2020	2.55	Adenosylmethionine transferase
2022	2.47	Biotin synthesis protein BioC
2023	3.24	Dethiobiotin synthetase
2024	2.24	Ribosomal large subunit pseudouridine synthase B
2026	3.12	Segregation and condensation protein A
2029	4.04	COG1399 protein with ribosomal protein L32p
2030	3.10	LSU ribosomal protein L32p
2031	2.78	Malonyl CoA-acyl carrier protein transacylase
2032	3.58	3-oxoacyl-[acyl-carrier protein] reductase

Peg Number	Fold Change	Gene Name
2033	2.98	Acyl carrier protein
2043	3.30	Ribose-phosphate pyrophosphokinase
2044	3.05	4-diphosphocytidyl-2-C-methyl-D-erythritol kinase
2072	2.01	SSU ribosomal protein S7p (S5e)
2073	2.48	Translation elongation factor G
2083	2.66	Hypothetical protein
2086	2.22	Hypothetical protein
2089	2.29	Hypothetical protein
2091	2.29	Hypothetical protein
2098	2.00	1-acyl-sn-glycerol-3-phosphate acyltransferase
2115	2.57	Hypothetical protein
2135	2.90	Hypothetical protein
2140	3.30	LSU ribosomal protein L13p (L13Ae)
2141	2.82	SSU ribosomal protein S9p (S16e)
2151	2.76	Acyclic terpenes utilisation regulator AtuR, TetR
2159	3.08	Hypothetical protein
2160	2.04	Hypothetical protein
2161	3.66	Universal stress protein
2162	6.25	Sulfate permease
2168	3.12	Aminoglycoside 3'-phosphotransferase, StrB
2169	2.37	Aminoglycoside 3'-phosphotransferase
2179	2.62	Hypothetical protein
2191	2.13	Threonine synthase
2194	2.77	Tyrosine recombinase XerD
2195	6.44	Ferrous iron transport protein
2196	3.49	Ferrous iron transport protein B
2210	2.02	Fe(2+)-trafficking protein YggX
2229	2.75	Membrane fusion component
2234	2.25	Hypothetical protein
2235	2.03	Hypothetical protein
2236	5.70	Hypothetical protein
2237	2.28	5 methylenetetrahydrofolate reductase

Peg Number	Fold Change	Gene Name
2244	2.27	Hypothetical protein
2262	3.08	Hypothetical protein
2263	3.33	Hemolysin
2264	6.83	Channel-forming transporter TpsB family
2267	3.30	N-acetyl-L L-diaminopimelate deacetylase
2274	2.01	Transcriptional regulator TetR family
2306	2.24	Hypothetical protein
2307	2.32	Hypothetical protein
2316	2.12	Hypothetical protein
2324	2.75	Hypothetical protein
2341	2.72	Hypothetical protein
2366	6.36	Hypothetical protein
2389	2.20	Transcriptional regulator MarR family
2402	2.54	Hypothetical protein
2416	2.56	Phosphate cytidylyltransferase
2419	4.03	Enolase
2420	3.06	Phosphate synthase
2422	2.17	Internalin putative
2448	2.88	Transposase and inactivated derivatives
2451	3.14	Vitamin B12 ABC transporter permease BtuC
2470	2.18	Organic hydroperoxide resistance protein
2476	2.29	Integral membrane protein YggT (osmotic shock)
2479	2.01	Acetyl-coenzyme A carboxyl transferase α- chain
2482	2.51	Transcription termination factor Rho
2483	2.71	Hypothetical protein
2489	2.16	Uncharacterised domain COG3236
2493	2.20	Probable membrane protein YPO3302
2497	2.58	Acyl-CoA synthase
2498	2.58	Sodium-dependent phosphate transporter
2505	2.35	Late competence protein ComEA DNA receptor
2518	4.75	NAD(P) transhydrogenase subunit beta

Peg Number	Fold Change	Gene Name
2520	5.51	NAD(P) transhydrogenase alpha subunit
2521	2.44	Permease of the drug/metabolite transporter (DMT)
2535	2.08	Hypothetical protein
2543	2.36	Hypothetical protein
2550	3.13	Enoyl acyl-carrier protein reductase [NADH]
2552	2.90	3'-to-5' oligoribonuclease (orn)
2556	2.56	Protein export cytoplasm chaperone protein
2557	2.28	4'-phosphopantetheinyl transferase
2565	2.57	Membrane protein exporter
2566	2.87	Putative TM protein
2567	2.32	Hydroxybenzoyl-CoA thioesterase domain protein
2569	2.10	Lysophospholipid acyltransferase
2570	2.22	Glycosyl transferase
2571	2.68	Conserved hypothetical protein
2572	3.03	Hypothetical protein
2573	4.50	Acyl carrier protein (ACP2)
2574	5.39	Acyl carrier protein (ACP1)
2575	4.86	Glycerol phosphate acyltransferase
2576	3.37	3-oxoacyl-[ACP] synthase
2585	2.04	Nucleoside diphosphate kinase
2601	2.45	Phosphate acetyltransferase
2607	2.95	Cell division trigger factor
2608	4.47	Ferrichrome-iron receptor
2627	2.60	Putative membrane protein
2629	5.60	Biopolymer transport protein ExbD/TolR
2630	8.52	MotA/TolQ/ExbB proton channel family protein
2631	9.13	Ferric siderophore transport system TonB
2632	3.31	Formyltetrahydrofolate deformylase
2635	5.03	LSU ribosomal protein L28p
2636	4.80	LSU ribosomal protein L33p zinc-independent
2640	2.09	Hypothetical protein
2654	4.53	Glutamate-Asp carrier protein

Peg Number	Fold Change	Gene Name
2662	3.61	Translation initiation factor 1
2664	2.66	Hypothetical protein
2669	3.25	Hypothetical protein
2670	2.50	Cys regulon transcriptional activator CysB
2671	3.02	Hypothetical protein
2672	2.18	Probable TM protein
2685	2.18	Ribonuclease E
2688	2.05	Dehydrogenases
2695	16.34	LSU ribosomal protein L31p zinc-independent
2696	3.37	Type III effector HopPmaJ
2700	2.48	Probable methyltransferase
2722	2.34	Polyribonucleotide nucleotidyltransferase
2745	2.00	Ribosome-binding factor A
2746	2.21	Translation initiation factor 2
2747	2.20	Transcription termination protein NusA
2748	2.81	Clustered with transcription termination NusA
2755	2.39	Permease of the drug/metabolite transporter (DMT)
2757	2.10	Putative cytoplasmic protein
2762	2.54	Hypothetical protein
2763	2.21	Hypothetical protein
2771	2.03	Hypothetical protein
2773	2.54	Fe(2+)/α-ketoglutarate-dependent LpxO
2777	4.14	Hypothetical protein
2783	2.29	Hypothetical protein
2787	3.75	His permease YuiF
2804	2.46	Hypothetical protein
2805	3.27	ATP synthase epsilon chain
2806	3.24	ATP synthase beta chain
2807	3.93	ATP synthase gamma chain
2808	3.58	ATP synthase alpha chain
2809	3.87	ATP synthase delta chain

Peg Number	Fold Change	Gene Name
2811	3.45	ATP synthase C chain
2812	2.60	ATP synthase A chain
2813	2.71	ATP synthase protein I
2814	2.41	Zinc ABC transporter binding protein ZnuA
2817	2.01	Zinc ABC transporter permease ZnuB
2820	2.15	Hypothetical protein
2833	2.03	DedA protein
2847	2.71	Regulatory protein LuxR
2848	2.42	Hypothetical protein
2858	3.92	D-serine/D-alanine/glycine transporter
2859	35.74	D-serine/D-alanine/glycine transporter
2860	23.01	Translation initiation inhibitor
2861	12.71	Alanine racemase
2862	3.89	D-amino acid dehydrogenase small subunit
2863	4.29	Transcriptional regulator for lrp regulon AsnC
2864	6.42	Hypothetical protein
2865	7.88	Ferrichrome-iron receptor
2872	13.38	Short-chain dehydrogenase/reductase SDR
2874	3.09	MutT/nudix family protein
2879	2.35	Methylcitrate synthase
2882	2.01	Biosynthetic aromatic amino acid aminotransferase
2883	6.55	D-Lactate dehydrogenase
2884	9.32	L-lactate dehydrogenase
2885	13.62	Lactate-responsive regulator Enterobacteria GntR
2886	43.19	L-lactate permease
2892	2.07	UTP glucose phosphate uridylyltransferase
2894	2.41	Glycosyltransferases, cell wall biogenesis
2895	3.52	Glycosyl transferase family 2
2896	3.89	conserved hypothetical protein
2897	2.53	Hypothetical protein
2898	2.41	Hypothetical protein
2899	2.06	Potential multiple membrane spanning domains

Peg Number	Fold Change	Gene Name
2905	2.52	UDP acetylglucosamine dehydratase
2909	2.07	Tyrosine-protein kinase Wzc
2941	2.09	FKBP-type peptidyl-prolyl cis-trans isomerase SlpA
2943	3.18	Hypothetical protein
2951	2.68	Hypothetical protein
2959	3.59	Mobile element protein
2960	2.77	Mobile element protein
2963	2.17	Hypothetical protein
2967	2.00	Hypothetical protein
2968	2.77	putative bacteriophage protein
2973	2.14	Secretion activator protein
2974	6.62	TonB-dependent receptor
2989	11.83	Transporter LysE family
3005	6.31	Ferrichrome-iron receptor
3009	2.08	Argininosuccinate synthase
3011	3.66	Peptidase M48
3012	3.76	Thymidylate kinase
3021	3.00	Hypothetical protein
3024	6.47	Hypothetical protein
3026	2.24	Aromatic amino acid transport protein AroP
3032	3.36	4-aminobutyraldehyde dehydrogenase
3033	2.07	Putative transcription regulator (AsnC family)
3034	4.17	Transaminase
3035	11.96	Arginine N-succinyltransferase
3049	2.66	TonB protein
3052	2.83	Xanthine phosphoribosyltransferase
3059	2.44	Nitroreductase family protein
3061	2.46	Phosphoserine phosphatase
3069	2.96	Hypothetical protein
3073	4.31	LSU ribosomal protein L17p
3074	4.06	DNA-directed RNA polymerase alpha subunit
3075	3.95	SSU ribosomal protein S4p (S9e)

Peg Number	Fold Change	Gene Name
3076	3.92	SSU ribosomal protein S11p (S14e)
3077	3.71	SSU ribosomal protein S13p (S18e)
3078	2.95	LSU ribosomal protein L36p
3079	3.23	Preprotein translocase secY subunit (TC 3.A.5.1.1)
3080	2.80	LSU ribosomal protein L15p (L27Ae)
3081	3.44	LSU ribosomal protein L30p (L7e)
3082	3.32	SSU ribosomal protein S5p (S2e)
3083	3.09	LSU ribosomal protein L18p (L5e)
3084	3.61	LSU ribosomal protein L6p (L9e)
3085	3.05	SSU ribosomal protein S8p (S15Ae)
3086	3.14	SSU ribosomal protein S14p zinc-independent
3087	2.87	LSU ribosomal protein L5p (L11e)
3088	2.46	LSU ribosomal protein L24p (L26e)
3089	2.46	LSU ribosomal protein L14p (L23e)
3090	2.04	SSU ribosomal protein S17p (S11e)
3091	2.14	LSU ribosomal protein L29p (L35e)
3092	2.34	LSU ribosomal protein L16p (L10e)
3093	2.78	SSU ribosomal protein S3p (S3e)
3094	3.17	LSU ribosomal protein L22p (L17e)
3095	3.01	SSU ribosomal protein S19p (S15e)
3096	2.93	LSU ribosomal protein L2p (L8e)
3097	2.98	LSU ribosomal protein L23p (L23Ae)
3098	3.28	LSU ribosomal protein L4p (L1e)
3099	2.87	LSU ribosomal protein L3p (L3e)
3100	2.69	SSU ribosomal protein S10p (S20e)
3125	3.45	ATP-dependent RNA helicase NGO0650
3131	2.14	Hypothetical protein
3144	2.00	Transcriptional regulators LysR family
3152	2.20	Succinylglutamic semialdehyde dehydrogenase
3153	2.66	Arginine N-succinyltransferase
3154	3.10	Succinylornithine transaminase
3155	6.97	NAD-specific glutamate dehydrogenase

Peg Number	Fold Change	Gene Name
3174	3.73	Putative lipoprotein
3175	3.02	Ribonuclease HII
3181	2.06	Adenylosuccinate synthetase
3182	5.66	Hypothetical protein
3197	2.32	Carbamoyl-phosphate synthase large chain
3198	2.87	Carbamoyl-phosphate synthase small chain
3200	2.83	Hypothetical protein
3201	2.57	RNA binding protein
3205	5.05	Hypothetical protein
3206	5.48	Hypothetical protein
3209	2.38	Hypothetical protein
3214	3.32	Phosphoenolpyruvate carboxykinase GTP
3227	2.79	tRNA(Cytosine32)-2-thiocytidine synthetase
3233	3.20	Hypothetical protein
3275	2.51	DNA internalisation-related protein ComEC/Rec2
3276	2.24	Lipid A biosynthesis lauroyl acyltransferase
3279	4.11	Phosphoribosylglycinamide formyltransferase
3280	2.43	Phosphoribosylformylglycinamidine cyclo-ligase
3288	2.17	Putative tRNA/rRNA methyltransferase (EC:2.1.1)
3300	2.51	dNTP triphosphohydrolase broad substrate
3313	3.90	Queuosine Biosynthesis QueE Radical SAM
3314	2.21	Tetrahydropyridine dicarboxylate transferase
3325	2.69	Thymidylate kinase
3333	2.72	Ribonuclease III
3338	2.04	tRNA-(ms[2]io[6]A)-hydroxylase
3349	2.29	RarD protein
3350	3.39	NADPH-dependent dehydrogenase
3380	2.22	Phenazine biosynthesis protein PhzF like
3381	2.26	Hypothetical protein
3392	2.68	Unsaturated fatty acid biosythesis repressor FabR
3395	2.35	Hypothetical protein
3400	7.38	Aldehyde dehydrogenase

Peg Number	Fold Change	Gene Name
3401	5.01	Transcriptional regulator AsnC family
3402	27.78	Pyruvate decarboxylase Indole decarboxylase
3403	8.31	Aromatic amino acid transport protein AroP
3411	3.02	Adenylosuccinate lyase
3416	2.48	D-alanyl-D-alanine carboxypeptidase
3418	3.65	Hypothetical protein
3419	2.43	5-nucleotidase SurE
3421	2.01	Transcriptional regulator LysR family
3429	2.18	Lysyl-lysine 2 3-aminomutase
3430	2.67	Translation elongation factor P
3435	2.01	Hypothetical protein
3452	2.49	Permease of the drug/metabolite transporter (DMT)
3464	3.27	Threonine dehydratase catabolic
3465	2.79	YheO-like PAS domain
3466	23.91	Iron-chelator utilisation protein
3467	25.61	Siderophore biosynthesis non-ribosomal synthetase
3468	65.91	Non-ribosomal peptide synthetase
3470	435.32	Iron transport protein
3471	56.18	Iron compound ABC up-taketransporter PiuC
3472	126.16	Iron(III) dicitrate transport ATP-binding FecE
3473	48.64	Iron compound ABC up-taketransporter protein
3474	30.40	Ferrichrome-iron receptor
3475	43.77	Siderophore biosynthesis protein monooxygenase
3476	26.18	Non-ribosomal peptide synthetase biosynthesis
3477	137.72	2 3-dihydroxybenzoate-AMP ligase
3478	118.98	Isochorismatase
3479	45.76	His decarboxylase
3481	50.43	Transport ATP-binding protein CydCD
3482	45.80	ABC transporter related
3483	26.06	Putative thioesterase
3484	17.60	4'-phosphopantetheinyl transferase entD
3485	50.10	Isochorismate synthase of siderophore biosynthesis

Peg Number	Fold Change	Gene Name
3488	2.60	Hypothetical protein
3490	2.88	putative outermembrane protein
3496	2.14	GTP cyclohydrolase I type 1
3502	4.12	SSU ribosomal protein S20p
3511	5.19	Ferredoxin 2Fe-2S
3512	4.42	Chaperone protein HscA
3513	4.66	Chaperone protein HscB
3514	2.43	Iron binding protein IscA for iron-sulfur
3516	3.27	Cysteine desulfurase IscS subfamily
3517	4.61	Iron-sulfur cluster regulator IscR
3518	2.32	Hypothetical protein putative membrane protein
3520	2.83	DNA-binding protein HU-beta
3521	2.21	Peptidyl-prolyl cis-trans isomerase ppiD
3529	46.72	Siderophore S biosynthesis protein AcsD-like
3530	33.32	Probable Lysine n(6)-hydroxylase
3531	35.01	Permease major facilitator, siderophore biosynthesis
3532	6.85	Uncharacterised siderophore S biosynthesis protein
3533	12.74	Uncharacterised siderophore S biosynthesis AcsA
3534	5.28	Atr protein
3535	4.72	Putative siderophore biosynthesis protein
3536	9.00	Outer membrane receptor siderophore TonB
3537	4.33	Hypothetical protein
3538	5.28	Putative iron-regulated membrane protein
3539	6.60	Hypothetical protein
3540	79.33	Siderophore synthetase acetyltransferase
3546	2.86	Alpha-ribazole-5'-phosphate phosphatase
3551	2.58	Hypothetical protein
3552	4.97	Iron-regulated membrane protein
3553	8.62	Hypothetical protein
3554	4.49	Outer membrane receptor for ferric coprogen
3569	3.93	Hypothetical protein
3570	4.15	TolA protein

Peg Number	Fold Change	Gene Name
3578	2.64	Ribonuclease D
Down Regulated		
18	-3.15	Predicted protein
19	-2.12	Hypothetical protein
41	-2.57	5-nucleotidase SurE
44	-2.61	Hypothetical protein
72	-2.38	Chromosome segregation ATPases
86	-2.62	Hypothetical protein
90	-2.09	Putative membrane protein
92	-4.80	Ammonium transporter
119	-2.87	Phosphoadenylyl-sulfate reductase
121	-5.27	Hypothetical protein
132	-2.02	Hypothetical protein putative signal peptide
137	-2.50	UPF0028 protein YchK
148	-3.48	Hypothetical protein DUF454
150	-7.85	Bacteriolytic lipoprotein entericidin B
162	-3.84	Hypothetical protein
165	-8.72	Hypothetical protein
170	-2.63	FMN oxidoreductase
187	-8.04	PhnB protein putative DNA binding
188	-3.45	Quaternary ammonium compound-resistance
190	-3.30	Sulfite reductase [NADPH] hemoprotein
193	-2.41	Glucose-selective porin OprB
194	-2.23	Alpha-methylacyl-CoA racemase
206	-12.62	Alkyl hydroperoxide reductase subunit C-like
234	-2.29	Hypothetical protein putative signal peptide
253	-4.77	Putative sensory transduction HK
285	-2.99	ClpB protein
286	-2.06	CinA-like protein
287	-2.34	Conserved Hypothetical, putative exported protein
292	-5.42	Outer membrane lipoprotein omp16 precursor
298	-3.58	Conserved hypothetical, putative exported protein

Peg Number	Fold Change	Gene Name
301	-3.11	O-methyltransferase
302	-7.31	Hypothetical protein
314	-2.29	Copper chaperone
316	-2.04	Cu(I)-responsive transcriptional regulator
317	-2.47	Gfa-like protein
318	-85.98	Ferredoxin
320	-2.17	CmaU
333	-38.84	Hypothetical protein
334	-15.34	Hypothetical protein
335	-13.42	Phage putative head morphogenesis protein
340	-111.63	Hypothetical protein
341	-22.26	Hypothetical protein
353	-8.28	UspA-related nucleotide-binding protein
370	-2.52	3-hydroxyacyl-CoA dehydrogenase
371	-6.18	Hypothetical protein
380	-4.01	Mn2+/Fe2+ transporter NRAMP family
381	-3.13	Lactam utilisation protein LamB
382	-2.85	Lactam utilisation, allophanate hydrolase
383	-3.14	Allophanate hydrolase subunit
384	-3.07	Biotin carboxylase of acetyl-CoA carboxylase
390	-43.69	Uncharacterised zinc-type alcohol dehydrogenase
425	-2.23	Probable deaminase
448	-27.19	L-Asp-beta-decarboxylase
449	-38.94	Putative transport protein
456	-6.80	L-sorbosone dehydrogenase
457	-5.69	GCN5-related N-acetyltransferase
458	-2.11	Major facilitator superfamily
460	-4.11	Putative C4-dicarboxylate transport protein
461	-9.01	Hypothetical protein
471	-31.85	Hypothetical protein
473	-12.83	Hypothetical protein
475	-5.01	Protein containing domains DUF404, DUF407

Peg Number	Fold Change	Gene Name
476	-7.00	Hypothetical protein
477	-4.82	Transglutaminase domain protease
478	-4.20	Hypothetical protein
498	-2.35	Hypothetical protein
505	-2.37	ABC-type nitrate/sulfonate/bicarbonate transport
535	-7.80	Hypothetical protein
536	-2.85	Ribosomal small subunit pseudouridine synthase
537	-2.11	Acetyltransferase GNAT family
542	-7.07	tRNA dimethylallyltransferase
552	-2.60	Ethanolamine ammonia-lyase light chain
553	-3.39	Ethanolamine ammonia-lyase heavy chain
564	-26.56	Hypothetical protein
576	-15.83	Hypothetical protein
577	-20.80	Hypothetical protein
582	-29.68	Hypothetical protein
584	-72.84	Protein ycgK precursor
586	-2.90	Putative universal stress protein family
620	-2.09	Hypothetical protein
621	-3.73	Hypothetical protein
627	-3.35	L-lysine permease
636	-3.26	Outer membrane lipoprotein omp16 precursor
639	-3.74	Phosphomannomutase
640	-2.02	Acetylglutamate kinase
643	-3.45	Putative hemerythrin-like protein
686	-3.03	Hypothetical protein
694	-2.04	Enoyl-CoA hydratase
704	-2.73	Mannose-6-phosphate isomerase
705	-2.75	Putative hydrolase
707	-4.38	Probable L-Asp dehydrogenase
708	-3.07	Aldehyde dehydrogenase
717	-2.39	Aldose 1-epimerase
733	-2.33	4-hydroxyproline epimerase

Peg Number	Fold Change	Gene Name
761	-2.11	Hypothetical protein
770	-2.22	Aldehyde dehydrogenase
792	-2.20	Enoyl-[acyl-carrier-protein] reductase
806	-2.16	Acyl-CoA dehydrogenase
822	-128.83	Hypothetical protein putative exported protein
823	-22.47	Hypothetical protein
824	-7.94	Hypothetical protein
825	-580.47	Hypothetical protein
826	-1664.78	Hypothetical protein
827	-33.59	CinA-like protein
828	-58.95	Hypothetical protein
829	-55.79	Catalase
830	-75.25	3-oxoacyl-[acyl-carrier protein] reductase
831	-64.66	Hypothetical protein
832	-114.36	General stress protein
833	-2.21	Hypothetical protein
838	-4.96	Two-component hybrid sensor and regulator
843	-9.75	GlnQ protein
844	-4.89	Putative amino-acid transporter periplasmic protein
845	-6.16	Lysine-arginine-ornithine-binding protein
846	-2.39	Hypothetical protein
851	-6.46	Serine acetyltransferase
852	-14.98	Rhodanese-like domain protein
855	-2.44	Glutathione S-transferase
856	-2.68	Probable glutathione S-transferase YfcF homolog
876	-7.78	Hypothetical protein
877	-8.08	Putative Cytochrome bd2 subunit II
878	-8.38	Putative Cytochrome bd2 subunit I
879	-6.90	Hypothetical protein
880	-2.22	Hypothetical protein
881	-7.72	Acyl-CoA dehydrogenase dibenzothiophene
884	-2.66	Hypothetical protein

Peg Number	Fold Change	Gene Name
885	-49.68	Taurine-binding periplasmic protein TauA
886	-98.36	Taurine transport ATP-binding protein TauB
887	-69.61	Taurine transport system permease protein TauC
888	-40.78	Alpha-ketoglutarate-dependent taurine dioxygenase
889	-24.03	Hydantoin racemase
894	-3.10	Exoenzymes regulatory protein AepA precursor
900	-2.36	Chromate transport protein ChrA
901	-2.46	Chromate transport protein ChrA
911	-2.51	Peptide methionine sulfoxide reductase MsrB
922	-2.89	Conserved hypothetical putative exported protein
926	-3.41	Methionine ABC transporter permease protein
927	-2.53	Methionine ABC transporter ATP-binding protein
928	-2.52	Methionine ABC transporter substrate-binding
929	-2.28	Methionine ABC transporter substrate-binding
930	-10.38	Coenzyme tetrahydromethanopterin reductase
931	-4.12	Acyl-CoA dehydrogenase desulfurisation enzyme
932	-7.59	Acyl-CoA dehydrogenase desulfurisation enzyme
945	-22.88	Hypothetical protein
949	-15.63	Hypothetical protein
957	-4.29	Hypothetical protein
966	-2.40	Beta-lactamase
969	-2.94	Hypothetical protein
974	-3.13	Putative exported protein
977	-4.91	Hypothetical protein
1058	-3.59	Hypothetical protein putative signal peptide
1059	-15.20	Hypothetical protein
1061	-5.70	Glycine dehydrogenase glycine cleavage system P
1081	-4.08	Chromosome undetermined SCAF14611
1085	-2.60	Aquaporin Z
1110	-6.82	Hypothetical protein
1128	-3.37	Sulfate-binding protein Sbp
1146	-2.43	Glutamate synthase [NADPH] large chain

Peg Number	Fold Change	Gene Name
1147	-2.40	Glutamate synthase [NADPH] small chain
1149	-2.52	LemA family protein
1150	-2.54	Beta-propeller domains of methanol dehydrogenase
1151	-3.74	Hypothetical protein
1155	-3.34	Bacterioferritin
1173	-3.98	Lipase precursor
1177	-9.34	Hypothetical protein
1178	-2.94	Putative DMT superfamily metabolite efflux protein
1182	-2.65	Hypothetical protein
1183	-2.18	YgiN protei involved in menadione metabolism
1185	-2.37	Hypothetical protein
1188	-3.94	Superoxide dismutase [Cu-Zn] precursor
1192	-5.58	Hypothetical protein putative signal peptide
1210	-2.50	Lysophospholipase
1221	-2.16	Adenosylhomocysteinase
1224	-3.16	Butyryl-CoA dehydrogenase
1230	-3.24	Outer membrane protein W
1237	-3.35	Putative PRS2 protein
1256	-2.36	Extracellular solute-binding protein family 3
1261	-2.86	4Fe-4S ferredoxin iron-sulfur binding
1262	-13.84	Putative protease
1264	-3.30	Phenazine biosynthesis protein PhzF like
1267	-3.07	MgtC family
1284	-3.43	Hypothetical protein
1285	-2.70	Aminoacyl-His dipeptidase
1297	-6.69	Putative signal peptide
1321	-401.57	Hypothetical protein
1322	-24.70	Acyl-CoA dehydrogenase/oxidase domain protein
1323	-21.60	LmbE-like protein
1324	-14.85	Methyltransferase type 12
1325	-14.34	Glycosyl transferase group 2 family protein
1326	-97.53	Hypothetical protein

Peg Number	Fold Change	Gene Name
1332	-24.05	Hypothetical protein
1342	-2.17	Arylesterase precursor
1353	-2.75	Hypothetical protein
1357	-4.23	Hypothetical protein
1358	-4.65	Sulfate adenylyltransferase subunit 2
1359	-3.13	Sulfate adenylyltransferase subunit 1
1366	-3.44	Lipoprotein
1369	-5.39	Urease accessory protein UreD
1370	-4.53	Urease gamma subunit
1371	-3.58	Urease beta subunit
1372	-3.64	Urease alpha subunit
1373	-2.64	Urease accessory protein UreE
1374	-2.42	Urease accessory protein UreF
1375	-2.91	Urease accessory protein UreG
1376	-3.19	HupE-UreJ family metal transporter
1385	-4.01	NADP-specific glutamate dehydrogenase
1387	-3.11	Putative cytoplasmic protein
1396	-3.84	AdeT
1412	-19.20	Hypothetical protein
1436	-7.74	Arabidopsis thaliana genomic DNA chromosome
1450	-6.67	Hypothetical protein
1455	-8.66	Acetoin dehydrogenase E1 component alpha
1456	-5.76	Acetoin dehydrogenase E1 component beta
1458	-7.80	Dihydrolipoamide dehydrogenase of acetoin
1459	-9.11	2 3-butanediol dehydrogenase S-alcohol forming
1460	-10.00	2 3-butanediol dehydrogenase R-alcohol forming
1472	-5.73	Putative alkanesulfonate metabolism regulator
1473	-3.84	Adenylylsulfate reductase alpha-subunit
1475	-2.42	Organosulfonate ABC transporter
1476	-2.11	Alkanesulfonates transport system permease
1477	-3.80	Organosulfonate ABC transporter ATP-binding
1522	-3.84	Hypothetical protein putative signal peptide

Peg Number	Fold Change	Gene Name
1537	-2.43	Aldo-keto reductase
1543	-2.01	Gfa-like protein
1546	-3.30	Pirin
1547	-2.56	Nicotinamidase family protein YcaC
1549	-2.57	Succinate-semialdehyde dehydrogenase [NADP+]
1550	-2.69	Gamma-aminobutyrate aminotransferase
1552	-2.31	Aromatic amino acid transport protein AroP
1562	-2.32	Putative oxidoreductase SMc00968
1563	-2.30	Transcriptional regulator TetR family
1564	-2.63	Excinuclease ABC subunit A
1573	-3.28	Hypothetical protein
1575	-5.67	FMN reductase
1576	-6.44	Coenzyme F420-dependent methylene reductase
1590	-5.44	Hypothetical protein
1617	-3.19	Hypothetical protein
1627	-2.34	Putative xanthine/uracil permease
1629	-2.46	Salicylate hydroxylase
1630	-2.18	Allantoicase
1643	-2.64	Hypothetical protein
1644	-2.58	Hypothetical protein
1645	-2.18	Asp aminotransferase
1647	-2.15	Hypothetical protein
1649	-2.62	Phosphate regulon transcriptional regulatory PhoB
1651	-3.33	Hypothetical protein
1652	-3.09	Hypothetical protein
1660	-2.15	Hypothetical protein
1696	-2.04	Hypothetical protein
1697	-2.07	Putative transport
1698	-2.32	DNA polymerase III subunits gamma and tau
1699	-19.12	PQQ-dependent oxidoreductase gdhB family
1701	-43.34	conserved hypothetical putative menbrane protein
1702	-2.02	Dienelactone hydrolase family

Peg Number	Fold Change	Gene Name
1731	-7.87	Hypothetical protein
1737	-2.34	Cytochrome d ubiquinol oxidase subunit II
1738	-2.89	Protein ybgE
1743	-2.94	Hypothetical protein
1744	-28.25	Hypothetical protein
1746	-2.54	Hypothetical protein
1764	-24.32	Putative universal stress protein
1765	-2.84	Hypothetical protein
1766	-6.28	Hypothetical protein
1768	-5.07	Alkaline serine exoprotease A precursor
1805	-19.84	Hypothetical protein
1807	-4.17	UDP-glucose 4-epimerase
1808	-4.08	tRNA methylaminomethyl thiouridine TusD
1824	-2.47	Nitrite reductase [NAD(P)H] large subunit
1825	-2.65	RR NasT
1833	-4.28	BenABC operon transcriptional activator BenR
1836	-2.07	short-chain dehydrogenase/reductase
1840	-2.08	bBnABC operon transcriptional activator BenR
1842	-2.07	Anthranilate dioxygenase small subunit
1859	-41.57	Hypothetical protein
1860	-50.37	Hypothetical protein
1863	-2.61	Hypothetical protein
1864	-89.85	Hypothetical protein
1865	-5.00	Catalase
1866	-5.05	Phage capsid and scaffold
1885	-26.38	Ribosome hibernation protein YhbH
1892	-2.24	Type IV fimbrial biogenesis protein PilY1
1911	-5.25	Cobalt-zinc-cadmium resistance protein CzcD
1916	-3.55	Adenosine deaminase
1919	-3.62	Glutaryl-CoA dehydrogenase
1922	-2.34	TcuB works with TcuA to oxidise tricarballylate
1926	-3.64	TcuC integral membrane protein used to transport

Peg Number	Fold Change	Gene Name
1929	-2.06	N-acetyl-L L-diaminopimelate deacetylase
1934	-25.69	Hypothetical protein
1935	-24.12	Methyltetrahydropteroyltri glutamate
1936	-7.00	Flavin reductase RutF pyrimidine catabolism
1941	-18.81	Hypothetical protein
1961	-2.58	Transcriptional regulatory protein RstA
1983	-66.93	Hypothetical protein
1984	-12.30	Small-conductance mechanosensitive channel
1992	-15.77	Hypothetical protein
1994	-14.29	Hypothetical protein
2000	-2.00	Hypothetical protein
2001	-2.06	Hypothetical protein
2004	-4.23	FilA
2015	-6.98	Bacterioferritin
2016	-5.03	Putative transport protein (permease)
2017	-101.34	Alpha trehalose-phosphate synthase UDP-forming
2018	-140.05	Trehalose-6-phosphate phosphatase
2027	-2.33	Hypothetical YciO protein TsaC/YrdC paralog
2034	-2.49	Hypothetical protein
2058	-2.07	Tartrate dehydrogenase Tartrate decarboxylase
2062	-2.61	Succinate-semialdehyde dehydrogenase [NADP+]
2070	-4.20	Hypothetical protein
2076	-3.10	Hypothetical protein
2110	-2.16	Phage-related protein
2148	-2.18	Geranyl-CoA carboxylase carboxyl transferase
2149	-2.84	Citronellol and citronellal dehydrogenase
2155	-2.41	Mobile element protein
2190	-3.32	Murein-DD-endopeptidase
2206	-2.01	Transcriptional regulator TetR family
2254	-2.07	D-glucarate permease
2260	-68.31	Hypothetical protein
2270	-3.68	Putative glucose dehydrogenase precursor

Peg Number	Fold Change	Gene Name
2272	-6.89	Isochorismatase family
2273	-6.27	Antibiotic biosynthesis monooxygenase
2278	-6.58	ThiJ/PfpI family protein
2280	-2.00	Dihydrofolate reductase
2281	-5.77	Putative integral membrane protein
2282	-3.13	Reductase [NADPH]
2288	-2.00	Catalase
2289	-6.97	Non-heme chloroperoxidase
2291	-2.14	Aldehyde dehydrogenase Probable coniferyl
2292	-2.39	Quinone oxidoreductase
2298	-2.44	Acyl-CoA dehydrogenase short-chain specific
2327	-18.48	Hypothetical protein
2329	-3.11	Hypothetical protein
2351	-2.16	Hypothetical protein
2369	-2.24	Muconolactone isomerase
2370	-2.12	Catechol dioxygenase
2371	-2.88	3-oxoadipate CoA-transferase subunit A
2374	-2.54	Beta-ketoadipate enol-lactone hydrolase
2382	-2.46	3-oxoacyl-[acyl-carrier protein] reductase
2409	-2.39	4-carboxymuconolactone decarboxylase
2411	-3.35	Beta-ketoadipate enol-lactone hydrolase
2412	-2.89	3-carboxy-cis cis-muconate cycloisomerase
2413	-2.39	Acetyl-CoA acetyltransferase Beta-ketoadipyl
2414	-2.55	3-oxoadipate CoA-transferase subunit B
2415	-2.60	3-oxoadipate CoA-transferase subunit A
2418	-2.74	Hypothetical protein
2430	-2.40	Keto-deoxy-arabino-heptulosonate phosphate
2441	-2.44	Hypothetical protein
2455	-3.98	Transcriptional regulator
2459	-2.05	Nitrate/nitrite transporter
2484	-2.77	Integration host factor alpha subunit
2515	-2.35	Hydroxypyruvate isomerase

Peg Number	Fold Change	Gene Name
2525	-2.07	Hypothetical protein
2530	-11.12	Aconitate hydratase
2587	-14.87	Membrane-associated phospholipid phosphatase
2588	-4.73	Glycosyltransferase
2602	-2.42	Fumarate hydratase class aerobic
2604	-2.19	Hypothetical protein
2610	-4.36	2-isopropylmalate synthase
2613	-2.04	Hypothetical protein
2638	-4.57	Hypothetical protein
2643	-13.09	Hypothetical protein
2667	-2.65	3-isopropylmalate dehydratase small subunit
2668	-2.63	3-isopropylmalate dehydratase large subunit
2690	-3.60	Integral membrane protein
2692	-5.28	Acyl-CoA dehydrogenase family protein
2693	-4.02	Acyl-CoA dehydrogenase dibenzothiophene
2712	-6.66	Hypothetical protein
2719	-6.57	DnaJ-class molecular chaperone CbpA
2720	-12.49	Hypothetical protein
2729	-3.18	Hypothetical protein
2730	-2.01	UDP-galactose-lipid carrier transferase
2776	-2.97	Putative peptide signal
2778	-12.24	Hypothetical protein
2780	-4.63	Hypothetical protein
2782	-2.05	Hypothetical protein
2785	-5.97	Putative secreted protein
2786	-10.83	Outer membrane protein W precursor
2793	-2.00	Primosomal protein I
2796	-2.15	Hypothetical protein
2798	-3.34	Hypothetical protein
2832	-2.31	Inner membrane protein YqjF
2866	-2.42	Hypothetical protein
2867	-2.73	Hypothetical protein

Peg Number	Fold Change	Gene Name
2869	-5.08	Acid-resistant locus arl7 (Fragment)
2876	-3.01	Hypothetical protein
2926	-5.11	Putative oxidoreductase
2927	-2.50	putative signal peptide
2930	-5.95	Alkanesulfonates-binding protein
2931	-8.49	Alkanesulfonates-binding protein
2932	-5.68	Alkanesulfonate monooxygenase
2934	-3.33	Alkanesulfonates ABC transporter SsuB
2942	-2.28	Putative reductase
2954	-3.26	Hypothetical protein
2958	-2.31	Gentamicin 3'-N-acetyltransferase
2982	-2.42	2-octaprenyl-6-methoxyphenol hydroxylase
2987	-7.35	Co/Zn/Cd efflux system
2988	-5.34	Cobalt-zinc-cadmium resistance protein CzcD
3041	-2.05	Hypothetical protein
3042	-7.01	Hypothetical protein
3045	-2.16	Soluble lytic murein transglycosylase precursor
3063	-2.30	Oligopeptidase A
3104	-2.95	Flavohemoprotein (Flavohemoglobin)
3129	-11.07	Coproporphyrinogen III oxidase aerobic
3134	-5.99	Putative stress-responsive transcriptional regulator
3145	-2.98	Hypothetical protein putative signal peptide
3146	-2.04	Hypothetical protein
3148	-2.45	Conserved hypothetical putative signal peptide
3170	-2.55	Hypothetical protein
3187	-2.26	Mobile element protein
3189	-2.69	Large repetitive protein
3194	-2.37	Universal stress protein family
3213	-2.78	Aerobic glycerol 3 phosphate dehydrogenase
3215	-2.21	Transcription regulator
3232	-2.05	Long chain fatty acid CoA ligase
3236	-2.71	Hypothetical protein

Peg Number	Fold Change	Gene Name
3240	-2.13	Transcriptional regulator TetR family
3242	-4.15	Putative formate dehydrogenase oxidoreductase
3260	-3.66	Hypothetical protein
3269	-2.11	Hypothetical protein
3285	-2.24	Hypothetical protein
3286	-3.45	Hypothetical protein
3287	-3.55	Putative RNA polymerase sigma factor
3290	-3.28	Hypothetical protein
3304	-6.34	Hypothetical protein
3305	-2.25	Hypothetical protein
3315	-5.55	Outer membrane protein G1b
3317	-2.57	Sulfate and thiosulfate import ATP-binding CysA
3318	-7.44	Sulfate transport system permease protein CysW
3319	-19.79	Sulfate transport system permease protein CysT
3321	-68.42	Hypothetical protein
3322	-100.38	Sulfate and thiosulfate binding protein CysP
3340	-3.30	Hypothetical protein
3347	-2.29	Excinuclease ABC subunit B
3348	-4.55	Hypothetical protein
3359	-2.56	Hypothetical protein
3360	-5.76	Hypothetical protein
3361	-3.80	UDP-N-acetylglucosamine epimerase
3363	-3.54	Hypothetical protein
3364	-2.93	Mannosyl transferase in oligosaccharide synthesis
3365	-3.81	Hypothetical protein
3366	-2.69	Hypothetical protein
3374	-5.19	Isocitrate dehydrogenase [NADP]
3384	-2.52	Adenylate cyclase
3385	-3.53	Putative TM protein
3446	-2.36	Aldehyde dehydrogenase
3449	-2.82	Ethanolamine utilisation protein eutQ
3454	-7.52	Hypothetical protein

Peg Number	Fold Change	Gene Name
3459	-3.24	Transcriptional regulator TetR family
3463	-9.37	Hypothetical protein
3492	-2.36	Aminoglycoside 3' phosphotransferase
3495	-2.00	Xanthine dehydrogenase iron-sulfur cluster
3497	-3.31	Hypothetical protein
3503	-2.84	Oxidoreductase
3508	-2.07	Transcription-repair coupling factor
3527	-2.25	Hypothetical protein
3541	-9.79	CbbY family protein
3542	-6.45	Hypothetical protein
3550	-6.47	Putative sulfate permease
3557	-2.44	Predicted membrane fusion protein (MFP) YbhG
3558	-2.37	ABC transporter multidrug efflux ATP-binding
3568	-13.26	Hypothetical protein
3575	-4.28	Hypothetical protein
3581	-65.10	Hypothetical protein
3589	-2.03	Phytochrome-like protein Cph2

Appendix D: Gene expression of the Δ*stkR* mutant compared to the WT in M9 media

Peg Number	Fold Change	Gene Name
Up regulated		
4	2.17	Hypothetical protein
5	2.85	Hypothetical protein
10	2.04	Putative bacteriophage protein
11	2.01	Hypothetical protein
13	4.46	Fimbrial protein precursor
22	3.36	RND efflux system lipoprotein NodT
23	6.95	RND multidrug efflux transporter Acriflavin resistance
24	8.85	RND efflux system membrane fusion protein CmeA
32	2.60	Hypothetical protein
48	3.41	Indoleacetamide hydrolase
49	2.63	transcriptional activator
50	2.06	Hypothetical protein
51	2.20	Hypothetical protein
54	3.40	Hypothetical protein
56	2.29	Hypothetical protein
57	10.34	Hypothetical protein
58	3.61	Hypothetical protein
59	3.20	Hypothetical protein
69	2.44	tRNA methyltransferase
75	2.04	LSU ribosomal protein L21p
80	2.05	RND efflux system inner membrane transporter CmeB
97	3.16	DcaP
98	2.57	Hypothetical protein
100	5.10	1 acyl sn glycerol 3 phosphate acyltransferase
101	2.03	UPF0028 protein YchK
112	2.87	Undecaprenyl diphosphatase
113	2.82	Phenylacetic acid degradation operon regulatory paaX
123	2.57	Septum formation protein Maf
124	2.11	Rod shape determining protein MreD

Peg Number	Fold Change	Gene Name
128	2.07	Aspartyl tRNA(Asn) amidotransferase subunit A
129	2.16	Aspartyl tRNA(Asn) amidotransferase subunit B
130	2.59	Hypothetical protein
135	2.89	SbmA protein
138	6.58	Sodium/alanine symporter family protein
139	4.42	Hypothetical protein
140	3.31	Hypothetical protein
143	2.58	Putative efflux (PET) family inner membrane YccS
145	13.14	Iron regulated, Iron up-take factor PiuB
151	2.58	N succinyl L L diaminopimelate desuccinylase
158	2.81	Hypothetical protein
161	2.22	Prolyl tRNA synthetase bacterial type
163	3.45	Alkylphosphonate utilisation operon protein PhnA
164	2.17	Probable uroporphyrin III c methyltransferase
167	2.39	Thiol:disulfide interchange protein DsbC
180	2.41	Ribosomal RNA small subunit methyltransferase C
181	2.72	Lysine specific permease
182	2.93	Protein RtcB
183	3.05	Hypothetical protein
185	2.86	Putative type 4 fimbrial biogenesis protein FimT
191	2.44	Glucose dehydrogenase PQQ dependent
203	2.92	ABC transporter membrane spanning protein
208	2.80	Protein tyrosine/serine phosphatase
209	2.07	TolA protein
210	2.31	Dihydrofolate synthase / Folylpolyglutamate synthase
211	2.12	Acetyl coenzyme A carboxyl transferase beta chain
216	2.23	Hypothetical protein
237	24.64	Zinc regulated outer membrane receptor
239	2.11	Conserved membrane spanning protein
240	3.44	Aspartyl tRNA synthetase Aspartyl tRNA(Asn)
241	3.56	Exopolysaccharide phosphotransferase SCO6023
242	2.25	Hypothetical protein
243	3.28	Hypothetical protein

Peg Number	Fold Change	Gene Name
246	2.01	Poly(glycerol phosphate) alpha glucosyltransferase
247	2.57	Beta 1 4 glucosyltransferase
251	2.70	Branched chain amino acid aminotransferase
254	2.13	Hypothetical protein
255	2.34	Hypothetical protein
256	4.49	Hypothetical protein
257	2.41	S adenosylmethionine:tRNA ribosyltransferase
258	2.38	Hypothetical protein
259	3.30	Uncharacterised conserved membrane protein LemA
260	2.22	tRNA guanine transglycosylase
261	3.05	Preprotein translocase subunit YajC
262	3.73	Protein export membrane protein SecD
263	2.82	Protein export membrane protein SecF
270	2.04	Hypothetical protein putative signal peptide
271	2.28	tRNA methyltransferase
273	3.51	Hypothetical protein YajQ
274	2.93	Hypothetical protein
281	2.39	cAMP receptor protein
294	2.51	Uncharacterised glutathione S transferase like protein
297	3.80	Glutathione S transferase
313	2.53	Aromatic hydrocarbon utilisation regulator CatR
324	3.87	Fragment of transposase
328	4.50	Hypothetical protein
329	3.70	Cold shock protein CspG
330	5.81	Hypothetical protein
331	2.38	Pyrroline 5 carboxylate reductase
348	2.98	Hypothetical protein
349	4.14	Putative ATP binding component of a transport system
350	6.13	HlyD family secretion protein
354	2.22	Putative O methyltransferase protein
357	3.79	Hypothetical protein
362	2.63	Putative DMT superfamily metabolite efflux precursor
366	22.35	4 hydroxybenzoate transporter

Peg Number	Fold Change	Gene Name
367	9.85	Hypothetical protein
374	2.59	Beta lactamase
377	2.56	Hypothetical protein
378	6.60	Hypothetical protein putative exported protein
387	6.08	Hypothetical protein
409	2.64	Uncharacterised protein ImpF
410	3.06	Protein ImpG/VasA
411	2.85	Uncharacterised protein ImpH/VasB
412	2.55	Hypothetical protein
413	2.23	IcmF related protein
414	2.36	Hypothetical protein
421	2.10	Conserved hypothetical protein
422	2.49	Probable TM protein
423	2.05	Transcriptional regulator LysR family
427	2.29	Putative cytoplasmic protein
428	2.39	Histone acetyltransferase and related acetyltransferases
430	3.31	Hypothetical protein
431	2.69	Transcriptional regulator AraC family
434	2.30	Putative ATP/GTP binding protein
435	2.66	Transcriptional regulator GntR family
436	3.61	Hypothetical protein
437	3.22	Transcriptional regulator TetR family
438	3.52	Sigma fimbriae uncharacterised paralogous subunit
439	3.99	CsuA
440	3.92	Sigma fimbriae uncharacterised paralogous subunit
441	2.59	Sigma fimbriae chaperone protein
442	2.32	Sigma fimbriae usher protein
444	2.93	Hypothetical protein
453	2.57	Ortholog of Bordetella pertussis (BX470248) BP2750
454	2.84	Asp racemase
464	2.59	Methionine ABC transporter ATP binding protein
481	2.64	LSU ribosomal protein L9p
482	2.89	SSU ribosomal protein S18p zinc independent

Peg Number	Fold Change	Gene Name
483	2.66	SSU ribosomal protein S6p
484	2.10	Heme O synthase protoheme IX farnesyltransferase
489	2.09	Hypothetical protein
492	2.44	Biofilm PGA outer membrane secretin PgaA
495	2.09	Biofilm PGA synthesis auxiliary protein PgaD
499	2.06	Hypothetical protein
507	2.52	3 hydroxyacyl CoA dehydrogenase
508	2.86	Butyryl CoA dehydrogenase
514	3.25	Hydroxymethyldihydropteridine pyrophosphokinase
521	2.20	Putative signal peptide
528	2.58	Hypothetical protein
530	2.73	Putative permease (MFS superfamily)
531	6.80	Hypothetical protein
532	55.32	Hypothetical protein
546	3.55	Hypothetical protein
547	2.33	UDP 2 3 diacylglucosamine hydrolase
548	2.55	Peptidyl prolyl cis trans isomerase PpiB
551	2.95	Glutamine amidotransferase class I
560	3.20	5 carboxymethyl 2 hydroxymuconate delta isomerase
561	3.06	Putative transcriptional regulator (AraC family)
571	10.25	Hypothetical protein
573	7.04	Outer membrane receptor proteins mostly Fe transport
580	11.74	Putative OMR family iron siderophore receptor
585	2.33	ABC type transport system ATPase component
587	2.46	Hypothetical protein
588	2.74	Hypothetical protein
592	2.00	Benzoate transport protein
593	3.00	Leucine responsive regulatory protein transport system
596	3.00	Transcriptional regulator LysR family
597	2.60	Hypothetical protein
603	4.31	Methyl viologen resistance protein smvA
609	4.89	3 carboxymuconate cyclase
610	3.10	Low molecular weight protein tyrosine phosphatase

Peg Number	Fold Change	Gene Name
611	2.80	UDP N acetylenolpyruvoylglucosamine reductase
614	2.12	Ferredoxin dependent glutamate synthase
617	2.02	Putative transcriptional regulator (TetR family)
628	5.36	Tyrosyl tRNA synthetase mitochondrial
629	17.36	Tyrosyl tRNA synthetase mitochondrial
638	2.65	Deoxyuridine 5' triphosphate nucleotidohydrolase
647	2.59	FUR regulation protein
651	2.15	Exonuclease SbcC
661	2.77	Inner membrane component MDR
662	2.49	Gamma glutamyltranspeptidase
663	2.75	Putative ABC oligo/dipeptide transport ATP binding
664	2.35	DNA methyltransferase
665	3.67	Conserved hypothetical protein
666	2.96	Hypothetical protein
669	2.27	Transporter MFS superfamily
672	4.21	Hypothetical protein
689	2.72	YaeQ protein
693	2.63	Biofilm PGA synthesis auxiliary protein PgaD
702	2.25	Ferredoxin reductase
703	2.76	Probable glucarate transporter
708	2.53	Aldehyde dehydrogenase
711	2.24	L Proline/Glycine betaine transporter ProP
715	2.35	Transcriptional regulator AraC family
718	2.07	Hypothetical protein
719	3.10	Glycine cleavage system transcriptional activator
720	2.71	3 oxoacyl [acyl carrier protein] reductase
726	2.18	Phosphate transporter
727	2.23	D serine dehydratase
728	2.22	Redox sensitive transcriptional activator SoxR
730	2.13	1 pyrroline 4 hydroxy 2 carboxylate deaminase
732	2.68	Predicted regulator PutR for proline utilisation GntR
741	2.73	L serine dehydratase
742	85.64	Phenylacetic acid degradation protein PaaN

Peg Number	Fold Change	Gene Name
743	46.39	Phenylacetate CoA oxygenase PaaG subunit
744	35.00	Phenylacetate CoA oxygenase PaaH subunit
745	42.48	Phenylacetate CoA oxygenase PaaI subunit
746	45.47	Phenylacetate CoA oxygenase PaaJ subunit
747	43.27	Phenylacetate CoA oxygenase/reductase PaaK subunit
748	22.05	Phenylacetate degradation enoyl CoA hydratase PaaA
749	27.48	Phenylacetate degradation enoyl CoA hydratase PaaB
750	26.38	3 hydroxyacyl CoA dehydrogenase PaaC
751	7.50	Phenylacetic acid degradation protein PaaE
754	2.36	Phenylacetic acid degradation protein PaaY
756	2.42	Hypothetical protein
757	2.39	SEC C motif domain protein
758	2.72	Retron type reverse transcriptase
767	3.85	3 oxoadipate lactone hydrolase carboxymuconolactone
778	2.30	Pca regulon regulatory protein PcaR
780	2.18	Probable transcriptional regulator
781	2.63	Ferric iron ABC transporter iron binding protein
782	2.86	Ferric iron ABC transporter ATP binding protein
793	2.16	MFS permease protein
807	3.47	TesB like acyl CoA thioesterase 5
809	3.83	Transcriptional regulator
810	10.43	Hydroxymethylglutaryl CoA lyase
811	7.60	Methylcrotonyl CoA carboxylase biotin containing
812	7.99	Methylglutaconyl CoA hydratase
813	5.37	Methylcrotonyl CoA carboxylase carboxyl transferase
814	5.66	Isovaleryl CoA dehydrogenase
815	2.01	Transcriptional regulator LiuX, AcrR family
816	3.33	Acetoacetyl CoA synthetase / Long chain fatty acid
817	2.96	SAM dependent methyltransferases
819	2.01	Lipolytic enzyme
820	2.32	Transcriptional regulator LysR family
821	3.18	Hypothetical protein
840	2.27	Hypothetical protein

Peg Number	Fold Change	Gene Name
858	41.71	Holin like protein CidA
859	16.23	CidA associated membrane protein CidB
863	2.93	MFS permease
864	2.79	Hypothetical protein
865	4.93	Malonate decarboxylase alpha subunit
868	2.36	Malonate decarboxylase beta subunit
871	2.19	Malonyl CoA acyl carrier protein transacylase
892	2.54	Transcriptional regulator
896	2.36	Arsenate reductase
897	2.25	Arsenical resistance operon repressor
898	2.16	Arsenical resistance protein ACR3
904	2.10	Hypothetical protein
908	7.73	L asparaginase
909	2.19	Proton/glutamate symport protein
910	2.46	Asp aminotransferase
914	5.84	Arginine exporter protein ArgO
915	2.29	N succinyl L L diaminopimelate aminotransferase
918	5.76	Putative
919	3.58	Putative membrane protein
924	5.95	Membrane protein
933	2.23	Glutathione S transferase
934	2.03	Glutamate Asp periplasmic binding protein GltI
935	3.48	Glutamate Asp transport system permease GltJ
936	3.88	Glutamate Asp transport system permease GltK
937	2.63	Glutamate Asp transport ATP binding GltL
940	2.78	Hypothetical protein
941	2.88	Acyltransferase family protein
942	2.46	Putative transcriptional regulator (TetR family)
943	2.03	Hypothetical protein
944	2.61	Phage integrase
948	5.25	Cytosine/purine/uracil/thiamine/allantoin permease
951	2.57	Transcriptional regulator LysR family
953	5.27	Fimbrial adhesin precursor

Peg Number	Fold Change	Gene Name
954	2.88	Type 1 fimbriae anchoring protein FimD
955	2.07	P pilus assembly protein chaperone PapD
956	3.63	Fimbrial protein precursor
959	2.87	Biotin synthase
978	2.20	tRNA (uracil(54) C5) methyltransferase
979	2.85	Hypothetical protein
980	40.54	Transcript repressor of PutA and PutP / Proline
982	3.27	PutR transcriptional activator of PutA and PutP
983	11.83	Proline/sodium symporter PutP
985	3.89	Glycine cleavage system H protein
986	2.00	Transcriptional regulator AraC family
989	2.88	Nucleoprotein/polynucleotide associated enzyme
990	2.41	Conserved hypothetical protein putative membrane
991	3.01	Sodium/dicarboxylate symporter
993	2.13	Putative transcriptional regulator (TetR family)
994	2.87	Putative cytoplasmic protein
995	2.51	Maf/YceF/YhdE family protein
998	3.98	Hypothetical protein
1006	2.19	Chromosome (plasmid) partitioning protein ParB
1007	2.29	MotA/TolQ/ExbB proton channel family protein
1010	2.01	Tetraacyldisaccharide 4' kinase
1016	2.32	General secretion pathway protein G
1017	2.98	General secretion pathway protein I
1018	2.51	General secretion pathway protein J
1019	2.45	General secretion pathway protein K
1023	2.54	tRNA specific adenosine 34 deaminase
1025	2.13	Cytidylate kinase
1026	3.47	SSU ribosomal protein S1p
1030	3.21	Hypothetical protein
1033	3.24	ATPase AFG1 family
1041	2.25	Dipeptide binding ABC transporter periplasmic
1042	2.40	Dipeptide binding ABC transporter periplasmic
1043	2.06	Thimet oligopeptidase

Peg Number	Fold Change	Gene Name
1044	2.82	Dipeptide transport system permease protein DppB
1045	2.41	Oligopeptide transport system permease protein OppC
1048	3.04	Hypothetical protein
1052	2.78	LSU ribosomal protein L11p
1053	2.91	LSU ribosomal protein L1p
1054	3.90	LSU ribosomal protein L10p
1055	3.58	LSU ribosomal protein L7/L12
1060	2.44	Hypothetical protein
1062	2.12	Putative Na+/H+ antiporter
1066	2.46	Succinyl CoA ligase [ADP forming] alpha chain
1067	2.48	Succinyl CoA ligase [ADP forming] beta chain
1096	2.01	Exonuclease putative
1106	3.15	Carbonic anhydrase
1107	2.07	3 oxoacyl [acyl carrier protein] reductase
1112	3.21	Conserved hypothetical protein putative signal peptide
1115	2.41	Nickel cobalt cadmium resistance protein
1124	2.10	Hypothetical protein
1125	3.44	Arginine permease RocE
1133	2.04	UDP acetylmuramoylalanyl glutamyl ligase
1134	2.15	Phospho N acetylmuramoyl pentapeptide transferase
1139	2.68	Type IV pilus biogenesis protein PilN
1152	2.64	Type IV pilin PilA
1153	2.61	Hypothetical protein
1156	22.56	Bacterioferritin associated ferredoxin
1160	2.07	Guanylate kinase
1162	2.35	Type IV fimbrial biogenesis protein FimT
1171	2.00	tRNA (Guanine37 N1) methyltransferase
1172	2.82	LSU ribosomal protein L19p
1186	4.41	Multidrug translocase MdfA
1187	2.35	Putative efflux (PET) family inner membrane YccS
1195	3.88	Hypothetical protein
1196	3.46	Arginine permease RocE
1205	2.95	Xaa Pro aminopeptidase

Peg Number	Fold Change	Gene Name
1206	3.81	Di /tripeptide transporter
1211	2.13	Hypothetical protein
1212	5.57	Hypothetical protein
1217	2.25	NADP dependent malic enzyme
1233	2.99	Translation elongation factor Ts
1234	2.72	Hypothetical protein
1238	2.96	Hypothetical protein
1242	3.34	Hypothetical protein
1243	3.88	NADPH dependent 7 cyano 7 deazaguanine reductase
1244	6.00	ABC type multidrug transport system permease
1245	5.64	ABC type multidrug transport system ATPase
1246	4.60	Hypothetical protein
1247	2.72	Exodeoxyribonuclease X
1248	2.06	Lysophospholipase
1272	129.98	Hypothetical protein
1273	2.08	Mutator mutT protein pyrophosphorylase like protein
1281	19.18	IroE protein
1283	2.04	Cyclohexadienyl dehydrogenase synthase
1288	2.90	UPF0246 protein YaaA
1289	2.40	Hypothetical protein
1294	3.03	Hypothetical protein
1295	2.56	Cold shock protein CspA
1300	2.02	Phosphohistidine phosphatase SixA
1302	2.38	Hypothetical protein
1313	2.25	Hypothetical protein
1316	2.47	Serine/threonine protein kinase
1336	3.69	Rhomboid family protein
1337	3.11	NfuA Fe S protein maturation
1338	50.17	TonB dependent receptor ferrienterochelin and colicins
1339	4.00	Hypothetical protein
1341	2.78	Carbonic anhydrase
1365	2.42	Isocitrate lyase
1379	2.26	Putative signal peptide

Peg Number	Fold Change	Gene Name
1382	2.68	Hypothetical protein
1386	2.46	Putative signal peptide
1398	2.11	DedA protein
1401	2.04	DNA recombination and repair protein RecF
1404	2.74	LSU ribosomal protein L34p
1405	2.23	Ribonuclease P protein component
1406	3.68	Protein YidD
1407	2.51	Inner membrane protein translocase component YidC
1417	2.11	Similarity to glutathionylspermidine synthase group 1
1418	3.51	Hypothetical protein
1430	2.13	Hypothetical protein
1435	2.18	Hypothetical protein
1438	2.25	Peptidyl prolyl cis trans isomerase PpiA precursor
1440	2.88	Transcription regulatory protein opdE
1463	2.88	Beta lactamase like protein
1464	3.00	Oxidoreductase (flavoprotein)
1465	2.67	Cell division protein DivIC (FtsB) stabilises FtsL/RasP
1482	3.34	Asp ammonia lyase
1484	2.07	Hypothetical protein
1485	2.37	Putative transcriptional regulator (LysR family)
1487	5.18	Acetyl CoA acyltransferase
1488	5.59	Short chain fatty acids transporter
1489	12.20	Acetyl CoA:acetoacetyl CoA transferase beta subunit
1490	13.09	Acetyl CoA:acetoacetyl CoA transferase alpha subunit
1491	2.24	LysR family transcriptional regulator
1492	7.63	D beta hydroxybutyrate permease
1493	5.22	D beta hydroxybutyrate dehydrogenase
1497	2.34	Putative acetyltransferase
1511	2.90	CBS domain protein
1527	3.13	Hypothetical protein
1533	2.43	Hypothetical protein
1534	2.74	Hypothetical protein
1540	2.44	Permease of the drug/metabolite transporter (DMT)

Peg Number	Fold Change	Gene Name
1541	3.32	LysR family transcriptional regulator STM3121
1544	2.05	Gamma tocopherol C methyltransferase
1565	2.77	Hypothetical protein
1567	3.22	Outer membrane protein
1586	2.14	NADH:flavin oxidoreductases Old Yellow Enzyme
1591	2.18	Single stranded DNA specific exonuclease RecJ
1597	6.16	Ferrichrome iron receptor
1598	2.11	Probable TM protein
1602	2.17	Peptidase M23/M37 family
1612	3.84	Hypothetical protein
1613	20.38	Ferrichrome iron receptor
1616	2.72	Arsenate reductase
1633	2.07	Hypothetical protein
1636	2.09	Hypothetical protein
1637	4.87	Hypothetical protein
1638	3.33	Hypothetical protein
1646	2.04	Multi antimicrobial extrusion protein Na(+)/drug
1653	2.05	Hypothetical protein
1665	2.20	Transcription termination protein NusB
1669	2.08	N acetylglucosamine 1 phosphate uridyltransferase
1670	2.59	Glucosamine fructose 6 phosphate aminotransferase
1673	2.81	Formiminoglutamase
1674	5.40	Imidazolonepropionase
1675	4.24	His transport protein (permease)
1676	3.95	His ammonia lyase
1677	5.14	Urocanate hydratase
1678	2.46	Conserved hypothetical protein
1680	3.07	O antigen acetylase
1681	29.47	Putative metal chaperone Zn homeostasis GTPase of
1682	18.26	Hypothetical protein
1683	86.14	Aromatic amino acid transport protein AroP
1684	101.58	Fumarylacetoacetase
1685	226.44	Maleylacetoacetate isomerase transferase

Peg Number	Fold Change	Gene Name
1686	124.92	Glyoxalase family protein
1687	2.81	Transcriptional regulator IclR family
1688	111.18	4 hydroxyphenylpyruvate dioxygenase
1689	2.04	Purine nucleoside phosphorylase
1694	2.03	Putative lipoprotein 34 precursor (NlpB)
1703	2.02	HIT family hydrolase
1711	2.12	Hypothetical protein
1721	2.15	RND efflux membrane fusion protein
1730	2.29	Ribosomal RNA small subunit methyltransferase B
1733	2.62	Hypothetical protein
1734	2.54	Hypothetical protein
1735	2.20	Glutathione S transferase unnamed subgroup
1750	2.39	Hypothetical protein
1753	4.64	Branched chain amino acid transport system carrier
1754	5.81	Hypothetical protein
1757	2.55	Phosphoenolpyruvate protein phosphotransferase
1758	2.44	1 phosphofructokinase
1759	3.50	PTS system fructose component IIB & IIC
1762	2.54	Hypothetical protein
1773	2.17	Acetyltransferase GNAT family
1775	3.81	Hypothetical protein
1780	2.76	Regulatory protein RecX
1781	2.91	TPR repeat putative periplasmic protein
1782	2.81	Acyl carrier protein UDP acetylglucosamine
1783	3.72	Hydroxymyristoyl acyl carrier protein dehydratase
1784	2.43	UDP glucosamine N acyltransferase
1785	2.78	Outer membrane protein H precursor
1786	2.12	Outer membrane protein assembly factor YaeT
1787	2.13	Intramembrane protease RasP/YluC, FtsL cleavage
1788	2.01	1 deoxy D xylulose 5 phosphate reductoisomerase
1799	2.54	Hypothetical protein
1802	4.66	D amino acid dehydrogenase small subunit
1803	2.15	Hypothetical protein

Peg Number	Fold Change	Gene Name
1804	4.05	Hypothetical protein
1806	7.59	Fumarate hydratase class II
1810	2.34	Hypothetical protein
1811	2.12	tRNA 2 thiouridine synthesising protein E
1815	2.74	Molybdopterin biosynthesis protein MoeA
1817	2.16	Molybdenum cofactor biosynthesis protein MoaE
1827	3.38	Error prone lesion bypass DNA polymerase V
1828	5.96	3 dehydroquinate dehydratase II
1829	5.16	Biotin carboxyl carrier, of acetyl CoA carboxylase
1830	5.45	Biotin carboxylase of acetyl CoA carboxylase
1832	2.26	Nucleoside:H+ symporter MFS
1834	2.26	4 hydroxybenzoate transporter
1846	5.39	Molybdenum transport system permease protein ModB
1847	2.91	Molybdenum transport ATP binding protein ModC
1848	279.37	Dehydrogenase siderophore
1849	244.74	Isochorismatase of siderophore biosynthesis
1850	35.76	Hypothetical protein
1854	2.72	Coenzyme PQQ synthesis protein B
1855	2.01	Coenzyme PQQ synthesis protein C
1856	2.03	Coenzyme PQQ synthesis protein D
1857	2.20	Coenzyme PQQ synthesis protein E
1858	2.84	Microsomal dipeptidase
1871	3.10	P pilus assembly protein chaperone PapD
1880	7.65	Ferrichrome iron receptor
1884	2.01	RNA polymerase sigma 54 factor RpoN
1891	2.21	Para aminobenzoate synthase aminase component
1894	2.34	Hypothetical protein
1895	2.39	Long chain fatty acid transport protein
1896	2.19	FilE
1897	2.86	FilF
1900	2.13	Carbonic anhydrase family 3
1907	2.98	Putative hydrolase
1914	2.13	Glutamate N acetyltransferase / N acetylglutamate

Peg Number	Fold Change	Gene Name
1938	2.70	Hypothetical protein
1942	4.74	Hypothetical protein
1943	2.20	Hypothetical protein
1945	2.22	Hypothetical protein
1946	2.00	Hypothetical protein
1947	3.22	Hypothetical protein
1950	2.09	Hypothetical protein
1952	2.61	Hypothetical protein
1954	3.27	Phosphoadenylyl sulfate reductase thioredoxin
1955	2.88	Hypothetical protein
1957	2.01	Chromate transport protein ChrA
1958	2.18	Ribonucleotide reductase of class Ia (aerobic) beta
1963	2.38	Hypothetical protein
1964	2.21	Putative Heme regulated two component system
2009	2.50	Biotin protein ligase / Biotin operon repressor
2010	2.25	Protein of unknown function DUF81
2012	2.61	Chromosome partition protein smc
2020	3.05	Adenosylmethionine aminotransferase
2021	3.81	8 amino 7 oxononanoate synthase
2022	2.96	Biotin synthesis protein BioC
2023	3.72	Dethiobiotin synthetase
2029	2.42	COG1399 protein clustered with ribosomal protein
2031	3.65	Malonyl CoA acyl carrier protein transacylase
2032	5.34	3 oxoacyl [acyl carrier protein] reductase
2033	2.13	Acyl carrier protein
2034	2.68	Hypothetical protein
2043	2.25	Ribose phosphate pyrophosphokinase
2056	2.53	Hypothetical protein
2057	2.26	Positive regulator of Tartrate dehydrogenase enzyme
2061	2.57	Benzoate 1 2 dioxygenase
2062	2.33	Succinate semialdehyde dehydrogenase
2063	2.84	Ferredoxin
2066	2.33	Hypothetical protein

Peg Number	Fold Change	Gene Name
2067	2.69	Pirin like
2068	2.34	Protoporphyrinogen IX oxidase novel form HemJ
2069	2.49	3 oxoacyl [acyl carrier protein] synthase KASI
2073	2.10	Translation elongation factor G
2077	2.36	Hypothetical protein
2083	2.52	Hypothetical protein
2085	2.18	Hypothetical protein
2088	2.17	Hypothetical protein
2089	5.52	Hypothetical protein
2092	2.22	Hypothetical protein
2093	2.07	Uncharacterised protein YfiR precursor
2103	2.38	Hypothetical protein
2114	2.47	Hypothetical protein
2115	2.79	Hypothetical protein
2116	2.42	Hypothetical protein
2134	2.32	Hypothetical protein
2135	3.89	Hypothetical protein
2140	2.58	LSU ribosomal protein L13p (L13Ae)
2144	2.02	Hypothetical protein
2159	2.64	Hypothetical protein
2161	2.70	Universal stress protein
2162	3.48	Sulfate permease
2164	2.02	TET efflux protein TetA
2168	3.18	Aminoglycoside 3' phosphotransferase StrB
2169	2.64	Aminoglycoside 3' phosphotransferase
2170	2.17	Hypothetical protein
2179	4.65	Hypothetical protein
2180	2.33	Hypothetical protein
2181	2.23	DNA polymerase III chi subunit
2187	2.01	Helix turn helix Fis type
2191	2.31	Threonine synthase
2193	2.32	Thiol:disulfide interchange protein DsbC
2194	3.11	Tyrosine recombinase XerD

Peg Number	Fold Change	Gene Name
2195	10.59	Ferrous iron transport protein
2196	5.50	Ferrous iron transport protein B
2197	2.79	Hypothetical protein
2204	3.80	Thiamin biosynthesis protein ThiC
2210	2.70	Probable Fe(2+) trafficking protein YggX
2211	2.48	Argininosuccinate lyase
2217	2.62	Hypothetical protein
2218	3.01	Putative 4 hydroxybenzoyl CoA thioesterase
2229	2.24	Membrane fusion of tripartite MDR
2232	2.77	Hypothetical protein
2234	2.30	Hypothetical protein
2235	2.13	Hypothetical protein
2236	7.01	Hypothetical protein
2240	2.01	Ribose phosphate pyrophosphokinase
2247	3.17	Dimethylmenaquinone methyltransferase family
2259	2.21	Nitrate/nitrite transporter
2262	2.58	Hypothetical protein
2263	2.48	Hemolysin
2264	2.53	Channel forming transporter activator of TpsB
2267	2.68	N acetyl L L diaminopimelate deacetylase
2269	2.26	Putative Glutathione potassium efflux system KefB
2276	5.53	Predicted transcriptional regulator Rrf2 family
2284	3.87	Lipase
2304	2.68	Dihydropteroate synthase
2306	2.03	Hypothetical protein
2314	2.01	Hypothetical protein
2315	3.02	Hypothetical protein
2316	4.50	Hypothetical protein
2337	2.50	Hypothetical protein
2341	2.22	Hypothetical protein
2342	2.22	Hypothetical protein
2362	2.50	Sugar transport
2366	5.69	Hypothetical protein

Peg Number	Fold Change	Gene Name
2383	2.11	Aromatic ring hydroxylating dioxygenase beta subunit
2397	2.13	Transcriptional regulator LysR family
2402	2.70	Hypothetical protein
2416	2.90	Methyl erythritol 4 phosphate cytidylyltransferase
2419	3.66	Enolase
2420	2.75	2 Keto 3 deoxy D manno octulosonate 8 phosphate
2431	2.22	Protein of unknown function UPF0060
2436	3.05	Hypothetical protein
2448	2.94	Transposase and inactivated derivatives
2449	3.25	Histone acetyltransferase HPA2 acetyltransferases
2451	2.52	Vitamin B12 ABC transporter BtuC
2452	2.49	Vitamin B12 ABC transporter component BtuF
2470	3.54	Organic hydroperoxide resistance protein
2476	2.22	Integral membrane protein YggT extracytoplasmic
2477	2.22	Pyrroline 5 carboxylate reductase
2478	2.23	tRNA(Ile) lysidine synthetase
2479	2.69	Acetyl coenzyme A carboxyl transferase alpha chain
2482	2.08	Transcription termination factor Rho
2489	2.58	Uncharacterised domain COG3236
2492	2.00	MFS permease
2498	2.38	Sodium dependent phosphate transporter
2505	2.49	Late competence protein ComEA DNA receptor
2518	4.77	NAD(P) transhydrogenase subunit beta
2519	3.69	NAD(P) transhydrogenase alpha subunit
2520	3.82	NAD(P) transhydrogenase alpha subunit
2535	7.91	Hypothetical protein
2536	2.88	Putative transcriptional regulator (TetR family)
2537	4.54	Transcriptional regulator TetR family
2538	2.77	Diguanylate cyclase/PDE with PAS/PAC
2546	2.35	DNA polymerase III delta subunit
2550	3.17	Enoyl acyl carrier protein reductase [NADH]
2552	2.02	Oligoribonuclease
2556	2.22	Protein export cytoplasm chaperone protein SecB

Peg Number	Fold Change	Gene Name
2557	2.98	4' phosphopantetheinyl transferase
2558	4.09	Excinuclease ATPase subunit
2559	2.60	3 oxoacyl [ACP] synthase
2565	2.22	Membrane protein exporter
2566	2.46	Putative TM protein
2568	2.02	Putative His ammonia lyase protein
2571	2.24	Conserved hypothetical protein
2572	2.61	FIG017861: Hypothetical protein
2573	2.54	Acyl carrier protein (ACP2)
2574	2.46	Acyl carrier protein (ACP1)
2575	3.68	Glycerol phosphate acyltransferase
2576	2.36	3 oxoacyl [ACP] synthase
2591	2.49	O Methyltransferase in polyketide biosynthesis
2595	3.39	Glyceraldehyde 3 phosphate dehydrogenase putative
2596	4.17	Gluconokinase
2597	4.96	Gluconate transporter family protein
2598	2.24	Deoxyphosphogluconate aldolase
2599	2.48	Phosphogluconate dehydratase
2603	2.45	Conserved hypothetical protein putative signal peptide
2607	2.26	Cell division trigger factor
2608	3.46	Ferrichrome iron receptor
2627	2.44	Putative membrane protein
2629	6.07	Biopolymer transport protein ExbD/TolR
2630	12.23	MotA/TolQ/ExbB proton channel family protein
2631	13.43	Ferric siderophore transport system periplasmic TonB
2632	3.05	Formyltetrahydrofolate deformylase
2635	3.12	LSU ribosomal protein L28p
2636	2.90	LSU ribosomal protein L33p zinc independent
2640	2.33	Hypothetical protein
2644	2.75	Hypothetical protein
2654	4.92	Glutamate Asp carrier protein
2663	2.31	Hypothetical protein
2664	2.84	Hypothetical protein

Peg Number	Fold Change	Gene Name
2669	11.73	Hypothetical protein
2670	6.48	Cys regulon transcriptional activator CysB
2671	3.97	Hypothetical protein
2678	2.06	LysR family transcriptional regulator STM3121
2680	2.14	Glutathione S transferase
2685	2.13	Ribonuclease E
2695	62.10	LSU ribosomal protein L31p zinc independent
2696	3.42	Type III effector HopPmaJ
2713	2.11	General secretion pathway protein G
2722	2.07	Polyribonucleotide nucleotidyltransferase
2746	2.18	Translation initiation factor 2
2753	2.43	Leader peptidase methyltransferase
2755	2.67	Permease of the drug/metabolite transporter (DMT)
2760	2.00	UPF0301 protein YqgE
2761	2.20	Putative Holliday junction resolvase YggF
2762	2.81	Hypothetical protein
2763	3.78	Hypothetical protein
2772	2.91	Hypothetical protein
2777	4.86	Hypothetical protein
2781	2.04	Hydroxychromene carboxylate isomerase/DsbA
2783	2.12	Hypothetical protein
2787	2.22	His permease YuiF
2803	4.13	Glutathione peroxidase
2804	3.09	Hypothetical protein
2805	2.42	ATP synthase epsilon chain
2806	2.48	ATP synthase beta chain
2807	2.62	ATP synthase gamma chain
2808	2.43	ATP synthase alpha chain
2809	2.55	ATP synthase delta chain
2810	2.51	ATP synthase B chain
2811	2.07	ATP synthase C chain
2814	3.65	Zinc ABC transporter periplasmic binding ZnuA
2820	2.62	Hypothetical protein

Peg Number	Fold Change	Gene Name
2827	2.20	Hypothetical protein
2828	2.64	Transcriptional regulator PadR family
2833	2.01	DedA protein
2839	2.39	Phosphopantetheinyl transferase
2843	2.44	Long chain fatty acid CoA ligase
2844	5.09	Acyl carrier protein
2845	32.71	Acyl CoA dehydrogenase short chain specific
2846	5.78	Long chain fatty acid CoA ligase
2847	5.18	Regulatory protein LuxR
2850	2.02	Permeases of the major facilitator superfamily
2851	2.45	3 hydroxyisobutyryl CoA hydrolase
2858	5.01	D serine/D alanine/glycine transporter
2859	4.91	D serine/D alanine/glycine transporter
2860	3.31	Translation initiation inhibitor
2863	2.37	Transcriptional regulator for lrp regulon (AsnC family)
2864	27.09	Hypothetical protein
2865	24.84	Ferrichrome iron receptor
2870	2.76	Major facilitator family transporter
2871	2.26	Transcriptional regulator TetR family
2872	20.08	Short chain dehydrogenase/reductase SDR
2874	2.20	MutT/nudix family protein
2875	3.11	Hypothetical protein
2877	2.10	Hypothetical protein
2882	2.52	Biosynthetic Aromatic amino acid aminotransferase
2883	12.36	D Lactate dehydrogenase
2884	12.88	L lactate dehydrogenase
2885	20.61	Lactate responsive regulator LldR /GntR
2886	56.81	L lactate permease
2892	3.15	UTP glucose phosphate uridylyltransferase
2893	2.40	Lipid carrier UDP acetylgalactosaminyl transferase
2894	4.16	Glycosyltransferases involved in cell wall biogenesis
2895	8.71	Glycosyl transferase family 2
2896	10.45	Conserved hypothetical protein

Peg Number	Fold Change	Gene Name
2897	7.02	Hypothetical protein
2898	4.76	Hypothetical protein
2899	3.43	Potential multiple membrane spanning domains
2900	2.05	N acetylneuraminate synthase
2901	2.38	GCN5 related N acetyltransferase
2902	2.26	N Acetylneuraminate cytidylyltransferase
2904	2.14	Bacillosamine/Legionaminic acid biosynthesis
2905	3.76	UDP acetylglucosamine dehydratase
2906	2.02	UDP glucose dehydrogenase
2908	2.23	Low molecular weight, tyrosine phosphatase Wzb
2909	2.83	Tyrosine protein kinase Wzc
2919	2.20	Possible linoleoyl CoA desaturase
2922	2.11	Transcriptional regulator TetR family
2941	2.05	FKBP type peptidyl prolyl isomerase SlpA
2943	2.27	Hypothetical protein
2950	2.52	Hypothetical protein
2951	3.21	Hypothetical protein
2959	3.59	Mobile element protein
2960	3.20	Mobile element protein
2967	2.58	Hypothetical protein
2973	2.96	Secretion activator protein
2974	13.02	TonB dependent receptor
2989	3.61	Transporter LysE family
2997	2.14	Hypothetical protein
3005	12.24	Ferrichrome iron receptor
3011	2.85	Peptidase M48 Ste24p
3012	2.45	Thymidylate kinase
3013	2.81	Methionine ABC transporter substrate binding protein
3016	2.72	Transcriptional regulator TetR family
3020	2.15	Hypothetical protein
3021	6.70	Hypothetical protein
3022	3.94	Hypothetical protein
3024	3.49	Hypothetical protein

Peg Number	Fold Change	Gene Name
3028	2.19	Putrescine importer
3032	4.62	Aminobutyraldehyde dehydrogenase
3034	3.08	Succinylornithine transaminase
3035	5.53	Arginine succinyltransferase
3049	2.78	TonB protein
3059	2.74	Nitroreductase family protein
3061	3.35	Phosphoserine phosphatase
3069	2.22	Hypothetical protein
3073	4.01	LSU ribosomal protein L17p
3075	3.62	SSU ribosomal protein S4p (S9e)
3076	3.68	SSU ribosomal protein S11p (S14e)
3077	3.34	SSU ribosomal protein S13p (S18e)
3078	2.59	LSU ribosomal protein L36p
3080	2.60	LSU ribosomal protein L15p (L27Ae)
3081	3.22	LSU ribosomal protein L30p (L7e)
3082	2.93	SSU ribosomal protein S5p (S2e)
3083	3.05	LSU ribosomal protein L18p (L5e)
3084	3.19	LSU ribosomal protein L6p (L9e)
3085	2.57	SSU ribosomal protein S8p (S15Ae)
3086	2.62	SSU ribosomal protein S14p (S29e) zinc independent
3087	2.10	LSU ribosomal protein L5p (L11e)
3091	2.08	LSU ribosomal protein L29p (L35e)
3092	2.46	LSU ribosomal protein L16p (L10e)
3093	2.83	SSU ribosomal protein S3p (S3e)
3094	3.19	LSU ribosomal protein L22p (L17e)
3095	3.03	SSU ribosomal protein S19p (S15e)
3096	2.70	LSU ribosomal protein L2p (L8e)
3097	2.67	LSU ribosomal protein L23p (L23Ae)
3098	2.40	LSU ribosomal protein L4p (L1e)
3099	2.03	LSU ribosomal protein L3p (L3e)
3125	2.63	ATP dependent RNA helicase NGO0650
3130	2.03	Shikimate dehydrogenase I alpha
3131	2.69	Hypothetical protein

Peg Number	Fold Change	Gene Name
3144	2.49	Transcriptional regulators LysR family
3148	2.34	Conserved hypothetical protein putative signal peptide
3150	3.23	Succinylglutamate desuccinylase
3151	5.78	Succinylarginine dihydrolase
3152	4.41	Succinylglutamic semialdehyde dehydrogenase
3153	4.44	Arginine succinyltransferase
3154	3.22	Succinylornithine transaminase
3155	10.30	NAD specific glutamate dehydrogenase
3165	2.13	Transcriptional regulator TetR family
3173	2.35	Putative cytochrome
3174	3.24	Putative lipoprotein
3175	2.73	Ribonuclease HII
3190	4.13	poly (glycerol phosphate) alpha glucosyltransferase
3191	3.98	Mur ligase middle region
3192	2.48	Hypothetical protein
3195	2.66	CHL acetyltransferase
3196	2.12	Transcription elongation factor GreA
3200	2.14	Hypothetical protein
3205	2.75	Hypothetical protein
3206	3.60	Hypothetical protein
3209	2.29	Hypothetical protein
3211	2.09	Dicarboxylate MFS transporter
3214	2.44	Phosphoenolpyruvate carboxykinase [GTP]
3216	2.09	Putative 3' 5' cyclic nucleotide PDE
3217	3.03	Hypothetical protein
3233	2.80	Hypothetical protein
3239	3.75	Oxidoreductase short chain dehydrogenase/reductase
3249	3.25	Hypothetical protein
3250	3.10	D serine/D alanine/glycine transporter
3251	2.36	Lipoprotein
3257	2.09	Electron transfer flavoprotein alpha subunit
3263	3.24	ABC type multidrug transport system permease
3264	2.96	ABC type multidrug transport system permease

Peg Number	Fold Change	Gene Name
3265	2.27	Predicted membrane protein (MFP) efflux pump YbhG
3272	2.76	Permease of the drug/metabolite transporter (DMT)
3275	2.70	DNA internalisation related protein ComEC/Rec2
3279	2.83	Phosphoribosylglycinamide formyltransferase
3283	2.50	Rhombosortase
3284	2.67	Hypothetical protein
3297	2.23	N acetyl diaminopimelate deacetylase
3300	2.56	dNTP triphosphohydrolase broad substrate specificity
3311	2.11	Hypothetical protein
3312	2.34	Queuosine Biosynthesis QueC ATPase
3313	3.95	Queuosine Biosynthesis QueE Radical SAM
3325	2.30	Thymidylate kinase
3333	2.14	Ribonuclease III
3336	2.01	DNA recombination and repair protein RecO
3338	2.19	tRNA (ms[2]io[6]A) hydroxylase
3342	2.64	Gfa like protein
3345	2.36	Putative GGDEF family protein
3349	2.64	RarD protein
3350	3.40	NADPH glyceraldehyde phosphate dehydrogenase
3351	2.34	Hypothetical protein
3352	3.45	Hypothetical protein
3373	2.21	tRNA pseudouridine synthase A
3375	4.29	Hypothetical protein
3377	2.43	Major facilitator family transporter
3380	2.65	Phenazine biosynthesis protein PhzF like
3381	3.45	Hypothetical protein
3391	2.93	Membrane protein putative
3392	2.17	Unsaturated fatty acid biosythesis repressor FabR
3395	2.78	Hypothetical protein
3396	2.05	Hypothetical protein
3400	29.84	Aldehyde dehydrogenase
3401	12.31	Transcriptional regulator AsnC family
3402	93.58	Pyruvate decarboxylase Indole 3 pyruvate

Peg Number	Fold Change	Gene Name
3403	54.22	Aromatic amino acid transport protein AroP
3405	2.39	Phosphate transport system permease protein PstC
3406	2.67	Phosphate transport system permease protein PstA
3409	2.03	Hypothetical protein
3411	3.20	Adenylosuccinate lyase
3412	2.13	Hypothetical purine metabolism
3416	3.55	Carboxypeptidase
3418	3.35	Hypothetical protein
3419	2.12	Nucleotidase SurE
3421	2.33	Transcriptional regulator LysR family
3422	2.38	ATP dependent protease La Type II
3427	3.87	PAS/PAC domain
3429	2.29	Lysyl lysine 2 3 aminomutase
3430	2.21	Translation elongation factor P
3435	2.63	Hypothetical protein
3440	2.04	Methylmalonate semialdehyde dehydrogenase
3452	2.35	Permease of the drug/metabolite transporter (DMT)
3456	2.18	Muconate cycloisomerase
3464	5.91	Threonine dehydratase catabolic
3465	9.32	YheO like PAS domain
3466	156.46	Iron chelator utilisation protein
3467	144.70	Siderophore biosynthesis non ribosomal
3468	209.43	Non ribosomal peptide synthetase
3470	859.13	Iron transport protein
3471	120.69	Iron compound ABC up-take transporter permease
3472	218.55	Iron(III) dicitrate transport ATP binding protein FecE
3473	160.97	Iron compound ABC up-take transporter binding
3474	92.69	Ferrichrome iron receptor
3475	209.03	Siderophore biosynthesis protein monooxygenase
3476	57.48	Non ribosomal peptide synthetase modules
3477	385.05	Dihydroxybenzoate AMP ligase
3478	904.52	Isochorismatase
3479	156.21	His decarboxylase

Peg Number	Fold Change	Gene Name
3481	199.82	Transport ATP binding protein CydCD
3482	182.70	ABC transporter related
3483	83.19	Putative thioesterase
3484	142.53	Phosphopantetheinyl transferase entD
3485	640.18	Isochorismate synthase of siderophore biosynthesi
3488	2.13	Hypothetical protein
3489	2.14	Hypothetical protein
3490	3.56	Putative outermembrane protein
3494	3.07	Xanthine dehydrogenase molybdenum binding subunit
3507	2.33	Hypothetical protein
3511	3.39	Ferredoxin Fe
3512	3.16	Chaperone protein HscA
3513	2.93	Chaperone protein HscB
3516	4.46	Cysteine desulfurase IscS subfamily
3517	5.55	Iron sulfur cluster regulator IscR
3518	2.44	Hypothetical protein putative membrane protein
3519	2.75	Polyhydroxyalkanoate granule associated protein PhaI
3520	4.46	DNA binding protein HU beta
3521	2.27	Peptidyl prolyl cis trans isomerase ppiD
3529	169.94	Uncharacterized siderophore biosynthesis AcsD
3530	134.43	Probable Lysine hydroxylase siderophore biosynthesis
3531	154.40	Permease of the MFS siderophore biosynthesis operon
3532	21.02	Uncharacterised siderophore biosynthesis AcsC like
3533	40.07	Uncharacterised siderophore biosynthesis AcsA like
3534	9.74	Atr protein
3535	16.89	Putative siderophore biosynthesis protein
3536	20.42	Outer membrane receptor siderophore up-take TonB
3537	10.66	Hypothetical protein
3538	8.90	Putative iron regulated membrane protein
3539	10.38	Hypothetical protein
3540	416.81	Siderophore synthetase acetyltransferase
3546	2.91	Alpha ribazole 5' phosphate phosphatase
3551	2.06	Hypothetical protein

Peg Number	Fold Change	Gene Name
3552	7.12	Iron regulated membrane protein
3553	15.93	Hypothetical protein
3554	6.46	Outer membrane receptor for ferric rhodotorulic acid
3569	3.86	Hypothetical protein
3570	3.40	TolA protein
3578	3.32	Ribonuclease D
3579	2.03	Hypothetical protein
Down regulated		
62	-2.36	Proposed lipoate regulatory protein YbeD
68	-5.22	Transcriptional regulator HxlR family
92	-4.19	Ammonium transporter
119	-4.45	Phosphoadenylyl sulfate / Adenylyl sulfate reductase
121	-7.18	Hypothetical protein
148	-3.57	Hypothetical protein DUF454
187	-3.63	PhnB putative DNA binding 3 demethylubiquinone
190	-3.04	Sulfite reductase [NADPH] hemoprotein beta
206	-3.52	Alkyl hydroperoxide reductase subunit C like protein
253	-2.00	Putative sensory transduction HK
285	-2.79	ClpB protein
302	-2.02	Hypothetical protein
318	-39.75	Ferredoxin
332	-2.29	Hypothetical protein
333	-3.62	Hypothetical protein
334	-5.20	Hypothetical protein
335	-4.85	Phage putative head morphogenesis protein
340	-21.49	Hypothetical protein
341	-7.76	Hypothetical protein
353	-3.06	UspA related nucleotide binding protein
371	-2.72	Hypothetical protein
390	-6.96	Uncharacterised zinc dehydrogenase ybdR
400	-2.28	Allophanate hydrolase
448	-8.77	L Asp beta decarboxylase
449	-13.60	Putative transport protein

Peg Number	Fold Change	Gene Name
461	-5.14	Hypothetical protein
471	-8.04	Hypothetical protein
473	-6.29	Hypothetical protein
476	-2.20	Hypothetical protein
478	-2.01	Hypothetical protein
498	-2.98	Hypothetical protein
517	-2.56	Potassium transporting ATPase C chain
535	-2.77	Hypothetical protein
542	-4.17	tRNA dimethylallyltransferase
564	-30.97	Hypothetical protein
576	-3.86	Hypothetical protein
577	-4.93	Hypothetical protein
582	-10.01	Hypothetical protein
583	-3.94	Hypothetical protein
584	-6.23	Protein ycgK precursor
586	-2.13	Putative universal stress protein family
590	-2.57	Mg(2+) transport ATPase P type
621	-3.08	Hypothetical protein
627	-2.09	L lysine permease
643	-2.78	Putative hemerythrin like protein
670	-2.03	Dihydrodipicolinate synthase
686	-2.02	Hypothetical protein
822	-16.10	Hypothetical protein putative exported protein
823	-4.20	Hypothetical protein
825	-46.79	Hypothetical protein
826	-328.12	Hypothetical protein
827	-6.94	CinA like protein
828	-5.41	Hypothetical protein
829	-8.21	Catalase
830	-7.52	Oxoacyl [acyl carrier protein] reductase
831	-8.97	Hypothetical protein
832	-141.72	General stress protein
838	-2.32	Two component hybrid sensor and regulator

Peg Number	Fold Change	Gene Name
842	-3.93	ABC type amino acid transport system permease
843	-4.42	GlnQ protein
844	-3.96	Putative amino acid transporter periplasmic
845	-3.85	Lysine arginine ornithine binding periplasm precursor
846	-2.17	Hypothetical protein
851	-5.07	Serine acetyltransferase
852	-4.13	Rhodanese like domain protein
876	-5.81	Hypothetical protein
877	-2.67	Putative Cytochrome bd2 subunit II
878	-2.54	Putative Cytochrome bd2 subunit I
879	-3.13	Hypothetical protein
880	-3.31	Hypothetical protein
881	-4.13	Acyl CoA dehydrogenase probable
885	-27.07	Taurine binding periplasmic protein TauA
886	-76.81	Taurine transport ATP binding protein TauB
887	-38.06	Taurine transport system permease protein TauC
888	-26.92	Alpha ketoglutarate dependent taurine dioxygenase
889	-9.13	Hydantoin racemase
928	-2.49	Methionine ABC transporter substrate binding protein
930	-4.39	Coenzyme dependent tetrahydromethanopterin
931	-2.75	Acyl CoA dehydrogenase
932	-4.02	Dehydrogenase dibenzothiophene enzyme
945	-11.71	Hypothetical protein
949	-4.38	Hypothetical protein
969	-4.09	Hypothetical protein
977	-7.20	Hypothetical protein
1058	-2.98	Hypothetical protein putative signal peptide
1059	-12.28	Hypothetical protein
1110	-5.68	Hypothetical protein
1128	-2.53	Sulfate binding protein Sbp
1146	-3.50	Glutamate synthase [NADPH] large chain
1147	-3.78	Glutamate synthase [NADPH] small chain
1155	-7.13	Bacterioferritin

Peg Number	Fold Change	Gene Name
1177	-2.99	Hypothetical protein
1192	-3.14	Hypothetical protein putative signal peptide
1220	-2.16	Methylenetetrahydrofolate reductase
1221	-3.88	Adenosylhomocysteinase
1237	-3.59	Putative PRS2 protein
1256	-2.73	Extracellular solute binding protein family 3
1258	-2.14	His ABC transporter permease protein HisM
1262	-7.32	Putative protease
1285	-2.14	Aminoacyl His dipeptidase (Peptidase D)
1321	-19.69	Hypothetical protein
1322	-4.32	Acyl CoA dehydrogenase/oxidase domain protein
1323	-2.81	LmbE like protein
1324	-2.73	Methyltransferase type 12
1325	-2.05	Glycosyl transferase family protein
1326	-17.44	Hypothetical protein
1332	-17.05	Hypothetical protein
1357	-3.43	Hypothetical protein
1358	-3.78	Sulfate adenylyltransferase subunit 2
1359	-2.76	Sulfate adenylyltransferase subunit kinase
1369	-3.81	Urease accessory protein UreD
1370	-2.22	Urease gamma subunit
1371	-2.17	Urease beta subunit
1372	-2.55	Urease alpha subunit
1385	-3.08	NADP specific glutamate dehydrogenase
1392	-2.90	Probable iron binding protein HesB_IscA_SufA
1396	-2.33	AdeT
1412	-3.70	Hypothetical protein
1432	-2.80	Heat shock protein GrpE
1436	-2.13	Arabidopsis thaliana genomic DNA chromosome
1450	-4.28	Hypothetical protein
1455	-5.27	Acetoin dehydrogenase E1 component alpha subunit
1456	-3.79	Acetoin dehydrogenase E1 component beta subunit
1457	-3.45	Dihydrolipoamide acetyltransferase component

Peg Number	Fold Change	Gene Name
1458	-3.28	Dihydrolipoamide dehydrogenase
1459	-3.31	Butanediol dehydrogenase S alcohol forming acetoin
1460	-2.81	Butanediol dehydrogenase alcohol forming acetoin
1475	-2.06	Organosulfonate ABC transporter substrate binding
1522	-2.35	Hypothetical protein putative signal peptide
1546	-3.18	Pirin
1564	-2.08	Excinuclease ABC subunit A
1576	-3.57	Coenzyme methylene tetrahydromethanopterin
1590	-2.60	Hypothetical protein
1647	-3.23	Hypothetical protein
1652	-2.41	Hypothetical protein
1699	-6.36	PQQ dependent oxidoreductase gdhB family
1701	-19.04	Conserved hypothetical protein putative menbrane
1728	-2.07	Dihydroxy acid dehydratase
1731	-6.78	Hypothetical protein
1737	-2.20	Cytochrome d ubiquinol oxidase subunit II
1738	-2.65	Protein ybgE
1743	-2.34	Hypothetical protein
1744	-21.98	Hypothetical protein
1764	-12.87	Putative universal stress protein
1766	-2.35	Hypothetical protein
1805	-4.80	Hypothetical protein
1808	-2.33	tRNA 5 methylaminomethyl synthase TusD
1824	-2.21	Nitrite reductase [NAD(P)H] large subunit
1833	-3.12	BenABC operon transcriptional activator BenR
1859	-9.59	Hypothetical protein
1860	-8.24	Hypothetical protein
1864	-17.87	Hypothetical protein
1865	-3.13	Catalase
1885	-5.57	Ribosome hibernation protein YhbH
1911	-2.59	Cobalt zinc cadmium resistance protein CzcD
1934	-47.73	Hypothetical protein
1935	-38.95	5 methyltetrahydropteroyltriglutamate

Peg Number	Fold Change	Gene Name
1936	-8.60	Predicted flavin reductase RutF pyrimidine catabolism
1941	-4.08	Hypothetical protein
1944	-2.44	Quinate/shikimate dehydrogenase
1965	-2.09	NADH ubiquinone oxidoreductase chain A
1983	-15.30	Hypothetical protein
1992	-9.51	Hypothetical protein
2015	-12.13	Bacterioferritin
2016	-3.21	Putative transport protein (permease)
2017	-13.33	Alpha trehalose phosphate synthase [UDP forming]
2018	-19.87	Trehalose 6 phosphate phosphatase
2109	-2.58	Putative bacteriophage protein
2148	-2.08	Geranyl CoA carboxylase carboxyl transferase subunit
2150	-2.76	3 hydroxy 3isohexenylglutaryl CoA:acetate lyase
2207	-2.45	Permease of the drug/metabolite transporter (DMT)
2260	-156.76	Hypothetical protein
2278	-2.88	ThiJ/PfpI family protein
2281	-2.75	Putative integral membrane protein
2282	-2.51	2 4 dienoyl CoA reductase [NADPH]
2308	-2.87	Hypothetical protein
2327	-6.05	Hypothetical protein
2340	-2.68	Phage capsid protein
2355	-2.85	Hypothetical protein
2372	-2.13	3 oxoadipate CoA transferase subunit B
2374	-2.08	Beta ketoadipate enol lactone hydrolase
2412	-2.37	3 carboxy cis cis muconate cycloisomerase
2455	-2.62	Transcriptional regulator
2530	-4.30	Aconitate hydratase
2587	-5.76	Membrane associated phospholipid phosphatase
2588	-3.22	Glycosyltransferase
2600	-2.24	Acetate kinase
2602	-4.16	Fumarate hydratase class I aerobic
2610	-3.59	Isopropylmalate synthase
2634	-2.62	Aldehyde dehydrogenase

Peg Number	Fold Change	Gene Name
2638	-6.23	Hypothetical protein
2643	-3.23	Hypothetical protein
2667	-2.06	3 isopropylmalate dehydratase small subunit
2692	-2.27	Acyl CoA dehydrogenase family protein
2693	-2.12	Acyl CoA dehydrogenase dibenzothiophene enzyme
2711	-2.23	Protein secretion chaperonin CsaA
2712	-9.60	Hypothetical protein
2717	-2.29	Chaperonin (Heat shock protein 33)
2719	-2.30	DnaJ class molecular chaperone CbpA
2720	-4.51	Hypothetical protein
2776	-3.69	Putative peptide signal
2778	-4.49	Hypothetical protein
2786	-7.00	Outer membrane protein W precursor
2832	-2.14	Inner membrane protein YqjF
2834	-2.43	CmaU
2862	-2.24	D amino acid dehydrogenase small subunit
2869	-2.13	Acid resistant locus
2876	-2.80	Hypothetical protein
2926	-2.54	Putative oxidoreductase
2930	-7.10	Alkanesulfonates binding protein
2931	-3.38	Alkanesulfonates binding protein
2932	-5.75	Alkanesulfonate monooxygenase
2934	-2.43	Alkanesulfonates ABC transporter ATP binding
2954	-3.02	Hypothetical protein
2958	-3.04	GEN acetyltransferase
2987	-9.13	Co/Zn/Cd efflux system
2988	-14.90	Cobalt zinc cadmium resistance protein CzcD
3041	-2.91	Hypothetical protein
3042	-2.60	Hypothetical protein
3063	-2.18	Oligopeptidase A
3104	-7.28	Flavohemoprotein (Nitric oxide dioxygenase)
3129	-6.11	Coproporphyrinogen III oxidase aerobic
3134	-9.60	Putative stress responsive transcriptional regulator

Peg Number	Fold Change	Gene Name
3235	-2.32	Transcriptional regulator TetR family
3286	-2.15	Hypothetical protein
3287	-3.72	Putative RNA polymerase sigma factor
3290	-3.47	Hypothetical protein
3304	-2.12	Hypothetical protein
3321	-31.38	Hypothetical protein
3347	-2.53	Excinuclease ABC subunit B
3384	-2.36	Adenylate cyclase
3388	-2.09	Isochorismatase DhbB
3424	-2.22	Lactoylglutathione lyase
3426	-2.13	50S ribosomal protein L31
3454	-3.53	Hypothetical protein
3461	-2.46	Transcriptional regulator TetR family
3463	-9.84	Hypothetical protein
3527	-2.16	Hypothetical protein
3541	-3.83	CbbY family protein
3542	-4.40	Hypothetical protein
3550	-6.95	Putative sulfate permease
3568	-3.98	Hypothetical protein
3581	-41.91	Hypothetical protein

Appendix E: Gene expression of the Δ*stkR* mutant compared to the WT in blood

Peg Number	Fold Change	Gene Name
Up regulated		
571	3.69	Hypothetical protein
744	2.53	Phenylacetate CoA oxygenase PaaH subunit
840	6.56	Hypothetical protein
1163	2.24	Type IV fimbrial biogenesis protein PilV
1236	2.02	AzlC family protein
1451	2.01	Transcriptional regulator TetR family
1478	2.00	FOG HEAT repeat
1479	3.23	Hypothetical protein co-occurring HEAT repeat
1918	2.21	Transcriptional regulator LysR family
2337	2.08	Hypothetical protein
2344	2.28	Hypothetical protein
3069	2.41	Hypothetical protein
3304	2.24	Hypothetical protein
3316	2.07	Alkanesulfonate utilisation operon LysR-family
Down regulated		
29	-2.02	Alpha/beta hydrolase
292	-2.43	Outer membrane lipoprotein omp16 precursor
334	-2.04	Hypothetical protein
390	-2.38	Zinc-type alcohol dehydrogenase ybdR
448	-3.79	L-Asp-beta-decarboxylase
449	-4.11	Putative transport protein
471	-3.70	Hypothetical protein
553	-2.15	Ethanolamine ammonia-lyase heavy chain
554	-2.49	Ethanolamine permease
577	-2.04	Hypothetical protein
670	-3.02	Dihydrodipicolinate synthase
798	-2.09	Enoyl-CoA hydratase amino acid degradation
822	-3.03	Hypothetical protein putative export protein
825	-3.24	Hypothetical protein
826	-3.81	Hypothetical protein

Peg Number	Fold Change	Gene Name
829	-2.55	Catalase
830	-4.82	3-oxoacyl-[acyl-carrier protein] reductase
901	-2.55	Chromate transport protein ChrA
1085	-2.65	Aquaporin Z
1238	-2.50	Hypothetical protein
1258	-2.97	His ABC transporter permease protein HisM
1321	-3.22	Hypothetical protein
1322	-2.00	Acyl-CoA dehydrogenase/oxidase domain protein
1323	-2.42	LmbE-like protein
1324	-3.12	Methyltransferase type 12
1326	-3.27	Hypothetical protein
1371	-2.04	Urease beta subunit
1412	-2.01	Hypothetical protein
1455	-5.50	Acetoin dehydrogenase E1 alpha-subunit
1456	-4.38	Acetoin dehydrogenase E1 component beta-subunit
1457	-4.22	Dihydrolipoamide acetyltransferase component
1458	-3.60	Dihydrolipoamide dehydrogenase
1459	-3.40	22C3-butanediol dehydrogenase S-alcohol forming
1460	-2.18	22C3-butanediol dehydrogenase R-alcohol forming
1471	-2.11	Chromate transport protein ChrA
1554	-3.09	Hypothetical protein
1625	-2.38	Decarboxylase
1699	-2.04	PQQ-dependent oxidoreductase gdhB family
1701	-2.37	Conserved hypothetical protein putative protein
1859	-2.53	Hypothetical protein
1911	-2.00	Cobalt-zinc-cadmium resistance protein CzcD
1920	-2.97	Sialic acid transporter (permease) NanT
1983	-2.05	Hypothetical protein
1984	-2.22	Small-conductance mechanosensitive channel
1994	-2.13	Hypothetical protein
2017	-2.43	Alpha alpha-trehalose-phosphate synthase UDP
2109	-2.55	Putative bacteriophage protein
2124	-2.08	Hypothetical protein

Peg Number	Fold Change	Gene Name
2130	-2.04	Probable bacteriophage protein STY1048
2168	-2.53	Aminoglycoside phosphotransferase STR
2207	-2.27	Permease of the drug/metabolite transporter (DMT)
2306	-2.18	Hypothetical protein
2377	-2.14	Hypothetical protein
2386	-2.50	Hypothetical protein
2797	-2.06	Hypothetical protein
2800	-2.03	Hypothetical protein
2801	-2.03	Hypothetical protein
2953	-2.04	Resolvase
2954	-2.07	Hypothetical protein
3143	-2.11	Permease of the drug/metabolite transporter (DMT)
3315	-2.37	Outer membrane protein G1b

Appendix F: Giles *et al*. 2016; BMC Microbiology

Giles et al. BMC Microbiology (2015) 15:116
DOI 10.1186/s12866-015-0440-6

BMC Microbiology

RESEARCH ARTICLE Open Access

Identification of genes essential for pellicle formation in *Acinetobacter baumannii*

Sarah K. Giles[1], Uwe H. Stroeher[1], Bart A. Eijkelkamp[1,2] and Melissa H. Brown[1*]

Abstract

Background: *Acinetobacter baumannii* is an opportunistic pathogen, which has the ability to persist in the clinical environment, causing acute and chronic infections. A possible mechanism contributing to survival of *A. baumannii* is its ability to form a biofilm-like structure at the air/liquid interface, known as a pellicle. This study aimed to identify and characterise the molecular mechanisms required for pellicle formation in *A. baumannii* and to assess a broad range of clinical *A. baumannii* strains for their ability to form these multicellular structures.

Results: Random transposon mutagenesis was undertaken on a previously identified hyper-motile variant of *A. baumannii* ATCC 17978 designated 17978hm. In total three genes critical for pellicle formation were identified; *cpdA*, a phosphodiesterase required for degradation of cyclic adenosine monophosphate (cAMP), and A1S_0112 and A1S_0115 which are involved in the production of a secondary metabolite. While motility of the A1S_0112::Tn and A1S_0115::Tn mutant strains was abolished, the *cpdA*::Tn mutant strain displayed a minor alteration in its motility pattern. Determination of cAMP levels in the *cpdA*::Tn strain revealed a ~24-fold increase in cellular cAMP, confirming the role CpdA plays in catabolising this secondary messenger molecule. Interestingly, transcriptional analysis of the *cpdA*::Tn strain showed significant down-regulation of the operon harboring the A1S_0112 and A1S_0115 genes, revealing a link between these three genes and pellicle formation. Examination of our collection of 54 clinical *A. baumannii* strains revealed that eight formed a measurable pellicle; all of these strains were motile.

Conclusions: This study shows that pellicle formation is a rare trait in *A. baumannii* and that a limited number of genes are essential for the expression of this phenotype. Additionally, an association between pellicle formation and motility was identified. The level of the signalling molecule cAMP was found to be controlled, in part, by the *cpdA* gene product, in addition to playing a critical role in pellicle formation, cellular hydrophobicity and motility. Furthermore, cAMP was identified as a novel regulator of the operon A1S_0112-0118.

Keywords: Cyclic AMP, Motility, Virulence, Biofilm, Hydrophobicity

Background

Acinetobacter baumannii is an opportunistic Gram-negative human pathogen that causes severe nosocomial infections primarily in immune-compromised patients; disease states include pneumonia, meningitis and bacteraemia [1–5]. The bacterium can be found in intensive care units and is frequently isolated from medical devices [6–9]. The capacity to survive in these environments is possibly due to the ability of this organism to survive desiccation and resist a broad spectrum of antibiotics and disinfectants. As a result, *A. baumannii* has entrenched itself in the clinical environment [10–12].

Given the occurrence of *A. baumannii* in intensive care units and its high level of intrinsic and adapted resistance, there is increased pressure to identify novel drug targets. Therefore, understanding the molecular mechanisms contributing to virulence in *A. baumannii* is essential. Similar to numerous other organisms, *A. baumannii* has the ability to grow a multicellular structure known as a biofilm (reviewed by Longo *et al.* 2014) [13] of which the pellicle is a specialised form. The pellicle is localised to the interface between air and liquid, and is a structure of connected cells surrounded by a matrix of extracellular polymeric substance [14, 15]. The

* Correspondence: melissa.brown@flinders.edu.au
[1]School of Biological Sciences, Flinders University, GPO Box 2100S001 Adelaide, SA, Australia
Full list of author information is available at the end of the article

formation of a pellicle allows aerobic bacteria to have access in a stagnant environment to high levels of oxygen and nutrients [16]. The pellicle can increase bacterial survival under antibiotic pressure as well as contribute to longer than usual persistence in a hostile environment, such as under drying conditions [17–19].

There are numerous molecular mechanisms potentially involved in pellicle formation by *A. baumannii*. One such mechanism is the *csuA/BABCDE* pilus chaperone-usher assembly system which is responsible for the production of pili and is essential in the formation of a biofilm on solid surfaces [2, 9, 20]. In a study on *Bacillus subtilis*, 288 regulatory and potential regulatory genes were associated with pellicle formation [21]. Recent analyses of *A. baumannii* bacteria in the pellicle state have revealed alterations in the expression of at least 52 membrane proteins (32 up-regulated and 20 down-regulated) [22, 23]. These 52 proteins were found to be involved in; iron uptake systems, lipid and carbohydrate transport, cellular metabolism, starvation, in addition to porins and pili.

As bacteria encounter a wide range of environmental conditions, there is a requirement to respond to these changes, such as changing from a planktonic state to living within a biofilm and/or pellicle; this can involve deployment of a number of signalling molecules [24, 25]. Cyclic adenosine monophosphate (cAMP) is a ubiquitous signalling molecule used in conjunction with a variety of regulators for modulating gene expression in both prokaryotes and eukaryotes [26, 27]. In bacteria, it has been found to alter multiple virulence characteristics. For example, in *Vibrio cholerae* cAMP has been implicated in the regulation of cholera toxin, the toxin co-regulated pilus and other pathogenic factors [28]. In *Serratia marcesens* the importance of the cAMP receptor protein (CRP complex) in the formation of biofilm has been established [26]. In this case the type I fimbriae-dependant biofilm is tightly regulated and a deletion in the phosphodiesterase gene was found to increase cAMP within the bacteria cell and consequently decrease biofilm formation. Conversely, when increased copies of the phosphodiesterase gene are introduced into the bacterial cell, the bacteria enter into what is described as a "hyper biofilm" state [26]. Similarly in *Pseudomonas aeruginosa*, cAMP has been identified as a key component in biofilm formation, where increased levels of cAMP can inhibit adherence capabilities [29]. Furthermore, in this organism cAMP functions as a co-factor of the virulence factor regulator Vfr, where the cAMP-Vfr complex regulates type III secretion systems involved in exporting toxins and other compounds [30–32]. This complex also regulates virulence factors such as type IV pili, the *las* quorum sensing system and exotoxin A [32, 33]. Although a *vfr*-like gene is present in the *A. baumannii* genome, its role in regulation of virulence factors and interaction with cAMP has not been reported.

The proteomic analyses by Marti *et al.* (2011) and Nait Chabane *et al.* (2014) suggested that pellicle formation in *A. baumannii* is not the result of a single gene or operon [22, 23]. Instead, it is likely that pellicle formation is multifactorial, requiring surface-exposed molecular structures and an adequate level of transcriptional regulation. The aim of this study is to provide insight into the genetic elements that contribute to the ability of *A. baumannii* to migrate to a surface and form a pellicle as well as to assess the prevalence of pellicle formation in a number of clinically-relevant *A. baumannii* strains.

Results and discussion

Pellicle formation is a rare trait in clinical *A. baumannii* strains

In this study, we have defined the pellicle as a robust layer of connected cells covering the surface of a liquid. To assess the prevalence of pellicle formation, our collection of clinical *A. baumannii* strains [34] was screened for this phenotype. Pellicle formation was assessed using glass and polypropylene tubes, as these materials are used for a number of implements within the hospital environment and have different surface properties, which may influence the initial attachment and formation of a pellicle. Preliminary assessment of pellicle biomass was conducted at growth temperatures of 25 °C and 37 °C (data not shown), which revealed that pellicle growth predominantly occurred at 25 °C; these results coincide with Marti *et al.* (2011) [35], as such, all subsequent analyses were performed at 25 °C. Of the 54 clinical strains tested only eight formed a robust pellicle, suggesting that this is not a ubiquitous phenotype (Table 1). These eight strains produced varying amounts of total pellicle biomass when comparing glass and polypropylene strata (Table 1). Pellicle formation was categorised into three groups dependent on the amount of pellicle material measured at OD_{600} where a; "small pellicle" is considered >0.19, "moderate pellicle" is considered >0.20 and <0.50 and "well-developed pellicle" is >0.51. In glass tubes, strains ATCC 17978, 17978hm, WM98c, 04145027 and AYE produced a well-developed pellicle, while, AB0057, 11986752 and 2320495 produced a moderate to small pellicle. Analysis in polypropylene tubes showed that only two strains, 17978hm and 04145027, produced a strong pellicle, while four strains, ATCC 17978, 11986752, 2320495 and WM98c, produced a moderate to small pellicle. Both AYE and AB0057 formed a pellicle in glass tubes, but failed to form a measurable pellicle in polypropylene tubes. Hence, the ability to form a pellicle was not conserved across glass and polypropylene surfaces. These observed differences could be due to a number of factors related to the specific adherence strategies of each strain, such as the production of

Table 1 Pellicle formation in glass and polypropylene, cell hydrophobicity, motility status and isolation site

A. baumannii isolate	Glass (OD_{600})	Polypropylene (OD_{600})	Hydrophobicity (%)	Motility	Isolation site
Pellicle forming *A. baumannii* strains					
ATCC 17978	0.65 ± 0.16	0.44 ± 0.08	32 ± 0.25	+	Meningitis
17978hm	1.03 ± 0.01	0.94 ± 0.02	42 ± 0.19	+	Meningitis
11986752	0.13 ± 0.01	0.17 ± 0.04	98 ± 0.01	+	Pus
2320495	0.35 ± 0.08	0.28 ± 0.06	98 ± 0.03	+	Pus
WM98c	1.01 ± 0.02	0.37 ± 0.08	94 ± 0.10	+	Unknown
04145027	0.62 ± 0.00	0.79 ± 0.04	100 ± 0.00	+	Vaginal
AYE	0.65 ± 0.11	Not detected	92 ± 0.07	+	Urinary
AB0057	0.47 ± 0.06	Not detected	0	+	Blood
Surface film forming *A. baumannii* strains					
6772166	BD[a]	BD	0	+	Pus
685775	BD	BD	0	+	Sputum
PW01c	BD	BD	0	+	Unknown
6877889	BD	BD	9 ± 0.09	+	Sputum
6870155	BD	BD	5 ± 0.07	+	Sputum

[a] BD = below detection level

pili and other surface-exposed macromolecules. A number of strains, 6772166, 6856775, PW01c, 6877889 and 6870155 produced a weak surface film that could not be extracted using our protocol, attempts to do so by other means such as draining the planktonic growth resulted in destruction of this weak surface film. Structures such as pilin-like proteins and exopolysaccharides have been shown to be present in pellicles [23] and it is possible that these structures are expressed at a reduced level in these strains resulting in only a weak surface film. Interestingly, all pellicle forming strains and those that formed a weak surface film have been shown to be motile [34]. This finding highlights the possibility that the molecular mechanisms involved in motility and pellicle formation are linked.

Hydrophobicity across the clinical *A. baumannii* strains is not directly linked to pellicle formation ability

In a number of bacterial species, including *A. baumannii*, a positive association between cell surface hydrophobicity, biofilm formation and adherence capabilities has been reported [36–38]. We evaluated our set of clinical *A. baumannii* strains for cell surface hydrophobicity and identified major differences (Fig. 1). Using the divisions

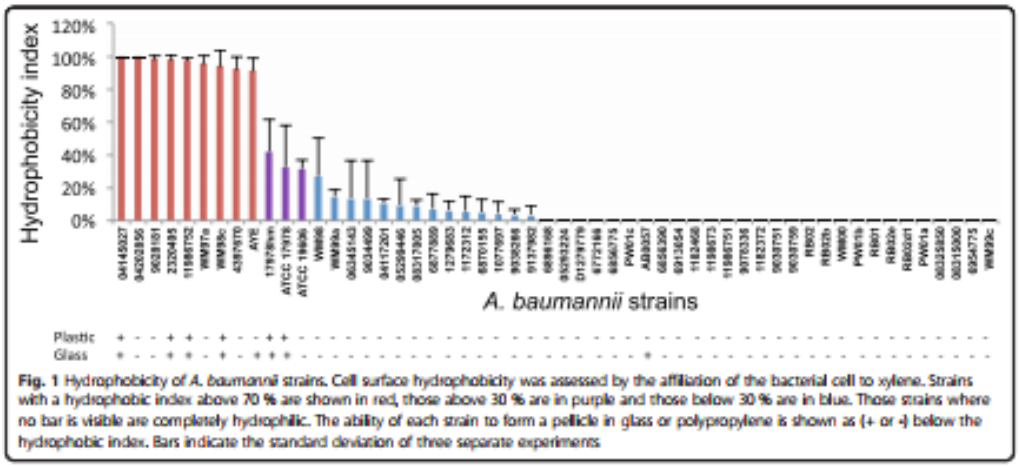

Fig. 1 Hydrophobicity of *A. baumannii* strains. Cell surface hydrophobicity was assessed by the affiliation of the bacterial cell to xylene. Strains with a hydrophobic index above 70 % are shown in red, those above 30 % are in purple and those below 30 % are in blue. Those strains where no bar is visible are completely hydrophilic. The ability of each strain to form a pellicle in glass or polypropylene is shown as (+ or -) below the hydrophobic index. Bars indicate the standard deviation of three separate experiments

of the hydrophobicity index as established by Pour *et al.* (2011) [36], 42 of the strains displayed a hydrophilic character, nine were found to have a strong hydrophobic character and three showed an intermediate level of cell surface hydrophobicity. Of the eight strains that formed a pellicle in glass (Table 1), five (11986752, 2320495, WM98c, 04145027 and AYE) were found to have a strong hydrophobicity index of >70 %, two (ATCC 17978 and 17978hm) showed an intermediate hydrophobic character and AB0057 was found to be hydrophilic. There are numerous proteins embedded within the outer membrane of Gram-negative bacteria that have a variety of functions including pili for adherence and possibly pellicle formation as well as other physical characteristics. Surface proteins can alter the surface chemistry of a cell and affect the surface hydrophobicity [39, 40]. The aforementioned results suggest a high level of correlation between the ability to form an extractable pellicle and an increase in cell surface hydrophobicity. The level of hydrophobicity may have an influence on what surface and how strongly bacteria interact due to a variety of proteins on the cell surface [41, 42]. Interestingly, the strains identified as producing a weak surface film all show a hydrophilic nature.

A1S_0112, A1S_0115 and *cpdA* are essential for pellicle formation in *A. baumannii* 17978hm

To further investigate the pellicle phenotype, we used our previously characterised *A. baumannii* 17978hm strain (harboring an insertion in *hns*) [43], which has the ability to produce increased amounts of pellicle material compared to the ATCC 17978 parent strain. This strain was chosen as it allows good discrimination between the pellicle and non-pellicle phenotype allowing ready identification in large scale screening procedures. To identify genes associated with this potential virulence factor a transposon bank of random mutants was constructed in the 17978hm strain using the plasmid pLOF mini::Tn*10*:*gfp*:*kan* [44]. Approximately 4000 individual transposon insertion mutants were examined in microtitre trays for their ability to form a pellicle. Initial screening identified nine transposon insertion mutants that were incapable of pellicle formation. Subsequent evaluation of these strains in polypropylene and glass tubes confirmed the complete loss of the pellicle phenotype (data not shown). The exact insertion site of the individual transposon insertions were identified by cloning the kanamycin resistance gene associated with the transposon (mini::Tn*10*:*gfp*:*kan*) and subsequent sequencing. Insertions were found to be within three genes: A1S_0249 (*cpdA*), a cAMP phosphodiesterase; A1S_0112, acyl-CoA synthetase/adenosine monophosphate (AMP) acid ligase II; and A1S_0115, which is annotated to be involved in amino acid adenylation. The precise insertion site of the transposon is given as the nucleotide position relative to the *A. baumannii* ATCC 17978 genome sequence (GenBank CP000521) (Additional file 1). Seven transposon insertions were identified to be within the A1S_0115 gene. A single representative of each of the three distinct insertions, designated transposon mutants 1, 2 and 5, was taken for further investigation (Additional file 1).

Transposon mutant 1 was identified as containing an insertion within *cpdA*, *cpdA*::Tn. Bacteria finely modulate intracellular cAMP levels through adenylate cyclases (synthesis) and cAMP phosphodiesterases, such as CpdA, which converts cAMP to AMP (degradation) [45]. Therefore, as the insertional inactivation of *cpdA* led to a loss of pellicle, this insertion identified the requirement for cAMP regulation in this process. To confirm that the observed phenotype can be attributed to disruption of *cpdA*, the *cpdA*::Tn mutant strain was complemented by cloning a wild-type copy of *cpdA* into the empty shuttle vector pWH1266 [46], producing pWH0249. The pWH0249 plasmid was subsequently electroporated into the *cpdA*::Tn mutant strain generating the strain *cpdA*::Tn(0249) (Table 2). This strain was found to successfully produce a pellicle in contrast to both the *cpdA*::Tn mutant strain or the *cpdA*::Tn control strain harboring the empty pWH1266 vector, *cpdA*::Tn(1266) (Table 2; Fig. 2).

Transposon mutant 2 A1S_0112::Tn and transposon mutant 5 A1S_0115::Tn have insertions within the open reading frame (ORFs) A1S_0112 and A1S_0115, which are located in a large operon comprised of seven genes, A1S_0112-0118 (Fig. 3). This operon has previously been associated with cell motility, potentially by production and secretion of a biosurfactant via a type-I secretion system or another mechanism [47, 48]. A recent report has shown that the genes within this operon are significantly up-regulated in biofilm cells in *A. baumannii* ATCC 17978 and a site-specific knockout of A1S_0114 abolished biofilm formation [49]. Efforts to complement the A1S_0112::Tn and A1S_0115::Tn transposon mutant strains with copies of the wild-type genes cloned into pWH1266 (Table 2), were unsuccessful possibly due to polar effects of the transposon insertions. In order to ensure that the lack of complementation was not due to a lack of transcription of our complementing genes, we undertook qRT-PCR that revealed adequate transcription occurred for the wild-type A1S_0112 and A1S_0115 genes cloned into the empty pWH1266 vector (Table 3, Additional file 2). As mentioned, pellicle formation was not restored in these mutants, possibly because, these ORFs are part of an operon which must be transcribed as a polycistronic message making complementation of these mutants not possible. This is supported by the work of Clemmer *et al.* (2011) who previously isolated transposon mutants in this region which abolished motility and

Table 2 *A. baumannii* 17978hm mutant derivatives constructed in this study

Abbreviated name	Description[a]
cpdA::Tn	Tn*Mobgf*plan insertion in *cpdA*, kan^R
cpdA::Tn(0249)	Tn*Mobgf*plan insertion in *cpdA* containing pWH0249, kan^R, amp^R
cpdA::Tn(1266)	Tn*Mobgf*plan insertion in *cpdA* containing shuttle vector pWH1266, kan^R, amp^R, tet^R
A1S_0112::Tn	Tn*Mobgf*plan insertion in A1S_0112, kan^R
A1S_0112::Tn(0112)	Tn*Mobgf*plan insertion in A1S_0112 containing pWH0112, kan^R, amp^R
A1S_0112::Tn(1266)	Tn*Mobgf*plan insertion in A1S_0112 containing shuttle vector pWH1266, kan^R, amp^R, tet^R
A1S_0115::Tn	Tn*Mobgf*plan insertion in A1S_0115, kan^R
A1S_0115::Tn(0115)	Tn*Mobgf*plan insertion in A1S_0115 containing pWH0115, kan^R, amp^R
A1S_0115::Tn(1266)	Tn*Mobgf*plan insertion in A1S_0115 containing shuttle vector pWH1266, kan^R, amp^R, tet^R

[a] kan^R, kanamycin resistance at 50 μg/mL; amp^R, ampicillin resistance at 100 μg/mL; tet^R, tetracycline resistance at 12.5 μg/mL

due to the nature of this operon were also unable to complement the mutants [47].

Characterisation of pellicle-deficient mutant strains *cpdA*::Tn, A1S_0112::Tn and A1S_0115::Tn

The three transposon insertion mutant strains described above were examined for potential growth perturbations in Luria-Bertani (LB) liquid cultures. All three *A. baumannii* transposon mutant strains showed comparable growth to the parent 17978hm strain (Additional file 3), indicating that the loss of the pellicle is not due to a general growth defect. Since pellicle formation is only one type of biofilm, the ability to form a biofilm at the liquid-surface interface was also examined. The three transposon mutants were assessed for both their planktonic growth potential and their ability to form a biofilm on polypropylene (Fig. 4a and b). All transposon mutants showed an increase in planktonic growth compared to the parent and *cpdA*::Tn(0249) complemented derivative (p-value <0.001) (Fig. 4a). The transposon insertion mutants were able to form a significantly increased amount of biofilm in polypropylene tubes compared to the parent strain (*cpdA*::Tn, A1S_0115::Tn and A1S_0112::Tn; p-values of 0.05, 0.05 and 0.01, respectively) (Fig. 4b), while, the complemented *cpdA*::Tn(0249) mutant strain returned the phenotype to that of the parent (Fig. 4). Carriage of wild-type copies of A1S_0112 and A1S_0115 in their respective Tn mutant derivatives did not result in functional complementation (data not shown).

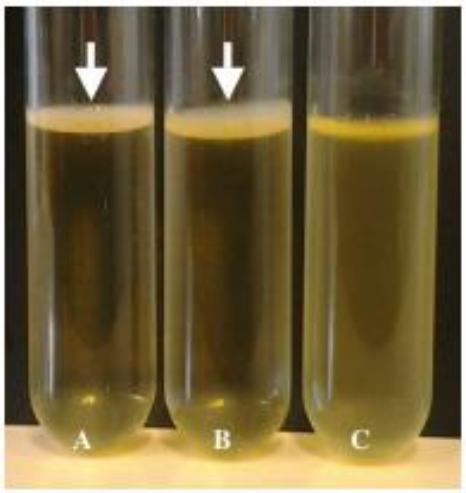

Fig. 2 Pellicle formation by *A. baumannii* 17978hm parent, *cpdA*::Tn(0249) and *cpdA*::Tn(1266) strains. *A. baumannii* strains were grown in Luria-Bertani broth and analysed after a 72 h incubation at 25 °C in the absence of light. Pellicle material was assessed visually. **(a)** 17978hm parent strain; **(b)** *cpdA*::Tn(0249) complemented mutant strain showing developed pellicles at the interface between the liquid and air; and **(c)** *cpdA*::Tn(1266) mutant strain negative for pellicle formation. Arrows identify the pellicle material

The three pellicle deficient transposon mutants all displayed a >80 % reduction in cell surface hydrophobicity compared to the parent strain, to essentially a hydrophilic nature (*cpdA*::Tn, A1S_0112::Tn and A1S_0115::Tn; p-values of 0.001, 0.01 and 0.01, respectively) (Fig. 5). This indicates that hydrophobicity is affected when *cpdA*, A1S_0112 or A1S_0115 genes are insertionally inactivated. The presence of the wild-type *cpdA* gene in the *A. baumannii cpdA*::Tn(0249) derivative not only complemented the hydrophobicity character, but increased the hydrophobicity index to 60 % which is above the parent strain (p-value <0.001) (Fig. 5); this would indicate that cAMP is involved in modulating cell surface hydrophobicity. The increase in hydrophobicity above the level seen with the parent strain is likely due to a copy number effect of the wild-type *cpdA* determinant residing on the pWH1266 plasmid.

Traditionally, *A. baumannii* has been considered non-motile due to its lack of flagella; however, two forms of

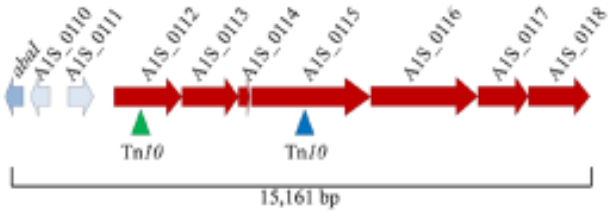

Fig. 3 Operon with transposon insertion sites within A1S_0112 and A1S_0115 identified. The genetic organisation of the A1S_0112-0118 operon is shown with the arrows representing open reading frames and depict the direction of transcription. The location of the transposon (Tn*10*) insertions in A1S_0112 (green triangle) and A1S_0115 (blue triangle) are shown. Flanking genes illustrate the position of the operon within the chromosome adjacent to the quorum sensing gene *abaI*; A1S_0110 hypothetical protein and A1S_0111 transcriptional regulator; the total size of the region shown is 15,161 bp in length

motility known as swarming and twitching have now been described in this species [34, 50, 51]. While sliding motility in non-flagellated bacteria can occur by surfactant production in other bacteria [48], twitching motility within *A. baumannii* is mediated by the extension and retraction of type IV pili as a form of surface translocation [5]. We have shown previously that *A. baumannii* strain 17978hm is motile via swarming on LB medium containing 0.25 % agar [34]. Therefore, we applied these conditions to examine the motility phenotypes of the three pellicle-deficient transposon mutant strains. The A1S_0112::Tn and A1S_0115::Tn mutant strains proved to be non-motile as they only grew at the initial inoculum site on the agar plate (Fig. 6). The A1S_0112::Tn and A1S_0115::Tn mutant strains harboring either a wild-type copy of A1S_0112 or A1S_0115 or an empty vector pWH1266 also gave a negative result (Fig. 6). Our data corroborate the findings by Clemmer *et al.* (2011) [47], that the A1S_0112-0118 operon is required for motility as insertions within this operon were found to be non-motile (Fig. 6). However, the loss of motility seen in the transposon mutant strains is not universal because the *cpdA*::Tn variant remained motile despite presenting a visually different motility pattern compared to the 17978hm parent strain (Fig. 6). The *cpdA*::Tn and *cpdA*::Tn(1266) strains presented a spoke like motility pattern, whereas the parent strain formed an even surface film of motile cells. The *cpdA*::Tn(0249) mutant strain returned the motility phenotype to that of the parent covering the 0.25 % agar plate with motile bacterial cells (Fig. 6). As such, motility was not substantially affected, however the manner by which the bacterial cells exercised their motility phenotype in the *cpdA*::Tn strain was altered. These results connect the clinical *A. baumannii* strains with the mutant derivatives of the 17978hm strain, in that, all pellicle forming strains including those that form a weak surface film are motile and when the pellicle is disrupted there is either an alteration in the motile phenotype as seen in the *cpdA*::Tn mutant or complete abolishment of motility.

Table 3 Fold change in gene expression of transposon mutant strains compared to the 17978hm parent strain

Strain	A1S_0112*	A1S_0115*	A1S_0118*
cpdA::Tn	-2.8 ± 0.21	ND	ND
cpdA::Tn(0249)	1.5 ± 0.44	ND	ND
cpdA::Tn(1266)	-5.6 ± 0.032	ND	ND
A1S_0112::Tn	NA	-335.46 ± 1.42	-28.44 ± 1.33
A1S_0112::Tn(0112)	-0.49 ± 1.39	-669.37 ± 1.24	-51.63 ± 1.70
A1S_0112::Tn(1266)	-171.25 ± 1.68	-325.53 ± 1.22	-85.43 ± 1.46
A1S_0115::Tn	-1.14 ± 1.59	NA	-83.29 ± 1.20
A1S_0115::Tn(0115)	-4.1 ± 1.09	-1.16 ± 1.63	-28.97 ± 1.54
A1S_0115::Tn(1266)	-0.99 ± 1.32	-347.29 ± 1.52	-72.50 ± 1.14

NA = not applicable
ND = not done
* = data from three biological replicates

Bacterial adherence is a critical virulence factor and aids in host and surface colonisation. The adherence of the *A. baumannii* mutant strains to human lung epithelial cells (A549) was assessed; all three transposon insertion strains had adherence capabilities that were not significantly different to that of the 17978hm parent strain (data not shown). This suggests that the mechanisms used by *A. baumannii* for pellicle formation are not essential for adherence to A549 human epithelial cells.

The levels of cAMP in the *cpdA*::Tn mutant strain are significantly increased compared to the 17978hm parent strain

The maintenance of intracellular cAMP levels is largely a result of controlling *cpdA* expression [52]. Therefore, if *cpdA* is inactivated, cAMP levels are expected to increase in the bacterial cell. Quantification of cAMP levels was achieved using a cyclic nucleotide XP enzymatic immunoassay kit. The *cpdA*::Tn mutant strain was found to have a level of cAMP approximately 24-fold greater than in the 17978hm parent strain (0.5 nM and 12 nM,

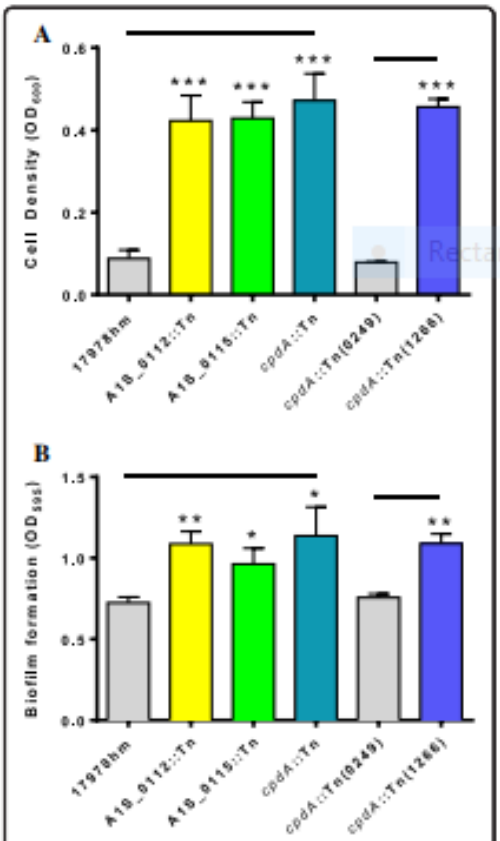

Fig. 4 Planktonic growth and biofilm formation in polypropylene tubes of the transposon mutants and 17978hm parent strain. Cells were cultured in Luria Bertani media without shaking at 37 °C in polypropylene tubes for 72 h. (a) Planktonic growth was assessed by removal of 1 mL of media and the optical density measured at OD_{600}. All three transposon insertion mutant strains showed a dramatic increase of planktonic growth; 4-fold greater than the 17978hm parent strain. Complementation of the *cdpA* mutation in the *cpdA*::Tn(0249) strain returned the phenotype to wild-type levels. (b) The level of biofilm produced was assessed by crystal violet staining. Transposon insertion mutant strains had an increased biomass of the surface/liquid biofilm by approximately 30 % compared to that of the 17978hm parent. The *cpdA*::Tn(0249) mutant strain that contains a wild-type copy of the gene, restored the biofilm phenotype to that of the parent. Bars indicate the standard deviation of three separate experiments. Asterisks indicate significant difference: one denotes a p-value <0.05, two a p-value <0.01 and three a p-value <0.001, as determined by a student *t*-test

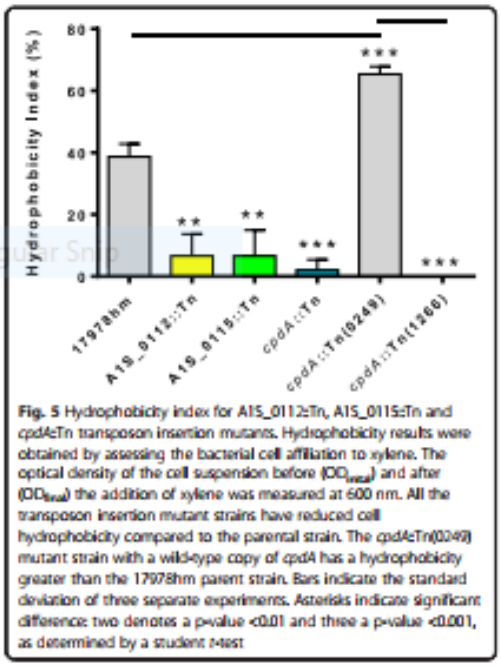

Fig. 5 Hydrophobicity index for A1S_0112::Tn, A1S_0115::Tn and *cpdA*::Tn transposon insertion mutants. Hydrophobicity results were obtained by assessing the bacterial cell affiliation to xylene. The optical density of the cell suspension before ($OD_{initial}$) and after (OD_{final}) the addition of xylene was measured at 600 nm. All the transposon insertion mutant strains have reduced cell hydrophobicity compared to the parental strain. The *cpdA*::Tn(0249) mutant strain with a wild-type copy of *cpdA* has a hydrophobicity greater than the 17978hm parent strain. Bars indicate the standard deviation of three separate experiments. Asterisks indicate significant difference: two denotes a p-value <0.01 and three a p-value <0.001, as determined by a student *t*-test

respectively) (p-value <0.001) (Fig. 7). This confirmed that *cpdA* is involved in cAMP homeostasis within the cell and that the disruption of this gene dramatically affects the accumulation of this secondary signalling molecule. Examination of cAMP levels in strains *cpdA*::Tn(0249) and *cpdA*::Tn(1266) showed that the phenotype could be specifically attributed to the inactivation of *cpdA* (Fig. 7).

Transcriptional profiling of the *cpdA*::Tn mutant strain under motility conditions

To assess the association between pellicle formation and motility qRT-PCR was undertaken on the *A. baumannii* 17978hm parent and the *cpdA*::Tn transposon mutant strain grown under previously identified motility conditions, i.e. on semi-solid LB agar [43]. Analysis of the operon A1S_0112-0118 (Fig. 3) was undertaken by quantifying the transcription of the A1S_0112 gene, which is the first gene in the operon. In the *cpdA*::Tn strain, the transcription level of A1S_0112 was 2.8-fold down-regulated compared to the 17978hm parent (Table 3). This indicated that CpdA via cAMP plays a role, either directly or indirectly, in regulation of the A1S_0112-0118 operon. This potential regulatory role of CpdA and cAMP on the A1S_0112-0118 operon could explain the altered motility phenotype seen in the *cpdA*::Tn mutant strain, possibly due to alteration in the production of a biosurfactant or through another unknown mechanism(s).

The A1S_0112-0118 operon described above has previously been shown to be activated by quorum-sensing signals in the form of homoserine lactone (*abaI*, A1S_0109) [47]. Furthermore, Saroj and Rather (2013) have shown that down-regulation of *abaI* leads to a

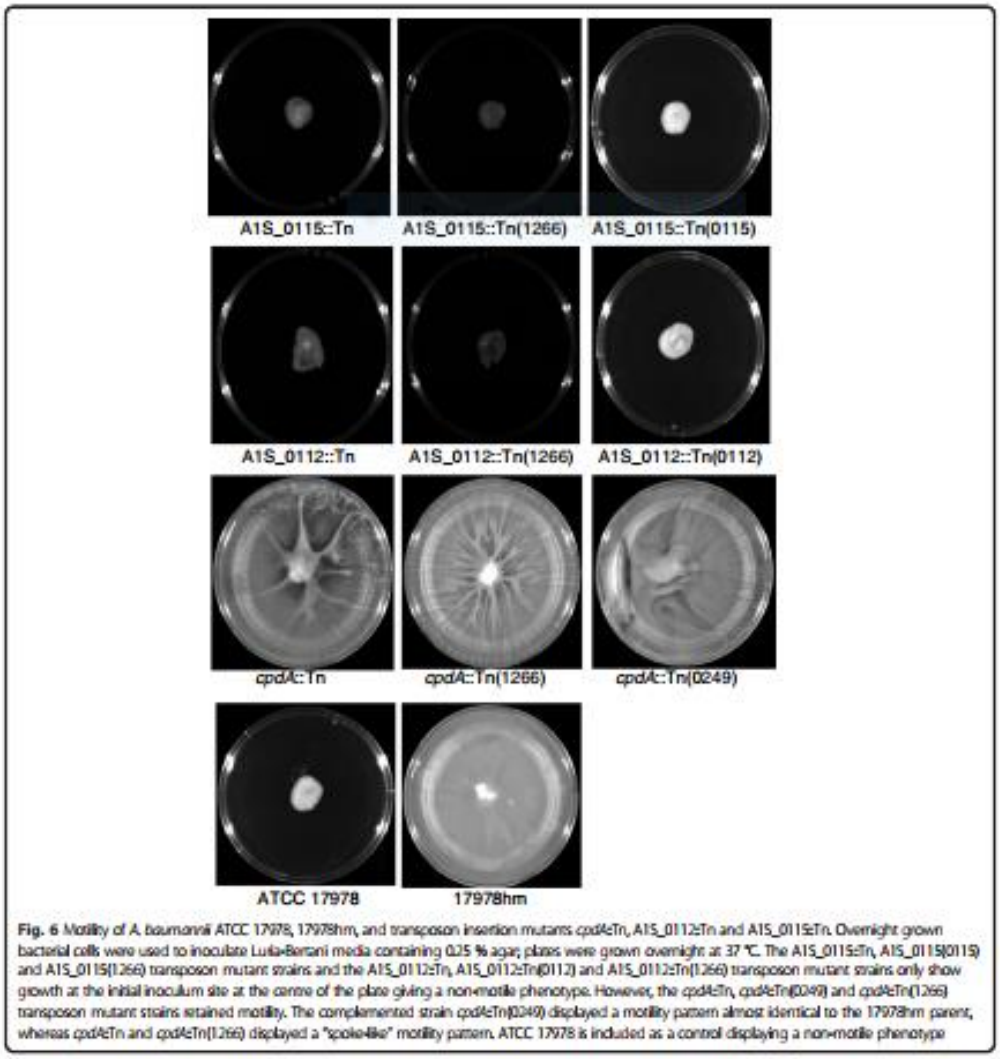

Fig. 6 Motility of *A. baumannii* ATCC 17978, 17978hm, and transposon insertion mutants *cpdA*::Tn, A1S_0112::Tn and A1S_0115::Tn. Overnight grown bacterial cells were used to inoculate Luria-Bertani media containing 0.35 % agar; plates were grown overnight at 37 °C. The A1S_0115::Tn, A1S_0115(0115) and A1S_0115(1266) transposon mutant strains and the A1S_0112::Tn, A1S_0112::Tn(0112) and A1S_0112::Tn(1266) transposon mutant strains only show growth at the initial inoculum site at the centre of the plate giving a non-motile phenotype. However, the *cpdA*::Tn, *cpdA*::Tn(0249) and *cpdA*::Tn(1266) transposon mutant strains retained motility. The complemented strain *cpdA*::Tn(0249) displayed a motility pattern almost identical to the 17978hm parent, whereas *cpdA*::Tn and *cpdA*::Tn(1266) displayed a "spoke-like" motility pattern. ATCC 17978 is included as a control displaying a non-motile phenotype

reduction in motility in *A. nosocomialis* strain M2 [53, 54]. Therefore, to examine whether the insertional inactivation of *cpdA* in the *cpdA*::Tn mutant had a regulatory effect on the quorum sensing gene *abaI* when grown on motility media, we assessed the levels of transcription of *abaI* using qRT-PCR. The results revealed that, despite the altered motility phenotype of the derivative, *abaI* is expressed at a level comparable to the parent strain (~1.2-fold increase). This suggests that the A1S_0112-0118 operon is regulated independently by two different factors; quorum-sensing (AbaI) and cAMP. Levels of cAMP act as one of the major signalling molecules within the cell and have been show to regulate numerous genes in other bacterial species such as *P. aeruginosa* and *Escherichia coli*, possibly through activation of Vfr [33]. In *P. aeruginosa*, *vfr* is auto-regulated and upon inactivation of *cpdA*, *vfr* expression increases by 12-fold [33, 45]. We investigated this possibility in our *cpdA*::Tn mutant strain by examining the transcript of the putative *vfr* gene (A1S_1182). The qRT-PCR results showed a 1.7-fold decrease in *vfr* expression in the *cpdA*::Tn mutant strain compared to the 17978hm

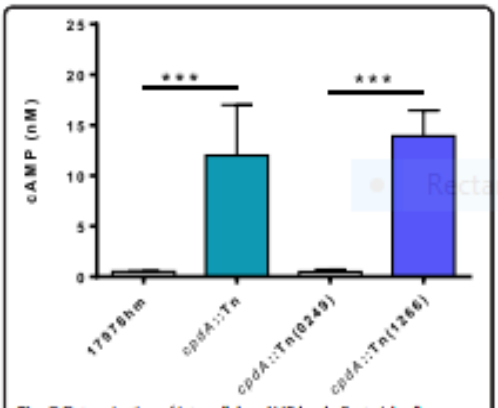

Fig. 7 Determination of intracellular cAMP levels. Bacterial cells were grown to an OD_{600} of 0.7, disrupted and cAMP levels determined using the Cyclic Nucleotide XP Enzymatic Immunoassay kit. The amount of cAMP is given in nM representing a sample corresponding to 1 mg of total cellular protein. Bars indicate the standard deviation of three separate experiments. The *cpdA*::Tn transposon mutant has 12 mM of cAMP compared to the parent 17978hm strain which has 0.5 mM of cAMP within the cell. The *cpdA*::Tn(8249) mutant strain returned the cAMP levels to that of the 17978hm parent strain. The *cpdA*::Tn mutant strain harboring the empty vector pWH1266 had no effect on the cAMP levels. Asterisks indicate significant difference (p-value <0.001) as determined by one-way Anova

parental strain, that, by a student *t*-test, was determined to be statistically insignificant. Thus, although a 1.7-fold reduction in *vfr* transcription was observed it is not known whether cAMP and Vfr work in concert in *A. baumannii*.

Whole transcriptome analysis of the CpdA mutant compared to the 17978hm *A. baumannii* parent strain

Alterations in the level of intracellular cAMP are known to affect a plethora of phenotypes, including alterations in metabolic processes, biofilm formation and cell surface hydrophobicity [52]. Therefore, RNA sequencing was used to investigate the transcriptome of the *cpdA*::Tn mutant grown in Mueller Hinton broth, in order to assess the impact high levels of cAMP have within the bacterial cell. Transcriptome sequencing revealed that many genes were differentially expressed in the *cpdA*::Tn mutant compared to the parent. Of the approximately 3400 annotated genes in ATCC 17978, 184 genes were more than 2-fold up-regulated and 494 genes were more than 2-fold down-regulated (Fig. 8). The most highly up-regulated gene is identified as an alcohol dehydrogenase (A1S_1274) which showed a 34-fold increase in expression, whereas the greatest down-regulated gene is a putative transcriptional regulator (A1S_1256) showing a 29-fold decrease of expression (Fig. 8).

A number of the genes down-regulated in the *cpdA*::Tn mutant include genes encoding phage-related proteins (A1S_2021-2033), putative acyl carrier proteins, ferric enterobactin receptors, porins, signal peptides, membrane proteins and numerous hypothetical ORFs with no known function (Fig. 8). Variations in the expression of multiple potential transcriptional regulators were also observed; this may be due to the significant alterations that cAMP levels have on the general metabolism of the cell. Genes of particular interest in this study that are down-regulated include the CsuA/BABCDE system (A1S_2213-2218) (9 to 20-fold), the *hms* operon which consists of three genes designated A1S_2160 to A1S_2162) (10 to12-fold), and a chaperone usher system (A1S_1507-1510) (2-fold). Proteins encoded by the *csu* cluster and chaperone usher system have been identified in pellicle and biofilm formations [2, 20, 22, 23, 34, 55, 56]. Interestingly, a single polynucleotide polymorphism leading to truncation of the *csuB* gene potentially inactivating this operon has been identified within ATCC 17978 [2, 22, 56]. Within the *hms* operon two proteins (A1S_2160 and A1S_2161) share an average of 44 % identity with the PgaBC proteins (A1S_0938-0939), the third protein within Hms (A1S_2162) has been designated as a biofilm synthesis protein and shares no homology to the Pga proteins in *A. baumannii* ATCC 17978. The Pga system has previously been identified as being important in biofilm formation [57]. Interestingly, a recent paper by Nait Chabane *et al.* (2014) [23] found that CsuA/BABCDE, PgaABC proteins and the chaperone usher system described above, are over represented within *A. baumannii* strains displaying a pellicle phenotype. This suggests that the Hms and chaperone usher pilus proteins could be key components in the formation of the pellicle matrix.

Numerous genes which are up-regulated encode proteins involved in oxidative phosphorylation (Fig. 8). In particular, these include those encoding ubiquinol oxidase subunit I and II (A1S_1434 and A1S_1433) which are 5.7- fold and 4.9-fold up-regulated, respectively. Other genes involved in oxidative phosphorylation include the NADH dehydrogenase complex (A1S_0762-0764) and the ATP synthetase complex (A1S_0148-0156). One of the most highly up-regulated genes (A1S_1387) is an oxidoreductase (18-fold); this class of enzymes is often involved in the FAD to $FADH_2$ conversion, where $FADH_2$ plays a major role in oxidative phosphorylation. Therefore, many of the up-regulated genes are involved in the energy, and by extension, the metabolic status of the cell which is not surprising given the central role cAMP plays in cell metabolism.

Other genes of interest which were significantly up-regulated are those involved in 50S and 30S ribosome assembly. The potential role of these up-regulated

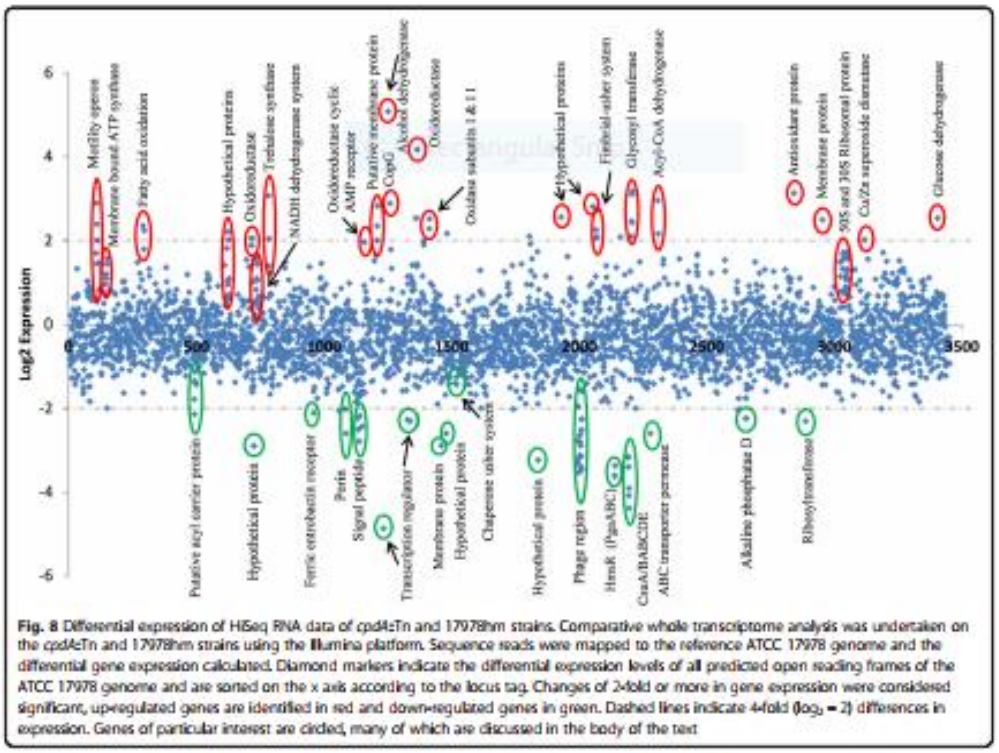

Fig. 8 Differential expression of HiSeq RNA data of *cpdA*::Tn and 17978hm strains. Comparative whole transcriptome analysis was undertaken on the *cpdA*::Tn and 17978hm strains using the Illumina platform. Sequence reads were mapped to the reference ATCC 17978 genome and the differential gene expression calculated. Diamond markers indicate the differential expression levels of all predicted open reading frames of the ATCC 17978 genome and are sorted on the x axis according to the locus tag. Changes of 2-fold or more in gene expression were considered significant, up-regulated genes are identified in red and down-regulated genes in green. Dashed lines indicate 4-fold ($\log_2 = 2$) differences in expression. Genes of particular interest are circled, many of which are discussed in the body of the text

ribosomal proteins maybe in the assembly of 100S ribosomes, as these are required for cells to survive long term nutrient stress in situations where glucose is low and cAMP is high [58]. Other up-regulated genes including those involved in fatty acid oxidation, trehalose synthase, membrane proteins, dehydrogenase proteins and a number of proteins which are annotated as hypothetical ORFs.

A small operon consisting of 4 genes (A1S_2088-2091) was identified as having 4-fold increase in expression. Proteins encoded by this region have recently been found in extracted pellicle material [23]. Since, *cpdA*::Tn is not capable of pellicle production it would seem unlikely that the A1S_2088-2091 operon is involved in this phenotype, however, *cpdA*::Tn does show an increase in biofilm formation compared to the parent strain and as such this operon may contribute to liquid/surface biofilm production.

The previously described motility operon A1S_0112-0118 [47] is up-regulated approximately 3.8-fold in the *cpdA*::Tn mutant transcriptome, which is in contrast to RT-PCR data (Table 3). These RT-PCR studies were conducted on motility agar to look at the influence of motility on the change in transcription of this operon. On motility agar both cAMP and quorum sensing may play a role in the control of this operon, however in liquid culture grown to mid-log phase used for the RNA-sequence analysis, cAMP appears to be solely responsible for the regulation of A1S_0112-0118.

Conclusions

This report has shown that pellicle formation is a phenotypic trait seen in a limited number of *A. baumannii* strains. For the first time, the secondary signalling molecule cAMP has been shown to play a critical role in pellicle formation as well as motility in *A. baumannii*. Additionally, this study has shown that insertions in CpdA, A1S_0112 and A1S_0115 completely abolish pellicle formation. Furthermore, transcriptional analyses identified that cAMP effects the expression of the A1S_0112-0118 operon essential for motility, thereby altering the migration pattern seen in the *cpdA*::Tn mutant strain grown on semi-sold agar; insertions in the above operon in A1S_0112 and A1S_0115 resulted in a non-motile phenotype. We thus speculate, that pellicle and motility phenotypes of *A. baumannii* are linked via the expression of cAMP and the

A1S_0112-0118 operon. Increased cell surface hydrophobicity was identified as an indicator of pellicle formation ability in the clinical strains tested herein. Whole transciptome analysis has identified an abundance of ORFs affected by the increase in cAMP within the *cpdA*::Tn mutant. A number of these correlate with genes previously known to be involved in pellicle formation including the *hms* locus and a chaperone usher system as well as the A1S_0112-0118 region identified in this study. Considering the importance of pellicle formation in the persistence and transmission of numerous bacterial species, this study has contributed to our understanding of the regulatory mechanisms behind these significant virulence traits in *A. baumannii*.

Methods

Bacterial strains

The 54 clinical *A. baumannii* bacterial strains used in this study and the hyper-motile derivative of *A. baumannii* ATCC 17978 designated 17978hm have been described previously [34, 59]. All *A. baumannii* strains were cultured on LB media containing 1 % agar overnight at 37 °C, and single colonies transferred to LB broth for subsequent use in assays, unless otherwise stated. For maintenance, conjugation, cloning and replicating plasmids *E. coli* DH5α, SM10 or JM109 cells were used [60–62].

Assessment of pellicle formation

The pellicle formation assay was adapted from previously described protocol [35]. In brief, overnight bacterial cultures were diluted 1:100 in 5 mL of LB broth and grown stagnant in polypropylene or glass tubes for 72 h at 25 °C without shaking in the dark [63, 64]. Quantitative measurement of the pellicle material was assessed by the addition of 1 mL of ethanol into the tube underneath the pellicle material. The floating pellicle was then removed and resuspended in phosphate buffered saline (PBS) and the OD_{600} measured using a spectrophotometer (Beckman DU 640). Quantitative data were collected from at least three experiments on three different days.

Motility assays

Motility was assessed by migration on semi-solid surfaces using media containing 0.25 % agar as described previously [34]. Briefly, an overnight colony was collected using a sterile loop and used to inoculate the centre of LB medium containing 0.25 % agar. The plate was then incubated overnight at 37 °C. Strains were considered motile if any movement of growth from the original inoculation site was observed.

Eukaryotic cell adherence assays

A. baumannii cell adherence to A549 (human type 2 pneumocytes) was investigated as previously described [34]. In brief, cell lines were grown in Dulbecco's Modified Eagle medium (Invitrogen, Australia) supplemented with 10 % foetal bovine serum (Bovogen, Australia). Washed A549 monolayers in 24-well tissue culture plates were infected with bacterial inoculums containing ~$1x10^7$ colony forming units. After incubation at 37 °C for 4 h the culture medium was removed and the monolayers washed with PBS. The cell monolayers were detached from the plate using a treatment of 100 μL of 0.25 % trypsin in PBS. Eukaryotic cells were subsequently lysed by the addition of 400 μL 0.025 % Triton X-100 and serial 10-fold dilutions were spread plated on LB agar to determine the number of colony forming units of adherent bacteria per well. The collated data for the adherence assay were obtained from at least three independent experiments and represent the data points from each experiment in quadruplicate wells.

Cell surface hydrophobicity tests

Cell surface hydrophobicity was examined as described previously [65]. In brief, overnight cultures were diluted in LB broth and incubated at 37 °C for 2 h. Potassium urea magnesium buffer was used to wash the cells twice, before incubation at 30 °C for 20 min. The cell suspension was adjusted to OD_{600} ~ 0.25 in the same buffer in glass vials before the addition of xylene (3 mL). The sample was vortexed for 20 sec and the aqueous phase transferred to a 1.5 mL tube. The OD_{600} of the cell suspension was determined before ($OD_{initial}$) and after (OD_{final}) the addition of xylene. The hydrophobicity index, expressed as a percentage, is calculated as $(OD_{initial} - OD_{final}/OD_{initial})*100$. Quantitative data were collected from at least three experiments from three different days.

Transposon mutagenesis

Transposon mutagenesis was undertaken using a modified mini Tn*10* transposon (mini::Tn*10*:*gfp*:*kan*) carried on the plasmid pLof [66]. The pLof mini::Tn*10*:*gfp*:*kan* plasmid was transformed into the donor *E. coli* SM10 strain and mated with the *A. baumannii* 17978hm recipient at a 1:10 ratio for 4 h at 37 °C on LB agar exconjugates were resuspended in 5 mL of LB broth and plated onto selective media containing 50 μg/mL kanamycin and 25 μg/mL chloramphenicol to select for transposition events and counter-select against the *E. coli* SM10 donor strain. Approximately, 4000 exconjugates were individually picked using sterile toothpicks to inoculate 200 μL of LB broth in 96 well microtitre plates. The cells were grown at 25 °C in the dark for 72 h and assessed visually for pellicle loss.

Identification of mini::Tn*10*:*gfp*:*kan* insertion in the chromosome

Chromosomal DNA isolated from *A. baumannii* 17978hm containing the mini::Tn*10*:*gfp*:*kan* was digested with restriction endonucleases *Xba*I and *Sac*II for 4 h at 37 °C. Digested products were cloned into pBluescript SK II (Agilent technologies, CA, USA) and clones were confirmed by sequencing (Australian Genome Research Facility, Adelaide, South Australia). The insertion site of the transposons in the chromosome was determined by Sanger sequencing using an oligonucleotide designed to read out of the end of the transposon (see Additional file 2).

Complementation of transposon insertions

For genetic complementation of the non-pellicle forming *A. baumannii* mutants, the genes corresponding to A1S_0112, A1S_0115 and *cpdA* were PCR amplified, cloned into the shuttle vector pWH1266, transformed into DH5α *E. coli* cells and sequenced. Plasmids were extracted and subsequently transformed via electroporation using a MicroPulser (Bio-Rad, CA, USA) at 2.5 kV, 200 ohms and 25 microfarads into their respective *A. baumannii* transposon insertion strains [46]. PCR was achieved with VELOCITY™ DNA polymerase (Bioline, Vic, Australia) and the oligonucleotides (Additional file 2) using the following PCR protocols. For amplification of *cpdA*, cycling conditions were 2 min at 94 °C, 30 cycles of 45 sec at 94 °C, 45 sec at 55 °C, and 90 sec at 72 °C, followed by a final extension of 4 min at 72 °C. Amplification of A1S_0112 used the same conditions with the exception of the annealing temperature which was increased to 60 °C. For amplification of A1S_0115, the cycling conditions were 2 min at 94 °C, 30 cycles of 90 sec at 94 °C, 90 sec at 60 °C, 4 min at 72 °C and a final extension of 6 min at 72 °C.

Measurement of intracellular cAMP levels

Assessment of cAMP levels within *A. baumannii* strains *cpdA*::Tn, *cpdA*::Tn(0249), *cpdA*::Tn(1266) and 17978hm was performed with cells were grown to an OD_{600} of 0.7. Cells were pelleted by centrifugation at 4500 *g* for 15 min, resuspended in PBS and disrupted at 30,000 lb per square inch using the One Shot Head from the TS series bench top disruptor (Constant Systems, United Kingdom). The resulting cellular material in the cell lysis solution was clarified by centrifugation at 4500 *g* for 30 min and the supernatant removed and stored at −80 °C until required. The concentration of cAMP was measured using the Cyclic Nucleotide XP Enzymatic Immunoassay kit (Cell Signalling Technology, MA, USA) according to the manufacturer's instructions. In brief, 50 μL of horseradish peroxidase-linked cAMP solution and 50 μL of sample were added to the supplied 96-well tray, which was then covered and incubated at room temperature for 3 h on a horizontal orbital plate shaker. The contents of the plate were discarded and the plate was washed 4 times with 200 μL/well of wash buffer. Next, 100 μL of 3,3',5,5'-tetramethylbenzidinesubstrate solution was added and incubated for 30 min at room temperature, after which 100 μL of stop solution was added and the absorbance measured at 450 nm. Using the inverse for the standards derived from a standard curve and adjusted for the amount of total protein added, the amount of cAMP was calculated. Total protein concentrations were quantified using the Lowry protein assay (Bio-Rad, CA, USA) following the manufacturer's instructions.

Isolation of total cellular RNA

To measure transcriptional levels for either RT-PCR or in Hiseq RNA transcriptome analysis conducted by SA Pathology (Central Adelaide local Health Network via an Illumina platform), cells were isolated and RNA extracted as below. Bacterial cells were harvested from either semi-solid media (0.25 % LB agar) for RT-PCR using pre-chilled PBS or harvested from Mueller Hinton broth at OD_{600} of 0.6 for Hiseq. Bacterial cells were pelleted by centrifugation at 4500 *g* for 15 min and lysed in 1 mL TRIzol reagent (Life Technologies, Australia) and 200 μL of chloroform. Following phase separation, the aqueous layer was collected and RNA isolated using the Isolate RNA Mini Kit (Bioline, NSW, Australia) following the manufacturer's recommendations. Samples for RT-PCR were subsequently treated with DNaseI (Promega, WI, USA) for 30 min at 37 °C and 1 μL of stop solution was added before a final incubation for 10 min at 65 °C. Triplicate samples were pooled and sent to SA Pathology for Ribosomal RNA reduction using Epicentre Ribo-Zero kit and RNA library bar-coding was undertaken on RNA for HiSeq. Samples were run on the Illumina HiSeq platform (1X50 base pair single reads). These data are accessible through GEO Series accession number GSE64935 (http://www.ncbi.nlm.nih.gov/geo/query/acc.cgi?acc= GSE64935).

Bioinformatic analysis

The quality of the cDNA reads obtained from the HiSeq was checked using 'Fastqc' (http://www.bioinformatics.babraham.ac.uk/projects/fastqc/). Reads were subsequently mapped to the reference genome using 'bowtie' aligner (http://bowtie-bio.sourceforge.net/index.shtml). For the reads obtained, approximately 95 % were mapped to the ATCC 17978 genome of which 78 % mapped to the coding regions. In order to determine changes in gene expression the number of reads obtained for each ORF was normalised using reads per kilobase of transcript per million reads mapped.

Quantitative reverse transcription PCR

M-MLV reverse-transcriptase (Promega) and random hexamers (GeneWorks, SA, Australia) were used to synthesise complementary deoxyribonucleic acid (cDNA) following the manufacturer's recommendations. qRT-PCR was performed on three biological replicates using DyNAmo SYBR green qRT-PCR kits (ThermoScientific, Vic, Australia) in conjunction with a Rotor-Gene RG-3000 (Corbett Life Science, Australia). A typical qRT-PCR run was as follows: 1 min at 95 °C, 40 cycles of 10 sec at 95 °C, 15 sec at 55 °C and 20 sec at 72 °C [67]. Transcriptional differences were calculated using the $\Delta\Delta C_T$ method [68]. The 16S rRNA (A1S_r01) and *gapDH* (A1S_2501) transcription levels were used as a reference.

Additional files

Additional file 1: Position of the Tn*10kan:gfp* insertion within the *A. baumannii* 17978hm non-pellicle forming mutants.

Additional file 2: Oligonucleotides used for cloning, sequencing and qRT-PCR.

Additional file 3: Growth curve of the transposon insertion mutants. *A. baumannii* insertion mutants were subcultured 1:100 dilution into fresh Luria-Bertani broth; 200 μL samples were taken every hour and the OD_{600} determined spectroscopically.

Competing interests

The authors declare that they have no competing interests.

Authors' contributions

SKG, BAE, UHS and MHB designed the research project. SKG, BAE and UHS carried out the experiments and SKG, BAE, UHS and MHB wrote the manuscript. All authors have read and approved the final manuscript.

Acknowledgements

This project was financially supported by the National Health and Medical Research Council Australia Project Grant 535053 and a Flinders Medical Research Foundation Grant. SKG is the recipient of a Flinders University Research Scholarship (FURS).

Author details

[1]School of Biological Sciences, Flinders University, GPO Box 21005001 Adelaide, SA, Australia. [2]Research Centre for Infectious Diseases, School of Biological Sciences University of Adelaide, Adelaide, Australia.

Received: 15 January 2015 Accepted: 11 May 2015
Published online: 06 June 2015

References

1. Bergogne-Bérézin E. Treatment of *Acinetobacter* infections. Expert Opin Investig Drugs. 1997;6(2):119–27.
2. McQueary CN, Actis LA. *Acinetobacter baumannii* biofilms: Variations among strains and correlations with other cell properties. J Microbiol. 2011;49(2):243–50.
3. Dijkshoorn L, Nemec A, Seifert H. An increasing threat in hospitals: multidrug-resistant *Acinetobacter baumannii*. Nat Rev Microbiol. 2007;5(12):939–51.
4. Shin JA, Chang YS, Kim HJ, Kim SK, Chang J, Ahn CM, et al. Clinical outcomes of tigecycline in the treatment of multidrug-resistant *Acinetobacter baumannii* infection. Yonsei Med J. 2012;53(5):974–84.
5. Roca I, Espinal P, Vila-Farrés X, Vila J. The *Acinetobacter baumannii* oxymoron: commensal hospital dweller turned pan-drug-resistant menace. Front Microbiol. 2012;3(3):148.
6. Peleg AY, Seifert H, Paterson DL. *Acinetobacter baumannii*: emergence of a successful pathogen. J Clin Microbiol Rev. 2008;21(3):538–82.
7. Ramirez MS, Don M, Merkier AK, Bistué AJ, Zorreguieta A, Centrón D, et al. Naturally competent *Acinetobacter baumannii* clinical isolate as a convenient model for genetic studies. J Clin Microbiol. 2010;48(4):1488–90.
8. Neely AN, Maley MP, Warden GD. Computer keyboards as reservoirs for *Acinetobacter baumannii* in a burn hospital. Clin Infect Dis. 1999;29(5):1358–60.
9. Donlan RM, Costerton JW. Biofilms: survival mechanisms of clinically relevant microorganisms. Clin Microbiol Rev. 2002;15(2):167–93.
10. Karaiskos I, Galani L, Baziaka F, Giamarellou H. Intraventricular and intrathecal colistin as the last therapeutic resort for the treatment of multidrug-resistant and extensively drug-resistant *Acinetobacter baumannii* ventriculitis and meningitis: a literature review. Int J Antimicrob Agents. 2013;41(6):499–508.
11. Stasiak P, Thom KA, Johnsonm JK, Leekha S, Lissauer M, Zhu J, et al. The effect of terminal cleaning on environmental contamination rates of multidrug-resistant *Acinetobacter baumannii*. Am J Infect Control. 2012;40(10):1005–7.
12. Karageorgopoulos DE, Falagas ME. Current control and treatment of multidrug-resistant *Acinetobacter baumannii* infections. Lancet Infect Dis. 2008;8(12):751–62.
13. Longo F, Vuotto C, Donelli G. Biofilm formation in *Acinetobacter baumannii*. New Microbiol. 2014;37(2):119–27.
14. Yamamoto K, Arai H, Ishii M, Igarashi Y. Involvement of flagella-driven motility and pili in *Pseudomonas aeruginosa* colonization at the air-liquid interface. Microbes Environ. 2012;27(3):330–3.
15. Moonmangmee S, Kawabata K, Tanaka S, Toyama H, Adachi O, Matsushita K. A novel polysaccharide involved in the pellicle formation of *Acetobacter aceti*. J Biosci Bioeng. 2002;93(2):192–200.
16. Yuan J, Chen Y, Zhou G, Chen H, Gao H. Investigation of roles of divalent cations in *Shewanella oneidensis* pellicle formation reveals unique impacts of insoluble iron. Biochim Biophys Acta. 2013;1830(11):5248–57.
17. Espinal P, Martí S, Vila J. Effect of biofilm formation on the survival of *Acinetobacter baumannii* on dry surfaces. J Hosp Infect. 2012;80(1):56–60.
18. Kanchanarach W, Theeragool G, Inoue T, Yakushi T, Adachi O, Matsushita K. Acetic acid fermentation of *Acetobacter pasteurianus*: relationship between acetic acid resistance and pellicle polysaccharide formation. J Biosci Bioeng. 2010;74(8):1591–7.
19. Sambandan D, Dao DN, Weinrick BC, Vilchèze C, Gurcha SS, Ojha A, et al. Keto-mycolic acid-dependent pellicle formation confers tolerance to drug-sensitive *Mycobacterium tuberculosis*. MBio. 2013;4(3):e00222–00213.
20. Tomaras AP, Dorsey CW, Edelmann RE, Actis LA. Attachment to and biofilm formation on abiotic surfaces by *Acinetobacter baumannii*: involvement of a novel chaperone-usher pili assembly system. Microbiol. 2003;149(12):3473–84.
21. Kobayashi K. *Bacillus subtilis* pellicle formation proceeds through genetically defined morphological changes. J Bacteriol. 2007;189(13):4920–31.
22. Martí S, Nait Chabane Y, Alexandre S, Coquet L, Vila J, Jouenne T, et al. Growth of *Acinetobacter baumannii* in pellicle enhanced the expression of potential virulence factors. PLoS One. 2011;6(10):e26030.
23. Nait Chabane Y, Martí S, Rihouey C, Alexandre S, Hardouin J, Lesouhaitier O, et al. Characterisation of pellicles formed by *Acinetobacter baumannii* at the air-liquid interface. PLoS One. 2014;9(10):e111660.
24. Lazar V. Quorum sensing in biofilms - How to destroy the bacterial citadels or their cohesion/power? Anaerobe. 2011;17(6):280–5.
25. de Kievit TR. Quorum sensing in *Pseudomonas aeruginosa* biofilms. Environ Microbiol. 2009;11(2):279–88.
26. Kalivoda EJ, Brothers KM, Stella NA, Schmitt MJ, Shanks RM. Bacterial cyclic AMP-phosphodiesterase activity coordinates biofilm formation. PLoS One. 2013;8(7):e71267.
27. Shemarova IV. cAMP-dependent signal pathways in unicellular eukaryotes. Crit Rev Microbiol. 2009;35(1):23–42.
28. Skorupski K, Taylor RK. Cyclic AMP and its receptor protein negatively regulate the coordinate expression of cholera toxin and toxin-coregulated pilus in *Vibrio cholerae*. Proc Natl Acad Sci U S A. 1997;94(1):265–70.
29. Ono K, Oka R, Toyofuku M, Sakaguchi A, Hamada M, Yoshida S, et al. cAMP signaling affects irreversible attachment during biofilm formation by *Pseudomonas aeruginosa* PAO1. Microbes Environ. 2014;29(1):104–6.
30. Wolfgang MC, Lee VT, Gilmore ME, Lory S. Coordinate regulation of bacterial virulence genes by a novel adenylate cyclase-dependent signaling pathway. Dev Cell. 2003;4(2):253–63.
31. Yahr TL, Vallis AJ, Hancock MK, Barbieri JT, Frank DW. ExoY, an adenylate cyclase secreted by the *Pseudomonas aeruginosa* type III system. Proc Natl Acad Sci U S A. 1998;95(23):13899–904.

32. Jimenez PN, Koch G, Thompson JA, Xavier KB, Cool RH, Quax WJ. The multiple signaling systems regulating virulence in *Pseudomonas aeruginosa*. Microbiol Mol Biol Rev. 2012;76(1):46–65.
33. Fuchs EL, Brutinel ED, Jones AK, Fulcher NB, Urbanowski ML, Yahr TL, et al. The *Pseudomonas aeruginosa* Vfr regulator controls global virulence factor expression through cyclic AMP-dependent and -independent mechanisms. J Bacteriol. 2010;192(14):3553–64.
34. Eijkelkamp BA, Stroeher UH, Hassan KA, Papadimitrious MS, Paulsen IT, Brown MH. Adherence and motility characteristics of clinical *Acinetobacter baumannii* isolates. FEMS Microbiol Lett. 2011;323(1):44–51.
35. Martí S, Rodríguez-Baño J, Catel-Ferreira M, Jouenne T, Vila J, Seifert H, et al. Biofilm formation at the solid-liquid and air-liquid interfaces by *Acinetobacter* species. BMC Res Notes. 2011;4(5):1–4.
36. Pour NK, Dusane DH, Dhakephalkar PK, Zamin FR, Zinjarde SS, Chopade BA. Biofilm formation by *Acinetobacter baumannii* strains isolated from urinary tract infection and urinary catheters. FEMS Immunol Med Microbiol. 2011;62(3):328–38.
37. Costa GF, Tognim MC, Cardoso CL, Carrara-Marrone FE, Garcia LB. Preliminary evaluation of adherence on abiotic and cellular surfaces of *Acinetobacter baumannii* strains isolated from catheter tips. Braz J Infect Dis. 2006;10(5):346–51.
38. Furuhata K, Kato Y, Goto K, Hara M, Fukuyama M. Diversity of heterotrophic bacteria isolated from biofilm samples and cell surface hydrophobicity. J Gen Appl Microbiol. 2009;55(1):69–74.
39. Kouidhi B, Zmantar T, Hentati H, Bakhrouf A. Cell surface hydrophobicity, biofilm formation, adhesives properties and molecular detection of adhesins genes in *Staphylococcus aureus* associated to dental caries. Microb Pathog. 2010;49(1–2):14–22.
40. Chiku K, Tsunemi K, Yamamoto M, Ohnishi-Kameyama M, Yoshida M, Ishii T, et al. Defects in D-rhamnosyl residue biosynthetic genes affect lipopolysaccharide structure, motility, and cell-surface hydrophobicity in *Pseudomonas syringae* pathovar *glycinea* race 4. Biosci Biotechnol Biochem. 2013;77(3):505–10.
41. Raut J, Rathod V, Karuppayil SM. Cell surface hydrophobicity and adhesion: a study on fifty clinical isolates of *Candida albicans*. Nippon Ishinkin Gakkai Zasshi. 2010;51(3):131–6.
42. Delcour AH. Outer membrane permeability and antibiotic resistance. Biochim Biophys Acta. 2009;1794(5):808–16.
43. Eijkelkamp BA, Stroeher UH, Hassan KA, Elbourne LD, Paulsen IT, Brown MH. H-NS plays a role in expression of *Acinetobacter baumannii* virulence features. Infect Immun. 2013;81(7):2574–83.
44. Stretton S, Techkarnjanaruk S, McLennan AM, Goodman AE. Use of green fluorescent protein to tag and investigate gene expression in marine bacteria. Appl Environ Microbiol. 1998;64(7):2554–9.
45. Fuchs EL, Brutinel ED, Klem ER, Fehr AR, Yahr TL, Wolfgang MC. In vitro and in vivo characterization of the *Pseudomonas aeruginosa* cyclic AMP (cAMP) phosphodiesterase CpdA, required for cAMP homeostasis and virulence factor regulation. J Bacteriol. 2010;192(11):2779–90.
46. Hunger M, Schmucker R, Kishan V, Hillen W. Analysis and nucleotide sequence of an origin of DNA replication in *Acinetobacter calcoaceticus* and its use for *Escherichia coli* shuttle plasmids. Gene. 1990;87(1):45–51.
47. Clemmer KM, Bonomo RA, Rather PN. Genetic analysis of surface motility in *Acinetobacter baumannii*. Microbiol. 2011;157(9):2534–44.
48. Stewart CR, Rossier O, Cianciotto NP. Surface translocation by *Legionella pneumophila*: a form of sliding motility that is dependent upon type II protein secretion. J Bacteriol. 2009;191(5):1537–46.
49. Rumbo-Feal S, Gómez MJ, Gayoso C, Álvarez-Fraga L, Cabral MP, Aransay AM, et al. Whole transcriptome analysis of *Acinetobacter baumannii* assessed by RNA-sequencing reveals different mRNA expression profiles in biofilm compared to planktonic cells. PLoS One. 2013;8(8):e72968.
50. Henrichsen J. The influence of changes in the environment on twitching motility. Acta Pathol Microbiol Scand B. 1975;83(3):179–86.
51. Skiebe E, de Berardinis V, Morczinek P, Kerrinnes T, Faber F, Lepka D, et al. Surface-associated motility, a common trait of clinical isolates of *Acinetobacter baumannii*, depends on 1,3-diaminopropane. Int J Med Microbiol. 2012;302(3):117–28.
52. McDonough KA, Rodriguez A. The myriad roles of cyclic AMP in microbial pathogens: from signal to sword. Nat Rev Microbiol. 2012;10(1):27–38.
53. Saroj SD, Rather PN. Streptomycin inhibits quorum sensing in *Acinetobacter baumannii*. Antimicrob Agents Chemother. 2013;57(4):1926–9.
54. Caruthers MD, Harding CM, Baker BD, Bonomo RA, Hujer KM, Rather PN, et al. Draft genome sequence of the clinical isolate *Acinetobacter nosocomialis* strain M2. Genome Announc. 2013;1(6):e00906–13.
55. Vallet I, Olson JW, Lory S, Lazdunski A, Filloux A. The chaperone/usher pathways of *Pseudomonas aeruginosa*: identification of fimbrial gene clusters (cup) and their involvement in biofilm formation. Proc Natl Acad Sci U S A. 2001;98(12):6911–6.
56. Eijkelkamp BA, Stroeher UH, Hassan KA, Paulsen IT, Brown MH. Comparative analysis of surface-exposed virulence factors of *Acinetobacter baumannii*. BMC Genomics. 2014;15:1020.
57. Choi AH, Slamti L, Avci FY, Pier GB, Maira-Litrán T. The pgaABCD locus of *Acinetobacter baumannii* encodes the production of poly-b-1-6-N-acetylglucosamine, which is critical for biofilm formation. J Bacteriol. 2009;191(19):5953–63.
58. Wada A, Mikkola R, Kurland CG, Ishihama A. Growth phase-coupled changes of the ribosome profile in natural isolates and laboratory strains of *Escherichia coli*. J Bacteriol. 2000;182(10):2893–9.
59. Eijkelkamp BA, Hassan KA, Paulsen IT, Brown MH. Investigation of the human pathogen *Acinetobacter baumannii* under iron limiting conditions. BMC Genomics. 2011;12(1):126.
60. Hanahan D. Studies on transformation of *Escherichia coli* with plasmids. J Mol Biol. 1983;166(4):557–80.
61. Simon R, Priefer U, Puhler A. A broad host range mobilization system for invivo genetic-engineering - transposon mutagenesis in Gram-negative bacteria. BioTechnol. 1983;1(9):784–91.
62. Yanisch-Perron C, Vieira J, Messing J. Improved M13 phage cloning vectors and host strains: nucleotide sequences of the M13mp18 and pUC19 vectors. Gene. 1985;33(1):103–19.
63. Musa MA, Gaddy JA, Cabruja M, Arivett BA, Viale AM, Riaia R, et al. The opportunistic human pathogen *Acinetobacter baumannii* senses and responds to light. J Bacteriol. 2010;192(24):6336–45.
64. Golic A, Vaneechoutte M, Nemec A, Viale AM, Actis LA, Mussi MA. Staring at the cold sun: blue light regulation is distributed within the genus *Acinetobacter*. PLoS One. 2013;8(1):e55059.
65. Rosenberg E, Gottlieb A, Rosenberg M. Inhibition of bacterial adherence to hydrocarbons and epithelial cells by emulsan. Infect Immun. 1983;39(3):1024–8.
66. Matthysse AG, Stretton S, Dandie C, McClure NC, Goodman AE. Construction of GFP vectors for use in gram-negative bacteria other than *Escherichia coli*. FEMS Microbiol Lett. 1996;145(1):87–94.
67. Brazma A, Vilo J. Gene expression data analysis. Microbes Infect. 2001;3(10):823–9.
68. Livak KJ, Schmittgen TD. Analysis of relative gene expression data using real-time quantitative PCR and the 2(-Delta Delta C(T)) method. Methods. 2001;25(4):402–8.

Appendix G: Giles *et al*. 2016; Bio-protocol

bio-protocol http://www.bio-protocol.org/e1792 Vol 6, Iss 8, Apr 20, 2016

Measurement of Intracellular cAMP Levels Using the Cyclic Nucleotide XP Enzymatic Immunoassay Kit in Bacteria

Sarah K Giles, Uwe H Stroeher and Melissa H Brown*

School of Biological Sciences, Flinders University, Adelaide, Australia
*For correspondence: melissa.brown@flinders.edu.au

[Abstract] Cyclic AMP (cAMP) is a ubiquitous secondary signaling molecule, commonly associated with many bacterial processes, including the regulation of virulence factors, such as biofilms, pellicles and motility (Wolfgang, 2003). The quantity of available cAMP is controlled by the interplay between the synthesis of adenosine triphosphate (ATP) to cAMP by adenylyl cyclases, and the degradation of cAMP by phosphodiesterase (McDonough *et al*., 2012). Adequate quantification of cAMP levels within a bacterial cell is an important step in identifying the impact that secondary signaling molecules play on the regulatory pathway within the cell. The principle of this method is to measure total cAMP levels within a bacterial cell, using crude bacterial whole cell lysate. The Cyclic AMP XP™ Assay kit used in this protocol was originally designed to be used for determining the level of cAMP in eukaryotic cells, however, the antibodies used in coating the wells will react with cAMP from any species and thus can be used for determining levels in bacterial cells. The measurement of cAMP in prokaryotic cells described here is a simple and cost effective method of producing quantifiable results.

Materials and Reagents

1. 1 ml cuvettes (SARSTEDT AG & Co., catalog number: 67.742)
2. 15 ml tubes (Falcon Tube) (DKSH, catalog number: LP021015)
3. 50 ml tubes (Falcon Tubes) (DKSH, catalog number: LP21050)
4. 96-well microtitre tray (tissue culture plate) (DKSH, catalog number: LP031096)
5. Aluminum foil
6. Bacterial cell culture
7. Mueller Hinton (MH) broth (prepared as per manufacturer's instructions) (Oxoid Australia, catalog number: CM0405)
8. MH agar media (25 ml/Petri dish) (prepared as per manufacturer's instructions) (Oxoid Australia, catalog number: CM0337)
9. Cyclic AMP XP™ Assay kit (Cell Signaling Technologies, catalog number: 4339)
10. Protein assay DC™ reagents A & B (Bio-Rad Laboratories, catalog number: 500-121)
11. Protein assay bovine serum albumin (BSA) standards (0, 0.125, 0.25, 0.5, 1, 2.5, 5 mg/ml of protein)
12. Milli Q water

bio-protocol http://www.bio-protocol.org/e1792 Vol 6, Iss 8, Apr 20, 2016

13. Sodium Chloride (NaCl) (Chem Supply, catalog number: SA046-5 kg)
14. Potassium Chloride (KCl) (Thermo Fisher Scientific, Ajax Finechem, catalog number: A383-500 g)
15. Sodium Phosphate (Na_2HPO_4) (Merck Millipore Corporation, catalog numer: 7558-79-4)
16. Potassium Phosphat (KH_2PO_4) (Merck Millipore Corporation, catalog number: 7778-77-0)
17. Phosphate buffered saline (PBS) (see Recipes)

Equipment

1. VIS spectrophotometer able to read OD_{600} nm [*e.g.* DU®640 (Beckman Coulter)]
2. ELISA plate reader able to read absorption at 450 nm [*e.g.* Multiskan EX original (Adelab Scientific)]
3. French pressure cell able to operate at 30,000 psi or cell disruptor [*e.g.* One Shot Head from the TS series bench top disruptor (Constant Systems)]
4. Ice bucket
5. Sterile inoculating loop
6. Shaking incubator (37 °C, at 200 rpm)
7. Centrifuge (able to hold 50 ml tubes, spin at 8,000 *x g* and hold a pre-cooled temperature of 4 °C) [*e.g.* Benchtop Centrifuge Hermle Z383K (DKSH)]
8. Horizontal orbital shaker (at ~30 rpm) [*e.g.* OM5 (Ratek, Adelab Scientific)]

Software

1. Software for use with the ELISA plate reader that can export raw OD_{600} nm values (*e.g.* Microsoft Excel)
2. Graphpad prism (Graphpad Software Inc)

Procedure

1. Grow an overnight culture (~16 h) of the required strain on an agar plate, including any antibiotic selection if required. Prepare MH broth media for culture and sterile PBS.
2. Next Day: Under sterile conditions, using a sterile inoculating loop remove a single colony from the agar plate and inoculate 5 ml of MH broth in a 50 ml tube including any antibiotic selection if required. Grow culture overnight (~16 h) at 37 °C at 200 rpm.
3. Next Day: Make a 1:100 dilution of the overnight culture into 15 ml of MH broth in a 50 ml tube. Grow culture at 37 °C shaking at 200 rpm until the culture reaches an OD_{600} = 0.7 (approximately 3-4 h), measure using a spectrophotometer.

bio-protocol http://www.bio-protocol.org/e1792 Vol 6, Iss 8, Apr 20, 2016

4. While the bacterial culture is growing, pre-cool the centrifuge to 4 °C, prepare ice bucket, pre-cool PBS on ice.
5. Remove bacterial cells from incubator and put on ice, centrifuge sample for 20 min, 4 °C at 8,000 *x g*, decant supernatant and keep cell pellet on ice; sample can be frozen at -20 °C for up to 6 months.
6. Resuspend the pellet in 3 ml of cooled PBS buffer and keep sample on ice.
7. Set up cell disruptor with a one shot head (pre-cooled to 4 °C); set to 30,000 psi, and process sample, collect lysed cells into a new 15 ml tube on ice.
8. Centrifuge sample at 8,000 *x g* for 20 min at 4 °C, remove the supernatant and store at -80 °C until required, up to 6 months.
9. Remove 10 µl of sample to quantify total protein in sample using the Protein assay DC™ kit following manufacturer's instructions.
10. Using a microtitre tray, add 20 µl of Reagent A across 7 wells of row A; this is to be used for the BSA standard samples. Add 20 µl of Reagent A across 3 wells of row B; this is to be used for your sample.
11. To the 20 µl of Reagent A in row A, add 5 µl of each BSA protein standard (0, 0.125, 0.25, 0.5, 1, 2.5, 5 mg/ml) to the 7 individual wells. To the 20 µl of Reagent A in row B, add 5 µl of your sample to each of the three wells.
12. Subsequently add 200 µl of Reagent B into all wells used and leave samples to react for 3 min at room temperature.
13. Measure the absorbance of the wells using a Multiskan at 600 nm; create a standard curve using the BSA protein standards in an Excel spread sheet. Then using the equation of the line calculate the amount of protein in your sample. See Note 3 for experimental details, as well as Table 1 and Figure 1 as a representative example.
14. Using the calculated protein concentration of your samples from step 13 adjust the final protein concentration to 1 mg/ml in PBS for cAMP analysis.
15. Put all Cyclic AMP XP™ assay kit solutions and the cAMP XP™ Rabbit mAb coated microwell strips at room temperature.
16. Dilute the 20x wash buffer in Milli-Q to 1x buffer.
17. Prepare a 1x cell lysis buffer from the 10x stock solution provided in Milli-Q water, then add 1 mM of phenylmethylsulfonyl fluoride provided.
18. Make fresh cAMP standards in 1x cell lysis buffer: In 450 µl of 1x cell lysis buffer add 50 µl of cAMP standard (2.4 M) to make 240 nM of cAMP.
19. Using the 240 nM cAMP solution make a 1:3 serial dilution in the cell lysis buffer producing the following concentrations: 80 nM, 26.7 nM, 8.9 nM, 3.0 nM, 1 nM, 0.3 nM and 0 nM.
20. For the unknown samples add 50 µl of the crude protein extract (at 1 mg/ml) in triplicate into the microwell strips. Subsequently, add 50 µl of provided horseradish peroxidase-linked cAMP solution to all standards and samples. Cover with aluminum

bio-protocol http://www.bio-protocol.org/e1792 Vol 6, Iss 8, Apr 20, 2016

foil and incubate at room temperature for 3 h on a horizontal orbital plate shaker (~30 rpm).

21. Tip out the solution in the microwell strips and wash 4 times with 200 µl/well of 1x wash buffer; discard all liquid each time but do not allow wells to dry.
22. Add 100 µl of 3, 3', 5, 5'-tetramethylbenzidinesubstrate solution provided in the kit and incubate the plate at room temperature for 30 min. Continue to monitor the wells as they will have a transparent color at the start of the reaction which will change to a yellow. Monitor wells for color change and when an intense yellow color is seen the reaction should be stopped; this may be necessary to do prior to the 30 min incubation time-frame described in the kit.
23. Add 100 µl of stop solution and then immediately measure the absorbance at 450 nm see representative data 3 for example (Table 2 and Figure 2).
24. Using the inverse for the standards derived from a standard curve, and adjusted for the amount of total protein added from the protein assay; calculate the amount of cAMP in nM/1 mg of crude protein extract.

Representative data

1. A representative experiment demonstrating quantification of cAMP in the bacterium *Acinetobacter baumannii* can be found in Giles *et al.* (2015) Investigation of genes essential for pellicle formation in *Acinetobacter baumannii*.
2. Below is an example of the excel BSA standard curve.

Table 1. BSA protein standards and their relative absorbance at OD_{600}

BSA Standard (mg/ml)[a]	OD_{600} (nm)
5	0.401
2.5	0.235
1	0.157
0.5	0.108
0.25	0.088
0.125	0.079
0	0.063

[a]Absorbance was determined using a Protein Assay DC™ kit and read using a Multiskan EX. Data was subsequently plotted as seen in Figure 1.

bio-protocol http://www.bio-protocol.org/e1792 Vol 6, Iss 8, Apr 20, 2016

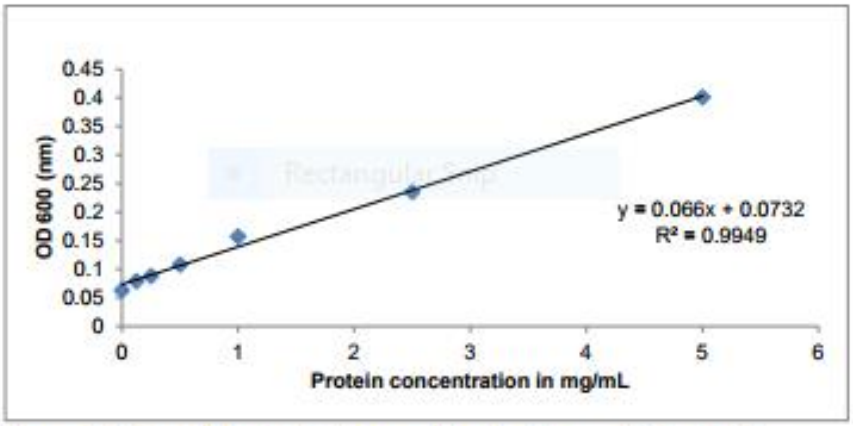

Figure 1. BSA protein standard curve. The absorbance at OD_{600} (nm) was determined for a range of BSA protein standards from 0-5 mg/mL. Protein concentration was determined using the Protein Assay DC™ kit. The line of best fit was plotted using y=mx+c (Excel 2003, Microsoft™).

3. A representative of the cAMP standards diluted in 1x cell lysis buffer is on page 1 of the Cyclic AMP XP™ assay kit manufacturer's instruction; an example (Table 2 and Figure 2) is also provided below.

Table 2. cAMP standards and their relative absorbance at OD_{450} (nm)

cAMP standards (nM)*	OD_{450} (nm)
80	0.09
26.7	0.14
8.9	0.24
3	0.375
1	0.5
0.3	0.6375

*The amount of cAMP (nM) was determined using the Cyclic AMP XP™ Assay kit and absorbance read using a Multiskan EX. Data was subsequently plotted as seen in Figure 2.

bio-protocol http://www.bio-protocol.org/e1792 Vol 6, Iss 8, Apr 20, 2016

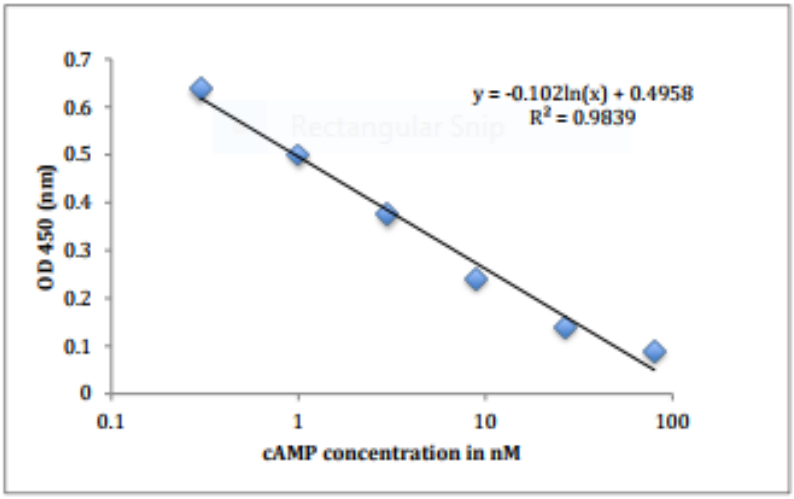

Figure 2. cAMP concentration standard curve. The absorbance at OD_{450} (nm) was determined for a range of cAMP standards from 0.3-80 nM. cAMP concentration was determined using the Cyclic AMP XP™ Assay kit. The line of best fit was plotted using y=mln(x)+c (Excel 2003, Microsoft™). Using this standard curve the quantity of cAMP can be determined for cell lysates.

Notes

1. This protocol is optimized for measuring intracellular cAMP levels in *Acinetobacter baumannii*. For other bacteria, use the appropriate growth medium, antibiotics, and growth conditions.
2. The method for reading OD_{600}: Under sterile conditions pipette 1 ml of culture into a 1 ml cuvette and measure cellular density at an OD_{600} length in the spectrophotometer; repeat this every 1 h or until the culture reaches the required OD_{600} = 0.7.
3. Protein assay using the Multiskan at OD_{600}: after waiting 3 min at room temperature measure the samples in the microtitre tray, then output the data to an excel spread sheet for data manipulation and save. Spread sheet 1 should contain your Multiskan raw data. Then in spread sheet 2 column A row 1 type in BSA standard, column B type in OD_{600}; In column A rows 2-8 type in the BSA standards numbers, in column B type in the Multiskan reads for the BSA standards (see Table 1). Then highlight all the data and make a scatter plot with no markers, add a trend line, add the equation of the line as well as a title and axis labels (see Figure 1). Your samples are in triplicate, average your samples, then insert your average number into the equation of the line as the Y

bio-protocol http://www.bio-protocol.org/e1792 Vol 6, Iss 8, Apr 20, 2016

intersect and find X: example Y = 0.066 X + 0.0732: if Y is 0.2, then 0.2 - 0.0732 = 0.1268/0.066 =1.92 mg/ml of protein in your sample.

4. When waiting for the color change to occur from clear to yellow before adding the stop solution, it is imperative that the microwell plates are continually monitored throughout this reaction. After approximately 15 min, depending on the concentration of cAMP within a sample, the development of an intense yellow color will occur. Once the entire well is yellow add the stop solution.
5. Cyclic AMP is stable for long periods of time when frozen (approximately 6 months at -20 °C), it can be stored for 2 weeks at 4 °C.
6. The use of the Constant System one shot head results in reliable disruption of *Acinetobacter baumannii* cells. The efficiency of cell disruption using other mechanical of chemical methods or the use of differing species will need to be determined empirically.

Recipes

1. Phosphate buffer saline (PBS)
   For 500 ml
   4.0 grams NaCl
   0.1 grams KCl
   0.7 grams Na_2HPO_4
   0.1 grams KH_2PO_4
   Add dH_2O up to 500 ml
   pH sample with HCl pH 7.4 final

Acknowledgements

This protocol was modified and adapted from the manufacturer's instructions specifically for eukaryotic cells using the Cyclic AMP XP™ Assay kit. This project was financially supported by the National Health and Medical Research Council Australia Project Grant 535053 and a Flinders Medical Research Foundation Grant. SKG is the recipient of a Flinders University Research Scholarship (FURS).

References

1. Giles, S. K., Stroeher, U. H., Eijkelkamp, B. A. and Brown, M. H. (2015). Identification of genes essential for pellicle formation in *Acinetobacter baumannii*. *BMC Microbiol* 15: 116.
2. McDonough, K. A. and Rodriguez, A. (2012). The myriad roles of cyclic AMP in microbial pathogens: from signal to sword. *Nat Rev Microbiol* 10(1): 27-38.

bio-protocol http://www.bio-protocol.org/e1792 Vol 6, Iss 8, Apr 20, 2016

3. Wolfgang, M. C., Lee, V. T., Gilmore, M. E. and Lory, S. (2003). Coordinate regulation of bacterial virulence genes by a novel adenylate cyclase-dependent signaling pathway. *Dev Cell* 4(2): 253-263.

REFERENCES

Abbo, A., S. Navon-Venezia, O. Hammer-Muntz, T. Krichali, Y. Siegman-Igra and Y. Carmeli (2005). "Multidrug-resistant *Acinetobacter baumannii*." Emerging Infectious Diseases **11**(1): 22-29.

Adams, F. G., U. H. Stroeher, K. A. Hassan, S. Marri and M. H. Brown (2018). "Resistance to pentamidine is mediated by AdeAB, regulated by AdeRS, and influenced by growth conditions in *Acinetobacter baumannii* ATCC 17978." PLOS One **13**(5): 1-18.

Adams, M. D., K. Goglin, N. Molyneaux, K. M. Hujer, H. Lavender, J. J. Jamison, I. J. MacDonald, K. M. Martin, T. Russo, A. A. Campagnari, A. M. Hujer, R. A. Bonomo and S. R. Gill (2008). "Comparative genome sequence analysis of multidrug-resistant *Acinetobacter baumannii*." Journal of Bacteriology **190**(24): 8053-8064.

Adams, M. D., G. C. Nickel, S. Bajaksouzian, H. Lavender, A. R. Murthy, M. R. Jacobs and R. A. Bonomo (2009). "Resistance to colistin in *Acinetobacter baumannii* associated with mutations in the PmrAB two-component system." Antimicrobial Agents and Chemotherapy **53**(9): 3628-3634.

Ahmad, S., S. Raza, R. Uddin and S. S. Azam (2018). "Comparative subtractive proteomics based ranking for antibiotic targets against the dirtiest superbug: *Acinetobacter baumannii*." Journal of Molecular Graphics and Modelling **82**: 74-92.

Ahn, S. J. and K. C. Rice (2016). "Understanding the *Streptococcus mutans* Cid/Lrg system through CidB function." Applied and Environmental Microbiology **82**(20): 6189-6203.

Alipour, M., Z. E. Suntres and A. Omri (2009). "Importance of DNase and alginate lyase for enhancing free and liposome encapsulated aminoglycoside activity against *Pseudomonas aeruginosa*." Journal of Antimicrobial Chemotherapy **64**(2): 317-325.

Almblad, H., M. Rybtke, S. Hendiani, J. B. Andersen, M. Givskov and T. Tolker-Nielsen (2019). "High levels of cAMP inhibit *Pseudomonas aeruginosa* biofilm formation through reduction of the c-di-GMP content." Microbiology **165**(3): 324-333.

Alves, C. S., M. N. Melo, H. G. Franquelim, R. Ferre, M. Planas, L. Feliu, E. Bardaji, W. Kowalczyk, D. Andreu, N. C. Santos, M. X. Fernandes and M. A. Castanho (2010). "*Escherichia coli* cell surface perturbation and disruption induced by antimicrobial peptides BP100 and *pepR*." Journal of Biological Chemistry **285**(36): 27536-27544.

Alves, L. A., E. N. Harth-Chu, T. H. Palma, R. N. Stipp, F. S. Mariano, J. F. Hofling, J. Abranches and R. O. Mattos-Graner (2017). "The two-component system VicRK regulates functions associated with *Streptococcus mutans* resistance to complement immunity." Molecular Oral Microbiology **32**(5): 419-431.

Anstey, N. M., B. J. Currie, M. Hassell, D. Palmer, B. Dwyer and H. Seifert (2002). "Community-acquired bacteremic *Acinetobacter* pneumonia in tropical Australia is caused by diverse strains of *Acinetobacter baumannii*, with carriage in the throat in at-risk groups." Journal of Clinical Microbiology **40**(2): 685-686.

Anstey, N. M., B. J. Currie and K. M. Withnall (1992). "Community-acquired *Acinetobacter* pneumonia in the Northern Territory of Australia." Clinical Infectious Diseases **14**(1): 83-91.

Antunes, L. C., F. Imperi, A. Carattoli and P. Visca (2011). "Deciphering the multifactorial nature of *Acinetobacter baumannii* pathogenicity." PLOS one **6**(8): e22674.

Arivett, B. A., D. C. Ream, S. E. Fiester, D. Kidane and L. A. Actis (2016). "Draft genome sequences of *Acinetobacter baumannii* isolates from wounded military personnel." Genome Announcements **4**(4): 1-2.

Arroyo, L. A., C. M. Herrera, L. Fernandez, J. V. Hankins, M. S. Trent and R. E. Hancock (2011). "The *pmrCAB* operon mediates polymyxin resistance in *Acinetobacter baumannii* ATCC 17978 and clinical isolates through phosphoethanolamine modification of Lipid A." Antimicrobial Agents and Chemotherapy **55**(8): 3743-3751.

Ashby, M. K. and J. Houmard (2006). "Cyanobacterial two-component proteins: structure, diversity, distribution, and evolution." Microbiology and Molecular Biology Reviews **70**(2): 472-509.

Avonce, N., A. Mendoza-Vargas, E. Morett and G. Iturriaga (2006). "Insights on the evolution of trehalose biosynthesis." BMC Evolutionary Biology **6**(109): 1-15.

Aydemir, H., D. Akduman, N. Piskin, F. Comert, E. Horuz, A. Terzi, F. Kokturk, T. Ornek and G. Celebi (2012). "Colistin vs. the combination of colistin and rifampicin for the treatment of carbapenem-resistant *Acinetobacter baumannii* ventilator-associated pneumonia." Epidemiology and Infection **141**(6): 1-9.

Baccigalupi, L., G. Castaldo, G. Cangiano, R. Isticato, R. Marasco, M. De Felice and E. Ricca (2004). "GerE-independent expression of cotH leads to CotC accumulation in the mother cell compartment during *Bacillus subtilis* sporulation." Microbiology **150**(10): 3441-3449.

Bakthavatchalam, Y. D., A. K. Pragasam, I. Biswas and B. Veeraraghavan (2018). "Polymyxin susceptibility testing, interpretative breakpoints and resistance mechanisms: An update." Journal of Global Antimicrobial Resistance **12**: 124-136.

Baquir, B., S. Lemaire, F. Van Bambeke, P. M. Tulkens, L. Lin and B. Spellberg (2012). "Macrophage killing of bacterial and fungal pathogens is not inhibited by intense intracellular accumulation of the lipoglycopeptide antibiotic oritavancin." Clinical Infectious Diseases **54**: 229-232.

Bartoszewicz, M., A. Rygiel, M. Krzeminski and A. Przondo-Mordarska (2007). "Penetration of a selected antibiotic and antiseptic into a biofilm formed on orthopedic steel implants." Ortopedia Traumatologia Rehabilitacja **9**(3): 310-318.

Batisson, I., M. P. Guimond, F. Girard, H. An, C. Zhu, E. Oswald, J. M. Fairbrother, M. Jacques and J. Harel (2003). "Characterization of the novel factor *paa* involved in the early steps of the adhesion mechanism of attaching and effacing *Escherichia coli*." Infection and Immunity **71**(8): 4516-4525.

Beceiro, A., E. Llobet, J. Aranda, J. A. Bengoechea, M. Doumith, M. Hornsey, H. Dhanji, H. Chart, G. Bou, D. M. Livermore and N. Woodford (2011). "Phosphoethanolamine modification of lipid A in colistin-resistant variants of *Acinetobacter baumannii* mediated by the *pmrAB* two-component regulatory system." Antimicrobial Agents and Chemotherapy **55**(7): 3370-3379.

Behlau, I. and M. S. Gilmore (2008). "Microbial biofilms in ophthalmology and infectious disease." Archives of Ophthalmology **126**(11): 1572-1581.

Bergogne-Bérézin, E. (1997). "Treatment of *Acinetobacter* infections." Expert Opinion on Investigational Drugs **6**(2): 119-127.

Bergogne-Berezin, E. and K. J. Towner (1996). "*Acinetobacter* spp. as nosocomial pathogens: microbiological, clinical, and epidemiological features." Clinical Microbiology Reviews **9**(2): 148-165.

Berlau, J., H. M. Aucken, E. Houang and T. L. Pitt (1999). "Isolation of *Acinetobacter* spp. including *A. baumannii* from vegetables: implications for hospital-acquired infections." Journal of Hospital Infection **42**(3): 201-204.

Boll, J. M., A. A. Crofts, K. Peters, V. Cattoir, W. Vollmer, B. W. Davies and M. S. Trent (2016). "A penicillin-binding protein inhibits selection of colistin-resistant, lipooligosaccharide-deficient *Acinetobacter baumannii*." Proceedings of the National Academy of Sciences of the United States of America **113**(41): 6228-6237.

Braun, V. (2003). "Iron uptake by *Escherichia coli*." Frontiers in Bioscience **8**: 1409-1421.

Brazma, A. and J. Vilo (2001). "Gene expression data analysis." Microbes and Infection **3**(10): 823-829.

Breland, E. J., A. R. Eberly and M. Hadjifrangiskou (2017). "An overview of two-component signal transduction systems implicated in extra-intestinal pathogenic *E. coli* Infections." Frontiers in Cellular and Infection Microbiology **7**: 1-14.

Breslow, J. M., J. J. Meissler, Jr., R. R. Hartzell, P. B. Spence, A. Truant, J. Gaughan and T. K. Eisenstein (2011). "Innate immune responses to systemic *Acinetobacter baumannii* infection in mice: neutrophils, but not interleukin-17, mediate host resistance." Infection and Immunity **79**(8): 3317-3327.

Brossard, K. A. and A. A. Campagnari (2012). "The *Acinetobacter baumannii* biofilm-associated protein plays a role in adherence to human epithelial cells." Infection and Immunity **80**(1): 228-233.

Bryant, R. E., K. Fox, G. Oh and V. H. Morthland (1992). "Beta-lactam enhancement of aminoglycoside activity under conditions of reduced pH and oxygen tension that may exist in infected tissues." Journal of the Infectious Diseases **165**(4): 676-682.

Buckler, D. R., G. S. Anand and A. M. Stock (2000). "Response-regulator phosphorylation and activation: a two-way street?" Trends in Microbiology **8**(4): 153-156.

Byrne-Bailey, K. G., W. H. Gaze, P. Kay, A. B. Boxall, P. M. Hawkey and E. M. Wellington (2009). "Prevalence of sulfonamide resistance genes in bacterial isolates from manured agricultural soils and pig slurry in the United Kingdom." Antimicrobial Agents and Chemotherapy **53**(2): 696-702.

Cai, S. J. and M. Inouye (2002). "EnvZ-OmpR interaction and osmoregulation in *Escherichia coli*." Journal of Biological Chemistry **277**(27): 24155-24161.

Calva, E. and R. Oropeza (2006). "Two-component signal transduction systems, environmental signals, and virulence." Microbial Ecology **51**(2): 166-176.

Cameranesi, M. M., J. Moran-Barrio, A. S. Limansky, G. D. Repizo and A. M. Viale (2018). "Site-specific recombination at XerC/D sites mediates the formation and resolution of plasmid co-integrates carrying a blaOXA-58- and TnaphA6-resistance module in *Acinetobacter baumannii*." Frontiers in Immunology **9**: 1-5.

Capra, E. J. and M. T. Laub (2012). "Evolution of two-component signal transduction systems." Annual Review of Microbiology **66**: 325-347.

Cardona, S. T., M. Choy and A. M. Hogan (2018). "Essential two-component systems regulating cell envelope functions: opportunities for novel antibiotic therapies." Journal of Membrane Biology **251**(1): 75-89.

Cardoso, K., R. F. Gandra, E. S. Wisniewski, C. A. Osaku, M. K. Kadowaki, V. Felipach-Neto, L. F. Haus and C. Simao Rde (2010). "DnaK and GroEL are induced in response to antibiotic and heat shock in *Acinetobacter baumannii*." Journal of Medical Microbiology **59**(9): 1061-1068.

Carretero-Ledesma, M., M. Garcia-Quintanilla, R. Martin-Pena, M. R. Pulido, J. Pachon and M. J. McConnell (2018). "Phenotypic changes associated with colistin resistance due to lipopolysaccharide loss in *Acinetobacter baumannii*." Virulence **9**(1): 930-942.

Carruthers, M. D., C. M. Harding, B. D. Baker, R. A. Bonomo, K. M. Hujer, P. N. Rather and R. S. Munson, Jr. (2013a). "Draft genome sequence of the clinical isolate *Acinetobacter nosocomialis* strain M2." Genome Announcements **1**(6): e00906-00913.

Carruthers, M. D., P. A. Nicholson, E. N. Tracy and R. S. Munson, Jr. (2013b). "*Acinetobacter baumannii* utilizes a type VI secretion system for bacterial competition." PLOS One **8**(3): e59388.

Casino, P., V. Rubio and A. Marina (2010). "The mechanism of signal transduction by two-component systems." Current Opinion in Structural Biology **20**(6): 763-771.

Castillo-Juarez, I., L. E. Lopez-Jacome, G. Soberon-Chavez, M. Tomas, J. Lee, P. Castaneda-Tamez, I. A. Hernandez-Barragan, M. Y. Cruz-Muniz, T. Maeda, T. K. Wood and R. Garcia-Contreras (2017). "Exploiting quorum sensing inhibition for the control of *Pseudomonas aeruginosa* and *Acinetobacter baumannii* biofilms." Current Topics in Medicinal Chemistry **17**(17): 1915-1927.

Catel-Ferreira, M., S. Marti, L. Guillon, L. Jara, G. Coadou, V. Molle, E. Bouffartigues, G. Bou, I. Shalk, T. Jouenne, X. Vila-Farres and E. De (2016). "The outer membrane porin OmpW of *Acinetobacter baumannii* is involved in iron uptake and colistin binding." FEBS Letters **590**(2): 224-231.

Celik, I. H., S. S. Oguz, G. Demirel, O. Erdeve and U. Dilmen (2012). "Outcome of ventilator-associated pneumonia due to multidrug-resistant *Acinetobacter baumannii* and *Pseudomonas aeruginosa* treated with aerosolized colistin in neonates: a retrospective chart review." European Journal of Pediatrics **171**(2): 311-316.

Cerqueira, G. M., X. Kostoulias, C. Khoo, I. Aibinu, Y. Qu, A. Traven and A. Y. Peleg (2014). "A global virulence regulator in *Acinetobacter baumannii* and its control of the phenylacetic acid catabolic pathway." Journal of the Infectious Diseases **210**(1): 46-55.

Cerqueira, G. M. and A. Y. Peleg (2011). "Insights into *Acinetobacter baumanni*i pathogenicity." IUBMB Life **63**(12): 1055-1060.

Cevahir, N., M. Demir, I. Kaleli, M. Gurbuz and S. Tikvesli (2008). "Evaluation of biofilm production, gelatinase activity, and mannose-resistant hemagglutination in *Acinetobacter baumannii* strains." Journal of Microbiology, Immunology and Infection **41**(6): 513-518.

Chalmers, S. A., S. J. Garcia, J. A. Reynolds, L. Herlitz and C. Putterman (2019). "NF-kB signaling in myeloid cells mediates the pathogenesis of immune-mediated nephritis." Journal of Autoimmunity **98**: 33-43.

Chamoun, M. N., A. Blumenthal, M. J. Sullivan, M. A. Schembri and G. C. Ulett (2018). "Bacterial pathogenesis and interleukin-17: interconnecting mechanisms of immune regulation, host genetics, and microbial virulence that influence severity of infection." Critical Reviews in Microbiology **44**(4): 465-486.

Chan, P. C., L. M. Huang, H. C. Lin, L. Y. Chang, M. L. Chen, C. Y. Lu, P. I. Lee, J. M. Chen, C. Y. Lee, H. J. Pan, J. T. Wang, S. C. Chang and Y. C. Chen (2007). "Control of an outbreak of pandrug-resistant *Acinetobacter baumannii* colonization and infection in a neonatal intensive care unit." Infection Control and Hospital Epidemiology **28**(4): 423-429.

Chanchaithong, P., N. Prapasarakul, N. Sirisopit Mehl, N. Suanpairintr, K. Teankum, A. Collaud, A. Endimiani and V. Perreten (2018). "Extensively drug-resistant community-acquired *Acinetobacter baumannii* sequence type 2 in a dog with urinary tract infection in Thailand." Journal of Global Antimicrobial Resistance **13**: 33-34.

Chen, H. D. and E. A. Groisman (2013). "The biology of the PmrA/PmrB two-component system: the major regulator of lipopolysaccharide modifications." Annual Review of Microbiology **67**: 83-112.

Chen, R., R. Lv, L. Xiao, M. Wang, Z. Du, Y. Tan, Y. Cui, Y. Yan, Y. Luo, R. Yang and Y. Song (2017). "A1S_2811, a CheA/Y-like hybrid two-component regulator from *Acinetobacter baumannii* ATCC17978, is involved in surface motility and biofilm formation in this bacterium." Microbiologyopen **6**(5): e00510.

Cheng, H. Y., Y. F. Chen and H. L. Peng (2010). "Molecular characterization of the PhoPQ-PmrD-PmrAB mediated pathway regulating polymyxin B resistance in *Klebsiella pneumoniae* CG43." Journal of Biomedical Science **17**(1): 60-76.

Chiku, K., K. Tsunemi, M. Yamamoto, M. Ohnishi-Kameyama, M. Yoshida, T. Ishii, F. Taguchi, M. Iwaki, Y. Ichinose and H. Ono (2013). "Defects in D-rhamnosyl residue biosynthetic genes affect lipopolysaccharide structure, motility, and cell-surface hydrophobicity in *Pseudomonas syringae pathovar glycinea* race 4." Bioscience, biotechnology, and biochemistry **77**(3): 505-510.

Chin, C. Y., K. A. Gregg, B. A. Napier, R. K. Ernst and D. S. Weiss (2015). "A PmrB-regulated deacetylase required for lipid A modification and polymyxin resistance in *Acinetobacter baumannii*." Antimicrobiol Agents and Chemotherapy **59**(12): 7911-7914.

Choi, A. H., L. Slamti, F. Y. Avci, G. B. Pier and T. Maira-Litrán (2009). "The *pgaABCD* locus of *Acinetobacter baumannii* encodes the production of poly-β-1-6-N-acetylglucosamine, which is critical for biofilm formation." Journal of Bacteriology **191**(19): 5953-5963.

Choi, C. H., J. S. Lee, Y. C. Lee, T. I. Park and J. C. Lee (2008). "*Acinetobacter baumannii* invades epithelial cells and outer membrane protein A mediates interactions with epithelial cells." BMC Microbiology **8**: 216-227.

Choi, J. Y., Y. Kim, E. A. Ko, Y. K. Park, W. H. Jheong, G. Ko and K. S. Ko (2012). "*Acinetobacter* species isolates from a range of environments: species survey and observations of antimicrobial resistance." Diagnostic Microbiology and Infectious Disease **74**(2): 177-180.

Chuang, Y. Y., Y. C. Huang, C. H. Lin, L. H. Su and C. T. Wu (2009). "Epidemiological investigation after hospitalising a case with pandrug-resistant *Acinetobacter baumannii* infection." Journal of Hospital Infection **72**(1): 30-35.

Chusri, S., K. Silpapojakul, E. McNeil, K. Singkhamanan and V. Chongsuvivatwong (2015). "Impact of antibiotic exposure on occurrence of nosocomial carbapenem-resistant *Acinetobacter baumannii* infection: a case control study." Journal of Infection and Chemotherapy **21**(2): 90-95.

Cirl, C., A. Wieser, M. Yadav, S. Duerr, S. Schubert, H. Fischer, D. Stappert, N. Wantia, N. Rodriguez, H. Wagner, C. Svanborg and T. Miethke (2008). "Subversion of Toll-like receptor signaling by a unique family of bacterial Toll/interleukin-1 receptor domain-containing proteins." Nature Medicine **14**(4): 399-406.

Clemmer, K. M., R. A. Bonomo and P. N. Rather (2011). "Genetic analysis of surface motility in *Acinetobacter baumannii*." Microbiology **157**(9): 2534-2544.

CLSI (2006). "Clinical Laboratory Standards Institute evaluation protocols." MLO-Medical Laboratory Observer **38**(8): 38, 40-41.

CLSI (2007). Performance standards for antimicrobial disk susceptibility testing; seventeenth information supplement, Wayne, PA.

Comeau, D. E., K. Ikenaka, K. L. Tsung and M. Inouye (1985). "Primary characterization of the protein products of the *Escherichia coli* ompB locus: structure and regulation of synthesis of the OmpR and EnvZ proteins." Journal of Bacteriology **164**(2): 578-584.

Costa, G. F., M. C. Tognim, C. L. Cardoso, F. E. Carrara-Marrone and L. B. Garcia (2006). "Preliminary evaluation of adherence on abiotic and cellular surfaces of *Acinetobacter baumannii* strains isolated from catheter tips." Brazilian Journal of Infectious Diseases **10**(5): 346-351.

Da Silva, G. J. and S. Domingues (2017). "Interplay between colistin resistance, virulence and fitness in *Acinetobacter baumannii*." Antibiotics (Basel) **6**(4): 1-11.

Darouiche, R. O. (2004). "Treatment of infections associated with surgical implants." New England Journal of Medicine **350**(14): 1422-1429.

Davis, K. A., K. A. Moran, C. K. McAllister and P. J. Gray (2005). "Multidrug-resistant *Acinetobacter* extremity infections in soldiers." Emerging Infectious Diseases **11**(8): 1218-1224.

de Breij, A., L. Dijkshoorn, E. Lagendijk, J. van der Meer, A. Koster, G. Bloemberg, R. Wolterbeek, P. van den Broek and P. Nibbering (2010). "Do biofilm formation and interactions with human cells explain the clinical success of *Acinetobacter baumannii*?" PLOS One **5**(5): e10732.

de Breij, A., M. Eveillard, L. Dijkshoorn, P. J. van den Broek, P. H. Nibbering and M. L. Joly-Guillou (2012). "Differences in *Acinetobacter baumannii* strains and host innate immune response determine morbidity and mortality in experimental pneumonia." PLOS One **7**(2): e30673.

de Kievit, T. R. (2009). "Quorum sensing in *Pseudomonas aeruginosa* biofilms." Environmental Microbiology **11**(2): 279-288.

De Silva, P. M. and A. Kumar (2018). "Effect of sodium chloride on surface-associated motility of *Acinetobacter baumannii* and the role of AdeRS two-component system." Journal of Membrane Biology **251**(1): 5-13.

Delcour, A. H. (2009). "Outer membrane permeability and antibiotic resistance." Biochimica et Biophysica Acta **1794**(5): 808-816.

Denys, G. A., J. C. Davis, P. D. O'Hanley and J. T. Stephens, Jr. (2011). "*In vitro* and *in vivo* activity of E-101 solution against *Acinetobacter baumannii* strains isolated from U.S. military personnel." Antimicrobial Agents and Chemotherapy **55**(7): 3603-3608.

Desai, M., T. Buhler, P. H. Weller and M. R. Brown (1998). "Increasing resistance of planktonic and biofilm cultures of *Burkholderia cepacia* to ciprofloxacin and ceftazidime during exponential growth." Journal of Antimicrobial Chemotherapy **42**(2): 153-160.

Deveson Lucas, D., B. Crane, A. Wright, M. L. Han, J. Moffatt, D. Bulach, S. L. Gladman, D. Powell, J. Aranda, T. Seemann, D. Machado, T. Pacheco, T. Marques, M. Viveiros, R. Nation, J. Li, M. Harper and J. D. Boyce (2018). "Emergence of high-level colistin resistance in an *Acinetobacter baumannii* clinical isolate mediated by inactivation of the global regulator H-NS." Antimicrobial Agents and Chemotherapy **62**: e02442-02416.

Dijkshoorn, L., A. Nemec and H. Seifert (2007). "An increasing threat in hospitals: multidrug-resistant *Acinetobacter baumannii*." Nature Reviews Microbiology **5**(12): 939-951.

Dikshit, N., S. D. Kale, H. J. Khameneh, V. Balamuralidhar, C. Y. Tang, P. Kumar, T. P. Lim, T. T. Tan, A. L. Kwa, A. Mortellaro and B. Sukumaran (2018). "NLRP3 inflammasome pathway has a critical role in the host immunity against clinically relevant *Acinetobacter baumannii* pulmonary infection." Mucosal Immunology **11**(1): 257-272.

Donlan, R. M. and J. W. Costerton (2002). "Biofilms: survival mechanisms of clinically relevant microorganisms." Clinical Microbiology Reviews **15**(2): 167-193.

Dorr, T., L. Alvarez, F. Delgado, B. M. Davis, F. Cava and M. K. Waldor (2016). "A cell wall damage response mediated by a sensor kinase/response regulator pair enables beta-lactam tolerance." Proceedings of the National Academy of Sciences of the United States of America **113**(2): 404-409.

Dorsey, C. W., M. S. Beglin and L. A. Actis (2003a). "Detection and analysis of iron uptake components expressed by *Acinetobacter baumannii* clinical isolates." Journal of Clinical Microbiology **41**(9): 4188-4193.

Dorsey, C. W., M. E. Tolmasky, J. H. Crosa and L. A. Actis (2003b). "Genetic organization of an *Acinetobacter baumannii* chromosomal region harbouring genes related to siderophore biosynthesis and transport." Microbiology **149**(5): 1227-1238.

Draughn, G. L., M. E. Milton, E. A. Feldmann, B. G. Bobay, B. M. Roth, A. L. Olson, R. J. Thompson, L. A. Actis, C. Davies and J. Cavanagh (2018). "The structure of the biofilm-controlling response regulator BfmR from *Acinetobacter baumannii* reveals details of its DNA-binding mechanism." Journal of Molecular Biology **430**(6): 806-821.

Eijkelkamp, B. A., K. A. Hassan, I. T. Paulsen and M. H. Brown (2011a). "Investigation of the human pathogen *Acinetobacter baumannii* under iron limiting conditions." BMC Genomics **12**(1): 126-140.

Eijkelkamp, B. A., U. H. Stroeher, K. A. Hassan, L. D. Elbourne, I. T. Paulsen and M. H. Brown (2013). "H-NS plays a role in expression of *Acinetobacter baumannii* virulence features." Infection and Immunity **81**(7): 2574-2583.

Eijkelkamp, B. A., U. H. Stroeher, K. A. Hassan, M. S. Papadimitrious, I. T. Paulsen and M. H. Brown (2011b). "Adherence and motility characteristics of clinical *Acinetobacter baumannii* isolates." FEMS Microbiology Letters **323**(1): 44-51.

Eijkelkamp, B. A., U. H. Stroeher, K. A. Hassan, I. T. Paulsen and M. H. Brown (2014). "Comparative analysis of surface-exposed virulence factors of *Acinetobacter baumannii*." BMC Genomics **15**: 1020-1032.

Elhosseiny, N. M. and A. S. Attia (2018). "*Acinetobacter*: an emerging pathogen with a versatile secretome." Emerging Microbes and Infections **7**(1): 33-34.

Espinal, P., S. Martí and J. Vila (2012). "Effect of biofilm formation on the survival of *Acinetobacter baumannii* on dry surfaces." Journal of Hospital Infection **80**(1): 56-60.

Evans, M. E., D. J. Feola and R. P. Rapp (1999). "Polymyxin B sulfate and colistin: old antibiotics for emerging multiresistant gram-negative bacteria." Annals of Pharmacotherapy **33**(9): 960-967.

Eveillard, M., M. Kempf, O. Belmonte, H. Pailhories and M. L. Joly-Guillou (2013). "Reservoirs of *Acinetobacter baumannii* outside the hospital and potential involvement in emerging human community-acquired infections." International Journal of Infectious Diseases **17**(10): e802-805.

Ewann, F., M. Jackson, K. Pethe, A. Cooper, N. Mielcarek, D. Ensergueix, B. Gicquel, C. Locht and P. Supply (2002). "Transient requirement of the PrrA-PrrB two-component system for early intracellular multiplication of *Mycobacterium tuberculosis*." Infection and Immunity **70**(5): 2256-2263.

Fagon, J. Y., J. Chastre, Y. Domart, J. L. Trouillet and C. Gibert (1996). "Mortality due to ventilator-associated pneumonia or colonization with *Pseudomonas* or *Acinetobacter* species: assessment by quantitative culture of samples obtained by a protected specimen brush." Clinical Infectious Diseases **23**(3): 538-542.

Falagas, M. E., E. A. Karveli, I. Kelesidis and T. Kelesidis (2007). "Community-acquired *Acinetobacter* infections." European Journal of Clinical Microbiology and Infectious Diseases **26**(12): 857-868.

Falagas, M. E., P. I. Rafailidis, E. Ioannidou, V. G. Alexiou, D. K. Matthaiou, D. E. Karageorgopoulos, A. Kapaskelis, D. Nikita and A. Michalopoulos (2010). "Colistin therapy for microbiologically documented multidrug-resistant Gram-negative bacterial infections: a retrospective cohort study of 258 patients." International Journal of Antimicrobial Agents **35**(2): 194-199.

Falghoush, A., H. Beyenal, T. E. Besser, A. Omsland and D. R. Call (2017). "Osmotic compounds enhance antibiotic efficacy against *Acinetobacter baumannii* biofilm communities." Applied and Environmental Microbiology **83**(19): e01297-01217.

Fang, C., X. Chen and M. Zhou (2016). "Epidemiology and cytokine levels among children with nosocomial multidrug-resistant *Acinetobacter baumannii* complex in a tertiary hospital of Eastern China." PLOS One **11**(8): e0161690.

Feng, J., M. R. Atkinson, W. McCleary, J. B. Stock, B. L. Wanner and A. J. Ninfa (1992). "Role of phosphorylated metabolic intermediates in the regulation of glutamine synthetase synthesis in *Escherichia coli*." Journal of Bacteriology **174**(19): 6061-6070.

Fernandez-Cuenca, F., Y. Smani, M. C. Gomez-Sanchez, F. Docobo-Perez, F. J. Caballero-Moyano, J. Dominguez-Herrera, A. Pascual and J. Pachon (2011). "Attenuated virulence of a slow-growing pandrug-resistant *Acinetobacter baumannii* is associated with decreased expression of genes encoding the porins CarO and OprD-like." International Journal of Antimicrobial Agents **38**(6): 548-549.

Fiester, S. E., C. C. Nwugo, W. F. Penwell, J. M. Neary, A. C. Beckett, B. A. Arivett, R. E. Schmidt, S. C. Geiger, P. L. Connerly, S. M. Menke, A. P. Tomaras and L. A. Actis (2015). "Role of the carboxy terminus of *secA* in iron acquisition, protein translocation, and virulence of the bacterial pathogen *Acinetobacter baumannii*." Infection and Immunity **83**(4): 1354-1365.

Fitzsimons, T. C., J. M. Lewis, A. Wright, O. Kleifeld, R. B. Schittenhelm, D. Powell, M. Harper and J. D. Boyce (2018). "Identification of novel *Acinetobacter baumannii* type VI secretion system anti-bacterial effector and immunity pairs." Infection and Immunity **86**(8): e00297.

Fomsgaard, A., M. A. Freudenberg and C. Galanos (1990). "Modification of the silver staining technique to detect lipopolysaccharide in polyacrylamide gels." Journal of Clinical Microbiology **28**(12): 2627-2631.

Forst, S., D. Comeau, S. Norioka and M. Inouye (1987). "Localization and membrane topology of EnvZ, a protein involved in osmoregulation of OmpF and OmpC in *Escherichia coli*." Journal of Biological Chemistry **262**(34): 16433-16438.

Fournier, P. E., D. Vallenet, V. Barbe, S. Audic, H. Ogata, L. Poirel, H. Richet, C. Robert, S. Mangenot, C. Abergel, P. Nordmann, J. Weissenbach, D. Raoult and J. M. Claverie (2006). "Comparative genomics of multidrug resistance in *Acinetobacter baumannii*." PLOS Genetics **2**(1): 62-72.

Fuchs, E. L., E. D. Brutinel, A. K. Jones, N. B. Fulcher, M. L. Urbanowski, T. L. Yahr and M. C. Wolfgang (2010a). "The *Pseudomonas aeruginosa* Vfr regulator controls global virulence factor expression through cyclic AMP-dependent and -independent mechanisms." Journal of Bacteriology **192**(14): 3553-3564.

Fuchs, E. L., E. D. Brutinel, E. R. Klem, A. R. Fehr, T. L. Yahr and M. C. Wolfgang (2010b). "In vitro and in vivo characterization of the *Pseudomonas aeruginosa* cyclic AMP (cAMP) phosphodiesterase CpdA, required for cAMP homeostasis and virulence factor regulation." Journal of Bacteriology **192**(11): 2779-2790.

Furuhata, K., Y. Kato, K. Goto, M. Hara and M. Fukuyama (2009). "Diversity of heterotrophic bacteria isolated from biofilm samples and cell surface hydrophobicity." Journal of General and Applied Microbiology **55**(1): 69-74.

Gaddy, J. A. and L. A. Actis (2009a). "Regulation of *Acinetobacter baumannii* biofilm formation." Future Microbiology **4**(3): 273-278.

Gaddy, J. A., B. A. Arivett, M. J. McConnell, R. Lopez-Rojas, J. Pachon and L. A. Actis (2012). "Role of acinetobactin-mediated iron acquisition functions in the interaction of *Acinetobacter baumannii* strain ATCC 19606T with human lung epithelial cells, *Galleria mellonella* caterpillars, and mice." Infection and Immunity **80**(3): 1015-1024.

Gaddy, J. A., A. P. Tomaras and L. A. Actis (2009b). "The *Acinetobacter baumannii* 19606 OmpA protein plays a role in biofilm formation on abiotic surfaces and in the interaction of this pathogen with eukaryotic cells." Infection and Immunity **77**(8): 3150-3160.

Galperin, M. Y. (2006). "Structural classification of bacterial response regulators: diversity of output domains and domain combinations." Journal of Bacteriology **188**(12): 4169-4182.

Garcia-Patino, M. G., R. Garcia-Contreras and P. Licona-Limon (2017). "The immune response against *Acinetobacter baumannii*, an emerging pathogen in nosocomial infections." Frontiers in Immunology **8**: 1-6.

Garlantezec, R., C. Bourigault, J. M. Boles, G. Prat, R. Baron, J. M. Tonnelier, M. Cosse, M. Lefevre, S. Jourdain, G. Lelay, L. Daniel, M. Virmaux, I. Le Du, D. Tande, A. Renault and B. Lejeune (2011). "Cost-analysis of an intensive care unit closure due to an imipenem-resistant oxa-23 *Acinetobacter baumannii* outbreak." Journal of Hospital Infection **77**(2): 174-175.

Garnacho-Montero, J. and R. Amaya-Villar (2010). "Multiresistant *Acinetobacter baumannii* infections: epidemiology and management." Current Opinion in Infectious Diseases **23**(4): 332-339.

Gauthier, J. D., M. K. Jones, P. Thiaville, J. L. Joseph, R. A. Swain, C. J. Krediet, P. A. Gulig, M. Teplitski and A. C. Wright (2010). "Role of GacA in virulence of *Vibrio vulnificus*." Microbiology **156**(12): 3722-3733.

Gebhardt, M. J. and H. A. Shuman (2017). "GigA and GigB are master regulators of antibiotic resistance, stress responses, and virulence in *Acinetobacter baumannii*." Journal of Bacteriology **199**(10): 1-17.

Geisinger, E. and R. R. Isberg (2015). "Antibiotic modulation of capsular exopolysaccharide and virulence in *Acinetobacter baumannii*." PLOS Pathogens **11**(2): e1004691.

Gholamalipour, Y., A. Karunanayake Mudiyanselage and C. T. Martin (2018). "3' end additions by T7 RNA polymerase are RNA self-templated, distributive and diverse in character-RNA-Seq analyses." Nucleic Acids Research **46**(18): 9253-9263.

Giles, S. K., U. H. Stroeher, B. A. Eijkelkamp and M. H. Brown (2015). "Identification of genes essential for pellicle formation in *Acinetobacter baumannii*." BMC Microbiology **15**: 116-129.

Girardello, R., M. Visconde, R. Cayo, R. C. Figueiredo, M. A. Mori, N. Lincopan and A. C. Gales (2017). "Diversity of polymyxin resistance mechanisms among *Acinetobacter baumannii* clinical isolates." Diagnostic Microbiology and Infectious Disease **87**(1): 37-44.

Gohl, O., A. Friedrich, M. Hoppert and B. Averhoff (2006). "The thin pili of *Acinetobacter* sp. strain BD413 mediate adhesion to biotic and abiotic surfaces." Applied and Environmental Microbiology **72**(2): 1394-1401.

Gold, B., G. M. Rodriguez, S. A. Marras, M. Pentecost and I. Smith (2001). "The *Mycobacterium tuberculosis* IdeR is a dual functional regulator that controls transcription of genes involved in iron acquisition, iron storage and survival in macrophages." Molecular Microbiology **42**(3): 851-865.

Golic, A., M. Vaneechoutte, A. Nemec, A. M. Viale, L. A. Actis and M. A. Mussi (2013). "Staring at the cold sun: blue light regulation is distributed within the genus *Acinetobacter*." PLOS One **8**(1): e55059.

Gordon, N. C. and D. W. Wareham (2010). "Multidrug-resistant *Acinetobacter baumannii*: mechanisms of virulence and resistance." International Journal of Antimicrobial Agents **35**(3): 219-226.

Gotoh, Y., Y. Eguchi, T. Watanabe, S. Okamoto, A. Doi and R. Utsumi (2010). "Two-component signal transduction as potential drug targets in pathogenic bacteria." Current Opinion in Microbiology **13**(2): 232-239.

Griffith, M. E., D. R. Lazarus, P. B. Mann, J. A. Boger, D. R. Hospenthal and C. K. Murray (2007). "*Acinetobacter* skin carriage among US army soldiers deployed in Iraq." Infection Control and Hospital Epidemiology **28**(6): 720-722.

Gross, R. and D. Beier (2012). Two-component Systems in Bacteria. Great Britian, Caister Academic Press.

Gui, S., R. Li, Y. Feng and S. Wang (2014). "Transmission electron microscopic morphological study and flow cytometric viability assessment of *Acinetobacter baumannii* susceptible to Musca domestica cecropin." ScientificWorldJournal **2014**: 1-6.

Gunn, J. S. (2008). "The *Salmonella* PmrAB regulon: lipopolysaccharide modifications, antimicrobial peptide resistance and more." Trends in Microbiology **16**(6): 284-290.

Guo, N., W. Xue, D. Tang, J. Ding and B. Zhao (2016). "Risk factors and outcomes of hospitalized patients with blood infections caused by multidrug-resistant *Acinetobacter baumannii* complex in a hospital of Northern China." American Journal of Infection Control **44**(4): 37-39.

Haag, A. F. and F. Bagnoli (2016). The role of two-component signal transduction systems in *Staphylococcus aureus* virulence regulation. Current Topics in Microbiology and Immunology, Springer Berlin Heidelberg. **1:** 1-54.

Hammond, A. A., K. G. Miller, C. J. Kruczek, J. Dertien, J. A. Colmer-Hamood, J. A. Griswold, A. R. Horswill and A. N. Hamood (2011). "An *in vitro* biofilm model to examine the effect of antibiotic ointments on biofilms produced by burn wound bacterial isolates." Burns **37**(2): 312-321.

Hanahan, D. (1983). "Studies on transformation of *Escherichia coli* with plasmids." Journal of Molecular Biology **166**(4): 557-580.

Hancock, R. E. (1997). "Peptide antibiotics." The Lancet **349**(9049): 418-422.

Hantke, K. (2001). "Bacterial zinc transporters and regulators." Biometals **14**(3-4): 239-249.

Harding, C. M., S. W. Hennon and M. F. Feldman (2018). "Uncovering the mechanisms of *Acinetobacter baumannii* virulence." Nature Reviews Microbiology **16**(2): 91-102.

Harding, C. M., E. N. Tracy, M. D. Carruthers, P. N. Rather, L. A. Actis and R. S. Munson, Jr. (2013). "*Acinetobacter baumannii* strain M2 produces type IV pili which play a role in natural transformation and twitching motility but not surface-associated motility." MBio **4**(4): e00360-00313.

Hazan, R., J. He, G. Xiao, V. Dekimpe, Y. Apidianakis, B. Lesic, C. Astrakas, E. Deziel, F. Lepine and L. G. Rahme (2010). "Homeostatic interplay between bacterial cell-cell signaling and iron in virulence." PLOS Pathogens **6**(3): e1000810.

Henrichsen, J. (1975). "The influence of changes in the environment on twitching motility." Acta Pathologica et Microbiologica Scandinavica. Section B, Microbiology **83**(3): 179-186.

Henry, R., N. Vithanage, P. Harrison, T. Seemann, S. Coutts, J. H. Moffatt, R. L. Nation, J. Li, M. Harper, B. Adler and J. D. Boyce (2012). "Colistin-resistant, lipopolysaccharide-deficient *Acinetobacter baumannii* responds to lipopolysaccharide loss through increased expression of genes involved in the synthesis and transport of lipoproteins, phospholipids, and poly-beta-1,6-N-acetylglucosamine." Antimicrobial Agents and Chemotherapy **56**(1): 59-69.

Higgins, P. G., C. Dammhayn, M. Hackel and H. Seifert (2010). "Global spread of carbapenem-resistant *Acinetobacter baumannii*." Journal of Antimicrobial Chemotherapy **65**(2): 233-238.

Hoch, J. A. (2000). "Two-component and phosphorelay signal transduction." Current Opinion in Microbiology **3**(2): 165-170.

Hoiby, N., T. Bjarnsholt, M. Givskov, S. Molin and O. Ciofu (2010). "Antibiotic resistance of bacterial biofilms." International Journal of Antimicrobial Agents **35**(4): 322-332.

Hoiby, N., O. Ciofu, H. K. Johansen, Z. J. Song, C. Moser, P. O. Jensen, S. Molin, M. Givskov, T. Tolker-Nielsen and T. Bjarnsholt (2011). "The clinical impact of bacterial biofilms." International Journal of Oral Science **3**(2): 55-65.

Houang, E. T., Y. W. Chu, C. M. Leung, K. Y. Chu, J. Berlau, K. C. Ng and A. F. Cheng (2001). "Epidemiology and infection control implications of *Acinetobacter* spp. in Hong Kong." Journal of Clinical Microbiology **39**(1): 228-234.

Howell, A., S. Dubrac, D. Noone, K. I. Varughese and K. Devine (2006). "Interactions between the YycFG and PhoPR two-component systems in *Bacillus subtilis*: the PhoR kinase phosphorylates the non-cognate YycF response regulator upon phosphate limitation." Molecular Microbiology **59**(4): 1199-1215.

Hsueh, P. R., L. J. Teng, C. Y. Chen, W. H. Chen, C. J. Yu, S. W. Ho and K. T. Luh (2002). "Pandrug-resistant *Acinetobacter baumannii* causing nosocomial infections in a university hospital, Taiwan." Emerging Infectious Diseases **8**(8): 827-832.

Hu, C., Y. Li, Z. Zhao, S. Wei, Z. Zhao, H. Chen and P. Wu (2018). "*In vitro* synergistic effect of amlodipine and imipenem on the expression of the AdeABC efflux pump in multidrug-resistant *Acinetobacter baumannii*." PLOS One **13**(6): e0198061.

Huang, B., M. Eberstadt, E. T. Olejniczak, R. P. Meadows and S. W. Fesik (1996). "NMR structure and mutagenesis of the Fas (APO-1/CD95) death domain." Nature **384**(6610): 638-641.

Huang, H. H., W. C. Chen, C. W. Lin, Y. T. Lin, H. C. Ning, Y. C. Chang and T. C. Yang (2017). "Relationship of the CreBC two-component regulatory system and inner membrane protein CreD with swimming motility in *Stenotrophomonas maltophilia*." PLOS One **12**(4): e0174704.

Hujer, K. M., A. M. Hujer, E. A. Hulten, S. Bajaksouzian, J. M. Adams, C. J. Donskey, D. J. Ecker, C. Massire, M. W. Eshoo, R. Sampath, J. M. Thomson, P. N. Rather, D. W. Craft, J. T. Fishbain, A. J. Ewell, M. R. Jacobs, D. L. Paterson and R. A. Bonomo (2006). "Analysis of antibiotic resistance genes in multidrug-resistant *Acinetobacter* sp. isolates from military and civilian patients treated at the Walter Reed Army Medical Center." Antimicrobial Agents and Chemotherapy **50**(12): 4114-4123.

Hunger, M., R. Schmucker, V. Kishan and W. Hillen (1990). "Analysis and nucleotide sequence of an origin of DNA replication in *Acinetobacter calcoaceticus* and its use for *Escherichia coli* shuttle plasmids." Gene **87**(1): 45-51.

Hurley, J. C. (2018). "Paradoxical *Acinetobacter* associated ventilator associated pneumonia incidences within prevention studies using respiratory tract applications of topical polymyxin: benchmarking the evidence base." Journal of Hospital Infection **100**(1): 105-113.

Huys, G., K. Bartie, M. Cnockaert, D. T. Hoang Oanh, N. T. Phuong, T. Somsiri, S. Chinabut, F. M. Yusoff, M. Shariff, M. Giacomini, A. Teale and J. Swings (2007). "Biodiversity of chloramphenicol-resistant mesophilic heterotrophs from Southeast Asian aquaculture environments." Research in Microbiology **158**(3): 228-235.

Island, M. D. and R. J. Kadner (1993). "Interplay between the membrane-associated UhpB and UhpC regulatory proteins." Journal of Bacteriology **175**(16): 5028-5034.

Jaidane, N., T. Naas, W. Mansour, B. B. Radhia, S. Jerbi, N. Boujaafar, O. Bouallegue and R. A. Bonnin (2018). "Genomic analysis of *in vivo* acquired resistance to colistin and rifampicin in *Acinetobacter baumannii*." International Journal of Antimicrobial Agents **51**(2): 266-269.

Jang, T. N., S. H. Lee, C. H. Huang, C. L. Lee and W. Y. Chen (2009). "Risk factors and impact of nosocomial *Acinetobacter baumannii* bloodstream infections in the adult intensive care unit: a case-control study." Journal of Hospital Infection **73**(2): 143-150.

Jimenez, P. N., G. Koch, J. A. Thompson, K. B. Xavier, R. H. Cool and W. J. Quax (2012). "The multiple signaling systems regulating virulence in *Pseudomonas aeruginosa*." Microbiology and Molecular Biology Reviews **76**(1): 46-65.

John, T. M., C. N. Jacob, C. C. Ittycheria, A. M. George, A. G. Jacob, S. Subramaniyam, J. Puthiyaveettil and R. Jayaprakash (2012). "Macrophage activation syndrome following *Acinetobacter baumannii* sepsis." International Journal of Infectious Diseases **16**(3): e223-224.

Jones, C. L., S. S. Singh, Y. Alamneh, L. G. Casella, R. K. Ernst, E. P. Lesho, P. E. Waterman and D. V. Zurawski (2017). "*In vivo* fitness adaptations of colistin-resistant *Acinetobacter baumannii* isolates to oxidative stress." Antimicrobial Agents and Chemotherapy **61**(3): e00598-00516.

Jos, D. d. and O. E. Conatantin (2009). "Bacterial biofilms formation at air liquid interfaces." Innovative Romanian Food Biotechnology **5**(12): 18-22.

Ju, M. H., Y. L. Yao, C. L. Du, S. Chen and Y. L. Song (2018). "Subsequent multidrug-resistant bacteremia is a risk factor for short-term mortality of patients with ventilator-associated pneumonia caused by *Acinetobacter baumannii* in intensive care unit: a multicenter experience." Chinese Medical Journal **131**(3): 361-363.

Jun, S. H., J. H. Lee, B. R. Kim, S. I. Kim, T. I. Park, J. C. Lee and Y. C. Lee (2013). "*Acinetobacter baumannii* outer membrane vesicles elicit a potent innate immune response via membrane proteins." PLOS One **8**(8): e71751.

Jyot, J., J. K. Gautam, M. Raje and A. Ghosh (1999). "Localization of DnaK and GroEL in *Vibrio cholerae*." FEMS Microbiology Letters **172**(2): 165-171.

Kalivoda, E. J., K. M. Brothers, N. A. Stella, M. J. Schmitt and R. M. Shanks (2013). "Bacterial cyclic AMP-phosphodiesterase activity coordinates biofilm formation." PLOS One **8**(7): e71267.

Kamoshida, G., T. Kikuchi-Ueda, S. Nishida, S. Tansho-Nagakawa, T. Ubagai and Y. Ono (2018). "Pathogenic bacterium *Acinetobacter baumannii* inhibits the formation of neutrophil extracellular traps by suppressing neutrophil adhesion." Frontiers in Immunology **9**: 1-8.

Kanchanarach, W., G. Theeragool, T. Inoue, T. Yakushi, O. Adachi and K. Matsushita (2010). "Acetic acid fermentation of *Acetobacter pasteurianus*: relationship between acetic acid resistance and pellicle polysaccharide formation." Journal of Bioscience and Bioengineering **74**(8): 1591-1597.

Karageorgopoulos, D. E. and M. E. Falagas (2008). "Current control and treatment of multidrug-resistant *Acinetobacter baumannii* infections." The Lancet Infectious Diseases **8**(12): 751-762.

Karaiskos, I., L. Galani, F. Baziaka and H. Giamarellou (2013). "Intraventricular and intrathecal colistin as the last therapeutic resort for the treatment of multidrug-resistant and extensively drug-resistant *Acinetobacter baumannii* ventriculitis and meningitis: a literature review." International Journal of Antimicrobial Agents **41**(6): 499-508.

Kentache, T., A. Ben Abdelkrim, T. Jouenne, E. De and J. Hardouin (2017). "Global dynamic proteome study of a pellicle-forming *Acinetobacter baumannii* strain." Mol Cell Proteomics **16**(1): 100-112.

Kim, S., D. S. Patel, S. Park, J. Slusky, J. B. Klauda, G. Widmalm and W. Im (2016). "Bilayer properties of lipid A from various Gram-negative bacteria." Biophysical Journal **111**(8): 1750-1760.

Kim, S. W., C. H. Choi, D. C. Moon, J. S. Jin, J. H. Lee, J. H. Shin, J. M. Kim, Y. C. Lee, S. Y. Seol, D. T. Cho and J. C. Lee (2009). "Serum resistance of *Acinetobacter baumannii* through the binding of factor H to outer membrane proteins." FEMS Microbiology Letters **301**(2): 224-231.

Kim, Y. A., J. J. Kim, D. J. Won and K. Lee (2018). "Seasonal and temperature-associated increase in community-onset *Acinetobacter baumannii* complex colonization or infection." Annals of Laboratory Medicine **38**(3): 266-270.

King, L. B., E. Swiatlo, A. Swiatlo and L. S. McDaniel (2009). "Serum resistance and biofilm formation in clinical isolates of *Acinetobacter baumannii*." FEMS Immunology and Medical Microbiology **55**(3): 414-421.

Knapp, S., C. W. Wieland, S. Florquin, R. Pantophlet, L. Dijkshoorn, N. Tshimbalanga, S. Akira and T. van der Poll (2006). "Differential roles of CD14 and toll-like receptors 4 and 2 in murine *Acinetobacter pneumonia*." American Journal of Respiratory and Critical Care Medicine **173**(1): 122-129.

Kobayashi, K. (2007). "*Bacillus subtilis* pellicle formation proceeds through genetically defined morphological changes." Journal of Bacteriology **189**(13): 4920-4931.

Koenigs, A., J. Stahl, B. Averhoff, S. Gottig, T. A. Wichelhaus, R. Wallich, P. F. Zipfel and P. Kraiczy (2016). "CipA of *Acinetobacter baumannii* is a novel plasminogen binding and complement inhibitory protein." Journal of the Infectious Diseases **213**(9): 1388-1399.

Kouidhi, B., T. Zmantar, H. Hentati and A. Bakhrouf (2010). "Cell surface hydrophobicity, biofilm formation, adhesives properties and molecular detection of adhesins genes in *Staphylococcus aureus* associated to dental caries." Microbial Pathogenesis **49**(1): 14-22.

Kroger, C., S. C. Kary, K. Schauer and A. D. Cameron (2016). "Genetic regulation of virulence and antibiotic resistance in *Acinetobacter baumannii*." Genes (Basel) **8**(1): 1-12.

Krueger, B., T. Friedrich, F. Forster, J. Bernhardt, R. Gross and T. Dandekar (2012). "Different evolutionary modifications as a guide to rewire two-component systems." Bioinformatics and Biology Insights **6**: 97-128.

Kuhn, M. L., K. A. Majorek, W. Minor and W. F. Anderson (2013). "Broad-substrate screen as a tool to identify substrates for bacterial Gcn5-related N-acetyltransferases with unknown substrate specificity." Protein Science **22**(2): 222-230.

Laub, M. T. and M. Goulian (2007). "Specificity in two-component signal transduction pathways." Annual Review of Genetics **41**: 121-145.

Lawrence, T. (2009). "The nuclear factor NF-kappaB pathway in inflammation." Cold Spring Harbor Perspectives in Biology **1**(6): a001651.

Lazar Adler, N. R., E. M. Allwood, D. Deveson Lucas, P. Harrison, S. Watts, A. Dimitropoulos, P. Treerat, P. Alwis, R. J. Devenish, M. Prescott, B. Govan, B. Adler, M. Harper and J. D. Boyce (2016). "Perturbation of the two-component signal transduction system, BprRS, results in attenuated virulence and motility defects in *Burkholderia pseudomallei*." BMC Genomics **17**(1): 331-342.

Lazar, V. (2011). "Quorum sensing in biofilms - How to destroy the bacterial citadels or their cohesion/power?" Anaerobe **17**(6): 280-285.

Lee, B. Y., S. M. McGlone, Y. Doi, R. R. Bailey and L. H. Harrison (2010). "Economic impact of *Acinetobacter baumannii* infection in the intensive care unit." Infection Control and Hospital Epidemiology **31**(10): 1087-1089.

Lee, C. R., J. H. Lee, M. Park, K. S. Park, I. K. Bae, Y. B. Kim, C. J. Cha, B. C. Jeong and S. H. Lee (2017). "Biology of *Acinetobacter baumannii*: pathogenesis, antibiotic

resistance mechanisms, and prospective treatment options." Frontiers in Cellular and Infection Microbiology **7**: 55-62.

Lee, H. W., Y. M. Koh, J. Kim, J. C. Lee, Y. C. Lee, S. Y. Seol and D. T. Cho (2008). "Capacity of multidrug-resistant clinical isolates of *Acinetobacter baumannii* to form biofilm and adhere to epithelial cell surfaces." Clinical Microbiology and Infection **14**(1): 49-54.

Lees-Miller, R. G., J. A. Iwashkiw, N. E. Scott, A. Seper, E. Vinogradov, S. Schild and M. F. Feldman (2013). "A common pathway for O-linked protein-glycosylation and synthesis of capsule in *Acinetobacter baumannii*." Molecular Microbiology **89**(5): 816-830.

Lemos, J. A., Y. Luzardo and R. A. Burne (2007). "Physiologic effects of forced down-regulation of *dnaK* and *groEL* expression in *Streptococcus* mutans." Journal of Bacteriology **189**(5): 1582-1588.

Leslie, S. B., E. Israeli, B. Lighthart, J. H. Crowe and L. M. Crowe (1995). "Trehalose and sucrose protect both membranes and proteins in intact bacteria during drying." Applied and Environmental Microbiology **61**(10): 3592-3597.

Lewis, L. A., B. Choudhury, J. T. Balthazar, L. E. Martin, S. Ram, P. A. Rice, D. S. Stephens, R. Carlson and W. M. Shafer (2009). "Phosphoethanolamine substitution of lipid A and resistance of *Neisseria gonorrhoeae* to cationic antimicrobial peptides and complement-mediated killing by normal human serum." Infect Immun **77**(3): 1112-1120.

Li, M. F., L. Sun and J. Li (2015). "*Edwardsiella tarda* evades serum killing by preventing complement activation via the alternative pathway." Fish and Shellfish Immunology **43**(2): 325-329.

Liu, Q., K. A. Hassan, H. E. Ashwood, H. Gamage, L. Li, B. C. Mabbutt and I. T. Paulsen (2018). "Regulation of the aceI multidrug efflux pump gene in *Acinetobacter baumannii*." Journal of Antimicrobial Chemotherapy **73**(6): 1492-1500.

Liu, Y. Y., Y. Wang, T. R. Walsh, L. X. Yi, R. Zhang, J. Spencer, Y. Doi, G. Tian, B. Dong, X. Huang, L. F. Yu, D. Gu, H. Ren, X. Chen, L. Lv, D. He, H. Zhou, Z. Liang, J. H. Liu and J. Shen (2016). "Emergence of plasmid-mediated colistin resistance mechanism MCR-1 in animals and human beings in China: a microbiological and molecular biological study." The Lancet Infectious Diseases **16**(2): 161-168.

Livak, K. J. and T. D. Schmittgen (2001). "Analysis of relative gene expression data using real-time quantitative PCR and the 2(-Delta Delta C(T)) method." Methods **25**(4): 402-408.

Loehfelm, T. W., N. R. Luke and A. A. Campagnari (2008). "Identification and characterization of an *Acinetobacter baumannii* biofilm-associated protein." Journal of Bacteriology **190**(3): 1036-1044.

Longo, F., C. Vuotto and G. Donelli (2014). "Biofilm formation in *Acinetobacter baumannii*." New Microbiologica **37**(2): 119-127.

Lukat, G. S., W. R. McCleary, A. M. Stock and J. B. Stock (1992). "Phosphorylation of bacterial response regulator proteins by low molecular weight phospho-donors." Proceedings of the National Academy of Sciences of the United States of America **89**(2): 718-722.

Machado, D., J. Antunes, A. Simoes, J. Perdigao, I. Couto, M. McCusker, M. Martins, I. Portugal, T. Pacheco, J. Batista, C. Toscano and M. Viveiros (2018). "Contribution of efflux to colistin heteroresistance in a multidrug resistant *Acinetobacter baumannii* clinical isolate." Journal of Medical Microbiology **67**(6): 740-749.

Mah, T. F. and G. A. O'Toole (2001). "Mechanisms of biofilm resistance to antimicrobial agents." Trends in Microbiology **9**(1): 34-39.

Makris, D., E. Petinaki, V. Tsolaki, E. Manoulakas, K. Mantzarlis, O. Apostolopoulou, D. Sfyras and E. Zakynthinos (2018). "Colistin versus colistin combined with ampicillin-sulbactam for multiresistant *Acinetobacter baumannii* ventilator-associated pneumonia

treatment: an open-label prospective study." Indian Journal of Critical Care Medicine **22**(2): 67-77.

Mangas, E. L., A. Rubio, R. Alvarez-Marin, G. Labrador-Herrera, J. Pachon, M. E. Pachon-Ibanez, F. Divina and A. J. Perez-Pulido (2019). "Pangenome of *Acinetobacter baumannii* uncovers two groups of genomes, one of them with genes involved in CRISPR/Cas defence systems associated with the absence of plasmids and exclusive genes for biofilm formation." Microbial Genomics: DOI: 10.1099/mgen.1090.000309.

Maragakis, L. L. and T. M. Perl (2008). "*Acinetobacter baumannii*: epidemiology, antimicrobial resistance, and treatment options." Clinical Infectious Diseases **46**(8): 1254-1263.

Marchand, I., L. Damier-Piolle, P. Courvalin and T. Lambert (2004). "Expression of the RND-type efflux pump AdeABC in *Acinetobacter baumannii* is regulated by the AdeRS two-component system." Antimicrobial Agents and Chemotherapy **48**(9): 3298-3304.

Marchenkov, V. V., N. V. Kotova, T. A. Muranova and G. V. Semisotnov (2018). "Limited trypsinolysis of GroES: the effect on the interaction with GroEL and assembly *in vitro*." Molekuliarnaia Biologiia **52**(1): 82-87.

Markogiannakis, A., G. Fildisis, S. Tsiplakou, A. Ikonomidis, A. Koutsoukou, S. Pournaras, E. N. Manolis, G. Baltopoulos and A. Tsakris (2008). "Cross-transmission of multidrug-resistant *Acinetobacter baumannii* clonal strains causing episodes of sepsis in a trauma intensive care unit." Infection Control and Hospital Epidemiology **29**(5): 410-417.

Martí, S., Y. Nait Chabane, S. Alexandre, L. Coquet, J. Vila, T. Jouenne and E. Dé (2011a). "Growth of *Acinetobacter baumannii* in pellicle enhanced the expression of potential virulence factors." PLOS One **6**(10): e26030.

Martí, S., J. Rodríguez-Bano, M. Catel-Ferreira, T. Jouenne, J. Vila, H. Seifert and E. Dé (2011b). "Biofilm formation at the solid-liquid and air-liquid interfaces by *Acinetobacter* species." BMC Research Notes **4**(5): 1-4.

Matthysse, A. G., S. Stretton, C. Dandie, N. C. McClure and A. E. Goodman (1996). "Construction of GFP vectors for use in gram-negative bacteria other than *Escherichia coli*." FEMS Microbiology Letters **145**(1): 87-94.

Mattick, J. S. (2002). "Type IV pili and twitching motility." Annual Review of Microbiology **56**: 289-314.

McDonough, K. A. and A. Rodriguez (2012). "The myriad roles of cyclic AMP in microbial pathogens: from signal to sword." Nature Reviews Microbiology **10**(1): 27-38.

McQueary, C. N. and L. A. Actis (2011). "*Acinetobacter baumannii* biofilms: variations among strains and correlations with other cell properties." Journal of Microbiology **49**(2): 243-250.

Mejean, V. (2016). "Two-component regulatory systems: the moment of truth." Research in Microbiology **167**(1): 1-3.

Merighi, M., A. Carroll-Portillo, A. N. Septer, A. Bhatiya and J. S. Gunn (2006). "Role of *Salmonella enterica serovar Typhimurium* two-component system PreA/PreB in modulating PmrA-regulated gene transcription." Journal of Bacteriology **188**(1): 141-149.

Merighi, M., A. N. Septer, A. Carroll-Portillo, A. Bhatiya, S. Porwollik, M. McClelland and J. S. Gunn (2009). "Genome-wide analysis of the PreA/PreB (QseB/QseC) regulon of *Salmonella enterica* serovar Typhimurium." BMC Microbiology **9**: 42-58.

Micheau, O. and J. Tschopp (2003). "Induction of TNF receptor I-mediated apoptosis via two sequential signaling complexes." Cell **114**(2): 181-190.

Mihara, K., T. Tanabe, Y. Yamakawa, T. Funahashi, H. Nakao, S. Narimatsu and S. Yamamoto (2004). "Identification and transcriptional organization of a gene cluster

involved in biosynthesis and transport of acinetobactin, a siderophore produced by *Acinetobacter baumannii* ATCC 19606T." Microbiology **150**(8): 2587-2597.

Milton, M. E., B. M. Minrovic, D. L. Harris, B. Kang, D. Jung, C. P. Lewis, R. J. Thompson, R. J. Melander, D. Zeng, C. Melander and J. Cavanagh (2018). "Re-sensitizing multidrug resistant bacteria to antibiotics by targeting bacterial response regulators: characterization and comparison of interactions between 2-Aminoimidazoles and the response regulators BfmR from *Acinetobacter baumannii* and QseB from *Francisella* spp." Frontiers in Bioscience **5**: 1-15.

Miyake, Y., T. Inaba, H. Watanabe, J. Teramoto, K. Yamamoto and A. Ishihama (2019). "Regulatory roles of pyruvate-sensing two-component system PyrSR (YpdAB) in *Escherichia coli* K-12." FEMS Microbiology Letters **366**(2): DOI: 10.1093/femsle/fnz1009.

Moatamed, O. (2012). "Bacterial virulence factors." Retrieved 27/8/2013, 2013, from https://www.slideshare.net/MansManchester/virulence-12307872.

Moffatt, J. H., M. Harper, P. Harrison, J. D. Hale, E. Vinogradov, T. Seemann, R. Henry, B. Crane, F. St Michael, A. D. Cox, B. Adler, R. L. Nation, J. Li and J. D. Boyce (2010). "Colistin resistance in *Acinetobacter baumannii* is mediated by complete loss of lipopolysaccharide production." Antimicrobial Agents and Chemotherapy **54**(12): 4971-4977.

Mohamed, Y. F., H. M. Abou-Shleib, A. M. Khalil, N. M. El-Guink and M. A. El-Nakeeb (2016). "Membrane permeabilization of colistin toward pan-drug resistant Gram-negative isolates." Brazilian Journal of Microbiology **47**(2): 381-388.

Moonmangmee, S., K. Kawabata, S. Tanaka, H. Toyama, O. Adachi and K. Matsushita (2002). "A novel polysaccharide involved in the pellicle formation of *Acetobacter aceti*." Journal of Bioscience and Bioengineering **93**(2): 192-200.

Mussi, M. A., J. A. Gaddy, M. Cabruja, B. A. Arivett, A. M. Viale, R. Rasia and L. A. Actis (2010). "The opportunistic human pathogen *Acinetobacter baumannii* senses and responds to light." Journal of Bacteriology **192**(24): 6336-6345.

Nairn, B. L., Z. R. Lonergan, J. Wang, J. J. Braymer, Y. Zhang, M. W. Calcutt, J. P. Lisher, B. A. Gilston, W. J. Chazin, V. de Crecy-Lagard, D. P. Giedroc and E. P. Skaar (2016). "The response of *Acinetobacter baumannii* to zinc starvation." Cell Host and Microbe **19**(6): 826-836.

Nait Chabane, Y., S. Martí, C. Rihouey, S. Alexandre, J. Hardouin, O. Lesouhaitier, J. Vila, J. B. Kaplan, T. Jouenne and E. Dé (2014). "Characterisation of pellicles formed by *Acinetobacter baumannii* at the air-liquid interface." PLOS One **9**(10): e111660.

Neely, A. N., M. P. Maley and G. D. Warden (1999). "Computer keyboards as reservoirs for *Acinetobacter baumannii* in a burn hospital." Clinical Infectious Diseases **29**(5): 1358-1360.

Nemec, A., L. Krizova, M. Maixnerova, T. J. van der Reijden, P. Deschaght, V. Passet, M. Vaneechoutte, S. Brisse and L. Dijkshoorn (2011). "Genotypic and phenotypic characterization of the *Acinetobacter calcoaceticus-Acinetobacter baumanni*i complex with the proposal of *Acinetobacter pittii* sp. nov. (formerly *Acinetobacter* genomic species 3) and *Acinetobacter nosocomialis* sp. nov. (formerly *Acinetobacter* genomic species 13TU)." Research in Microbiology **162**(4): 393-404.

Nigro, S. J., M. H. Brown and R. M. Hall (2019). "AbGRI1-5, a novel AbGRI1 variant in an *Acinetobacter baumannii* GC2 isolate from Adelaide, Australia." Journal of Antimicrobial Chemotherapy **74**(3): 821-823.

Nixon, B. T., C. W. Ronson and F. M. Ausubel (1986). "Two-component regulatory systems responsive to environmental stimuli share strongly conserved domains with the

nitrogen assimilation regulatory genes *ntrB* and *ntrC*." Proceedings of the National Academy of Sciences of the United States of America **83**(20): 7850-7854.

Nucleo, E., L. Steffanoni, G. Fugazza, R. Migliavacca, E. Giacobone, A. Navarra, L. Pagani and P. Landini (2009). "Growth in glucose-based medium and exposure to subinhibitory concentrations of imipenem induce biofilm formation in a multidrug-resistant clinical isolate of *Acinetobacter baumannii*." BMC Microbiology **9**: 270-281.

Olson, A. L., R. J. Thompson, C. Melander and J. Cavanagh (2012). "Chemical shift assignments and secondary structure prediction of the C-terminal domain of the response regulator BfmR from *Acinetobacter baumannii*." Biomolecular NMR assignments **8**: 67-70.

Ong, C. W., D. C. Lye, K. L. Khoo, G. S. Chua, S. F. Yeoh, Y. S. Leo, P. A. Tambyah and A. C. Chua (2009). "Severe community-acquired *Acinetobacter baumannii* pneumonia: an emerging highly lethal infectious disease in the Asia-Pacific." Respirology **14**(8): 1200-1205.

Ono, K., R. Oka, M. Toyofuku, A. Sakaguchi, M. Hamada, S. Yoshida and N. Nomura (2014). "cAMP signaling affects irreversible attachment during biofilm formation by *Pseudomonas aeruginosa* PAO1." Microbes and Environments **29**(1): 104-106.

Pagano, M., A. F. Martins and A. L. Barth (2016). "Mobile genetic elements related to carbapenem resistance in *Acinetobacter baumannii*." Brazilian Journal of Microbiology **47**(4): 785-792.

Pakharukova, N., M. Tuittila, S. Paavilainen, H. Malmi, O. Parilova, S. Teneberg, S. D. Knight and A. V. Zavialov (2018). "Structural basis for *Acinetobacter baumannii* biofilm formation." Proceedings of the National Academy of Sciences of the United States of America **115**(21): 5558-5563.

Palmer, K. L., L. M. Aye and M. Whiteley (2007). "Nutritional cues control *Pseudomonas aeruginosa* multicellular behavior in cystic fibrosis sputum." Journal of Bacteriology **189**(22): 8079-8087.

Parchem, N. L., K. A. Bauer, C. H. Cook, J. E. Mangino, C. D. Jones, K. Porter and C. V. Murphy (2016). "Colistin combination therapy improves microbiologic cure in critically ill patients with multi-drug resistant gram-negative pneumonia." European Journal of Clinical Microbiology and Infectious Diseases **35**(9): 1433-1439.

Park, M., W. J. Mitchell and F. Rafii (2016). "Effect of trehalose and trehalose transport on the tolerance of *Clostridium perfringens* to environmental stress in a wild type strain and its fluoroquinolone-resistant mutant." International Journal of Microbiology **2016**: 1-9.

Park, Y. K., J. Y. Choi, D. Shin and K. S. Ko (2011). "Correlation between overexpression and amino acid substitution of the PmrAB locus and colistin resistance in *Acinetobacter baumannii*." International Journal of Antimicrobial Agents **37**(6): 525-530.

Parkins, M. D., H. Ceri and D. G. Storey (2001). "*Pseudomonas aeruginosa* GacA, a factor in multihost virulence, is also essential for biofilm formation." Molecular Microbiology **40**(5): 1215-1226.

Parkinson, J. S. and E. C. Kofoid (1992). "Communication modules in bacterial signaling proteins." Annual Review of Genetics **26**: 71-112.

Peleg, A. Y., A. de Breij, M. D. Adams, G. M. Cerqueira, S. Mocali, M. Galardini, P. H. Nibbering, A. M. Earl, D. V. Ward, D. L. Paterson, H. Seifert and L. Dijkshoorn (2012). "The success of *Acinetobacter species*; genetic, metabolic and virulence attributes." PLOS One **7**(10): e46984.

Peleg, A. Y., H. Seifert and D. L. Paterson (2008). "*Acinetobacter baumannii*: emergence of a successful pathogen." Journal of Clinical Microbiology Reviews **21**(3): 538-582.

Perraud, A. L., V. Weiss and R. Gross (1999). "Signalling pathways in two-component phosphorelay systems." Trends in Microbiology **7**(3): 115-120.

Piletska, E. V., G. Stavroulakis, L. D. Larcombe, M. J. Whitcombe, A. Sharma, S. Primrose, G. K. Robinson and S. A. Piletsky (2011). "Passive control of quorum sensing: prevention of *Pseudomonas aeruginosa* biofilm formation by imprinted polymers." Biomacromolecules **12**(4): 1067-1071.

Pour, N. K., D. H. Dusane, P. K. Dhakephalkar, F. R. Zamin, S. S. Zinjarde and B. A. Chopade (2011). "Biofilm formation by *Acinetobacter baumannii* strains isolated from urinary tract infection and urinary catheters." FEMS Immunology and Medical Microbiology **62**(3): 328-338.

Prabhu, Y. and P. S. Phale (2003). "Biodegradation of phenanthrene by *Pseudomonas* sp. strain PP2: novel metabolic pathway, role of biosurfactant and cell surface hydrophobicity in hydrocarbon assimilation." Applied Microbiology and Biotechnology **61**(4): 342-351.

Prigent-Combaret, C., O. Vidal, C. Dorel and P. Lejeune (1999). "Abiotic surface sensing and biofilm-dependent regulation of gene expression in *Escherichia coli*." Journal of Bacteriology **181**(19): 5993-6002.

Purevdorj-Gage, B., W. J. Costerton and P. Stoodley (2005). "Phenotypic differentiation and seeding dispersal in non-mucoid and mucoid *Pseudomonas aeruginosa* biofilms." Microbiology **151**(5): 1569-1576.

Qin, Y., J. Zhang, L. Wu, D. Zhang, L. Fu and X. Xue (2018). "Comparison of the treatment efficacy between tigecycline plus high-dose cefoperazone-sulbactam and tigecycline monotherapy against ventilator-associated pneumonia caused by extensively drug-resistant *Acinetobacter baumannii*." International Journal of Clinical Pharmacology and Therapeutics **56**(3): 120-129.

Qiu, H., R. KuoLee, G. Harris, N. Van Rooijen, G. B. Patel and W. Chen (2012). "Role of macrophages in early host resistance to respiratory *Acinetobacter baumannii* infection." PLOS One **7**(6): e40019.

Quesada, A., M. C. Porrero, S. Tellez, G. Palomo, M. Garcia and L. Dominguez (2015). "Polymorphism of genes encoding PmrAB in colistin-resistant strains of *Escherichia coli* and *Salmonella enterica* isolated from poultry and swine." Journal of Antimicrobial Chemotherapy **70**(1): 71-74.

Raad, I., R. Reitzel, Y. Jiang, R. F. Chemaly, T. Dvorak and R. Hachem (2008). "Anti-adherence activity and antimicrobial durability of anti-infective-coated catheters against multidrug-resistant bacteria." Journal of Antimicrobial Chemotherapy **62**(4): 746-750.

Rahbar, M. R., I. Rasooli, S. L. Mousavi Gargari, J. Amani and Y. Fattahian (2010). "In silico analysis of antibody triggering biofilm associated protein in *Acinetobacter baumannii*." Journal of Theoretical Biology **266**(2): 275-290.

Ramirez, M. S., M. Don, A. K. Merkier, A. J. Bistué, A. Zorreguieta, D. Centrón and M. E. Tolmasky (2010). "Naturally competent *Acinetobacter baumannii* clinical isolate as a convenient model for genetic studies." Journal of Clinical Microbiology **48**(4): 1488-1490.

Ranjit, D. K., J. L. Endres and K. W. Bayles (2011). "*Staphylococcus aureus* CidA and LrgA proteins exhibit holin-like properties." Journal of Bacteriology **193**(10): 2468-2476.

Raut, J., V. Rathod and S. M. Karuppayil (2010). "Cell surface hydrophobicity and adhesion: a study on fifty clinical isolates of *Candida albicans*." Nihon Ishinkin Gakkai Zasshi **51**(3): 131-136.

Richmond, G. E., L. P. Evans, M. J. Anderson, M. E. Wand, L. C. Bonney, A. Ivens, K. L. Chua, M. A. Webber, J. M. Sutton, M. L. Peterson and L. J. Piddock (2016). "The *Acinetobacter baumannii* two-component system AdeRS regulates genes required for

multidrug efflux, biofilm formation, and virulence in a strain-specific manner." MBio **7**(2): e00430-00416.

Robinson, V. L., D. R. Buckler and A. M. Stock (2000). "A tale of two components: a novel kinase and a regulatory switch." Nature Structural and Molecular Biology **7**(8): 626-633.

Roca, I., P. Espinal, X. Vila-Farrés and J. Vila (2012). "The *Acinetobacter baumannii* oxymoron: commensal hospital dweller turned pan-drug-resistant menace." Frontiers in Immunology **23**(3): 1-8.

Ronish, L. A., E. Lillehoj, J. K. Fields, E. J. Sundberg and K. H. Piepenbrink (2019). "The structure of PilA from *Acinetobacter baumannii* AB5075 suggests a mechanism for functional specialization in *Acinetobacter* type IV pili." The Journal of Biological Chemistry **294**(1): 218-230.

Rosenberg, E., A. Gottlieb and M. Rosenberg (1983). "Inhibition of bacterial adherence to hydrocarbons and epithelial cells by emulsan." Infection and Immunity **39**(3): 1024-1028.

Roychoudhury, S., N. A. Zielinski, A. J. Ninfa, N. E. Allen, L. N. Jungheim, T. I. Nicas and A. M. Chakrabarty (1993). "Inhibitors of two-component signal transduction systems: inhibition of alginate gene activation in *Pseudomonas aeruginosa*." Proceedings of the National Academy of Sciences of the United States of America **90**(3): 965-969.

Rumbo-Feal, S., M. J. Gómez, C. Gayoso, L. Álvarez-Fraga, M. P. Cabral, A. M. Aransay, N. Rodríguez-Ezpeleta, A. Fullaondo, J. Valle, M. Tomás, G. Bou and M. Poza (2013). "Whole transcriptome analysis of *Acinetobacter baumannii* assessed by RNA-sequencing reveals different mRNA expression profiles in biofilm compared to planktonic cells." PLOS One **8**(8): e72968.

Rumbo, C., E. Fernandez-Moreira, M. Merino, M. Poza, J. A. Mendez, N. C. Soares, A. Mosquera, F. Chaves and G. Bou (2011). "Horizontal transfer of the OXA-24 carbapenemase gene via outer membrane vesicles: a new mechanism of dissemination of the carbapenem resistance genes in *Acinetobacter baumannii*." Antimicrobial Agents and Chemotherapy **55**(7): 3084-3090.

Russo, T. A., N. R. Luke, J. M. Beanan, R. Olson, S. L. Sauberan, U. MacDonald, L. W. Schultz, T. C. Umland and A. A. Campagnari (2010). "The K1 capsular polysaccharide of *Acinetobacter baumannii* strain 307-0294 is a major virulence factor." Infection and Immunity **78**(9): 3993-4000.

Russo, T. A., A. Manohar, J. M. Beanan, R. Olson, U. MacDonald, J. Graham and T. C. Umland (2016). "The response regulator BfmR is a potential drug target for *Acinetobacter baumannii*." mSphere **1**(3): e00082-00016.

Sambandan, D., D. N. Dao, B. C. Weinrick, C. Vilchéze, S. S. Gurcha, A. Ojha, L. Kremer, G. S. Besra, G. F. Hatfull and W. R. Jacobs, Jr. (2013). "Keto-mycolic acid-dependent pellicle formation confers tolerance to drug-sensitive *Mycobacterium tuberculosis*." MBio **4**(3): e00222-00213.

Samuels, M. L., J. A. Witmer and A. A. Schaffner (2012). Statistics for the life sciences. Boston, MA, Pearson Education.

Santos, C. L., M. Correia-Neves, P. Moradas-Ferreira and M. V. Mendes (2012). "A walk into the LuxR regulators of *Actinobacteria:* phylogenomic distribution and functional diversity." PLOS One **7**(10): e46758.

Sarkar, S., G. C. Ulett, M. Totsika, M. D. Phan and M. A. Schembri (2014). "Role of capsule and O antigen in the virulence of uropathogenic *Escherichia coli*." PLOS One **9**(4): e94786.

Saroj, S. D. and P. N. Rather (2013). "Streptomycin inhibits quorum sensing in *Acinetobacter baumannii*." Antimicrobial Agents and Chemotherapy **57**(4): 1926-1929.

Sato, Y., Y. Unno, T. Ubagai and Y. Ono (2018). "Sub-minimum inhibitory concentrations of colistin and polymyxin B promote *Acinetobacter baumannii* biofilm formation." PLOS One **13**(3): e0194556.

Seifert, H. (1999). "*Acinetobacter bacteremia* in the tropics." Clinical Infectious Diseases **28**(1): 31-32.

Seifert, H., A. Strate and G. Pulverer (1995). "Nosocomial bacteremia due to *Acinetobacter baumannii*. Clinical features, epidemiology, and predictors of mortality." Medicine **74**(6): 340-349.

Sepahvand, S., M. A. Davarpanah, A. Roudgari, A. Bahador, V. Karbasizade and Z. Kargar Jahromi (2017). "Molecular evaluation of colistin-resistant gene expression changes in *Acinetobacter baumannii* with real-time polymerase chain reaction." Infection and Drug Resistance **10**: 455-462.

Serna, M., J. L. Giles, B. P. Morgan and D. Bubeck (2016). "Structural basis of complement membrane attack complex formation." Nature Communications **7**: 1-7.

Serota, D. P., M. E. Sexton, C. S. Kraft and F. Palacio (2018). "Severe community-acquired pneumonia due to *Acinetobacter baumannii* in North America: case report and review of the literature." Open Forum Infectious Diseases **5**(3): 1-3.

Shashkov, A. S., M. M. Shneider, S. N. Senchenkova, A. V. Popova, A. S. Nikitina, V. V. Babenko, E. S. Kostryukova, K. A. Miroshnikov, N. V. Volozhantsev and Y. A. Knirel (2015). "Structure of the capsular polysaccharide of *Acinetobacter baumannii* 1053 having the KL91 capsule biosynthesis gene locus." Carbohydrate Research **404**: 79-82.

Shemarova, I. V. (2009). "cAMP-dependent signal pathways in unicellular eukaryotes." Critical Reviews in Microbiology **35**(1): 23-42.

Sheng, X., M. Huvet, J. W. Pinney and M. P. Stumpf (2012). "Evolutionary characteristics of bacterial two-component systems." Advances in Experimental Medicine and Biology **751**: 121-137.

Shin, J. A., Y. S. Chang, H. J. Kim, S. K. Kim, J. Chang, C. M. Ahn and M. K. Byun (2012). "Clinical outcomes of tigecycline in the treatment of multidrug-resistant *Acinetobacter baumannii* infection." Yonsei Medical Journal **53**(5): 974-984.

Shin, J. H., H. W. Lee, S. M. Kim and J. Kim (2009). "Proteomic analysis of *Acinetobacter baumannii* in biofilm and planktonic growth mode." Journal of Microbiology **47**(6): 728-735.

Simon, R., U. Priefer and A. Puhler (1983). "A broad host range mobilization system for invivo genetic-engineering: transposon mutagenesis in Gram-negative bacteria." Bio-Technology **1**(9): 784-791.

Singh, N. P., M. Rani, K. Gupta, T. Sagar and I. R. Kaur (2017). "Changing trends in antimicrobial susceptibility pattern of bacterial isolates in a burn unit." Burns **43**(5): 1083-1087.

Siryaporn, A., B. S. Perchuk, M. T. Laub and M. Goulian (2010). "Evolving a robust signal transduction pathway from weak cross-talk." Molecular Systems Biology **21**(6): 1-26.

Skerker, J. M., M. S. Prasol, B. S. Perchuk, E. G. Biondi and M. T. Laub (2005). "Two-component signal transduction pathways regulating growth and cell cycle progression in a bacterium: a system-level analysis." PLOS Biology **3**(10): 1-19.

Skiebe, E., V. de Berardinis, P. Morczinek, T. Kerrinnes, F. Faber, D. Lepka, B. Hammer, O. Zimmermann, S. Ziesing, T. A. Wichelhaus, K. P. Hunfeld, S. Borgmann, S. Gröbner, P. G. Higgins, H. Seifert, H. J. Busse, W. Witte, Y. Pfeifer and G. Wilharm (2012). "Surface-associated motility, a common trait of clinical isolates of *Acinetobacter*

baumannii, depends on 1,3-diaminopropane." International Journal of Medical Microbiology **302**(3): 117-128.

Skindersoe, M. E., M. Alhede, R. Phipps, L. Yang, P. O. Jensen, T. B. Rasmussen, T. Bjarnsholt, T. Tolker-Nielsen, N. Hoiby and M. Givskov (2008). "Effects of antibiotics on quorum sensing in *Pseudomonas aeruginosa*." Antimicrobial Agents and Chemotherapy **52**(10): 3648-3663.

Skorupski, K. and R. K. Taylor (1997). "Cyclic AMP and its receptor protein negatively regulate the coordinate expression of cholera toxin and toxin-coregulated pilus in *Vibrio cholerae*." Proceedings of the National Academy of Sciences of the United States of America **94**(1): 265-270.

Smith, M. G., T. A. Gianoulis, S. Pukatzki, J. J. Mekalanos, L. N. Ornston, M. Gerstein and M. Snyder (2007). "New insights into *Acinetobacter baumannii* pathogenesis revealed by high-density pyrosequencing and transposon mutagenesis." Genes and Development **21**(5): 601-614.

Solomon, J. M. and A. D. Grossman (1996). "Who's competent and when: regulation of natural genetic competence in bacteria." Trends in Genetics **12**(4): 150-155.

Soon, R. L., J. Li, J. D. Boyce, M. Harper, B. Adler, I. Larson and R. L. Nation (2012). "Cell surface hydrophobicity of colistin-susceptible vs resistant *Acinetobacter baumannii* determined by contact angles: methodological considerations and implications." Journal of Applied Microbiology **113**(4): 940-951.

Srinivasan, V. B., V. Vaidyanathan and G. Rajamohan (2015). "AbuO, a TolC-like outer membrane protein of *Acinetobacter baumannii*, is involved in antimicrobial and oxidative stress resistance." Antimicrobial Agents and Chemotherapy **59**(2): 1236-1245.

Stanley, N. R. and B. A. Lazazzera (2004). "Environmental signals and regulatory pathways that influence biofilm formation." Molecular Microbiology **52**(4): 917-924.

Stephenson, K. and J. A. Hoch (2002). "Evolution of signalling in the sporulation phosphorelay." Molecular Microbiology **46**(2): 297-304.

Stewart, C. R., O. Rossier and N. P. Cianciotto (2009). "Surface translocation by *Legionella pneumophila*: a form of sliding motility that is dependent upon type II protein secretion." Journal of Bacteriology **191**(5): 1537-1546.

Stewart, P. S. and J. William Costerton (2001). "Antibiotic resistance of bacteria in biofilms." The Lancet **358**(9276): 135-138.

Stock, A. M., V. L. Robinson and P. N. Goudreau (2000). "Two-component signal transduction." Annual Review of Biochemistry **69**: 183-215.

Stojiljkovic, I., A. J. Baumler and K. Hantke (1994). "Fur regulon in gram-negative bacteria. Identification and characterization of new iron-regulated *Escherichia coli* genes by a fur titration assay." Journal of Molecular Biology **236**(2): 531-545.

Strassle, P., K. A. Thom, J. K. Johnsonm, S. Leekha, M. Lissauer, J. Zhu and A. D. Harris (2012). "The effect of terminal cleaning on environmental contamination rates of multidrug-resistant *Acinetobacter baumannii*." American Journal of Infection Control **40**(10): 1005-1007.

Stretton, S., S. Techkarnjanaruk, A. M. McLennan and A. E. Goodman (1998). "Use of green fluorescent protein to tag and investigate gene expression in marine bacteria." Applied and Environmental Microbiology **64**(7): 2554-2559.

Suleyman, G., G. Alangaden and A. C. Bardossy (2018). "The role of environmental contamination in the transmission of nosocomial pathogens and healthcare-associated infections." Current Infectious Disease Reports **20**(6): 12-16.

Sunenshine, R. H., M. O. Wright, L. L. Maragakis, A. D. Harris, X. Song, J. Hebden, S. E. Cosgrove, A. Anderson, J. Carnell, D. B. Jernigan, D. G. Kleinbaum, T. M. Perl, H. C. Standiford and A. Srinivasan (2007). "Multidrug-resistant *Acinetobacter* infection mortality rate and length of hospitalization." Emerging Infectious Diseases **13**(1): 97-103.

Sutherland, I. W. (2001). "The biofilm matrix an immobilized but dynamic microbial environment." Trends in Microbiology **9**(5): 222-227.

Tahrioui, A., E. Quesada and I. Llamas (2013). "Genetic and phenotypic analysis of the GacS/GacA system in the moderate halophile *Halomonas anticariensis*." Microbiology **159**(Pt 3): 462-474.

Takeuchi, O., S. Sato, T. Horiuchi, K. Hoshino, K. Takeda, Z. Dong, R. L. Modlin and S. Akira (2002). "Cutting edge: role of Toll-like receptor 1 in mediating immune response to microbial lipoproteins." Journal of Immunology **169**(1): 10-14.

Tamura, H., A. Yamada, H. Saito, S. Murai and H. Kato (2004). "Identification of another surface protein antigen I/II gene, *paaB*, and a putative transcriptional regulator gene, *par*, from *Streptococcus cricetus*." Genes and Genetic Systems **79**(3): 129-137.

Telang, N. V., M. G. Satpute, P. K. Dhakephalkar, K. B. Niphadkar and S. G. Joshi (2011). "Fulminating septicemia due to persistent pan-resistant community-acquired metallo-beta-lactamase (IMP-1)-positive *Acinetobacter baumannii*." Indian Journal of Pathology and Microbiology **54**(1): 180-182.

Thompson, R. J., B. G. Bobay, S. D. Stowe, A. L. Olson, L. Peng, Z. Su, L. A. Actis, C. Melander and J. Cavanagh (2012). "Identification of BfmR, a response regulator involved in biofilm development, as a target for a 2-Aminoimidazole-based antibiofilm agent." Biochemistry **51**(49): 9776-9778.

Tipton, K. A. and P. N. Rather (2016). "An OmpR/EnvZ two-component system ortholog regulates phase variation, osmotic tolerance, motility, and virulence in *Acinetobacter baumannii* strain AB5075." Journal of Bacteriology **199**(3): e00705-00716

Tiwari, S., S. B. Jamal, S. S. Hassan, P. Carvalho, S. Almeida, D. Barh, P. Ghosh, A. Silva, T. L. P. Castro and V. Azevedo (2017). "Two-component signal transduction systems of pathogenic bacteria as targets for antimicrobial therapy: an overview." Frontiers in Immunology **8**(1878): 1-7.

Tiwari, V., V. Patel and M. Tiwari (2018). "In-silico screening and experimental validation reveal L-Adrenaline as anti-biofilm molecule against biofilm-associated protein (Bap) producing *Acinetobacter baumannii*." International Journal of Biological Macromolecules **107**: 1242-1252.

Tomaras, A. P., C. W. Dorsey, R. E. Edelmann and L. A. Actis (2003). "Attachment to and biofilm formation on abiotic surfaces by *Acinetobacter baumannii*: involvement of a novel chaperone-usher pili assembly system." Microbiology **149**(12): 3473-3484.

Tomaras, A. P., M. J. Flagler, C. W. Dorsey, J. A. Gaddy and L. A. Actis (2008). "Characterization of a two-component regulatory system from *Acinetobacter baumannii* that controls biofilm formation and cellular morphology." Microbiology **154**(11): 3398-3409.

Trimble, M. J., P. Mlynarcik, M. Kolar and R. E. Hancock (2016). "Polymyxin: alternative mechanisms of action and resistance." Cold Spring Harbor Perspectives in Medicine **6**(10): 1-12.

Tsai, C. M. and C. E. Frasch (1982). "A sensitive silver stain for detecting lipopolysaccharides in polyacrylamide gels." Analytical Biochemistry **119**(1): 115-119.

Tuttobene, M. R., P. Cribb and M. A. Mussi (2018). "BlsA integrates light and temperature signals into iron metabolism through Fur in the human pathogen *Acinetobacter baumannii*." Scientific Reports **8**(1): 1-3.

Vallet, I., J. W. Olson, S. Lory, A. Lazdunski and A. Filloux (2001). "The chaperone/usher pathways of *Pseudomonas aeruginosa*: identification of fimbrial gene clusters (*cup*) and their involvement in biofilm formation." Proceedings of the National Academy of Sciences of the United States of America **98**(12): 6911-6916.

van Faassen, H., R. KuoLee, G. Harris, X. Zhao, J. W. Conlan and W. Chen (2007). "Neutrophils play an important role in host resistance to respiratory infection with *Acinetobacter baumannii* in mice." Infection and Immunity **75**(12): 5597-5608.

Vila, J., S. Marti and J. Sanchez-Cespedes (2007). "Porins, efflux pumps and multidrug resistance in *Acinetobacter baumannii*." Journal of Antimicrobial Chemotherapy **59**(6): 1210-1215.

Vogeleer, P., Y. D. Tremblay, A. A. Mafu, M. Jacques and J. Harel (2014). "Life on the outside: role of biofilms in environmental persistence of Shiga-toxin producing *Escherichia coli*." Frontiers in Microbiology **5**(317): 1-12.

Wada, A., R. Mikkola, C. G. Kurland and A. Ishihama (2000). "Growth phase-coupled changes of the ribosome profile in natural isolates and laboratory strains of *Escherichia coli*." Journal of Bacteriology **182**(10): 2893-2899.

Wand, M. E., L. J. Bock, L. C. Bonney and J. M. Sutton (2016). "Mechanisms of increased resistance to chlorhexidine and cross-resistance to colistin following exposure of *Klebsiella pneumoniae* clinical isolates to chlorhexidine." Antimicrobial Agents and Chemotherapy **61**: e01162-01116.

Wang, D., H. Liang, J. Chen, Y. Mou and Y. Qi (2014). "Structural and environmental features of novel *mdfA* variant and *mdfA* genes in recombinant regions of *Escherichia coli*." Microbial Drug Resistance **20**(5): 392-398.

Wang, J., C. Wang, H. B. Yu, S. Dela Ahator, X. Wu, S. Lv and L. H. Zhang (2019). "Bacterial quorum-sensing signal IQS induces host cell apoptosis by targeting POT1-p53 signalling pathway." Cellular Microbiology **21**(10): e13076.

Wang, L., J. K. Yang, V. Kabaleeswaran, A. J. Rice, A. C. Cruz, A. Y. Park, Q. Yin, E. Damko, S. B. Jang, S. Raunser, C. V. Robinson, R. M. Siegel, T. Walz and H. Wu (2010). "The Fas-FADD death domain complex structure reveals the basis of DISC assembly and disease mutations." Nature Structural and Molecular Biology **17**(11): 1324-1329.

Wang, Y., P. Hao, B. Lu, H. Yu, W. Huang, H. Hou and K. Dai (2010). "Causes of infection after earthquake, China, 2008." Emerging Infectious Diseases **16**(6): 974-975.

Wang, Y., Z. Wang, Y. Chen, X. Hua, Y. Yu and Q. Ji (2019). "A highly efficient CRISPR-Cas9-based genome engineering platform in *Acinetobacter baumannii* to understand the H2O2-sensing mechanism of OxyR." Cell Chemical Biology: DOI: 10.1016/j.chembiol.2019.1009.1003.

Wang, Y., X. Zhang, X. Feng, X. Liu, L. Deng and Z. A. Liang (2016). "Expression of Toll-like receptor 4 in lungs of immune-suppressed rat with *Acinetobacter baumannii* infection." Experimental and Therapeutic Medicine **12**(4): 2599-2605.

Warner, W. A., S. N. Kuang, R. Hernandez, M. C. Chong, P. J. Ewing, J. Fleischer, J. Meng, S. Chu, D. Terashita, L. English, W. Chen and H. H. Xu (2016). "Molecular characterization and antimicrobial susceptibility of *Acinetobacter baumannii* isolates obtained from two hospital outbreaks in Los Angeles County, California, USA." BMC Infectious Disease **16**: 194.

Weber, B. S., C. M. Harding and M. F. Feldman (2015a). "Pathogenic *Acinetobacter*: from the cell surface to infinity and beyond." Journal of Bacteriology **198**(6): 880-887.

Weber, B. S., P. M. Ly, J. N. Irwin, S. Pukatzki and M. F. Feldman (2015b). "A multidrug resistance plasmid contains the molecular switch for type VI secretion in

Acinetobacter baumannii." Proceedings of the National Academy of Sciences of the United States of America **112**(30): 9442-9447.

Wei, J. R., D. L. Richie, M. Mostafavi, L. E. t. Metzger, C. M. Rath, W. S. Sawyer, K. T. Takeoka and C. R. Dean (2017). "LpxK is essential for growth of *Acinetobacter baumannii* ATCC 19606: relationship to toxic accumulation of lipid A pathway intermediates." mSphere **2**(4): e00199-00117.

Weiss, G. and U. E. Schaible (2015). "Macrophage defense mechanisms against intracellular bacteria." Immunological Reviews **264**(1): 182-203.

Wessels, M. R. (2016). Cell wall and surface molecules: Capsule. *Streptococcus pyogenes*: basic biology to clinical manifestations. J. J. Ferretti, D. L. Stevens and V. A. Fischetti. University of Oklahoma Health Sciences Center, Oklahoma City, OK.

Whitworth, D. E. and P. J. Cock (2008). "Two-component systems of the myxobacteria: structure, diversity and evolutionary relationships." Microbiology **154**(2): 360-372.

WHO. (2017, 27 Feb 2017). "Essential medicines and health products: Global priority list of antibiotic-resistant bacteria to guide researcher, discovery, and development of new antibiotics." 2017, from www.who.int/medicines/publications/global-priority-list-antibiotic-resistant-bacteria/en/.

Wiegand, I., K. Hilpert and R. E. Hancock (2008). "Agar and broth dilution methods to determine the minimal inhibitory concentration (MIC) of antimicrobial substances." Nature Protocols **3**(2): 163-175.

Wolfgang, M. C., V. T. Lee, M. E. Gilmore and S. Lory (2003). "Coordinate regulation of bacterial virulence genes by a novel adenylate cyclase-dependent signaling pathway." Developmental Cell **4**(2): 253-263.

Wood, C. R., L. E. Mack and L. A. Actis (2018). "An update on the *Acinetobacter baumannii* regulatory circuitry." Trends in Microbiology **26**(7): 560-562.

Wuichet, K., B. J. Cantwell and I. B. Zhulin (2010). "Evolution and phyletic distribution of two-component signal transduction systems." Current Opinion in Microbiology **13**(2): 219-225.

Xu, K. D., G. A. McFeters and P. S. Stewart (2000). "Biofilm resistance to antimicrobial agents." Microbiology **146** 547-549.

Xu, L., P. Venkataramani, Y. Ding, Y. Liu, Y. Deng, G. L. Yong, L. Xin, R. Ye, L. Zhang, L. Yang and Z. X. Liang (2016). "A cyclic di-GMP-binding adaptor protein interacts with histidine kinase to regulate two-component signaling." The Journal of Biological Chemistry **291**(31): 16112-16123.

Yahr, T. L., A. J. Vallis, M. K. Hancock, J. T. Barbieri and D. W. Frank (1998). "ExoY, an adenylate cyclase secreted by the *Pseudomonas aeruginosa* type III system." Proceedings of the National Academy of Sciences of the United States of America **95**(23): 13899-13904.

Yamamoto, K., H. Arai, M. Ishii and Y. Igarashi (2012). "Involvement of flagella-driven motility and pili in *Pseudomonas aeruginosa* colonization at the air-liquid interface." Microbes and Environments **27**(3): 320-323.

Yamamoto, K., K. Hirao, T. Oshima, H. Aiba, R. Utsumi and A. Ishihama (2005). "Functional characterization in vitro of all two-component signal transduction systems from *Escherichia coli*." The Journal of Biological Chemistry **280**(2): 1448-1456.

Yan, Q., L. D. Lopes, B. T. Shaffer, T. A. Kidarsa, O. Vining, B. Philmus, C. Song, V. O. Stockwell, J. M. Raaijmakers, K. L. McPhail, F. D. Andreote, J. H. Chang and J. E. Loper (2018). "Secondary metabolism and interspecific competition affect accumulation of spontaneous mutants in the GacS-GacA regulatory system in *Pseudomonas protegens*." MBio **9**(1): e01845-01817.

Yanisch-Perron, C., J. Vieira and J. Messing (1985). "Improved M13 phage cloning vectors and host strains: nucleotide sequences of the M13mp18 and pUC19 vectors." Gene **33**(1): 103-119.

Yoon, E. J., P. Courvalin and C. Grillot-Courvalin (2013). "RND-type efflux pumps in multidrug-resistant clinical isolates of *Acinetobacter baumannii*: major role for AdeABC overexpression and AdeRS mutations." Antimicrobial Agents and Chemotherapy **57**(7): 2989-2995.

Yoshida, T., S. Cai and M. Inouye (2002). "Interaction of EnvZ, a sensory histidine kinase, with phosphorylated OmpR, the cognate response regulator." Molecular Microbiology **46**(5): 1283-1294.

Yuan, J., Y. Chen, G. Zhou, H. Chen and H. Gao (2013). "Investigation of roles of divalent cations in *Shewanella oneidensis* pellicle formation reveals unique impacts of insoluble iron." Biochimica et Biophysica Acta **1830**(11): 5248-5257.

Yue, D., C. Song, B. Zhang, Z. Liu, J. Chai, Y. Luo and H. Wu (2017). "Hospital-wide comparison of health care-associated infection among 8 intensive care units: A retrospective analysis for 2010-2015." American Journal of Infection Control **45**(1): e7-e13.

Zarrilli, R., S. Pournaras, M. Giannouli and A. Tsakris (2013). "Global evolution of multidrug-resistant *Acinetobacter baumannii* clonal lineages." International Journal of Antimicrobial Agents **41**(1): 11-19.

Zeana, C., E. Larson, J. Sahni, S. J. Bayuga, F. Wu and P. Della-Latta (2003). "The epidemiology of multidrug-resistant *Acinetobacter baumannii*: does the community represent a reservoir?" Infection Control and Hospital Epidemiology **24**(4): 275-279.

Zhang, D. F., J. Z. Ye, H. H. Dai, X. M. Lin, H. Li and X. X. Peng (2018). "Identification of ethanol tolerant outer membrane proteome reveals OmpC-dependent mechanism in a manner of EnvZ/OmpR regulation in *Escherichia coli*." Journal of Proteomics **179**: 92-99.

Zimbler, D. L., W. F. Penwell, J. A. Gaddy, S. M. Menke, A. P. Tomaras, P. L. Connerly and L. A. Actis (2009). "Iron acquisition functions expressed by the human pathogen *Acinetobacter baumannii*." Biometals **22**(1): 23-32.

Ziolkowski, G., I. Pawlowska, L. Krawczyk and J. Wojkowska-Mach (2018). "Antibiotic consumption versus the prevalence of multidrug-resistant *Acinetobacter baumannii* and *Clostridium difficile* infections at an ICU from 2014-2015." Journal of Infection and Public Health **11**(5): 626-630.